UNIVERSIDAD COMPLUTENSE DE MADRID

FACULTAD DE FARMACIA

TESIS DOCTORAL

Hybrid nanocarriers for the selective treatment of complex diseases

Nanotransportadores híbridos para el tratamiento selectivo de enfermedades complejas

MEMORIA PARA OPTAR AL GRADO DE DOCTOR

PRESENTADA POR

María Rocío Villegas Díaz

Director

Alejandro Baeza García

Madrid 2019

Hybrid Nanocarriers for the Selective Treatment of Complex Diseases

Nanotransportadores Híbridos para el Tratamiento Selectivo de Enfermedades Complejas

María Rocío Villegas Díaz

Memoria para optar al grado de Doctor
por la Universidad Complutense de Madrid

Departamento de Química en Ciencias Farmacéuticas
Facultad de Farmacia, UCM

Madrid 2018

Director: Alejandro Baeza García

Departamento de Química en Ciencias Farmacéuticas.

Facultad de Farmacia.

UNIVERSIDAD
COMPLUTENSE
MADRID

Hybrid Nanocarriers for the Selective Treatment of Complex Diseases.

Nanotransportadores Híbridos para el Tratamiento Selectivo de Enfermedades Complejas.

Memoria presentada por

María Rocío Villegas Díaz

Director

Alejandro Baeza García

Para optar el grado de Doctor con Mención Internacional por la Universidad Complutense de Madrid

Agradecimientos

Nunca me ha costado dar las gracias, sin embargo, estás hojas serán probablemente las más difíciles de escribir de la tesis, y todo se debe a que significan el final de una etapa de mi vida en la que he sido inmensamente feliz.

Empezaré agradeciendo a la Profesora María Vallet Regí el haberme dado la oportunidad de trabajar en su grupo de investigación y de aprender y desarrollarme en un mundo hasta entonces desconocido para mí.

Me gustaría agradecer a mi director Alejandro básicamente todo. Antes de pisar este laboratorio yo nunca había sabido lo que quería hacer, pero al llegar aquí descubrí una disciplina que me encantaba y a lo que quería dedicarme. Esto no habría sido así si no me hubieras propuesto miles de proyectos emocionantes y no te hubieras involucrado en que los lograrás. Gracias por confiar en mí. Gracias por preocuparte en formarme y motivarme, por las horas de rotulador y pizarra aprendiendo química, bueno y algo de historia sobre un tal Hernán Cortes que aparecía en negrita en mis libros. Gracias por tu paciencia y por estar dispuesto a ayudarme siempre. Ninguno de los dos teníamos todas con nosotros de que algún día esta tesis llegaría a ser realidad, pero ya ves, unos tres años después has logrado que una física opte a un título de doctora en…..Farmacia…..bueno espero que alguien abra la tesis para que se dé cuenta que tiene más que ver con la química. Ha sido todo un placer trabajar contigo, espero que mucha más gente tenga la gran suerte que he tenido yo de formarme a tu lado, porque hace falta que haya gente tan motivada y comprometida como tú. Gracias, gracias y gracias. Espero tener muchas más veces la oportunidad de investigar a tu lado, porque eso es sin ninguna duda un lujo más que un trabajo. Te admiro profundamente y te deseo la mejor de las suertes, no conozco a nadie que se la merezca más que tú.

Me gustaría agradecer también a mi tutora Vicky por su inmejorable ayuda. especialmente en esta última etapa de la tesis, gracias por estar siempre dispuesta a ayudar y por pensar siempre en todos.

Gracias al Departamento de Química en Ciencias Farmacéuticas, a la Unidad de Química inorgánica y Bioinorgánica, a la Facultad de Farmacia y a la Universidad Complutense de Madrid. En este departamento he conocido a gente excepcional tanto académica como personalmente hablando. Gracias a su director Juan Carlos por su constante preocupación en que todos podamos trabajar en las mejores condiciones posibles. Gracias a Pili y a Jose porque son, sin duda, imprescindibles y están dispuestos siempre a echar una mano. Gracias a todos los profesores y resto del personal del departamento Blanca, África, María Teresa, Antonio, Montse, Isabel, Dani, Rafa, Antonio Luis, Juan, Vicky, Miguel, Sandra, Ana y tantos otros. Gracias también a los distintos Centros de Apoyo a la Investigación, Especialmente al Centro Nacional de Microscopía Electrónica y el CAI de Difracción de Rayos X.

Gracias a todos mis compañeros de laboratorio.

Gracias al Maño por estar dispuesto a ayudarme siempre, por preocuparte de mí, por venir a verme y hacer más amenas las jornadas interminables en el laboratorio. Gracias por ser mi amigo y por sacarme siempre una sonrisa, estoy segura que con toda la motivación

que tienes y tu capacidad de trabajo llegarás muy lejos. Gracias a Nati por ser mi compañera y mi amiga, esta experiencia no habría sido la misma sin ti, eres increíble y contigo he conocido a alguien con la que comerme el mundo, lo haremos, estoy segura. Gracias a los dos por estar siempre a mi lado, sois lo mejor que me llevo de esta experiencia, ya no me imagino mi vida sin vosotros asique espero que sigamos viviendo muchas más aventuras juntos.

Gracias a Juan Luis por ser un compañero increíble y un gran amigo. Gracias por ser tan inteligente y por saber hacer que eso se convierta en una motivación para todos los que estamos a tu lado. No creo que nunca encuentre a un compañero mejor con el que picarme a poner reacciones a horas en las que el resto del mundo ya debe de estar cenando, eres increíble y es todo un placer haber vivido esta etapa contigo.

Gracias a Gonzalo porque es difícil saber tanto y mostrarlo de una forma tan "sin más". Tienes unos principios que admiro y que estoy segura te llevarán, si no lejos, al menos al lado de gente que merece la pena. Tienes una gran capacidad para ayudar a todo aquel que lo necesita de una forma altruista y un fin tan sincero como mejorar el mundo con tu ciencia y eso Gonzalo, es muy difícil de encontrar. Muy buena suerte amigo, te la mereces.

Gracias a Edu, porque a veces las personas que te empiezan imponiendo se acaban convirtiendo en gente guay, que no sabes muy bien cómo, pero se convierten en imprescindibles y hacen de cada momento uno mejor.

Gracias a Marina, porque fue todo un placer ser tu "sub-becaria" en mi primera etapa en este laboratorio, me alegro mucho de haber vivido una época tan importante a tu lado, gracias por estar dispuesta a repetirme todas las cosas las veces que hicieran falta y por estar siempre de buen humor.

Gracias a Ángel, desde que te fuiste este laboratorio se convirtió en una pequeña jungla, una jungla increíble, pero una jungla al fin y al cabo.

Gracias a mi GoldMan Sergio, ha sido todo un placer trabajar contigo, las sesiones de TEM son mucho más aburridas sin nuestras continuas discusiones matrimoniales. Ha sido muy divertido trabajar a tu lado, por aquí se te echa de menos.

Gracias a Víctor, mi compañero de tesis. Eres un tipo increíble y un estupendo químico. Me gustaría seguir aprendiendo mucho de ti y trabajar a tu lado. Es difícil encontrar a un "hater" con esa capacidad de hacer reír a todo el mundo. Espero seguir teniéndote cerca para salir de fiesta y acabar escuchándote cantar la Marseillaise. Muchas gracias mi pequeño Koala.

Gracias David por todos los meses de piques y risas, me va a ser difícil encontrar a alguien con el que entenderme también. Estoy segura de que encontrarás un sitio en el que poder hacer tu doctorado y disfrutar de la ciencia como a ti te gusta.

Gracias a Anna y a Noemí por haber elegido este sitio como hospedaje y venir a verme siempre a la hora de comer. Las comidas no serían ni la mitad de divertidas sin vosotras.

Gracias Patri por estar siempre con la sonrisa puesta, por saber dar abrazos cuando son necesarios y por estar pendiente de los demás, estoy deseando leer tu primer paper.

Gracias a Elena y Nai porque son capaces de sacar una sonrisa a cualquiera.

Gracias a Clara, por hacerme reír con todas sus historias, te habría dejado un “posit”, pero se me han acabado =).

Gracias a Adrián por haber formado parte de esta etapa, me alegro mucho de lo bien que te va en tu doctorado, muy buena suerte.

Gracias a Inés, digo Irene, por haber elegido este grupo para hacer la FPU, ha sido todo un placer conocerte.

Gracias a Sandra y a Ana porque sois geniales y ha sido un placer conoceros.

Gracias a Rebeca y a Javi por todo lo que nos hemos reído juntos, trabajar con gente así es todo un lujo.

Gracias a Mateo, porque me lo paso genial contigo y porque te voy a echar mucho de menos.

Gracias a Iciar porque es uno de mis grandes descubrimientos en esta tesis. Me encanta tu humor sagaz y la forma tan tuya de hacer personal todas mis luchas. Mi primer año en este laboratorio fue increíble gracias en gran parte a ti. Eres una gran amiga y espero tenerte siempre a mi lado.

Gracias a todos los que habéis pasado por este laboratorio, porque habéis hecho de esta aventura una de las etapas más felices de mi vida.

Thanks to Professor Jeffrey Brinker for taking me into his research group. It was a wonderful experience for me to work with such exceptional people. I would also like to specially acknowledge Achraf for being so helpful with everything, for the travels and for those three months at your side. It was a pleasure working with you, boss.

Gracias a todos mis amigos, Pili, Guille, Ángel, Claudia, Vir, Vivi, Elena, Marta, Mary, Faty, Belén, Álvaro, Miguel, Julián, Héctor, Lidia, Anahí, Elena, Carlos. Sois todos increíbles, gracias por hacerme tan feliz a vuestro lado.

Quiero dar las gracias especialmente a mis padres sin cuyo esfuerzo y sacrificio me habría sido imposible formarme y disfrutar haciendo lo que más me gusta. Todo lo que consiga en mi vida será gracias a vosotros, sois las personas a las que más admiro en este mundo y espero compensaros algún día. al menos en una ínfima parte. todo lo que me habéis dado. Esta tesis es especialmente vuestra. Estoy profundamente orgullosa de vosotros y os quiero. Gracias también a mis abuelas porque dudo mucho que vuelva a conocer a alguien con tanto coraje como ellas. Gracias Simona por quererme como me quieres, no tengo vidas para devolvértelo. Gracias a mi hermana por sufrirme en esta dura etapa, por estar siempre de buen humor y por ser tan ella.

Gracias por último a todos aquellos que lean esta tesis, espero que les pueda servir de ayuda y que leyéndola puedan sentir, aunque sea ligeramente, la emoción que yo he vivido durante su desarrollo.

Abbreviations

- Enhance Permeation and Retention (EPR)
- Extracellular Matrix (ECM)
- Transmission Electron Microscopy (TEM)
- Field Ion Microscope (FIM)
- Polyethyleneglicol (PEG)
- Mononuclear Phagocyte System (MPS)
- Poly(lactic-co-glycolic acid) (PLGA)
- Fluorescent Resonant Energy Transfer (FRET)
- Mesoporous Silica Nanoparticles (MSNs)
- Hexadecyltrimethylammonium (CTAB)
- Tetraethylortosilicate (TEOS)
- Fourier Transform Infrared Spectroscopy (FTIR)
- X Ray Diffraction (XRD)
- Dynamic Light Scattering (DLS)
- Scanning Electronic Microscopy (SEM)
- World Health Organization (WHO)
- Triphenylphosphinium (TPP)
- Food Drug Administration (FDA)
- Multidrug Resistance (MDR)
- ATP-binding cassette (ABC)
- Red Blood Cells (RBC)
- Bovine Serum Albumin (BSA)
- N,N´-methylene bisacrylamide (MBA)
- Indole Acetic (IAA)
- Horseradish Peroxidase (HRP)
- Glutathione (GSH)
- Caspase 3 (CP3)
- Acrylamide (AAm)
- 2-Aminoethyldimethacrylate Hydrochloride (Am)
- Ethylene Glycol dimethacrylate (EG)
- N,N,N´,N´-Tetramethylenediamine (TMEDA)
- Vascular Endothelial Growth Factor (VEGF)
- Poly (ethyleneglycol)-poly(Ɛ-caprolactone) (PEG-PCL)
- Blood Brain Barrier (BBB)
- Topotecan (TOP)
- Collagenase Clostridium Histolyticum (CCH)

INDEX

Summary

This doctoral thesis is focused on the design, synthesis and evaluation of smart nanosystems for the treatment of complex diseases such as cancer and fibrosis.

Cancer is a malignant and multifaceted disease with a significant incidence in the world population. Surgery, radiotherapy and chemotherapy have been traditionally employed for cancer treatment. However, the complete eradication of tumors simply by surgical operations is not always possible, while radiotherapy and chemotherapy affects equally to both, healthy and tumoral cells. Therefore, these treatments are not usually effective for the definitive elimination of tumors being their effectiveness limited by the appearance of severe side effects, because of their lack of selectivity. Nanomedicine is an emergent and potent sub-field of nanotechnology which tries to provide more efficient treatment for complex diseases. The use of nanomaterials in cancer is based on their capacity to be accumulated in tumoral masses due to the particular characteristics of malignant tissues. This effect is the so called *Enhance Permeation and Retention* (EPR) effect, and its discovery in 1986 supposed the starting point for the nanomedicine applied to oncological therapy. In this way, the use of nanoparticles as drug carriers allows to deliver high amounts of antitumoral drugs to the tumor in a selective and controlled way, reducing the appearance of the side effects associated with the high toxicity of these drugs. Unfortunately, the progress of these antitumoral nanodevices in the clinical field has not been as fast and successful as was expected at the beginning. This discouraging fact is due to the high complexity of tumoral mass and the presence of biological barriers which a nanodevice must be able to overcome for achieving an effective treatment. One of these barriers, which is common to all nanomedicines, is the presence of an abnormally dense extracellular matrix (ECM) in the tumoral tissues. Thus, when a nanoparticle

arrives to a tumor, the existence of these dense ECM hampers its penetration within the tissue. This fact strongly limits its therapeutic effect on the periphery of the diseased tissue. In order to alleviate this liability, the scientific community has struggled to provide different strategies. One of them consist in the surface decoration of the nanodevice with proteolytic enzymes, which are able to degrade the ECM facilitating the penetration of the nanocarriers. However, the efficacy of this strategy is strongly limited by the low physico-chemical stability of enzymes in living tissues.

In this thesis, a novel approach for overcoming this important barrier has been addressed. Our strategy was based on the encapsulation of proteolytic enzymes (collagenase) in order to preserve their catalytic activity against many different insults present in the body (as other proteolytic enzymes, temperature, oxidative agents and so on). Moreover, as collagenase acts on large substrates, these nanocapsules should be provided with the disassembly capacity in order to release the enzyme allowing its capacity to degrade the ECM. The mild acidic conditions, typical of many solid tumors, were chosen as stimulus which triggers the collagenase release. The attachment of these collagenase nanocapsules on the surface of a nanocarrier allows its deep penetration within a solid tumor because, the collagenase released in the zone destroys the tumoral ECM facilitating the particle penetration into the tissue. Thus, a higher penetration into the solid tumor ensures an effective treatment.

Collagenase nanocapsules were synthetized by free radical polymerization in aqueous medium using three different monomers: acrylamide, as neutral and structural monomer, 2-aminoethylmethacrylate hydrochloride, as positively charged monomer and ethylene glycoldimethacrylate, as pH-responsive crosslinker. The positive monomer plays a dual function in this process, on one hand, it favors the encapsulation process by electrostatic interactions with the negatively charged surface of the collagenase and, on the second

hand, provides anchoring points for the further attachment of the capsule on the particle surface. Once synthesized these collagenase nanocapsules, they were anchored on a model nanocarrier (mesoporous silica nanoparticles) and the efficacy of the nanodevices to achieve a homogenous distribution within tumoral tissues was examined employing 3D collagen scaffolds with the tumoral cells embedded. These collagen scaffolds were employed as models because they provide a realistic environment which present similar rheological properties than real human tissues. Nanosystems, decorated or not with collagenase nanocapsules, were placed on the top of these 3D models showing that only the nanoparticles which have collagenase nanocapsules on their surface were able to penetrate homogeneously in all around the tissue, whereas the naked particles were retained on the top.

Once proved the efficacy of the particle decoration with collagenase nanocapsules to achieve an enhanced penetration into the tissue, these capsules were attached on the surface of a nanocarrier able to present two important characteristics: to recognize the tumoral cells and to retain the cytotoxic compounds until the system reaches the inner space of these malignant cells. The chosen system for this aim was a Protocell, which is a nanodevice composed by a mesoporous silica core coated with a lipid bilayer. The mesoporous core provides high drug loading capacity due to its elevated porosity while the lipid bilayer offers colloidal stability and avoids the premature release of the cargo. The lipid bilayer was engineered in order to present two different functional groups (carboxylic acids and amino) in which an antibody (anti-VEGFR) able to recognize the tumoral cells (in this case, A549 lung cancer cells) and collagenase nanocapsules, were respectively attached.

The performance of this system was evaluated in a tridimensional tumoral tissue model consisted of a tumoral cell monolayer covered with a collagen gel of 200 μm of thickness

which also contains tumoral cells embedded. Fluorescently labeled protocells, decorated or not with the collagenase nanocapsules, were placed on the top of these gels and their capacity to reach the inner cell monolayer was evaluated by fluorescence confocal microscopy. Only the system that carried collagenase nanocapsules was able to reach this deep monolayer showing the importance to transport these proteolytic enzymes. Moreover, the presence of the antibody allowed an enhanced protocell internalization within the tumoral cells. Finally, the capacity to destroy the tumoral cells located in deep zones of the tissue was tested employing these systems loaded with a potent cytotoxic drug (topotecan). The results showed again that only the system which carried collagenase nanocapsules was able to destroy the tumoral cells located in the inner zone of the 3D model. This sophisticated system was able to achieve three paramount properties: enhanced penetration within tumoral tissues, selective internalization within tumoral cells and selective destruction of these malignant cells. This design could be easily extrapolated to other nanomedicines and would improve their efficacy in the treatment against cancer.

Other objective which has been explored in this thesis has been the development of nanocarriers able to present a dual and sequential targeting capacity from tumoral cells to important organelles inside them. The reason is that the release of antitumoral drugs close to certain organelles inside the cells (mitochondria or nucleus, among others) supposes, in many cases, an enhanced therapeutic effect. As proof of concept, nanocarriers were synthesized with two targeting moieties: folic acid for providing selectivity against prostate tumoral cells and a triphenylphosphine derivative, which present high affinity by the mitochondria membrane. These targeting agents were distributed in opposite hemisphere of the nanocarrier in order to avoid undesired interactions between them. Dual targeted nanoparticles achieved a significantly higher therapeutic effect in tumoral

cell models than mono-functionalized systems, validating the premise of this work and represents an important advancement in the design of nanosystems.

Finally, the use of collagenase nanocapsules for the treatment of different diseases than cancer, in this case fibrotic lesions, was evaluated. Fibrosis is a common lesion in several diseases that consists in the excessive formation of connective fibrotic tissues in organs or tissues. Therefore, an excessive accumulation of collagen characterizes a fibrotic tissue. A common clinical treatment of these lesions consists in the administration of collagenase to destroy these collagen depots. However, the labile nature of this enzyme which lost almost all its activity in one day reduces the efficacy of this treatment. Therefore, several injections of collagenase are often required supposing a strong inconvenient for the patients. Moreover, the repetitive administration of this enzyme increases the appearance of side effects due to overdose. The collagenase nanocapsules described for improving the penetration of nanomedicines in tumoral tissues were designed to be disassembled in mild acid conditions, but they are also hydrolyzed at physiological pH in one day. This rapid release does not provide a significant advantage in comparison with conventional treatment. Therefore, the design of collagenase nanocapsules able to provide a sustained and prolonged collagenase release during long periods of time was addressed. As a first approximation, the amount of degradable crosslinker was reduced in order to extent the degradation time. However, this strategy only improved the release time for 2-3 days which was still not enough. Since the presence of crosslinker is strictly necessary for the formation of the polymeric nanocapsule, to keep reducing its amount was not consider a valid approach. Instead, the addition of a second crosslinker in the monomer composition, in this case a non-degradable one, was studied. This strategy yielded nanocapsules able to release collagenase in a sustained way for more than 7 days, when the degradable versus non

degradable crosslinker ratio was fixed at 50-50%. These collagenase nanocapsules were tested in a fibrotic mouse model and compared with the conventional treatment, the administration of free collagenase. Collagenase nanocapsules achieved a significantly higher collagen reduction into the diseased tissue in comparison with free enzymes providing a promising alternative for the treatment of fibrotic pathologies.

In summary, the strategies developed during this doctoral thesis have tried to address important liabilities present in the treatment of complex diseases and the obtained results showed a promising potential which could be incorporated in the nanomedicine arsenal. The systems developed are collected in the **Figure 1**.

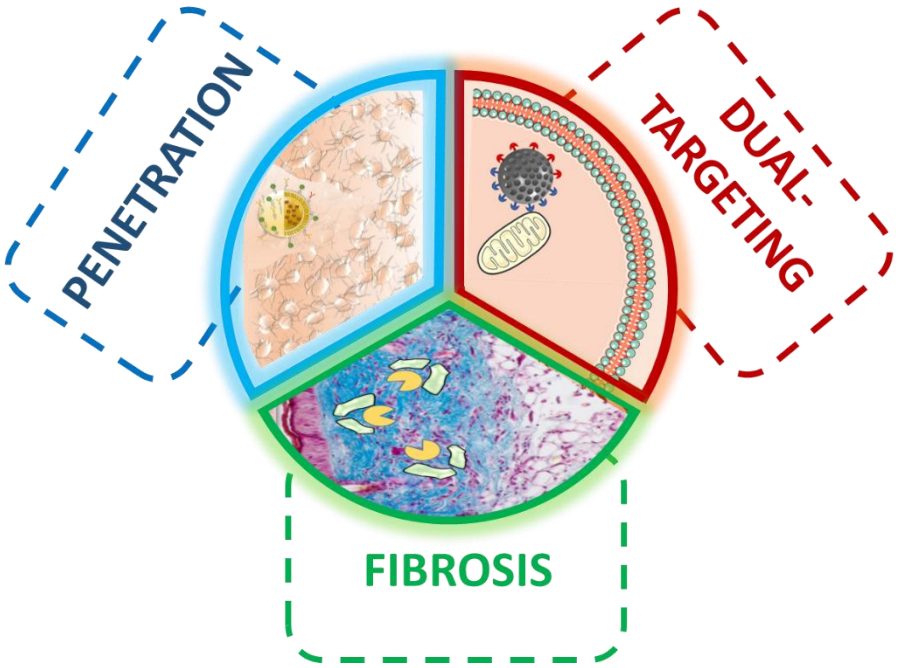

Figure 1. *Summary of systems developed in Doctoral Thesis.*

Resumen

Esta tesis doctoral se centra en el diseño, síntesis y evaluación de nanosistemas inteligentes para el tratamiento de enfermedades complejas como el cáncer y la fibrosis.

El cáncer es una enfermedad maligna y multifacética con una incidencia significativa en la población mundial. Tradicionalmente se ha tratado con cirugía, radioterapia y quimioterapia. Sin embargo, la extirpación total de tumores mediante cirugía no siempre es posible y la radioterapia y la quimioterapia no presentan selectividad hacia las masas tumorales. Por lo tanto, estos tratamientos no suelen ser eficaces para la eliminación completa de los tumores y su eficacia se ve a menudo limitada por la aparición de efectos secundarios graves. La nanomedicina es un subcampo emergente de la nanotecnología que trata de proporcionar un tratamiento más eficaz de enfermedades complejas. El uso de nanomateriales en el cáncer se basa en su capacidad de acumularse en masas tumorales debido a las características particulares de estos tejidos malignos. Este efecto recibe el nombre de *Enhance Permeation and Retention* (EPR) effect, y su descubrimiento en 1986 supuso el punto de partida para la nanomedicina aplicada a la terapia oncológica. De esta manera, el uso de nanopartículas como portadores de fármacos permite transportar una alta cantidad de fármacos antitumorales de forma selectiva y controlada al tumor, reduciendo la aparición de los efectos secundarios asociados a la alta toxicidad de estos fármacos. Desafortunadamente, el progreso de estos nanodispositivos antitumorales en el campo clínico no ha sido tan rápido y exitoso como se esperaba al principio. Este desalentador hecho se debe a la alta complejidad de la masa tumoral y a la presencia de barreras biológicas que un nanodispositivo debe ser capaz de superar para conseguir un tratamiento eficaz. Una de estas barreras, común a todos los nanomedicamentos, es la presencia de una matriz extracelular (MEC) altamente densa en los tejidos tumorales.

Así, cuando una nanopartícula llega a un tumor, la existencia de esta densa MEC dificulta su penetración en el tejido. Este hecho limita fuertemente su efecto terapéutico en la periferia del tejido enfermo. Con el fin de aliviar esta responsabilidad, la comunidad científica ha luchado para proporcionar diferentes estrategias. Una de ellas consiste en la decoración de la superficie del nanodispositivo con enzimas proteolíticas, que son capaces de degradar el MEC facilitando la penetración de los nanotransportadores. Sin embargo, la eficacia de esta estrategia está fuertemente limitada por la baja estabilidad físico-química de las enzimas en los tejidos vivos.

En esta tesis se ha abordado un enfoque novedoso para superar esta importante barrera. Nuestra estrategia se basó en la encapsulación de enzimas proteolíticas (colagenasa) con el fin de preservar su actividad catalítica frente a los diferentes agentes presentes en el cuerpo (como otras enzimas proteolíticas, temperatura, agentes oxidativos, etc.). Además, como la colagenasa actúa sobre un sustrato grande, estas nanocápsulas deben ser capaces de desensamblarse para liberar la enzima, permitiendo su capacidad de degradar el MEC. Las condiciones ácidas leves, típicas de muchos tumores sólidos, se eligieron como estímulo que desencadena la liberación de colagenasa. El anclaje de estas nanocápsulas de colagenasa en la superficie de un nanotransportador permitió su profunda penetración dentro de un tumor sólido porque, la colagenasa liberada en la zona degrada la tumoral MEC facilitando la penetración de partículas en el tejido. Así, una mayor penetración en el tumor sólido asegura un tratamiento eficaz.

Las nanocápsulas de colagenasa fueron sintetizadas mediante polimerización de radicales libres en medio acuoso utilizando tres monómeros diferentes: acrilamida, como monómero estructural neutro, clorhidrato de 2-aminoetilmetacrilato, como monómero con carga positiva y etilenglicol dimetacrilato, como agente entrecruzante sensible al pH. El monómero positivo desempeña una doble función en este proceso; por un lado,

favorece el proceso de encapsulación mediante interacciones electrostáticas con la superficie cargada negativamente de la colagenasa y, por otro lado, proporciona puntos de anclaje para la posterior fijación de la cápsula en la superficie de la partícula. Una vez sintetizadas estas nanocápsulas de colagenasa, se anclaron en un nanotransportador modelo (nanopartículas mesoporosas de sílice) y se examinó su eficacia para lograr una distribución homogénea de los nanotransportadores dentro de los tejidos tumorales empleando un modelo de colágeno 3D con las células tumorales embebidas. Este tipo de modelos proporcionan un entorno realista con consistencia similar a los tejidos tumorales humanos reales. Nanosistemas, decorados o no con nanocápsulas de colagenasa, fueron colocados en la parte superior de estos modelos 3D mostrando que sólo las nanopartículas que tienen nanocápsulas de colagenasa en su superficie fueron capaces de penetrar homogéneamente en todo el tejido, mientras que las partículas desnudas fueron retenidas en la parte superior.

Una vez comprobada la eficacia de la decoración de partículas con nanocápsulas de colagenasa para conseguir una mayor penetración en el tejido, estas cápsulas se fijaron en la superficie de un nanotransportador capaz de presentar dos características importantes: reconocer las células tumorales y retener los compuestos citotóxicos hasta que el sistema alcance el espacio interior de estas células malignas. El sistema elegido para este objetivo fue una protocélula, que es un nanodispositivo compuesto por un núcleo de sílice mesoporosa recubierto con una bicapa lipídica. El núcleo mesoporoso proporciona una alta capacidad de carga del fármaco debido a su elevada porosidad, mientras que la bicapa lipídica ofrece estabilidad coloidal y evita la liberación prematura de la carga. La bicapa lipídica fue diseñada para presentar dos grupos funcionales diferentes (ácidos carboxílicos y aminos) en los que un anticuerpo (anti-VEGFR) capaz

de reconocer las células tumorales (en este caso, células de cáncer de pulmón A549) y nanocápsulas de colagenasa fueron anclados respectivamente.

La efectividad de este sistema fue evaluada en un modelo de tejido tumoral tridimensional consistente en una monocapa de células tumorales recubierta con un gel de colágeno de 200 μm de espesor que también contenía células tumorales embebidas. En la parte superior de estos geles se colocaron protocélulas marcadas con fluorescencia, decoradas o no con nanocápsulas de colagenasa, y se evaluó la capacidad de alcanzar la monocapa celular interna mediante microscopía confocal de fluorescencia. Sólo el sistema que transportaba las nanocápsulas de colagenasa pudo alcanzar esta profunda monocapa, lo que demostró la importancia de transportar estas enzimas proteolíticas. Además, la presencia del anticuerpo permitió una mayor internalización de las protocélulas dentro de las células tumorales. Finalmente, se probó la capacidad de destruir las células tumorales ubicadas en zonas profundas del tejido utilizando estos sistemas cargados con un potente fármaco citotóxico (topotecán). Los resultados mostraron nuevamente que sólo el sistema que transportaba nanocápsulas de colagenasa era capaz de destruir las células tumorales ubicadas en la zona interna del modelo 3D. Este sofisticado sistema fue capaz de proporcionar tres importantes propiedades: mayor penetración dentro de los tejidos tumorales, internalización selectiva dentro de las células tumorales y destrucción selectiva de estas células malignas. Este diseño podría ser fácilmente extrapolable a otras nanomedicinas y mejoraría su eficacia en el tratamiento contra el cáncer.

Otro objetivo que se ha explorado en esta tesis ha sido el desarrollo de nanosistemas capaces de presentar una doble y secuencial capacidad de vectorización a las células tumorales y a importantes orgánulos en su interior. La razón es que la liberación de fármacos antitumorales cerca de ciertos orgánulos dentro de las células (mitocondrias o núcleos, entre otros) supone, en muchos casos, un mayor efecto terapéutico. Como prueba

de concepto, los nanotransportadores fueron sintetizados con dos agentes de vectorización : el ácido fólico para proporcionar selectividad por las células tumorales de próstata y un derivado de la trifenilfosfina, que presenta alta afinidad por la membrana mitocondrial. Estos agentes se distribuyeron en hemisferios opuestos del nanocarrier para evitar interacciones no deseadas entre ellos. Las nanopartículas de doble vectorización lograron un efecto terapéutico significativamente mayor en células tumorales que los sistemas monofuncionales, validando la premisa de este trabajo y suponiendo un importante avance en el diseño de nanosistemas.

Finalmente, se evaluó el uso de nanocápsulas de colagenasa para el tratamiento de enfermedades diferentes al cáncer, en este caso lesiones fibróticas. La fibrosis es una lesión común en varias enfermedades que consiste en la formación de tejidos fibróticos conectivos en órganos o tejidos. Este tejido fibrótico se caracteriza por una acumulación excesiva de colágeno. Un tratamiento clínico normal de estas lesiones consiste en la administración de colagenasa. Sin embargo, la naturaleza lábil de esta enzima hace que esta pierda totalmente su actividad después de sólo un día. Esto hace que sea habitual la necesidad de repetir la administración de la enzima, suponiendo una molestia en el paciente. Además, la administración continuada de la misma genera en muchos casos la aparición de efectos secundarios debido a una sobredosis. Las nanocápsulas de colagenasa descritas anteriormente para aumentar la penetración de las nanomedicinas en los tumores sólidos fueron diseñadas para desensamblarse en condiciones de acidez leve, pero también son hidrolizadas a pH fisiológico en un día. Por tanto, su uso para el tratamiento de lesiones fibróticas no proporcionaría una ventaja significativa en comparación con el tratamiento convencional. Por lo tanto, se abordó el diseño de nanocápsulas de colagenasa capaces de proporcionar una liberación sostenida y prolongada de colagenasa durante largos períodos de tiempo. Como primera

aproximación, la cantidad de del agente entrecruzante degradable se redujo para extender el tiempo de desensamblaje de la cápsula. Sin embargo, esta estrategia sólo mejoró el tiempo de liberación durante 2-3 días, lo que aún no era suficiente. Dado que la presencia del agente entrecruzante es estrictamente necesaria para la formación de la nanocápsula polimérica, seguir reduciendo su cantidad no se consideró un enfoque válido. En cambio, se estudió la adición de un segundo agente entrecruzante en la composición de la cápsula, en este caso un agente no degradable. Esta estrategia generó nanocápsulas capaces de liberar colagenasa de forma sostenida durante más de 7 días, cuando la proporción de agente entrecruzante degradable versus no degradable se fijó en 50-50%, lo que se consideró suficiente para su evaluación en el tratamiento de lesiones fibróticas. Debido al prometedor resultado alcanzado, estas nanocápsulas de colagenasa fueron probadas en un modelo de ratón fibrótico y comparadas con el tratamiento convencional, la administración de colagenasa libre. Las nanocápsulas de colagenasa lograron una reducción significativamente mayor del colágeno en el tejido enfermo en comparación con las enzimas libres, proporcionando una alternativa prometedora para el tratamiento de patologías fibróticas.

En resumen, las estrategias desarrolladas durante esta tesis doctoral han tratado de abordar importantes barreras presentes en el tratamiento de enfermedades complejas y los resultados obtenidos han mostrado una alta potencialidad que podría ser incorporada en el arsenal de la nanomedicina. Los sistemas desarrollados se recogen en la **Figura 1**.

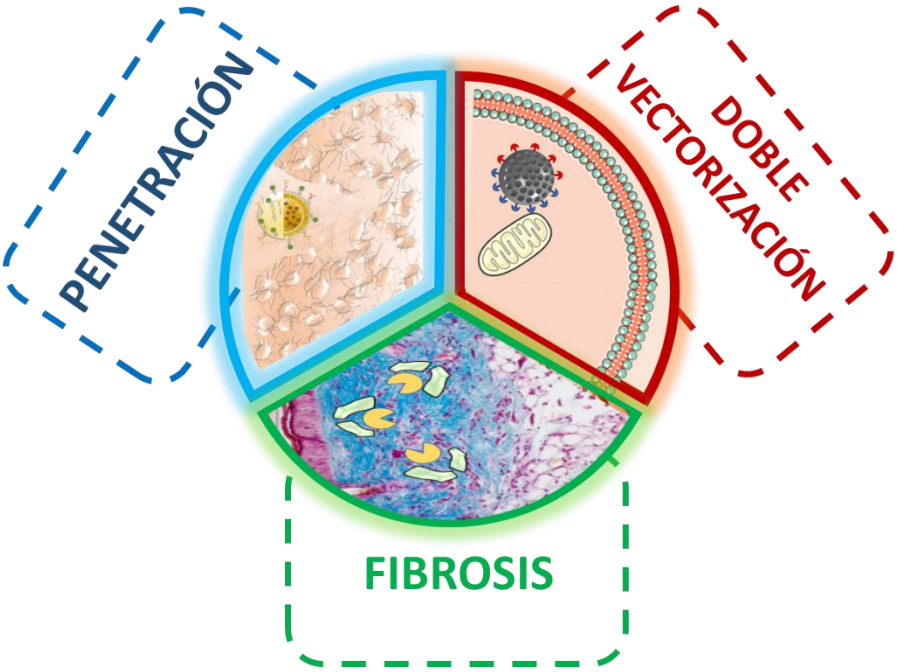

Figura 1. *Resumen de sistemas desarrollados en la Tesis Doctoral.*

Chapter I

Introduction

I.I. Nanotechnology and Nanomedicine.

The prefix "nano" comes from the Greek word νάνος which means dwarf. One nanometer (nm) is equivalent to one-billionth of meter or what is the same, 6 carbon atoms or 10 water molecules. Any atom is smaller than 1nm while some molecules are roughly of that size. For the sake of scale comparisons, the size of red blood cells is approximately 7000nm, and the diameter of human hair is 80000nm.[1]

The "nano world" has some important historic milestones. Around the year 1900, both Max Planck and Albert Einstein proposed theoretical models on the existence of tiny particles that follow their own laws. Unfortunately, the existent technology in those years was not sufficiently developed to find supporting evidences.[2] The invention of the light ultramicroscope in 1902 allowed the observation of structures smaller than 4nm in ruby glasses. A few years later, two inventions opened the way for the observation of a completely unexplored world, the nano world. These developments were the transmission electron microscopy (TEM) in 1931 developed by Max Knoll and Ernst Ruska[3] and the field ion microscope (FIM) invented by Erwin Müller in 1936.[4] These important progresses allowed the development of what today is called nanotechnology. The first mention of the aim to create and manipulate nanometer sized, and probably the origin of this discipline, is attributed to the historical lecture "There´s plenty of room at the bottom" given by Richard Feynman at an American Physical Society meeting at Caltech on December 29th, 1959.[5] Feynman explored the idea of manipulating matter at the atomic scale and described the huge possibilities hidden in the tiny world, both in storage information and also, in the production of nano-sized factories able to build therapeutic compounds or nanorobots capable of carrying out precise surgery inside the human body, to name just a few examples. Nevertheless, it was not until 1974 when Norio Taniguchi introduced for the first time the term "nanotechnology" at the international conference on industrial production in Tokyo. He used this name to refer to the ability to engineer materials precisely at the nanometer scale. The first steps in this direction came from the electronics industry which had the goal to produce nanometric electronic devices on silicon chips.[6] The ideas introduced by Feynman were subsequently developed by E. Drexler in his book "Vehicles of creation: the arrival of the nanotechnology era" that was published in 1986.[7] Other important events which paved the way for the birth of nanotechnology were the first nanotechnological program of the National Scientific Fund

which started to operate in USA in 1991, or the creation of institutions focused on their development such as the National Nanotechnology Initiative (NNI) established in the USA in 2000 by President Clinton. Nowadays, scientists from all around the world continue discovering unique and versatile properties of everyday materials at the nanoscale.[6]

Today, nanotechnology can be defined in a more general way as the science and engineering dealing with the design, production and application of systems at nanometric level. This multidisciplinary field is providing the ability to understand the systems at low scale and create a "nano-universe" of objects with exotic properties that cannot be obtained in the macroscopic world. Nanotechnology covers a vast and diverse number of areas in engineering, biology, medicine, physics and chemistry, among others. Along this field, a potent and emergent discipline is nanomedicine. Nanomedicine is referred to the use of nanotechnology for diagnostic and therapeutic applications or in the combination of both, thera-diagnostic.[8,9] This use has been explored to treat a wide type of pathologies such as infection,[10] degenerative diseases,[11,12] autoimmune pathologies,[13,14] cardiovascular disorders[15] and cancer.[16,17]

One important application of nanomedicine is the synthesis of nanosensors such as, for example, nanocrystals able to monitor biological signals, such as proteins released in response to inflammatory and cardiac events.[18] Nanotechnology has developed strategies for bone regeneration[19,20] and the avoidance of bacterial infection in implants.[21] Finally, it is necessary to highlight the use of nanomedicine for drugs delivery.[22,23]

Among all the outcome of nanomedicine, the "keystone" are the nanoparticles.[24] Nanoparticles are colloidal particles in a range of 10-100nm.[6] Applications of nanoparticles are specially promising in a wide number of applications due to their important and unique features such as high surface-mass ratio, unique optical and/or magnetic properties, and high catalytic power due to the high available surface of these systems. These interesting properties can be easily tuned by modifications in their surface and size and also by changes in their chemical composition. There are several types of nanoparticles studied for nanomedicine which can be broadly classified in function of their chemical nature as organic and inorganic nanoparticles, although they can also be designed in the form of hybrids combining the properties of both types (**Figure 1**). [22,25,26]

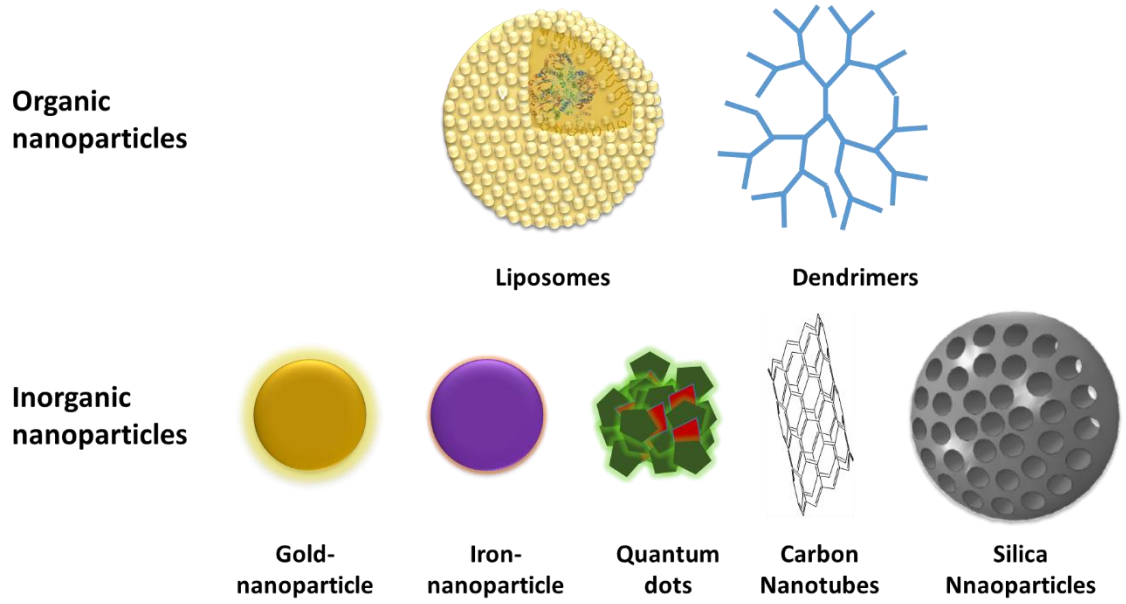

Figure 1. *Schematic representation of some of the most important types of nanoparticles used in nanomedicine.*

Organic nanoparticles are composed by organic molecules. These biodegradable and biocompatible materials are characterized by their high flexibility and versatility. [27]Among this type of particles, liposomes constitute one of the most important systems. Liposomes are vesicles with an aqueous core surrounded by one or more lipid bilayers.[28,29] They have been widely studied in nanomedicine due to their cell-like structure, high flexibility and excellent colloidal stability in biological fluids.[30,31,32] Liposomes combine a hydrophilic inner compartment and a lipophilic region formed by hydrophobic chains of phospholipids that compose the membrane vesicle. This fact allows to load them with hydrophilic compounds, which remain encapsulated in the aqueous core, and hydrophobic drugs, that are introduced in the phospholipid membrane structure.[33] All these properties render the liposomes extraordinary nanodevices for biomedical applications, so they have been already accepted by regulatory agencies for clinical use.[28] Liposomes must be coated with hydrophilic polymers, as polyethyleneglicol (PEG) in order to avoid their rapid clearance by mononuclear phagocyte system (MPS). Unfortunately, PEGylation induces a decrease in the melting temperature of the liposomes, which entails their destabilization.[34] Moreover, liposomes exhibit low mechanical stability, hence many of them break up upon administration due to the shear force exerted when are injected.[35] Another system considerating are Poly(lactic-co-glycolic acid) (PLGA) nanoparticles.[36] PLGA is a biodegradable polymer which produces harmless compounds (lactic and glycolic acid) during its hydrolysis.

PLGA-nanoparticles have been widely used in biomedical applications such as vaccine delivery system, targeting of the immune system, and cancer diagnosis and therapy, due to their excellent biocompatibility in combination with their higher robustness in comparison with liposomes. Polymeric micelles are an other type of organic nanosystems which are characterized by showing a core-shell structure. They are constituted by a di-block structure copolymer with a hydrophilic part (shell) and a hydrophobic one (core) that self-assembles in aqueous medium.[37] Polymeric micelles have been employed to carry insoluble drugs, photosensitizers for photodynamic therapy[38] and imaging contrast agents.[39] These micelles combines the high flexibility and dual cargo capacity of liposomes with the high mechanical stability of solid polymeric nanoparticles. Dendritic nanoparticles are macromolecules formed by sequences of polymeric branches regularly extended from a central core molecule.[40] Their surface exhibits a high number of reactive groups which can be used for multiple tasks such as the covalent or electrostatic grafting of drugs, imaging or targeting agents, among others. On contrary, the core of these macromolecules is strongly protected by dendritic architecture. This class of materials have been employed as carriers of small anticancer drugs or antimicrobial agents, as well as, tissue-repair scaffolds. Moreover, dendrimers have been explored as imaging agents by their conjugation with paramagnetic metal chelates.[41]

The other vast category of nanoparticles is the composed by inorganic materials. Inorganic nanoparticles have common properties such as sturdiness and high chemical stability. A subtype of inorganic nanoparticles are the based on metals such as gold, iron nanoparticles and quantum dots. Gold nanoparticles are generally harmless, bioinert and exhibit unique optical properties. They have distinctive extinction bands in a wide spectrum region. The optical properties are due to the plasmon resonance, which is associated to collective oscillation of conduction electrons in their surface. These characteristics have led to their use for optical diagnosis and photothermic therapy.[42,43]Iron oxide nanoparticles have been used as Magnetic Resonance Image (MRI) contrasts agents. This effect present especial importance for the visualization of bioevents such as gene expression and metastases at cellular and subcellular levels. Another use of iron oxide nanoparticles is their application as magnetic hyperthermia agents due to their capacity to induce an increment local of temperature when are exposed to alternating magnetic fields.[44,45,46] Quantum dots are small semiconductor nanocrystals aggregations in the range of 1-10nm. Their fluorescence emission can be tuned in a wide

wavelength range 400-2000nm. Moreover, they absorb energy and return it with other wavelength with high quantic performance. This class of materials has been used as tags for DNA hybridation detection, immunoassays and binding assays based on fluorescent resonant energy transfer (FRET).[47,48,49,50,51,52] Carbon based nanosystems show high absorption in the near infrared and convert this radiation in heat, and for this reason, they have been employed in photo thermal therapy. Furthermore, carbon nanotubes and graphene oxide nanoparticles have excellent electrical conductivity[53] so, carbon based nanocomposites have been proposed as supercapacitators. It has also been reported that carbon-based nanoparticles damage the bacteria membrane by oxidative stress, leading to their death.[54] Other uses of carbon based nanosystems have been the intracellular delivery of proteins and drugs and the formation of tissue repair scaffolds.[55,56]

Among the different types of inorganic materials, porous systems have been widely applied for drug delivery applications, as consequence of their extremely high loading capacity. The porous materials are classified in function of the pore size in microporous, with porous low then 2nm, mesoporous when the pore are in the range of 2-50nm and macroporous, up to 50nm.[83] Within this category, porous silica nanomaterials, specially with ordered mesoporous structure, are one of the most representative. They are characterized by their easy and fast preparation, they are robust, non-toxic and non-immunogenic materials and can be easily functionalized.[57] Ordered mesoporous silica based materials have been used for repairing bone defects[58,59,60,61,62,63,64,65] using two approaches, by loading with bisphosphonates or by its combination with bioactive glass.[66] Moreover, these materials have been widely explored for treat bacterial infections[67,20,68,69,70,71,72] In the form of nanoparticles, Mesoporous silica nanoparticles (MSNs) have been employed for multiple applications such as nanomotors,[73] diagnostic[74] or drug delivery.[75,75,76,77] Additionally, they can be functionalized in order to provide them with stealth properties in order to avoid their capture by MPS or targeting skills.[78,79,80,81,82] A more detailed description about the features that makes MSN as one of the most promising material for drug delivery applications will be discussed in the next section.

Mesoporous silica nanoparticles

Mesoporous silica nanoparticles were synthesized by the first time by Kuroda *et al* in 1990[84]and since then, this material has received huge attention in multiple fields such as catalysis, filter of contaminant agents and delivery of drugs.[84,85,86,87] Mesoporous silica is characterized by excellent physico-chemical stability, easy functionalization, biocompatibility and biodegradability.[88,89,90,91] Moreover, these materials exhibit precise pore distribution, high pore volume $1 cm^3/g$ and high superficial area of around 1000 $m^2 \cdot g^{-1}$ that allow the delivery of high amounts of cargo.[57,92] These properties confer them high potential as drug delivery systems and its application in this field has led to an exponential growth, since the pioneer work of Vallet-Regí *et al*. in which a drug (ibuprofen) was loaded by the first time within the pore matrix.[86,93]

Synthesis of mesoporous silica nanoparticles

The preparation method typically employed is based on the method described by Stöber *et al.* in 1968, for the synthesis of solid silica nanoparticles.[94] This method was based in the hydrolysis of tetraalkylsilicates in ethanoic medium, using ammonia as catalyst, that yields the formation of silica nucleous followed by a growth step.[94] The synthesis of mesoporous silica nanoparticles involves the use of surfactants, as porosity director agent and, a silica precursor that forms the silica matrix. This sol-gel method consists on a hydrolysis process followed by the polycondensation of silanol groups around the surfactant micelles. Typically, surfactants are amphiphilic polymers able to self-assemble in certain conformations that result in an ordered structured.[95] The pore size is determined by the length of the hydrophobic chain of the surfactant, as well as, by the addition of expander agents such as cyclohexane or 1,3,5-trimethylbenzene (**Figure 2**).[96] The reaction conditions can be both basic and acidic.[95] Once the nanoparticles are formed, the surfactant is removed from the pores by calcination or an ionic exchange process[97] in order to get the pore free for further cargo loading.[93]

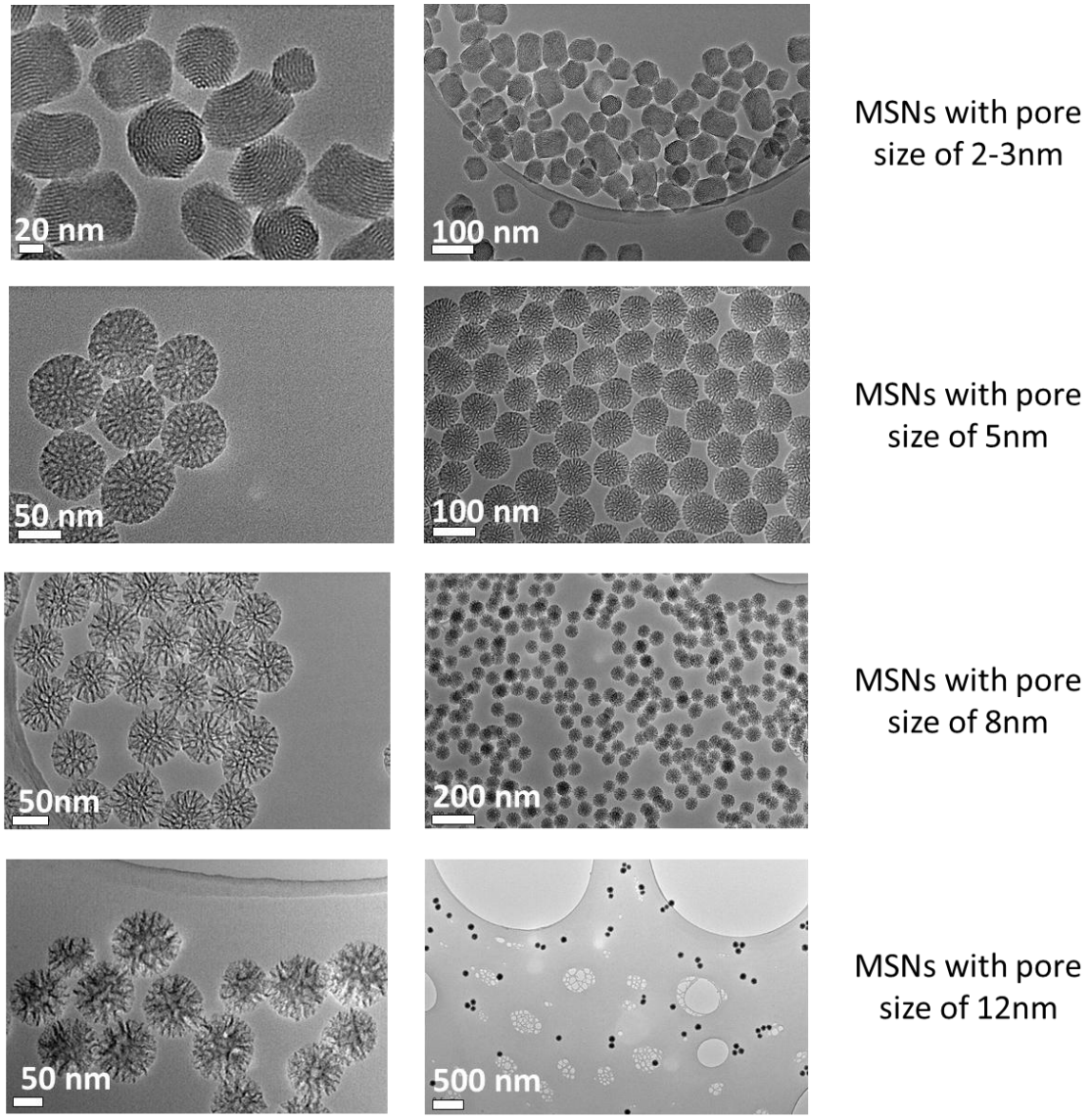

Figure 2. *Mesoporous silica nanoparticles with different pore size.*

Through the modification of the synthetic conditions, it is possible to obtain different types of mesoporous silica nanoparticles such as SBA-15 and MCM41, which exhibit different pore architecture. SBA-15 possesses a hexagonal array of mesoporous of 6nm of diameter, which is much larger than 2-3nm pores of MCM-41 structure.[67] MCM-41 has been chosen as core material in this thesis because this systems presents an unique pore distribution, in which the pores are parallel and do not present any interconnections between them, which allow a controlled release of the housed drug.[98,99,100] Specifically, MSN used along this thesis have been prepared employing hexadecyltrimethylammonium (CTAB) as surfactant and tetraethylortosilicate (TEOS) as silica precursor in basic medium.[90] Once the nanoparticles were formed, the surfactant was removed by ionic exchange with ammonium nitrate. The reason to choose this

method instead of calcination is that its mild conditions avoids the nanoparticles aggregation during the surfactant elimination and bypass the formation of toxic product, which are the main drawbacks of calcination.[98] Following this method, monodisperse MSNs with approximately 100nm of diameter and honeycomb ordered pore structure with unconnected pores with diameter of 2-3nm are obtained (**Figure 3**).[101]

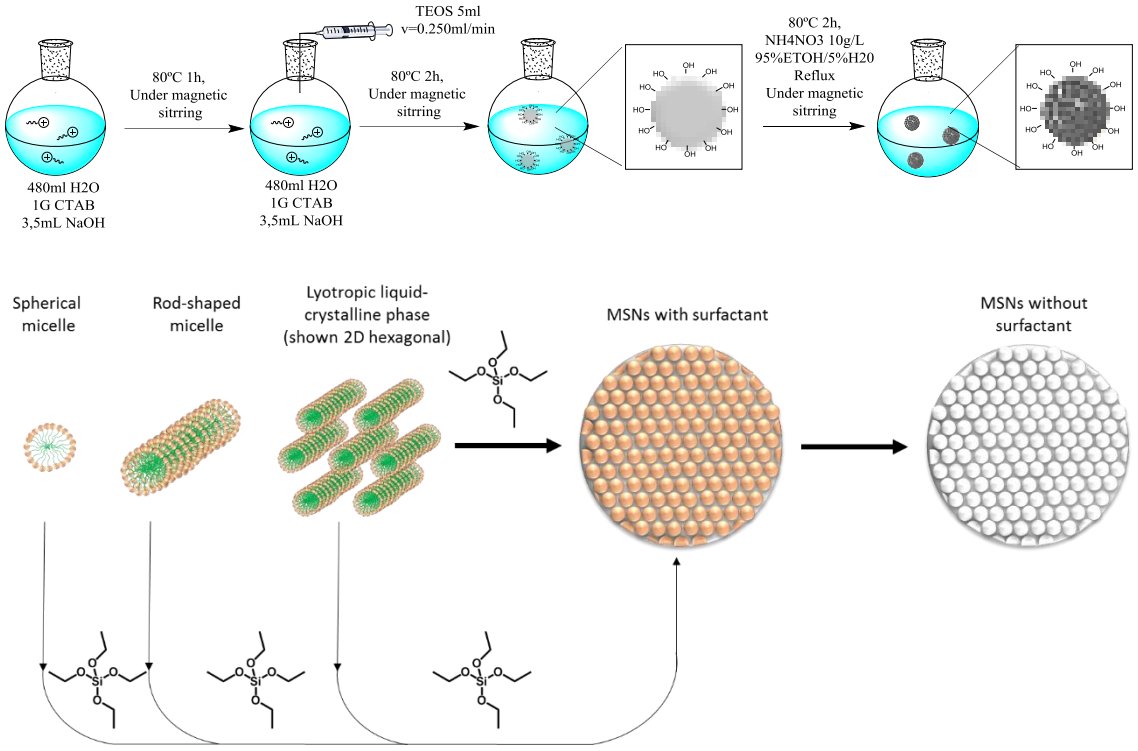

Figure 3. *Synthesis of MCM41 mesoporous silica nanoparticles.*

Characterization of mesoporous silica nanoparticles

The correct synthesis and functionalization of MSNs is evaluated by several characterization techniques. Some of the most important ones are Fourier Transform Infrared Spectroscopy (FTIR), X Ray Diffraction XRD, nitrogen adsorption/desorption and electronic microscopy among others. Mesoporous silica nanoparticles are characterized by FTIR showing the silica vibrational bands at 465cm^{-1} (Si-O bending), 800cm^{-1} (Si-o-Si bending), 942cm^{-1} (Si-OH bending) and at 1100cm^{-1} (Si-O stretching) (**Figure 4**). This technique allows to evaluate the correct surfactant removal, because the alkyl chains of the surfactant exhibit bands in 1400-1700cm^{-1} and 2800-300cm^{-1} and therefore, their disappearance confirms the complete elimination of the surfactant. Additionally, this technique has also been employed for the characterization of the

organic functionalization of the MSN surface, which can be followed by apparence of the new characteristic bands.[102,103]

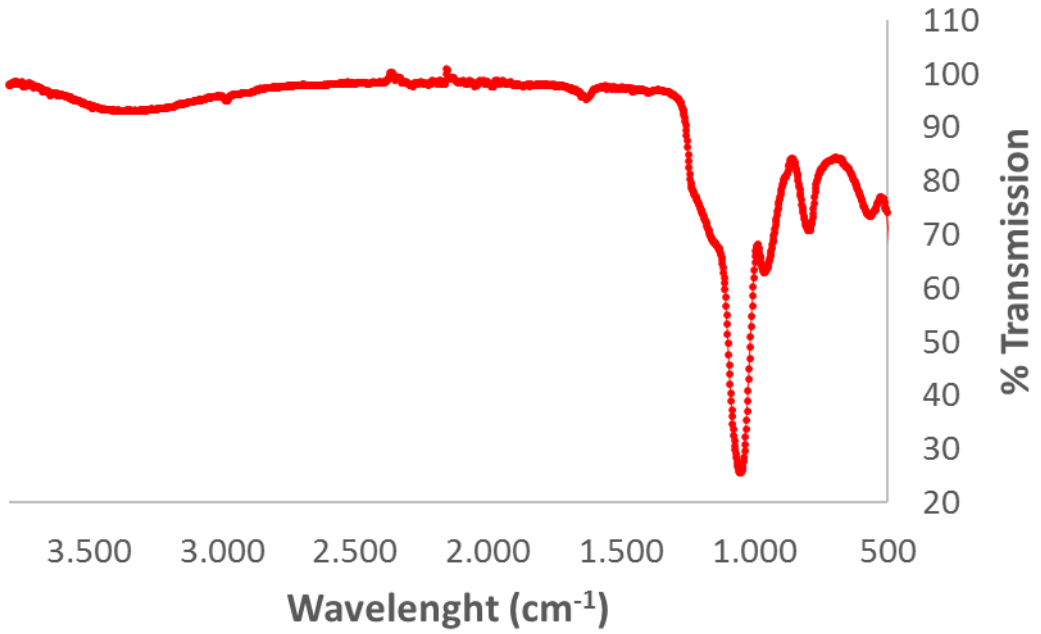

Figure 4. *FTIR spectrum of MSNs*

The nitrogen adsorption allows to calculate the diameter, pore volume and surface area of MSN (**Figure 5 y 6**).[86]

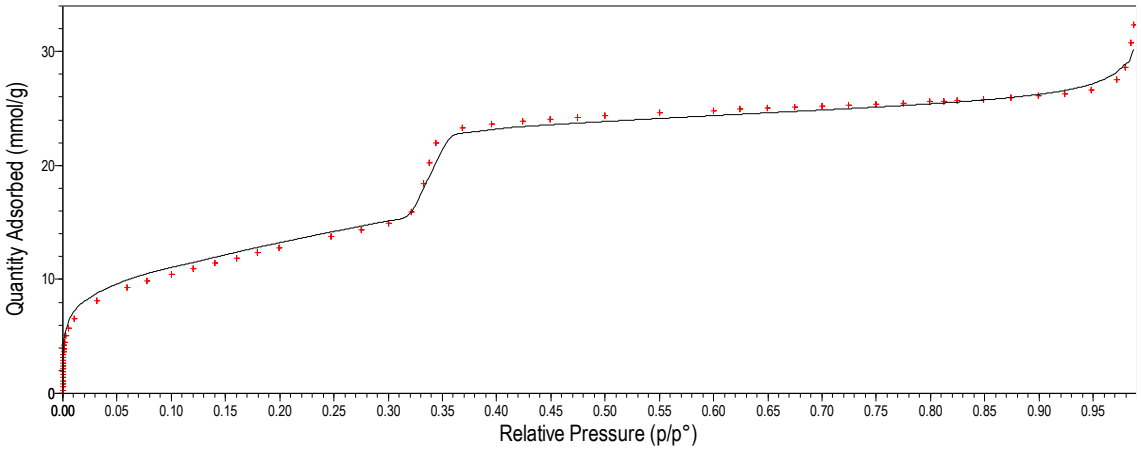

Figure 5. *Nitrogen adsorption isotherm*

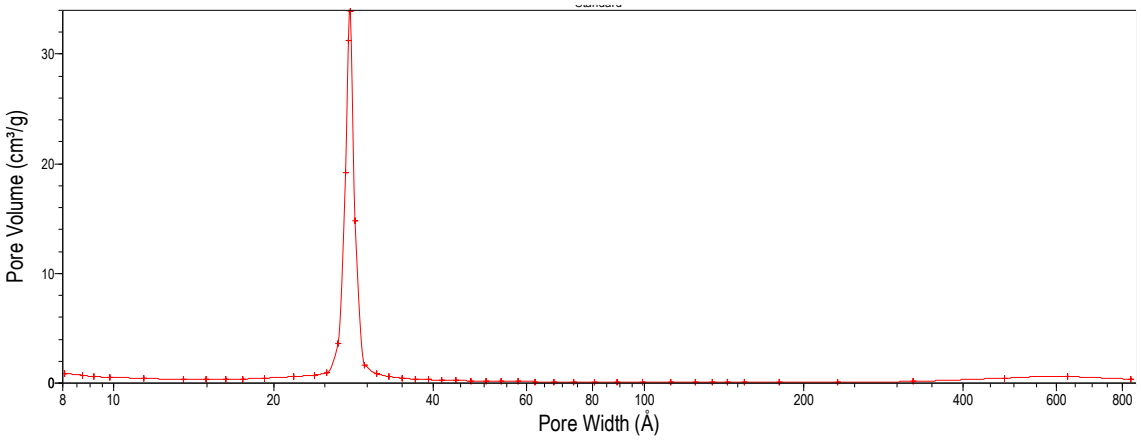

Figure 6. *diameter pore distribution by nitrogen adsorption.*

The pore order is evaluated by XRD diagram a low angle. The characteristic diagram of MCM-41 has four maxims at 2.2, 3.8, 4.4, and 5.8° which correspond with 100, 110, 200, 210 diffraction planes (**Figure 7**).[104]

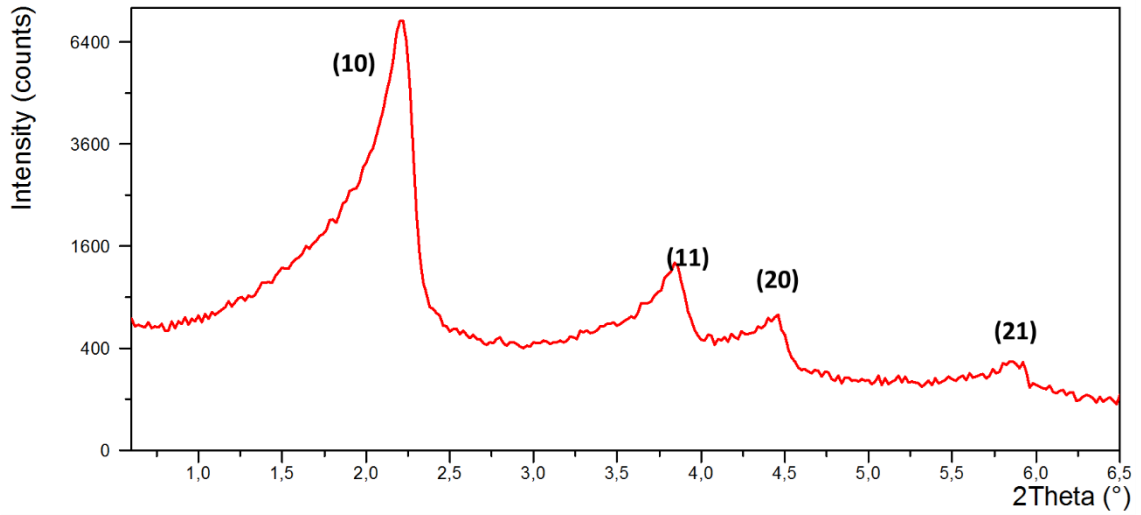

Figure 7. *XRD diagram a low angle of MSNs.*

The superficial charge of nanoparticles is estimated by Z-potential in function of their electrophoretic mobility. The hydrodynamic ratio is determined by Dynamic Light Scattering DLS and resulted in a range of 100-200nm (**Figure 8**).

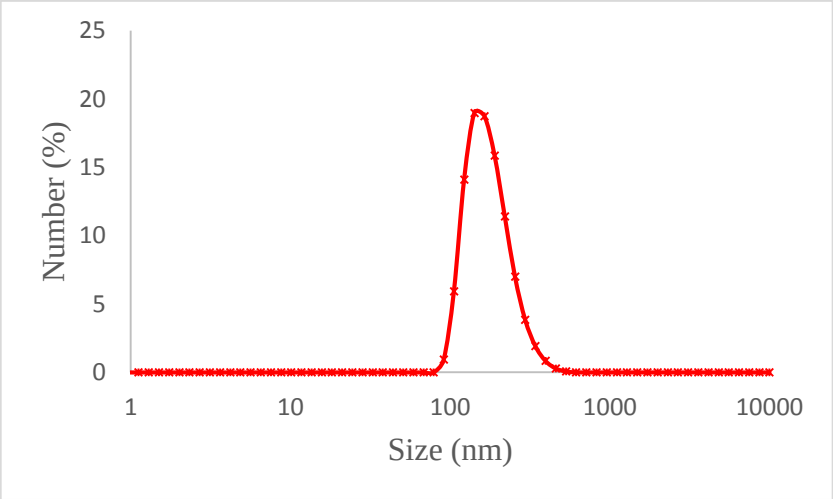

Figure 8. *Hydrodinamic ratio of MSNs by Dynamic Light Scattering.*

Finally, the morphology and size and porosity can be confirmed by transmission and scanning electronic microscopy TEM and SEM, respectively. The order of the porosity can be additionally confirmed by Fourier transform pattern of micrographs in TEM at high magnification (**Figure 9**).

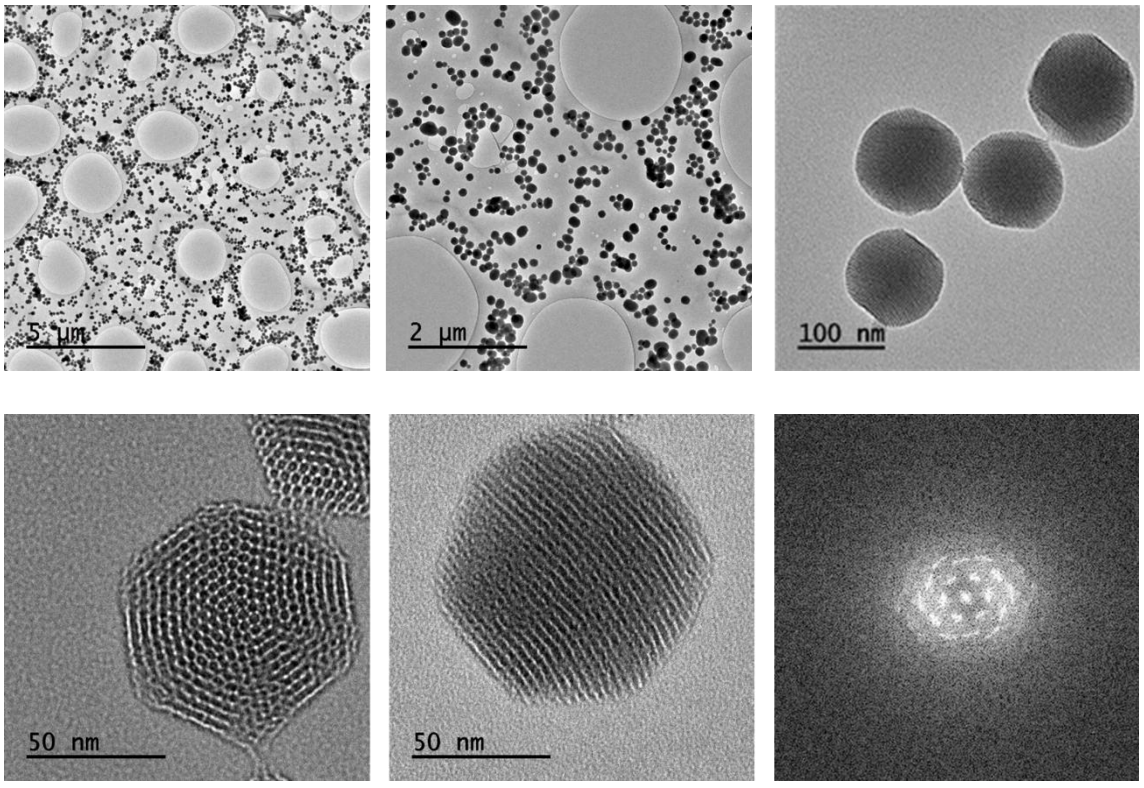

Figure 9. *TEM micrographs of MSNs.*

I.II. Cancer. Biology principles and conventional treatments.

Cancer is one of the most important causes of morbidity worldwide and is the second leading cause of death in the World. According to the World Health Organization (WHO),[105] 14 million of new cases were found in 2012 and produced 8.8 million of deaths in 2015. Cancer is responsible of 1 out of every 6 deaths. The economic impact of cancer in 2010 was estimated in US$ 1.16 trillion. For this reason, cancer is recognized as a common disease which has disastrous impact in the society.

Cancer can not be considered as a single disease but is a set of pathologies caused by deviant or malignant cells. The unstoppable growth of these cells form functional structures which proliferate anarchically and chronically invading the surrounding and distant tissues.[106] Despite its high complexity and variability, there are common set of functional biological capabilities in these class of diseases. These different biological abilities or hallmarks are acquired during the tumors growth, supporting their development and determining its structure and behavior.[107,108,109]

One important hallmark of cancer is its sustaining proliferative signals.[110] Healthy cells proliferate in a controlled mode when they receive instructions from the surrounding cells and by the paracrine system in form of growth factors, among others. In contrast, malignant cells often present mutational alterations of genes that act as active drivers of cell proliferation. These mutant genes, known as oncogenes, are overexpressed in the tumoral cells in comparison to their healthy cells counterparts and are responsible for their uncontrolled proliferation. Cancer cells can sustain the proliferative signals in multiple pathways such as the overproduction of growth factor receptors or transmitting growth-stimulatory signals to the surrounding healthy cells in such a way that these cells supply the growth factors.[111,112,113]

Tumors are characterized by being able to evade growth suppressors. Healthy cells enter in division phase only if they have all the resources and energy available to sustain the replication process, and their physiological state is appropriate. The control of the cell division process is orchestrated by proteins termed tumor suppressor genes.[114,115] Thus, these genes detect and repair cell genome damage, among other alterations, and ensure the correct advance of the cell. However, cancer cells have altered these genes in such a way that they cannot stop, in an effective manner, the cell-cycle replicative machinery when detect cellular alarms.[116] In addition, healthy cells have other mechanism to control

the division, as the inhibition by contact. This mechanism induces that cells stops the partition when they come into contact with other cells. Unfortunately, this mechanism is ineffective in cancer cells, which are continuously growing and dividing, regardless the signals or contacts sent by the surrounding cells.[117,118,119]

Other important hallmark of cancer is the enabling replicative immortality. Healthy cells do not have the ability to divide indefinitely. They have a limited number of successive cell growth-and-division cycles (Hayflick limit) before to enter in senescence, which consist in a cell state in which the cell is viable but it does not proliferate or in crisis, with involves cell death[120,121]. It has been found that tumoral cells are able to emerge from crisis state and exhibit unlimited replication potential. This ability is called immortalization, and allows a continuous expansion of malignant cells population evading the death. [122,123]

As consequence of the uncontrolled growth and division of cancer cells, they lead to high demand of oxygen and nutrients that yield in abnormally fast and continuous activated angiogenesis process induction, which is another hallmark of cancer.[124,125]

Other characteristic of tumor is that cancer cells use in different way the energy sources than healthy cells. This concept was introduced by Otto Warburg in 1992.[126] Warburg *et al.* found that cancer cells cultures present an enhanced uptake of glucose which is metabolized via glycolysis. This pathway to generate ATP was used by tumoral cells even when the oxygen is available. The high glycolytic ratio provides of several advantages to the proliferation of tumor cells. This effect allows the cells to use glucose for obtaining building blocks needed for biosynthetic pathways.[127,128,129,130,131]

One of the most well-known cancer hallmarks is the capacity of the cancer cells to develop resistance to death. Cells enter in programmed cell death in response to several abnormal physiologic conditions. The predominant pathway of programmed cell death is the apoptosis that consist in a genetically programmed fragmentation that triggers the cell mechanism of death. Tumoral cells suffer stress during the own progression of the disease or as a consequence of the antitumoral therapy. This stress should lead to programmed death of the malignant cell. Unfortunately, many tumors have attenuated apoptosis in such a way that cancer cells develop resistance to cell death.[132,133]

Other property to cancer cells is its ability to invade local surrounding tissues and distant metastasis. Cancer cells can be intravasated into blood vessels allowing the cell

dissemination to nearby and distant sites. For example, malignant cells can enter into lymphatic vessels[134] and then, they could reach the lymph nodes establishing a bridgehead required for the dissemination to distant tissues and metastasis progression.[135,136]

Moreover, cancer cells are able to avoid the immune destruction. One reason is the immune self-tolerance. Cancer cells often expressed antigens likely shared with the normal cells of origin in such a way that they are ignored by immune system. Other reason, is the capacity of cancer cells to develop strategies to avoid the detection by the immune system or their ability to hinder themselves from immunological killing. As example of this cancer skills, it has been demonstrated that several aggressive cancer cells express a transmembrane protein, CD47, which bind with macrophages reducing their capacity to kill them.[137,138]

These physiological changes provide to cancer cells with new acquireed abilities during tumor progression which protect them of the immune defensive mechanism. The process of the acquisition of these properties by the cancer cells can be compared with the Darwinian evolution and suppose a strong limitation to cancer eradication. Moreover, as it has been described above, tumors are not a homogeneous distribution of tumoral cells but in fact, they are really complex tissues with a myriad of different cell populations inside and therefore, they can even be pictured as functional organ.[139]

Nowadays, there are three common approximations to treat these pathologies: surgery, radiotherapy and chemotherapy.[140,141,142] Surgery is often employed when a tumor is in its early state, and it allows the physical removal of the tumor. When it is not possible because the tumor is deeply extended in the organ or its elimination by surgery could compromise the patient life, cancer is usually treated with radiotherapy and chemotherapy. Radiotherapy treatments are based in the use of high-energetic radiations in order to hamper the tumor growth by damaging the DNA of the diseased cells. Chemotherapy is based in the intravenously or oral administration of highly toxic drugs. These antitumoral drugs are designed to affect, in more grade, the dividing cells, which are usually the tumoral ones. Unfortunately, there are many different types of cells within the human body which are also in proliferative state such as hair follicles, cells of the digestive system or reproductive cells and therefore, these drugs are not selective. Both approaches, radiotherapy and chemotherapy cause several adverse effects in the patients due to this lack of selectivity between healthy and cancer cells. This fact leads to a higher systemic exposition to toxic agents and therefore, dose-limiting toxicity.[143] In order to

reduce the non-specific distribution of drugs throughout the body, many efforts have been done in the field of nanomedicine through the development of novel ways for the drug administration. In particular, nanoparticles have been widely studied as nanocarriers of antitumoral drugs. [25]

I.III. Nanoparticles in cancer

The use of nanoparticles as antitumoral drug carriers is based on their capacity to be selectively accumulated in the tumoral tissue. This tendency was discovered in 1986 by Maeda and Matsummura and it received the name *Enhanced Permeability and Retention* (EPR) effect (**Figure 10**).[144]

In contrast to healthy cells, tumoral cells are characterized by fast and uncontrolled growth that lead to an abnormal and accelerated angiogenesis processes in order to sustain their fast growing state.[125] As resulted of this fact, tumor-associated vasculature is usually aberrant both morphologically and functionally. Tumor blood vessels are irregular, tortuous, dilated and their endothelial walls present fenestrations of hundreds of nanometers.[145] When the nanoparticles are injected in the blood stream, they can not leave the blood vessels in healthy tissues because the interendothelial junctions are really tight but, when they reach the tumoral tissue, they can pass through these pores being accumulated there.[146]

On other hand, the uncontrolled proliferation of tumoral cells in the confined space of the tumoral tissue, in combination with the hyperproduction of interstitial matrix components give rise to the lymphatic vessels compression resulting in a deficient drainage system in the zone.[147,148] Thus, the nanoparticles are not only extravasated in the tumor but they are also accumulated there during long time, because they cannot be efficiently removed by the lack of lymphatic vessels.

This phenomenon is considered the arch-stone of the use of nanoparticles in oncology because they are passively accumulated in the tumoral zone simply by the nanometric nature of these systems and thus, this effect is also known as passive targeting..[146]

However, a tumoral mass is formed by heterogeneous composition that include both healthy and tumoral cells.[139] Therefore, once the nanoparticle have been extravasated and accumulated in the tumoral tissue, they should be able to recognize the tumoral cells in order to achieve a selective treatment. On one hand, the principal via by the uptake of

nanoparticles within mammalian cells is the endocytosis mediated by receptors.[149,150] On the other hand, tumoral cells usually express different membrane receptors than healthy cells or exhibit overexpression of certain receptors. Thus, nanocarriers surface can be decorated with (bio)-moieties able to bind with these specific cell membrane receptors of the tumoral cells in order to trigger a selective endocytosis (*active targeting*). One of the most employed types of targeting moieties are nutrients such as vitamins or sugars, because the accelerated metabolism of malignant cells demands high amount of nutrients, such as transferrin[100] and folic acid[151]. Transferrin is a glycoprotein that participates in the transport of iron to proliferating of cells.[152] Folic acid is necessary for the synthesis of purines and pyrimidines and therefore, is essential for the proper cell function. In addition to nutrients, a wide variety of targeting moieties such as antibodies and other ligands have been used to deliver the nanocarriers to tumoral cells *via* antigen-or-receptor-mediated interaction with the cell surface.[96,153,154]

Passive and active targeting ensure the specificity of the drug carriers for tumoral cells. However, nanomedicine can take one more step through the control of the intracellular fate of the nanocarrier. This fact is important because the cytotoxic effect of drugs is usually more severe in specific organelles. Therefore, targeting of intracellular organelle promotes the therapeutic effect of the drug carried.[155] Several drugs based their therapeutic effect on prevent the DNA replication or decrease or inhibit gene transcription. As the genetic material are contained in the nucleus, the nuclear targeting is an interesting strategy. The most common nuclear targeting moieties are small peptides from viruses that have nuclei localization capacity. Targeting the mitochondria is also attractive. Different clinically accepted drugs, such as Paclitaxel[156] or betulinic acid[157] act directly on the mitochondria. One ligand which shows high affinity to mitochondria is triphenylphosphinium (TPP) which interacts strongly with the negative charged mitochondrial membrane.

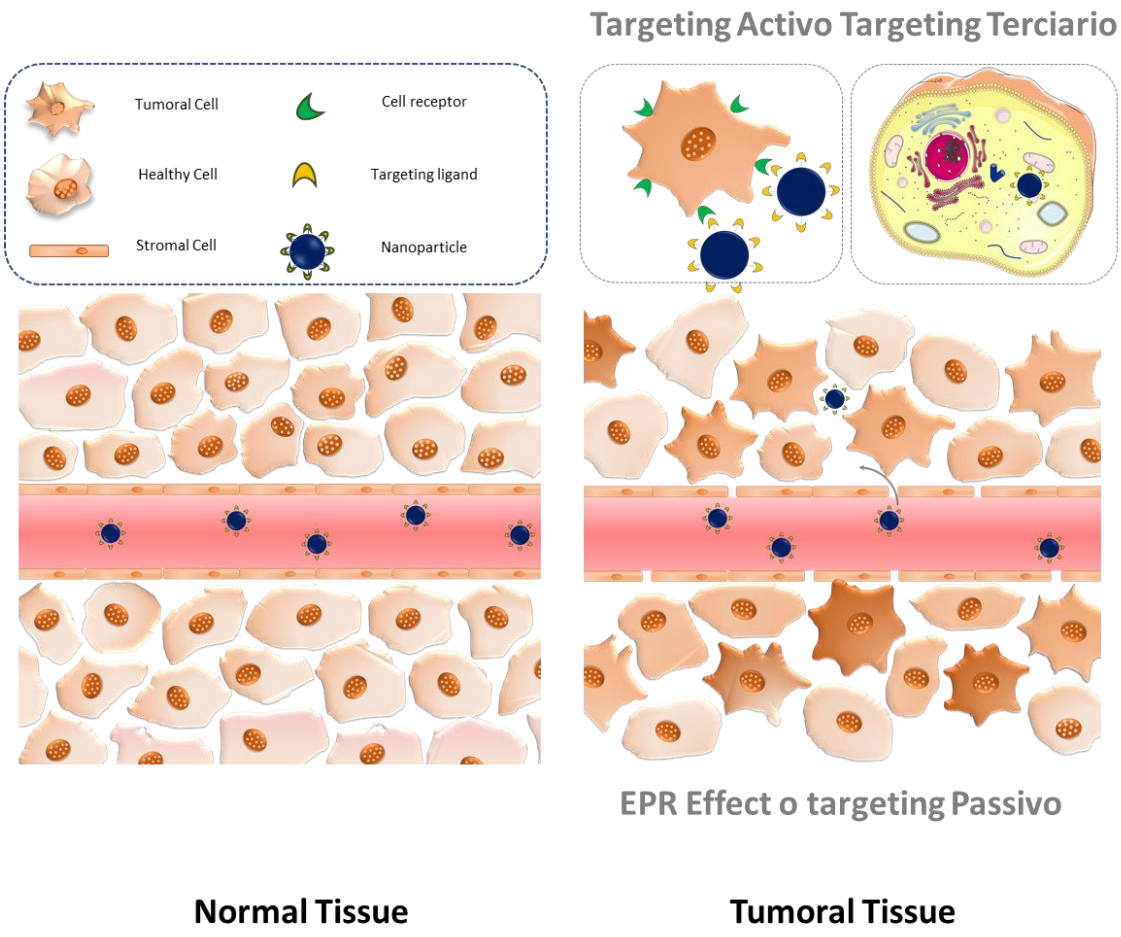

Figure 10. *EPR effect, active targeting and tertiary targeting.*

In spite of the fast significant advances of nanomedicine in the diagnosis and treatment of cancer, the incidence and mortality rates of this disease remain to be tremendously high.[158] Moreover, the implementation of nanodevices in clinic progresses slower than expected. Only over 20 nanoparticles have been approved by Food Drug Administration (FDA).[145] Some of the important reasons which cause this failure are originated by several barriers that a nanocarrier must overcome to achieve an effective therapy.[159,160,161]

A potential problem is the development of tumor resistance to conventional chemotherapy. Chemorresistance can be innate, existing since the beginning of the therapy, or acquired, developed after repeated administrations. The phenomenon by the tumor is able to survive of the chemotherapeutic treatments is known by Multidrug Resistance (MDR).[162] There are different mechanisms that confer the cell to drug resistance, as for example: an increment of drug efflux pump activity, such as the ATP-binding cassette (ABC) superfamily and a decrement of drug influx, as well as, the induction of DNA repair mechanisms, enzymatic degradation of drug, altered expression

of apoptosis-associated protein BCL-2 and tumor suppressor protein p53. Significant efforts have been carried out to overcome multidrug resistance. Nanomedicine has emerged as a potential strategy since nanocarriers are able to deliver high concentrations of chemotherapeutics drugs in combination or not with MDR inhibitors in a selective way to tumoral cells.[163,164]

Nanoparticles are mainly administrated via intravenous and circulate within the bloodstream until they arrive to the target place. During this travel, the nanoparticles are exposed to blood components that can hinders their function or result in a rapid clearance.[165] One of the mechanisms that have the human body for the elimination of foreign organisms or nanoparticles is the opsonization, followed by the pathogen capture by the cells that compose the Mononuclear Phagocytic System (MPS). Opsonization is the process in which the foreign body is covered by opsonins proteins making them more visible to phagocytic cells.[166] The opsonization can be produced by nonspecific adherence of phagocytes with serum proteins adsorbed on the particle surface or, by a conformational change of the adsorbed protein, which results in the macrophage recognition and particle clearance. Phagocyte cell are monocytes, macrophages, neutrophils, dendritic cells among others. Macrophages are localized in the liver (kupffer cells), lymph nodes and in the spleen and are the responsible for the rapid elimination of nanoparticles from the bloodstream. One method to reduce the interactions of nanoparticles with serum proteins consists in the grafting of hydrophilic polymer chains on the nanoparticle surface in order to reduce the protein adsorption. The most commonly employed polymer for this aim is PEG. Ethylene glycol unites that associate with water molecules and create a hydrating layer and hinders the protein adsorption.[167] Decoration with PEG, PEGylation, has demonstrated to increase the circulation time of nanoparticles from minutes to hours respect of non-modified nanoparticles.[168] Another option consists in surface decoration with "don´t eat me" peptides as CD47, that have demonstrated to avoid the phagocytic clearance of nanoparticles when are attached on the particle surface.[169,170] Other strategy to reduce the opsonization was developed by Tasciotti and co-workers[171] whose use a biomimetic particle coated with cell membranes isolated from leukocytes. The coating with these membranes reduced ten-fold the opsonization of particles with IgG and albumins proteins. Subsequently the coated nanoparticle showed 75% of less macrophages uptake. Finally, another interesting strategy consists in the wrapping of nanoparticles with red blood cells (RBC) membranes. Hu *et al.*[172]

demonstrated that the coating of nanoparticles with membranes isolated from RBC yield to particles that remain in circulation upon 72h.

Once the targeted nanocarrier has reached the tumor environment by passive targeting, it binds the receptor overexpressed on cell surface and is engulfed by the tumoral cells causing its destruction. However, if the interaction between the targeting moiety and the cell receptor is too strong, a paradoxical effect can appear. This effect receives the name of *binding site barrier* and induces an undesirable poor penetration of the nanoparticle within the tumoral tissue, as a consequence of the strong interaction between the targeted nanoparticle and the first tumoral cell line that it founds. One possible solution to this problem could be the use of hierarchical targeting in such a way that, the nanocarrier targeting ligands are not exposed until they are homogenously distributed in the malignant tissue. Once achieved the homogeneous distribution of the nanoparticles inside the tissue, the presence of certain stimuli (externally applied or internally present by the own pathological process) triggers the targeting activation and the subsequent particle uptake.[173,174]

Other important barrier is the high interstitial pressure present in many solid tumors.[175] This property was reported by Young *et al*. in 1950[176] and was hypothesized by Jain as an important barrier to drug nanocarriers in 1987. [177] The high porosity of the tumoral blood vessel walls in combination with dysfunctional lymphatic drainage, dense ECM and the contraction of interstitial space due to high stromal fibroblast fraction, in addition to infiltration of inflammatory cells, result in an unbalanced interstitial pressure. Thus, whereas net interstitial fluid pressure in healthy tissues is outward in the range of 0-3mmHg, [178,179,180,181] human solid tumors exhibit often a net inward pressure of 5-40mmHg. This value can even be increased to 15-130mmHg in desmoplastic pancreatic tumors. [160] The high interstitial pressure slow down the intravascular transport and reduce the perfusion rates decreasing the diffusion contribution of the interstitial transport. A way to address this problem is the tumor priming with anti-angiogenic therapy before the nanoparticle administration.[182,183]

Another important barrier common to practically all nanocarriers is the high density of extracellular matrix which strongly hamper the nanoparticle penetration within the tumor. The extracellular matrix is made mostly of collagen and glycoproteins, proteoglycans, elastin, hyaluronic acid and laminin among other structural proteins. In healthy tissues, extracellular matrix plays an important role not only providing structural integrity but

also allowing the transportation of important nutrients and oxygen maintaining the homeostasis. However, solid tumors exhibit an abnormally high stromal fraction that results in a desmoplastic state.[160] Thus, malignant masses are characterized by the formation of fibrotic tissues and present high levels of interstitial matrix components. Tumoral interstitial matrix consists in highly interconnected and tortuous network of collagen fibers. Due to the overproduction of structural proteins, tumoral extracellular matrices exhibit greater mechanical stiffness which complicate the penetration of the nanoparticle into deeper zones of the diseased tissue.

The interstitial transport, penetration and distribution of nanocarriers are ruled by two contributions: diffusion and convection.[145,160]

$$\frac{\partial C_i}{\partial t} = \underbrace{D \cdot \nabla^2 C_i}_{\substack{Diffusion \\ contribution}} + \underbrace{v_i \cdot \nabla C_i}_{\substack{Convection \\ contribution}}$$

Where

- C_i: nanoparticle concentration
- t: time
- D: diffusion coefficient.
- v_i: intersticial fluid velocity

$$v_i = -K_i \cdot \nabla p_i$$

  - K_i: is the hydraulic conductivity interstitial.
  - p_i: hydrostatic pressure.
  - R: is a term that takes into account the binding and degradation of nanoparticles

The fluid velocity depends on changes in the interstitial hydrostatic fluid pressure and diffusion coefficient depends of characteristics of the nanocarrier such as, surface charge, size, flexibility and also on the structure of the interstitial matrix. As have been mentioned above solid tumors exhibit high interstitial pressure that avoid the convection contribution.

The high stiffness of ECM results in a significant resistance to nanocarrier diffusion since the diffusion coefficient shows an inverse dependency with viscosity. The ineffective transport of nanocarriers inside the tumoral tissue limits the efficacy of the drug carrier,

because the effect of the nanomedicine is concentrated mainly in the malignant periphery yielding only a local effect.

Herculean efforts have been carried out in order to overcome this barrier due to the great impediment for the penetration of nanocarriers that suppose its presence and its universal role in all nanomedicines. Some important strategies which has been proposed for overwhelming this limitation are the use of ultrasounds to propel the nanocarrier inside the tissue and decoration of nanoparticles with proteolytic enzymes capable to degrade the ECM, which is one of the main topic developed in this thesis. These strategies are going to be discussed in detail in the following chapter.

References

(1) Whitesides, G. M. The "Right" Size in Nanobiotechnology. *Nat. Biotechnol.* **2003**, *21* (10), 1161–1165.

(2) MG, K.; V, K.; F, H. History and Possible Uses of Nanomedicine Based on Nanoparticles and Nanotechnological Progress. *J. Nanomed. Nanotechnol.* **2015**, *6* (6).

(3) Mappes, T.; Jahr, N.; Csaki, A.; Vogler, N.; Popp, J.; Fritzsche, W. The Invention of Immersion Ultramicroscopy in 1912-The Birth of Nanotechnology? *Angew. Chemie Int. Ed.* **2012**, *51* (45), 11208–11212.

(4) Kateb, B.; Heiss, J. D. *The Textbook of Nanoneuroscience and Nanoneurosurgery*; CRC Press/Taylor & Francis, 2013.

(5) Feynman, R. P. There's Plenty of Room at the Bottom An Invitation to Enter a New Field of Physics.

(6) Sahoo, S. K.; Parveen, S.; Panda, J. J. The Present and Future of Nanotechnology in Human Health Care. *Nanomedicine Nanotechnology, Biol. Med.* **2007**, *3* (1), 20–31.

(7) Tolochko, N. K. History of Nanotechnology. *Nanosci. nanotechnology. Encycl. life Support Syst. (EOLSS), Dev. under auspices UNESCO, SEolss Publ. oxford, 2009*, *3-4*. **2009**.

(8) Kim, J.; Piao, Y.; Hyeon, T. Multifunctional Nanostructured Materials for Multimodal Imaging, and Simultaneous Imaging and Therapy. *Chem. Soc. Rev.* **2009**, *38* (2), 372–390.

(9) Rizzo, L. Y.; Theek, B.; Storm, G.; Kiessling, F.; Lammers, T. Recent Progress in Nanomedicine: Therapeutic, Diagnostic and Theranostic Applications. *Curr. Opin. Biotechnol.* **2013**, *24*, 1159–1166.

(10) Akagi, T.; Akashi, M. Nanomedicine and Infection; Humana Press, New York, NY, 2016; pp 439–455.

(11) Zarbin, M. A.; Montemagno, C.; Leary, J. F.; Ritch, R. Regenerative Nanomedicine and the Treatment of Degenerative Retinal Diseases. *Wiley Interdiscip. Rev. Nanomedicine Nanobiotechnology* **2012**, *4* (1), 113–137.

(12) Zhang, C.; Wan, X.; Zheng, X.; Shao, X.; Liu, Q.; Zhang, Q.; Qian, Y. Dual-Functional Nanoparticles Targeting Amyloid Plaques in the Brains of Alzheimer's Disease Mice. **2014**.

(13) Serra, P.; Santamaria, P. Nanoparticle-Based Autoimmune Disease Therapy. *Clin. Immunol.* **2015**, *160* (1), 3–13.

(14) Clemente-Casares, X.; Santamaria, P. Nanomedicine in Autoimmunity. *Immunol. Lett.* **2014**, *158* (1–2), 167–174.

(15) McCarthy, J. R. Nanomedicine and Cardiovascular Disease. *Curr. Cardiovasc. Imaging Rep.* **2010**, *3* (1), 42–49.

(16) Ediriwickrema, A.; Saltzman, W. M. Nanotherapy for Cancer: Targeting and Multifunctionality in the Future of Cancer Therapies. *ACS Biomater. Sci. Eng.* **2015**, *1* (2), 64–78.

(17) Seigneuric, R.; Markey, L.; Nuyten, D. S. a; Dubernet, C.; Evelo, C. T. a; Finot, E.; Garrido, C. From Nanotechnology to Nanomedicine: Applications to Cancer Research. *Curr. Mol. Med.* **2010**, *10* (7), 640–652.

(18) Pelaz, B.; Alexiou, C.; Alvarez-Puebla, R. A.; Alves, F.; Andrews, A. M.; Ashraf, S.; Balogh, L. P.; Ballerini, L.; Bestetti, A.; Brendel, C.; et al. Diverse Applications of Nanomedicine. *ACS Nano* **2017**, *11* (3), 2313–2381.

(19) Vallet-Regí, M.; Ruiz-Hernández, E. Bioceramics: From Bone Regeneration to Cancer Nanomedicine. *Adv. Mater.* **2011**, *23* (44), 5177–5218.

(20) Meseguer-Olmo, L.; Ros-Nicolás, M.; Vicente-Ortega, V.; Alcaraz-Baños, M.; Clavel-Sainz, M.; Arcos, D.; Ragel, C. V.; Vallet-Regí, M.; Meseguer-Ortiz, C. A Bioactive Sol-Gel Glass Implant for in Vivo Gentamicin Release. Experimental Model in Rabbit. *J. Orthop. Res.* **2006**, *24* (3), 454–460.

(21) Izquierdo-Barba, I.; García-Martín, J. M.; Álvarez, R.; Palmero, A.; Esteban, J.; Pérez-Jorge, C.; Arcos, D.; Vallet-Regí, M. Nanocolumnar Coatings with Selective Behavior towards Osteoblast and Staphylococcus Aureus Proliferation. *Acta Biomater.* **2015**, *15*, 20–28.

(22) Agnieszka Z. Wilczewska, Katarzyna Niemirowicz, K. H. M.; Halina Car. Nanoparticles as Drug Delivery Systems. *Pharmacol. Reports* **2012**, No. 64, 1020–1037.

(23) Vallet-Regí, M.; Balas, F.; Arcos, D. Mesoporous Materials for Drug Delivery. *Angew. Chemie Int. Ed.* **2007**, *46* (40), 7548–7558.

(24) Parveen, S.; Misra, R.; Sahoo, S. K. Nanoparticles: A Boon to Drug Delivery, Therapeutics, Diagnostics and Imaging. *Nanomedicine Nanotechnology, Biol. Med.* **2012**, *8* (2), 147–166.

(25) Faraji, A. H.; Wipf, P. Nanoparticles in Cellular Drug Delivery. **2009**.

(26) Sanvicens, N.; Marco, M. P. Multifunctional Nanoparticles - Properties and Prospects for Their Use in Human Medicine. *Trends Biotechnol.* **2008**, *26* (8), 425–433.

(27) Shatrohan Lal, R. K.; Lal, S. Synthesis of Organic Nanoparticles and Their Applications in Drug Delivery and Food Nanotechnology: A Review. *J. Nanomater. Mol. Nanotechnol.* **2014**, *3* (4).

(28) Bozzuto, G.; Molinari, A. Liposomes as Nanomedical Devices. *Int. J. Nanomedicine* **2015**, *10*, 975.

(29) Akbarzadeh, A.; Rezaei-Sadabady, R.; Davaran, S.; Joo, S. W.; Zarghami, N.; Hanifehpour, Y.; Samiei, M.; Kouhi, M.; Nejati-Koshki, K. Liposome: Classification, Preparation, and Applications. *Nanoscale Res. Lett.* **2013**, *8*, 1.

(30) Deshpande, P. P.; Biswas, S.; Torchilin, V. P. Current Trends in the Use of Liposomes for Tumor Targeting. *Nanomedicine* **2013**, *8* (9), 1509–1528.

(31) Lasic, D. D.; Martin, F. J. *Stealth Liposomes*; CRC Press, 1995.

(32) Badran, M.; Shalaby, K.; Al-Omrani, A. Influence of the Flexible Liposomes on the Skin Deposition of a Hydrophilic Model Drug, Carboxyfluorescein: Dependency on Their Composition. *ScientificWorldJournal.* **2012**, *2012*, 134876.

(33) Morton, S. W.; Lee, M. J.; Deng, Z. J.; Dreaden, E. C.; Siouve, E.; Shopsowitz, K. E.; Shah, N. J.; Yaffe, M. B.; Hammond, P. T. A Nanoparticle-Based Combination Chemotherapy Delivery System for Enhanced Tumor Killing by Dynamic Rewiring of Signaling Pathways. *Sci. Signal.* **2014**, *7* (325).

(34) Liu, Y.; Li, J.; Lu, Y. Enzyme Therapeutics for Systemic Detoxification. *Adv. Drug Deliv. Rev.* **2015**, *90*, 24–39.

(35) Rwei, A. Y.; Paris, J. L.; Wang, B.; Wang, W.; Axon, C. D.; Vallet-Regí, M.; Langer, R.; Kohane, D. S. Ultrasound-Triggered Local Anaesthesia. *Nat. Biomed. Eng.* **2017**, *1* (8), 644–653.

(36) Fabienne Danhier; Eduardo Ansorena; Joana M. Silva; Régis Coco; Aude Le Breton; Véronique Préat. PLGA-Based Nanoparticles: An Overview of Biomedical Applications. *J. Control. Release* **2012**, No. 161, 505–522.

(37) Jones, M.-C.; Leroux, J.-C. Polymeric Micelles ± a New Generation of Colloidal Drug Carriers.

(38) van Nostrum, C. F. Polymeric Micelles to Deliver Photosensitizers for Photodynamic Therapy. *Adv. Drug Deliv. Rev.* **2004**, *56* (1), 9–16.

(39) Ai, H.; Flask, C.; Weinberg, B.; Shuai, X.; Pagel, M. D.; Farrell, D.; Duerk, J.; Gao, J. Magnetite-Loaded Polymeric Micelles as Ultrasensitive Magnetic-Resonance Probes. *Adv. Mater.* **2005**, *17* (16), 1949–1952.

(40) Nishi Mody, Rakesh Kumar Tekade, Neelesh Kumar Mehra,Prashant Chopdey, and N. K. J. Dendrimer, Liposomes, Carbon Nanotubes and PLGA Nanoparticles: One Platform Assessment of Drug Delivery Potential. *Am. Assoc. Pharm. Sci.* **2014**, *15* (2), 388–399.

(41) Svenson, S.; Tomalia, D. A. Dendrimers in Biomedical Applications-Reflections on the Field. *Adv. Drug Deliv. Rev.* **2012**, *64* (SUPPL.), 102–115.

(42) Dykman, L.; Khlebtsov, N. Gold Nanoparticles in Biomedical Applications: Recent Advances and Perspectives. *Chem. Soc. Rev.* **2012**, *41* (6), 2256–2282.

(43) Huang, X.; Jain, P. K.; El-Sayed, I. H.; El-Sayed, M. A. Gold Nanoparticles: Interesting Optical Properties and Recent Applications in Cancer Diagnostics and Therapy. *Nanomedicine* **2007**, *2* (5), 681–693.

(44) Ali, A.; Zafar, H.; Zia, M.; ul Haq, I.; Phull, A. R.; Ali, J. S.; Hussain, A. Synthesis, Characterization, Applications, and Challenges of Iron Oxide Nanoparticles. *Nanotechnol. Sci. Appl.* **2016**, *9*, 49–67.

(45) Schlorf, T.; Meincke, M.; Kossel, E.; Glüer, C.-C.; Jansen, O.; Mentlein, R. Biological Properties of Iron Oxide Nanoparticles for Cellular and Molecular Magnetic Resonance Imaging. *Int. J. Mol. Sci.* **2010**, *12* (1), 12–23.

(46) Silva, A. K. A.; Espinosa, A.; Kolosnjaj-Tabi, J.; Wilhelm, C.; Gazeau, F. *Medical Applications of Iron Oxide Nanoparticles*; 2016.

(47) Drbohlavova, J.; Adam, V.; Kizek, R.; Hubalek, J. Quantum Dots - Characterization, Preparation and Usage in Biological Systems. *Int. J. Mol. Sci.* **2009**, *10* (2), 656–673.

(48) Bailey, R. E.; Smith, A. M.; Nie, S. Quantum Dots in Biology and Medicine. *Phys. E Low-Dimensional Syst. Nanostructures* **2004**, *25* (1), 1–12.

(49) Radenkovic, D.; Kobayashi, H.; Remsey-Semmelweis, E.; Seifalian, A. M. Quantum Dot Nanoparticle for Optimization of Breast Cancer Diagnostics and Therapy in a Clinical Setting. *Nanomedicine Nanotechnology, Biol. Med.* **2016**, *12* (6), 1581–1592.

(50) Yaghini, E.; Turner, H. D.; Le Marois, A. M.; Suhling, K.; Naasani, I.; MacRobert, A. J. In Vivo Biodistribution Studies and Ex Vivo Lymph Node Imaging Using Heavy Metal-Free Quantum Dots. *Biomaterials* **2016**, *104*, 182–191.

(51) Park, Y.; Jeong, S.; Kim, S. Medically Translatable Quantum Dots for Biosensing and Imaging. *J. Photochem. Photobiol. C Photochem. Rev. J. Photochem. Photobiol. C* **2017**, *30*, 51–70.

(52) Martínez-Carmona, M.; Gun'ko, Y.; Vallet-Regí, M. ZnO Nanostructures for Drug Delivery and Theranostic Applications. *Nanomaterials* **2018**, *8* (4), 268.

(53) Jiang, H.; Lee, P. S.; Li, C. 3D Carbon Based Nanostructures for Advanced Supercapacitors. *Energy Environ. Sci.* **2013**, *6* (1), 41–53.

(54) Dizaj, S. M.; Mennati, A.; Jafari, S.; Khezri, K.; Adibkia, K. Antimicrobial Activity of Carbon-Based Nanoparticles. *Adv. Pharm. Bull.* **2015**, *5* (1), 19–23.

(55) Ji, S.; Liu, C.; Zhang, B.; Yang, F.; Xu, J.; Long, J.; Jin, C.; Fu, D.; Ni, Q.; Yu, X. Carbon Nanotubes in Cancer Diagnosis and Therapy. *Biochim. Biophys. Acta - Rev. Cancer* **2010**, *1806* (1), 29–35.

(56) Polizu, S.; Savadogo, O.; Poulin, P.; Yahia, L. Applications of Carbon Nanotubes-Based Biomaterials in Biomedical Nanotechnology. *J. Nanosci. Nanotechnol.* **2006**, *6* (7), 1883–1904.

(57) Manzano, M.; Vallet-Regí, M. New Developments in Ordered Mesoporous

Materials for Drug Delivery. *J. Mater. Chem.* **2010**, *20* (27), 5593.

(58) Francisco Balas; Miguel Manzano; Patricia Horcajada, and; Vallet-Regí*, M. Confinement and Controlled Release of Bisphosphonates on Ordered Mesoporous Silica-Based Materials. **2006**.

(59) Gómez-Cerezo, N.; Sánchez-Salcedo, S.; Izquierdo-Barba, I.; Arcos, D.; Vallet-Regí, M. In Vitro Colonization of Stratified Bioactive Scaffolds by Pre-Osteoblast Cells. *Acta Biomater.* **2016**, *44*, 73–84.

(60) López-Noriega, A.; Arcos, D.; Vallet-Regí, M. Functionalizing Mesoporous Bioglasses for Long-Term Anti-Osteoporotic Drug Delivery. *Chem. - A Eur. J.* **2010**, *16* (35), 10879–10886.

(61) Mas, N.; Arcos, D.; Polo, L.; Aznar, E.; Sánchez-Salcedo, S.; Sancenón, F.; García, A.; Marcos, M. D.; Baeza, A.; Vallet-Regí, M.; et al. Towards the Development of Smart 3D "gated Scaffolds" for on-Command Delivery. *Small* **2014**, *10* (23), 4859–4864.

(62) Philippart, A.; Gómez-Cerezo, N.; Arcos, D.; Salinas, A. J.; Boccardi, E.; Vallet-Regi, M.; Boccaccini, A. R. Novel Ion-Doped Mesoporous Glasses for Bone Tissue Engineering: Study of Their Structural Characteristics Influenced by the Presence of Phosphorous Oxide. *J. Non. Cryst. Solids* **2017**, *455*, 90–97.

(63) Polo, L.; Gómez-Cerezo, N.; Aznar, E.; Vivancos, J.-L.; Sancenón, F.; Arcos, D.; Vallet-Regí, M.; Martínez-Máñez, R. Molecular Gates in Mesoporous Bioactive Glasses for the Treatment of Bone Tumors and Infection. *Acta Biomater.* **2017**, *50*, 114–126.

(64) Gómez-Cerezo, N.; Izquierdo-Barba, I.; Arcos, D.; Vallet-Regí, M. Tailoring the Biological Response of Mesoporous Bioactive Materials. *J. Mater. Chem. B* **2015**, *3* (18), 3810–3819.

(65) Izquierdo-Barba, I.; Colilla, M.; Vallet-Regí, M. Zwitterionic Ceramics for Biomedical Applications. *Acta Biomater.* **2016**, *40*, 201–211.

(66) Horcajada, P.; Rámila, A.; Boulahya, K.; González-Calbet, J.; Vallet-Regí, M. Bioactivity in Ordered Mesoporous Materials. *Solid State Sci.* **2004**, *6*, 1295–1300.

(67) Doadrio, A. L.; Sousa, E. M. B.; Doadrio, J. C.; Pérez Pariente, J.; Izquierdo-Barba, I.; Vallet-Regí, M. Mesoporous SBA-15 HPLC Evaluation for Controlled Gentamicin Drug Delivery. *J. Control. Release* **2004**, *97* (1), 125–132.

(68) Izquierdo-Barba, I.; Vallet-Regí, M.; Kupferschmidt, N.; Terasaki, O.; Schmidtchen, A.; Malmsten, M. Incorporation of Antimicrobial Compounds in Mesoporous Silica Film Monolith. *Biomaterials* **2009**, *30* (29), 5729–5736.

(69) Izquierdo-Barba, I.; Sánchez-Salcedo, S.; Colilla, M.; Feito, M. J.; Ramírez-Santillán, C.; Portolés, M. T.; Vallet-Regí, M. Inhibition of Bacterial Adhesion on Biocompatible Zwitterionic SBA-15 Mesoporous Materials. *Acta Biomater.* **2011**, *7* (7), 2977–2985.

(70) García-Alvarez, R.; Izquierdo-Barba, I.; Vallet-Regí, M. 3D Scaffold with Effective Multidrug Sequential Release against Bacteria Biofilm. *Acta Biomater.* **2017**, *49*, 113–126.

(71) Sánchez-Salcedo, S.; Colilla, M.; Izquierdo-Barba, I.; Vallet-Regí, M. Design and Preparation of Biocompatible Zwitterionic Hydroxyapatite. *J. Mater. Chem. B* **2013**, *1* (11), 1595.

(72) Sánchez-Salcedo, S.; Shruti, S.; Salinas, A. J.; Malavasi, G.; Menabue, L.; Vallet-Regí, M. In Vitro Antibacterial Capacity and Cytocompatibility of SiO_2–CaO–P_2O_5 Meso-Macroporous Glass Scaffolds Enriched with ZnO. *J. Mater. Chem. B* **2014**, *2* (30), 4836–4847.

(73) Simmchen, J.; Baeza, A.; Ruiz, D.; Esplandiu, M. J.; Vallet-Regí, M. Asymmetric

Hybrid Silica Nanomotors for Capture and Cargo Transport: Towards a Novel Motion-Based DNA Sensor. *Small* **2012**, *8* (13), 2053–2059.

(74) Lee, J. E.; Lee, N.; Kim, T.; Kim, J.; Hyeon, T. Multifunctional Mesoporous Silica Nanocomposite Nanoparticles for Theranostic Applications. *Acc. Chem. Res.* **2011**, *44* (10), 893–902.

(75) Colilla, M.; González, B.; Vallet-Regí, M. Mesoporous Silicananoparticles for the Design of Smart Delivery Nanodevices. *Biomater. Sci.* **2013**, *1* (2), 114–134.

(76) Baeza, A.; Colilla, M.; Vallet-Regí, M. Advances in Mesoporous Silica Nanoparticles for Targeted Stimuli-Responsive Drug Delivery. *Expert Opin. Drug Deliv.* **2015**, *12* (2), 319–337.

(77) Baeza, A.; Manzano, M.; Colilla, M.; Vallet-Regí, M. Recent Advances in Mesoporous Silica Nanoparticles for Antitumor Therapy: Our Contribution. *Biomater. Sci.* **2016**, *4* (5), 803–813.

(78) Bitar, A.; Ahmad, N. M.; Fessi, H.; Elaissari, A. Silica-Based Nanoparticles for Biomedical Applications. *Drug Discov. Today* **2012**, *17* (19–20), 1147–1154.

(79) Villaverde, G.; Baeza, A.; Melen, G. J.; Alfranca, A.; Ramirez, M.; Vallet-Regí, M. A New Targeting Agent for the Selective Drug Delivery of Nanocarriers for Treating Neuroblastoma. *J. Mater. Chem. B* **2015**, *3* (24), 4831–4842.

(80) Vallet-Regí, M.; Ruiz-González, L.; Izquierdo-Barba, I.; González-Calbet, J. M. Revisiting Silica Based Ordered Mesoporous Materials: Medical Applications. *J. Mater. Chem.* **2006**, *16* (1), 26–31.

(81) Paris, J. L.; Cabañas, M. V.; Manzano, M.; Vallet-Regí, M. Polymer-Grafted Mesoporous Silica Nanoparticles as Ultrasound-Responsive Drug Carriers. *ACS Nano* **2015**, *9* (11), 11023–11033.

(82) Baeza, A.; Guisasola, E.; Torres-Pardo, A.; González-Calbet, J. M.; Melen, G. J.;

Ramirez, M.; Vallet-Regí, M. Hybrid Enzyme-Polymeric Capsules/Mesoporous Silica Nanodevice for In Situ Cytotoxic Agent Generation. *Adv. Funct. Mater.* **2014**, *24* (29), 4625–4633.

(83) Rouquerolt, J.; Avnir, D.; Fairbridge, C. W.; Everett, D. H.; Haynes, J. H.; Pernicone, N.; Ramsay, J. D. F.; Sing, K. S. W.; Unger, K. K. Recommendations for the Characterization of Porous Solids. *Pure Appl. Chem.* **1994**, *66* (8), 1739–1758.

(84) Yanagisawa, T.; Shimizu, T.; Kuroda, K.; Kato, C. The Preparation of Alkyltriinethylaininonium–Kaneinite Complexes and Their Conversion to Microporous Materials. *Bull. Chem. Soc. Jpn.* **1990**, *63* (4), 988–992.

(85) Beck, J. S.; Vartuli, J. C.; Roth, W. J.; Leonowicz, M. E.; Kresge, C. T.; Schmitt, K. D.; Chu, C. T. W.; Olson, D. H.; Sheppard, E. W.; McCullen, S. B.; et al. A New Family of Mesoporous Molecular Sieves Prepared with Liquid Crystal Templates. *J. Am. Chem. Soc.* **1992**, *114* (27), 10834–10843.

(86) Vallet-Regi, M.; Rámila, A.; del Real, R. P.; Pérez-Pariente, J. A New Property of MCM-41: Drug Delivery System. *Chem. Mater.* **2001**, *13* (2), 308–311.

(87) Walcarius, A.; Mercier, L. Mesoporous Organosilica Adsorbents: Nanoengineered Materials for Removal of Organic and Inorganic Pollutants. *J. Mater. Chem.* **2010**, *20* (22), 4478.

(88) Hoffmann, F.; Cornelius, M.; Morell, J.; Fröba, M. Silica-Based Mesoporous Organic-Inorganic Hybrid Materials. *Angew. Chemie - Int. Ed.* **2006**, *45* (20), 3216–3251.

(89) Manzano, M.; Colilla, M.; Vallet-Regí, M. Drug Delivery from Ordered Mesoporous Matrices. *Expert Opin. Drug Deliv.* **2009**, *6* (12), 1383–1400.

(90) He, Q.; Shi, J. Mesoporous Silica Nanoparticle Based Nano Drug Delivery

Systems: Synthesis, Controlled Drug Release and Delivery, Pharmacokinetics and Biocompatibility. *J. Mater. Chem.* **2011**, *21* (16), 5845–5855.

(91) Mamaeva, V.; Sahlgren, C.; Lindén, M. Mesoporous Silica Nanoparticles in medicine—Recent Advances ☆. **2013**.

(92) Lin, Y.-S.; Hurley, K. R.; Haynes, C. L. Critical Considerations in the Biomedical Use of Mesoporous Silica Nanoparticles. *J. Phys. Chem. Lett.* **2012**, *3* (3), 364–374.

(93) Muñ Oz, B.; Rá Mila, A.; Pérez-Pariente, J.; Díaz, I.; Vallet-Regí, M. MCM-41 Organic Modification as Drug Delivery Rate Regulator.

(94) Stöber, W.; Fink, A.; Bohn, E. Controlled Growth of Monodisperse Silica Spheres in the Micron Size Range. *J. Colloid Interface Sci.* **1968**, *26* (1), 62–69.

(95) Qiao, Z.-A.; Zhang, L.; Guo, M.; Liu, Y.; Huo, Q. Synthesis of Mesoporous Silica Nanoparticles via Controlled Hydrolysis and Condensation of Silicon Alkoxide. *Chem. Mater.* **2009**, *21* (16), 3823–3829.

(96) Durfee, P. N.; Lin, Y.-S.; Dunphy, D. R.; Muñiz, A. J.; Butler, K. S.; Humphrey, K. R.; Lokke, A. J.; Agola, J. O.; Chou, S. S.; Chen, I.-M.; et al. Mesoporous Silica Nanoparticle-Supported Lipid Bilayers (Protocells) for Active Targeting and Delivery to Individual Leukemia Cells. *ACS Nano* **2016**, *10* (9), 8325–8345.

(97) Vallet-Regí, M.; Manzano Garcia, M.; Colilla, M. *Biomedical Applications of Mesoporous Ceramics : Drug Delivery, Smart Materials, and Bone Tissue Engineering*.

(98) Wu, S.-H.; Mou, C.-Y.; Lin, H.-P. Synthesis of Mesoporous Silica Nanoparticles. *Chem. Soc. Rev.* **2013**, *42* (9), 3862.

(99) Argyo, C.; Weiss, V.; Bräuchle, C.; Bein, T. Multifunctional Mesoporous Silica Nanoparticles as a Universal Platform for Drug Delivery. *Chem. Mater.* **2014**, *26*

(1), 435–451.

(100) Martínez-Carmona, M.; Baeza, A.; Rodriguez-Milla, M. a.; García-Castro, J.; Vallet-Regí, M. Mesoporous Silica Nanoparticles Grafted with a Light-Responsive Protein Shell for Highly Cytotoxic Antitumoral Therapy. *J. Mater. Chem. B* **2015**, *3*, 5746–5752.

(101) Trewyn, B. G.; Nieweg, J. A.; Zhao, Y.; Lin, V. S.-Y. Biocompatible Mesoporous Silica Nanoparticles with Different Morphologies for Animal Cell Membrane Penetration. *Chem. Eng. J.* **2008**, *137* (1), 23–29.

(102) Chen, J.; Liu, M.; Chen, C.; Gong, H.; Gao, C. Synthesis and Characterization of Silica Nanoparticles with Well-Defined Thermoresponsive PNIPAM via a Combination of RAFT and Click Chemistry. *ACS Appl. Mater. Interfaces* **2011**, *3*, 3215–3223.

(103) Lu, J.; Liong, M.; Zink, J. I.; Tamanoi, F. Mesoporous Silica Nanoparticles as a Delivery System for Hydrophobic Anticancer Drugs. *Small* **2007**, *3* (8), 1341–1346.

(104) Ishii, Y.; Nishiwaki, Y.; Al-Zubaidi, A.; Kawasaki, S. Pore Size Determination in Ordered Mesoporous Materials Using Powder X‐ray Diffraction.

(105) WHO | Cancer. *WHO* **2018**.

(106) Floor, S. L.; Dumont, J. E.; Maenhaut, C.; Raspe, E. Hallmarks of Cancer: Of All Cancer Cells, All the Time? *Trends Mol. Med.* **2012**, *18* (9), 509–515.

(107) Hanahan, D.; Weinberg, R. A. Hallmarks of Cancer: The Next Generation. *Cell* **2011**, *144* (5), 646–674.

(108) Pietras, K.; Östman, A. Hallmarks of Cancer: Interactions with the Tumor Stroma. *Exp. Cell Res.* **2010**, *316*, 1324–1331.

(109) Hanahan, D.; Weinberg, R. A. 2 Biological Hallmarks of Cancer. **2017**, 7–16.

(110) Perona, R. Cell Signalling: Growth Factors and Tyrosine Kinase Receptors. *Clin. Transl. Oncol.* **2006**, *8* (2), 77–82.

(111) Cheng, N.; Chytil, A.; Shyr, Y.; Joly, A.; Research, H. M.-M. C.; 2008, undefined. Transforming Growth Factor-β Signaling–deficient Fibroblasts Enhance Hepatocyte Growth Factor Signaling in Mammary Carcinoma Cells to Promote Scattering and. *AACR*.

(112) Bhowmick, N.; Neilson, E.; Nature, H. M.-; 2004, undefined. Stromal Fibroblasts in Cancer Initiation and Progression. *nature.com*.

(113) DeBerardinis, R. J.; Lum, J. J.; Hatzivassiliou, G.; Thompson, C. B. The Biology of Cancer: Metabolic Reprogramming Fuels Cell Growth and Proliferation. *Cell Metab.* **2008**, *7* (1), 11–20.

(114) Burkhart, D. L.; Sage, J. Cellular Mechanisms of Tumour Suppression by the Retinoblastoma Gene. *Nat. Rev. Cancer* **2008**, *8* (9), 671–682.

(115) Deshpande, A.; Sicinski, P.; Oncogene, P. H.-; 2005, undefined. Cyclins and Cdks in Development and Cancer: A Perspective. *nature.com*.

(116) Sherr, C. J.; McCormick, F. The RB and p53 Pathways in Cancer. *Cancer Cell* **2002**, *2* (2), 103–112.

(117) Hezel, A. F.; Bardeesy, N. LKB1; Linking Cell Structure and Tumor Suppression. *Oncogene* **2008**, *27* (55), 6908–6919.

(118) Shaw, R. J. Tumor Suppression by LKB1: SIK-Ness Prevents Metastasis. *Sci. Signal.* **2009**, *2* (86), pe55.

(119) Okada, T.; Lopez-Lago, M.; Giancotti, F. G. Merlin/NF-2 Mediates Contact Inhibition of Growth by Suppressing Recruitment of Rac to the Plasma Membrane. *J. Cell Biol.* **2005**, *171* (2), 361–371.

(120) Sherr, C. J.; DePinho, R. A. Cellular Senescence: Mitotic Clock or Culture Shock?

Cell **2000**, *102* (4), 407–410.

(121) Wei, W.; Sedivy, J. M. Differentiation between Senescence (M1) and Crisis (M2) in Human Fibroblast Cultures. *Exp. Cell Res.* **1999**, *253* (2), 519–522.

(122) Blasco, M. A. Telomeres and Human Disease: Ageing, Cancer and beyond. *Nat. Rev. Genet.* **2005**, *6* (8), 611–622.

(123) Shay, J. W.; Wright, W. E. Hayflick, His Limit and Cellular Ageing. *Nat. Rev. Mol. Cell Biol.* **2000**, *1* (1), 72–76.

(124) Otrock, Z. K.; Mahfouz, R. A. R.; Makarem, J. A.; Shamseddine, A. I. Understanding the Biology of Angiogenesis: Review of the Most Important Molecular Mechanisms. *Blood Cells, Mol. Dis.* **2007**, *39* (2), 212–220.

(125) Jain, R. K. Tumor Angiogenesis and Accessibility: Role of Vascular Endothelial Growth Factor. *Semin. Oncol.* **2002**, *29* (6Q), 3–9.

(126) Warburg, O.; Wind, F.; Negelein, E. Über Den Stoffwechsel von Tumoren Im Körper. *Klin. Wochenschr.* **1926**, *5* (19), 829–832.

(127) Liberti, M. V.; Locasale, J. W. The Warburg Effect: How Does It Benefit Cancer Cells? *Trends Biochem Sci* **2016**, *41* (3), 211–218.

(128) Epstein, T.; Gatenby, R. A.; Brown, J. S. The Warburg Effect as an Adaptation of Cancer Cells to Rapid Fluctuations in Energy Demand. *PLoS One* **2017**, *12* (9), 1–14.

(129) Bensinger, S. J.; Christofk, H. R. New Aspects of the Warburg Effect in Cancer Cell Biology. *Semin. Cell Dev. Biol.* **2012**, *23* (4), 352–361.

(130) Vander Heiden, M.; Cantley, L.; Thompson, C. Understanding the Warburg Effect: The Metabolic Requiremetns of Cell Proliferation. *Science (80-.).* **2009**, *324* (5930), 1029–1033.

(131) Ferreira, L. M. R. Cancer Metabolism: The Warburg Effect Today. *Exp. Mol.*

Pathol. **2010**, *89* (3), 372–380.

(132) Adams, J. M.; Cory, S. The Bcl-2 Apoptotic Switch in Cancer Development and Therapy. *Oncogene* **2007**, *26* (9), 1324–1337.

(133) Lowe, S. W.; Cepero, E.; Evan, G. Intrinsic Tumour Suppression. *Nature* **2004**, *432* (7015), 307–315.

(134) Alitalo, A.; Detmar, M. Interaction of Tumor Cells and Lymphatic Vessels in Cancer Progression. *Oncogene* **2012**, *31* (42), 4499–4508.

(135) Fidler, I. J. The Organ Microenvironment and Cancer Metastasis. *Differentiation* **2002**, *70*, 498–505.

(136) Liotta, L. A.; Thorgeirsson, U. P.; Garbisa, S. Role of Collagenases in Tumor Cell Invasion. *Cancer Metastasis Rev.* **1982**, *1* (4), 277–288.

(137) Kim, R.; Emi, M.; Tanabe, K. Cancer Immunoediting from Immune Surveillance to Immune Escape. *Immunology* **2007**, *121* (1), 1–14.

(138) Teng, M. W. L.; Swann, J. B.; Koebel, C. M.; Schreiber, R. D.; Smyth, M. J. Immune-Mediated Dormancy: An Equilibrium with Cancer. *J. Leukoc. Biol.* **2008**, *84* (4), 988–993.

(139) Egeblad, M.; Nakasone, E. S.; Werb, Z. Tumors as Organs: Complex Tissues That Interface with the Entire Organism. *Dev. Cell* **2010**, *18* (6), 884–901.

(140) Lim, E.; Belcher, E.; Yap, Y. K.; Nicholson, A. G.; Goldstraw, P. The Role of Surgery in the Treatment of Limited Disease Small Cell Lung Cancer: Time to Reevaluate. *J. Thorac. Oncol.* **2008**, *3* (11), 1267–1271.

(141) Delaney, G.; Jacob, S.; Featherstone, C.; Barton, M. The Role of Radiotherapy in Cancer Treatment. *Cancer* **2005**, *104* (6), 1129–1137.

(142) Chabner, B. A.; Roberts, T. G. Chemotherapy and the War on Cancer. *Nat. Rev. Cancer* **2005**, *5* (1), 65–72.

(143) Wicki, A.; Witzigmann, D.; Balasubramanian, V.; Huwyler, J. Nanomedicine in Cancer Therapy: Challenges, Opportunities, and Clinical Applications. *J. Control. Release* **2015**, *200*, 138–157.

(144) Matsumura, Y.; Maeda, H. A New Concept for Macromolecular Therapeutics in Cancer-Chemotherapy - Mechanism of Tumoritropic Accumulation of Proteins and the Antitumor Agent Smancs. *Cancer Res.* **1986**, *46* (12), 6387–6392.

(145) Jain, R. K.; Stylianopoulos, T. Delivering Nanomedicine to Solid Tumors. *Nat. Rev. Clin. Oncol.* **2010**, *7* (11), 653–664.

(146) Nichols, J. W.; Bae, Y. H. EPR: Evidence and Fallacy. *J. Control. Release* **2014**, *190*, 451–464.

(147) Helmlinger, G.; Netti, P. A.; Lichtenbeld, H. C.; Melder, R. J.; Jain, R. K. Solid Stress Inhibits the Growth of Multicellular Tumor Spheroids. *Nat. Biotechnol.* **1997**, *15* (8), 778–783.

(148) Cheng, G.; Tse, J.; Jain, R. K.; Munn, L. L. Micro-Environmental Mechanical Stress Controls Tumor Spheroid Size and Morphology by Suppressing Proliferation and Inducing Apoptosis in Cancer Cells. *PLoS One* **2009**, *4* (2), e4632.

(149) Sahay, G.; Alakhova, D. Y.; Kabanov, A. V. Endocytosis of Nanomedicines. *J. Control. Release* **2010**, *145* (3), 182–195.

(150) Baeza, A. Ceramic Nanoparticles for Cancer Treatment. *Bio-Ceramics with Clin. Appl.* **2014**, 421–455.

(151) Stella, B.; Arpicco, S.; Peracchia, M. T.; Desmaële, D.; Hoebeke, J.; Renoir, M.; D'Angelo, J.; Cattel, L.; Couvreur, P. Design of Folic Acid-Conjugated Nanoparticles for Drug Targeting. *J. Pharm. Sci.* **2000**, *89* (11), 1452–1464.

(152) Singh, M. Transferrin As A Targeting Ligand for Liposomes and Anticancer

Drugs. *Curr. Pharm. Des.* **1999**, *5* (6), 443–451.

(153) Roland E. Kontermann. Dual Targeting Strategies with Bispecific Antibodies. *MAbs* **2012**, *4* (2), 182–197.

(154) Wang, M.; Thanou, M. Targeting Nanoparticles to Cancer. *Pharmacol. Res.* **2010**, *62* (2), 90–99.

(155) Sakhrani, N. M.; Padh, H. Organelle Targeting: Third Level of Drug Targeting. *Drug Des. Devel. Ther.* **2013**, *7*, 585–599.

(156) Kidd, J. F.; Pilkington, M. F.; Schell, M. J.; Fogarty, K. E.; Skepper, J. N.; Taylor, C. W.; Thorn, P. Paclitaxel Affects Cytosolic Calcium Signals by Opening the Mitochondrial Permeability Transition Pore. *J. Biol. Chem.* **2002**, *277* (8), 6504–6510.

(157) Fulda, S.; Scaffidi, C.; Susin, S. A.; Krammer, P. H.; Kroemer, G.; Peter, M. E.; Debatin, K. M. Activation of Mitochondria and Release of Mitochondrial Apoptogenic Factors by Betulinic Acid. *J. Biol. Chem.* **1998**, *273* (51), 33942–33948.

(158) Siegel, R. L.; Miller, K. D.; Jemal, A. Cancer Statistics, 2018. *CA. Cancer J. Clin.* **2018**, *68* (1), 7–30.

(159) Blanco, E.; Shen, H.; Ferrari, M. Principles of Nanoparticles Design for Overcoming Biologica Barriers for Drug Delivery. *Nat Biotechnol* **2015**, *33* (9), 941–951.

(160) Chauhan, V. P.; Stylianopoulos, T.; Boucher, Y.; Jain, R. K. Delivery of Molecular and Nanoscale Medicine to Tumors: Transport Barriers and Strategies. *Annu. Rev. Chem. Biomol. Eng.* **2011**, *2* (1), 281–298.

(161) Anchordoquy, T. J.; Barenholz, Y.; Boraschi, D.; Chorny, M.; Decuzzi, P.; Dobrovolskaia, M. A.; Farhangrazi, Z. S.; Farrell, D.; Gabizon, A.; Ghandehari,

H.; et al. Mechanisms and Barriers in Cancer Nanomedicine: Addressing Challenges, Looking for Solutions. *ACS Nano* **2017**, *11* (1), 12–18.

(162) Kunjachan, S.; Rychlik, B.; Storm, G.; Kiessling, F.; Lammers, T. Multidrug Resistance: Physiological Principles and Nanomedical Solutions. *Adv. Drug Deliv. Rev.* **2013**, *65* (13–14), 1852–1865.

(163) Xue, X.; Liang, X. J. Overcoming Drug Efflux-Based Multidrug Resistance in Cancer with Nanotechnology. *Chin. J. Cancer* **2012**, *31* (2), 100–109.

(164) Ganoth, A.; Merimi, K. C.; Peer, D. Overcoming Multidrug Resistance with Nanomedicines. *Expert Opin. Drug Deliv.* **2015**, *12* (2), 223–238.

(165) Moghimi, S. .; Patel, H. . Serum-Mediated Recognition of Liposomes by Phagocytic Cells of the Reticuloendothelial System – The Concept of Tissue Specificity. *Adv. Drug Deliv. Rev.* **1998**, *32* (1–2), 45–60.

(166) Tenzer, S.; Docter, D.; Kuharev, J.; Musyanovych, A.; Fetz, V.; Hecht, R.; Schlenk, F.; Fischer, D.; Kiouptsi, K.; Reinhardt, C.; et al. Rapid Formation of Plasma Protein Corona Critically Affects Nanoparticle Pathophysiology. *Nat. Nanotechnol.* **2013**, *8* (10), 772–781.

(167) Harris, J. M.; Chess, R. B. Effect of Pegylation on Pharmaceuticals. *Nat. Rev. Drug Discov.* **2003**, *2* (3), 214–221.

(168) Hamilton, A.; Biganzoli, L.; Coleman, R.; Mauriac, L.; Hennebert, P.; Awada, A.; Nooij, M.; Beex, L.; Piccart, M.; Van Hoorebeeck, I.; et al. EORTC 10968: A Phase I Clinical and Pharmacokinetic Study of Polyethylene Glycol Liposomal Doxorubicin (Caelyx(R), Doxil(R)) at a 6-Week Interval in Patients with Metastatic Breast Cancer. *Ann. Oncol.* **2002**, *13* (6), 910–918.

(169) Oldenborg, P. A.; Zheleznyak, A.; Fang, Y. F.; Lagenaur, C. F.; Gresham, H. D.; Lindberg, F. P. Role of CD47 as a Marker of Self on Red Blood Cells. *Science*

2000, *288* (5473), 2051–2054.

(170) Pia L. Rodriguez, Takamasa Harada, David A. Christian, D. A. P.; Richard K. Tsai, D. E. D. Minimal "Self" Peptides That Inhibit Phagocytic Clearance and Enhance Delivery of Nanoparticles. *Science (80-.).* **2013**, *339*.

(171) Parodi, A.; Quattrocchi, N.; van de Ven, A. L.; Chiappini, C.; Evangelopoulos, M.; Martinez, J. O.; Brown, B. S.; Khaled, S. Z.; Yazdi, I. K.; Enzo, M. V.; et al. Synthetic Nanoparticles Functionalized with Biomimetic Leukocyte Membranes Possess Cell-like Functions. *Nat. Nanotechnol.* **2013**, *8* (1), 61–68.

(172) Hu, C.-M. J.; Zhang, L.; Aryal, S.; Cheung, C.; Fang, R. H.; Zhang, L. Erythrocyte Membrane-Camouflaged Polymeric Nanoparticles as a Biomimetic Delivery Platform. *Proc. Natl. Acad. Sci. U. S. A.* **2011**, *108* (27), 10980–10985.

(173) Chen, Z.; Zhang, L.; Song, Y.; He, J.; Wu, L.; Zhao, C.; Xiao, Y.; Li, W.; Cai, B.; Cheng, H.; et al. Hierarchical Targeted Hepatocyte Mitochondrial Multifunctional Chitosan Nanoparticles for Anticancer Drug Delivery. *Biomaterials* **2015**, *52* (1), 240–250.

(174) Villaverde, G.; Nairi, V.; Baeza, A.; Vallet-Regí, M. Double Sequential Encrypted Targeting Sequence: A New Concept for Bone Cancer Treatment. *Chem. - A Eur. J.* **2017**, *23* (30), 7174–7179.

(175) Heldin, C.-H.; Rubin, K.; Pietras, K.; Ostman, A. High Interstitial Fluid Pressure - an Obstacle in Cancer Therapy. *Nat. Rev. Cancer* **2004**, *4* (10), 806–813.

(176) Young, J. S.; Llumsden, C. E.; Stalker, A. L. The Significance of the "tissue Pressure" of Normal Testicular and of Neoplastic (Brown-Pearce Carcinoma) Tissue in the Rabbit. *J. Pathol. Bacteriol.* **1950**, *62* (3), 313–333.

(177) Jain, R. K. Transport of Molecules in the Tumor Interstitium : A Review Transport of Molecules in the Tumor Interstitium : A Review1. *Cancer Res.* **1987**, *47* (17),

3039–3051.

(178) Khawar, I. A.; Kim, J. H.; Kuh, H.-J. Improving Drug Delivery to Solid Tumors: Priming the Tumor Microenvironment. *J. Control. Release* **2015**, *201*, 78–89.

(179) Milosevic, M.; Fyles, A.; Hedley, D.; Hill, R. The Human Tumor Microenvironment: Invasive (Needle) Measurement of Oxygen and Interstitial Fluid Pressure. *Semin. Radiat. Oncol.* **2004**, *14* (3), 249–258.

(180) Provenzano, P. P.; Cuevas, C.; Chang, A. E.; Goel, V. K.; Von Hoff, D. D.; Hingorani, S. R. Enzymatic Targeting of the Stroma Ablates Physical Barriers to Treatment of Pancreatic Ductal Adenocarcinoma. *Cancer Cell* **2012**, *21* (3), 418–429.

(181) Jacobetz, M. A.; Chan, D. S.; Neesse, A.; Bapiro, T. E.; Cook, N.; Frese, K. K.; Feig, C.; Nakagawa, T.; Caldwell, M. E.; Zecchini, H. I.; et al. Hyaluronan Impairs Vascular Function and Drug Delivery in a Mouse Model of Pancreatic Cancer. *Gut* **2013**, *62* (1), 112–120.

(182) Jain, R. K.; Tong, R. T.; Munn, L. L. Effect of Vascular Normalization by Antiangiogenic Therapy on Interstitial Hypertension, Peritumor Edema, and Lymphatic Metastasis: Insights from a Mathematical Model. *Cancer Res.* **2007**, *67* (6), 2729–2735.

(183) Jain, R. K. Normalization of Tumor Vasculature: An Emerging Concept in Antiangiogenic Therapy. *Science (80-.).* **2005**, *307* (5706), 58–62.

Chapter II

Objetives

II. Objetives

According to the importance of nanomedicine as a novel and promising field which can provide alternatives for unmet clinical situations, the main objective of this thesis has been to design smart nanocarriers able to operate in three specific areas:

The first of them was the development of drug nanocarriers capable to penetrate deeply within solid tumors in order to overcome one of the most important barrier of all nanomedicines, which is the dense extracellular matrix present in tumoral tissues. Our approach consisted in the synthesis of pH-sensitive polymeric nanocapsules which transport collagenase inside. These capsules were designed to present a dual function: protect the enzyme during its travel through the patient body and control release of the proteolytic enzymes when the capsules reach the mild acidic tumoral environment. The collagenase nanocapsules were attached on the surface of model nanocarriers (mesoporous silica and protocells) in order to evaluate the penetration capacity of the nanodevices and their capacity to destroy tumoral cells employing tridimensional tumoral tissue models showing excellent results in comparison with the nanodevices which did not carry the capsules.

The second one has been the development of dual-targeted nanodevices based on mesoporous silica nanoparticles asymmetrically decorated in a Janus configuration in order to accomplish a sequential targeting of tumoral cells and mitochondria. This system is based on the fact that releasing drugs in the vicinity of certain organelles increases their therapeutic effect by reducing the necessary doses.

Finally, the third area of this thesis was focused in the development of collagenase nanocapsules capable to maintain a prolonged release of the proteolytic enzymes during

more than 10 days, in order to treat fibrotic lesions. These capsules aim to improve the therapeutic effect of the current clinical treatment, which consists of the administration of the free enzyme.

II. Objetivos

De acuerdo con la importancia de la nanomedicina como un campo novedoso y prometedor que puede proporcionar alternativas a situaciones clínicas insatisfechas, el objetivo principal de esta tesis ha sido el diseño de nanomedicinas inteligentes capaces de operar en tres áreas específicas:

El primero de ellos ha sido el desarrollo de nanotransportadores de fármacos capaces de penetrar profundamente en los tumores sólidos superando una de las barreras más importantes de todas las nanomedicinas, que es la densa matriz extracelular presente en los tejidos tumorales. Nuestro enfoque consistió en la síntesis de nanocápsulas poliméricas sensibles al pH que transportan colagenasa en su interior. Estas cápsulas fueron diseñadas para presentar una doble función: la protección de la enzima durante su recorrido por el cuerpo del paciente y la liberación controlada de las enzimas proteolíticas cuando las cápsulas alcanzan el ambiente tumoral ácido leve. Las nanocápsulas de colagenasa se anclaron a la superficie de nanopartículas modelo (sílice mesoporosa y protocápsulas) a fin de evaluar su eficacia, en cuanto a la capacidad de penetración de los nanodispositivos y su capacidad de destrucción de las células tumorales, se evaluó empleando modelos tridimensionales de tejido tumoral.

El segundo ha sido el desarrollo de nanodispositivos de doble vectorización basados en nanopartículas de sílice mesoporosa decoradas asimétricamente en una configuración Janus para lograr un objetivo secuencial de células tumorales y mitocondrias. Este sistema se basa en el hecho de que liberar fármacos en la proximidad de ciertos orgánulos aumenta su efecto terapéutico disminuyendo las dosis necesarias.

Finalmente, la tercera área de esta tesis se centró en el desarrollo de nanocápsulas de colagenasa capaces de mantener una liberación prolongada de las enzimas proteolíticas durante más de 10 días, para tratar lesiones fibróticas. Estas cápsulas tienen como objetivo mejorar el efecto terapéutico del actual tratamiento en clínica, que consiste en la administración de la enzima libre.

Chapter III

Results and Discussion

III. Results and discussion

This chapter has been separated in three sections. The first of them, titled: "Collagenase nanocapsules to improve nanocarriers penetration in solid tumors" describes a novel strategy which tries to overcome one of the most important limitation of all nanomedicines in antitumoral therapy, which is their poor penetration within tumoral tissues. With this aim, Collagenase (an enzyme able to degrade the main component of ECM, collagen) has been encapsulated within pH-sensitive polymeric nanocapsules and them, these nanocapsules have been anchored on the surface of two nanocarrier models, mesoporous silica nanoparticles and protocells. Thus, the release of collagenase in the extracellular media has provided a remarkable improvement in the penetration of the nanodevices achieving a homogeneous distribution of them in deeper zones of the malignant tissue. This fact has resulted in a higher therapeutic efficacy than the systems without the collagenase nanocapsules.

In the second section titled: "Asymmetric nanoparticles as elements of dual targeting cell-organelle" Janus-type mesoporous silica nanoparticles with two targeting moieties asymmetrically distributed along the surface (one of them selective for tumoral cells and the other one for mitochondria) have been synthesized. Their capacity to be selectively engulfed by tumoral cells and once there, to induce a high therapeutic response, as a consequence of the close proximity to mitochondria, have been evaluated.

Finally, in the third section titled "Collagenase nanocapsule to treat fibrosis lesions" collagenase nanocapsules which exhibited a prolonged and controlled release of the

housed enzyme during long periods of time (up to more than 10 days) have been synthesized and evaluated *in vivo* as novel treatment to fibrotic lesions.

Section III.I.

Collagenase Nanocapsules to Improve Nanocarriers Penetration in Solid Tumors

Current strategies to improve the nanoparticles penetration in solid tumors. Use of proteolytic enzymes.

The abnormally dense extracellular matrix of solid tumors supposes a strong barrier that restrict the penetration of nanodevices in tumoral tissues (**Figure 1**), thereby limiting their efficacy for cancer imaging and therapy.

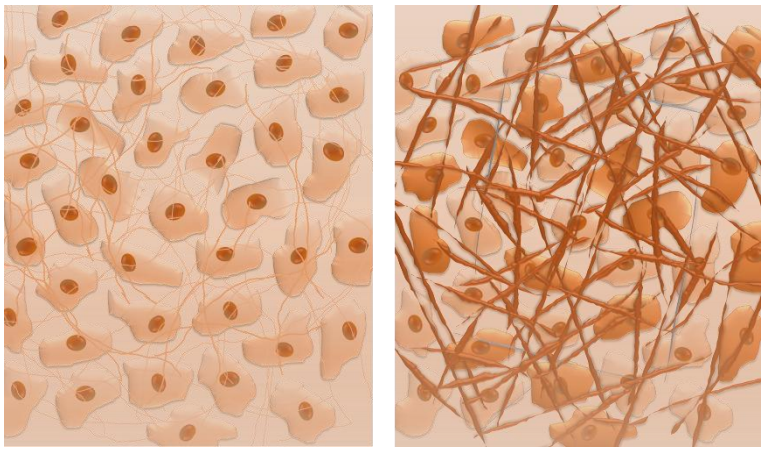

Figure 1. *Extracellular matrix (ECM) of a) normal tissue b) tumoral tissue.*

As was mentioned in the introduction, there are different approaches to overcome this barrier (**Figure 2**). One of them consist in the use of ultrasounds.[1] Ultrasounds are mechanical waves that can be focused in a local and deeper area in the body, inducing a propulsion force which can propel the nanocarrier into the tumoral tissue. In certain conditions, ultrasound can produce cavitation. This phenomenon consists in the formation of oscillations of a gas bubble in a fluid.[2] At high pressure, the gas bubble oscillations around the equilibrium radius can be unbalanced so, the gas bubble grows in an unstably way during decompression period and then, it suffers an abrupt collapse during the compression. This effect is called inertial cavitation and has been studied in order to improve the nanocarrier extravasation and penetration in simulated malignant tissues.[3] Furthermore, the use of polymeric nanocups, which act as cavitation nuclei, reduced the

pressure needed to achieve the inertial cavitation up to biologically acceptable pressure range enhancing the penetration of the nanocarriers.[4,5] However, this strategy requires the use of complex equipment, technical experts trained in the use of ultrasounds in clinic, the precise evaluation of the exposition period and the determination of the exact time when the nanodevices have reached the tumoral zone.

Other strategy available to improve the nanocarrier penetration inside the tumor is the normalization of the extracellular tumor matrix previously to the nanomedicine-based treatment.[6,7] Additionally, it is also possible to provide to the nanocarriers with the ability to digest the dense ECM during their route through the tumor.[8] These strategies are based on the co-administration of proteolytic enzymes together with the drug nanocarriers or the decoration of nanoparticle surface with these type of enzymes. It is expected that, a significant reduction of the matrix stiffness by the digestion of the compact ECM network, facilitates the diffusion of the nanocarriers within the ECM achieving a homogeneous distribution of the nanomedicines in the diseased zone. Different research groups have studied the effect of proteolytic enzymes in relation with the diffusion of nanoparticles. Magzoub *et al*. found that intratumoral injections of collagenase increased the diffusion of 10KDa dextran by 2-folds in all depths in the tumor tissue.[9] The similar treatment with Cathepsin C, that digest decorin ,which is a proteoglycan present in the ECM, give rise at similar improvement in the particle diffusion, similar to the case observed using collagenase.[9] In contrast, the administration of hyaluronidase showed a less pronounced effect. This fact is due to hyaluronidase treatment result in a collapse of water-swelled cage structures, increasing the viscous hindrance.[10] Relative to bigger molecules, such as albumin or 500kDa dextran, the administration of collagenase and Cathepsin C also supposed a significant improvement in the penetration capacity, higher than 10-fold efficient diffusion of these macromolecules at 2mm of depth in the tumor.

In other studies, it was found that collagenase treatment in tumors with high content in collagen, such as Human soft tissue HSTS26T sarcoma and Mu89 melanoma, induces a 2-fold improve in antibodies diffusion[10,11,9] and 3-fold in the case of herpes simplex virus.[6,12,13] On the other hand, it has been reported that multicellular spheroids treated with 0.1mg/ml of collagenase showed a significant decrease in collagen content, enough to achieve an increase in nanoparticle penetration.[14] The penetration of nanoparticles with 20, 40, 100 and 200 nm of diameter were evaluated in spheroids which were treated, or not, with collagenase. The administration of collagenase increased the penetration of 20 nm and 40 nm nanoparticles by 6.9 and 11.6 fold, whereas the effect in 100 and 200 nm nanoparticles was an increase of 3.2 and 1,5 fold respect to untreated spheroids.

High collagenase levels have been associated with more aggressive tumors because high proteolytic activity in the tissue favors the migration of the tumoral cells outside the tumors and therefore, it could lead to the apparition of metastasis in other tissues.[15] For this reason, it is reasonable to suppose that the administration of proteolytic enzymes previous to the nanoparticle treatment could enhance the metastasis risk. Thus, surface modification of drug nanocarriers with these enzymes has emerged as promising alternative due to the synchronized effect of the ECM digestion, which facilitates the nanoparticle diffusion, with the sustained release of cytotoxic drugs that simultaneously destroy the tumoral cells. As an example of this strategy, polystyrene nanoparticles were decorated with collagenase showing a 4-fold increase in particle penetration in comparison with nanoparticles coated with bovine serum albumin (BSA).[14] The penetration capacity of the nanoparticles decorated with proteolytic enzymes was also studied with mesoporous silica nanoparticles with bromelain on their surface. This coating induced a 2-fold increase in ECM penetration in comparison to naked nanoparticles.[8]

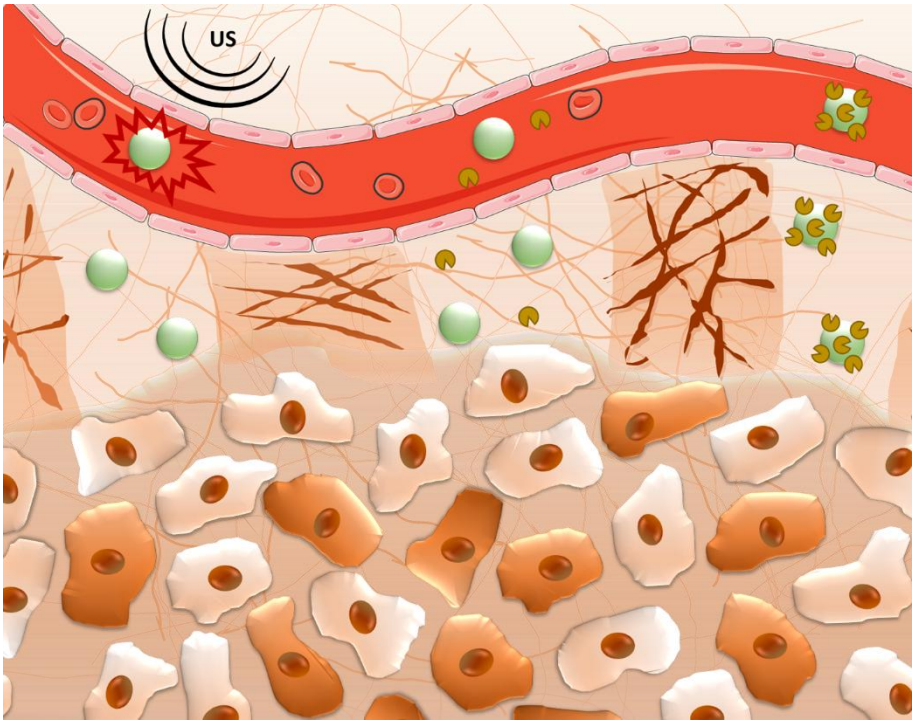

Figure 2. *Different strategies to improve nanocarriers penetration, such as ultrasound propulsion, co-administration with proteolytic enzymes and attachment of proteolytic enzymes on nanocarriers surfaces.*

The direct attachment of proteins on the particle surface is limited by the low physicochemical stability of proteins in biological fluids. Proteins are formed by peptide chains arranged in a three-dimensional conformation which confers them their function. The proteins function depends on both the aminoacid sequence and the specific folding. Unfortunately, the functional proteins folding is only slightly more stable that its unfolded form (the term unfold form is refereed to any non-functional conformational structure of the protein). The functional protein conformation was maintained by hydrophobic and hydrophilic and electrostatic interactions, Van der Waals forces and hydrogen bounding between chains of the protein which contribute to decrease the free energy of Gibbs of the folding process.[16] However, entropy is unfavorable to this process, and its contribution is proportional to temperature.

$$\Delta G = \Delta H - T \cdot \Delta S$$

- G: Free energy of Gibbs
- H: Enthalpy
- T: Temperature.
- S: Entropy

This functional structure resulted on a precise balance between stabilizing and disestablishing forces. Thus, small changes in the temperature or in the microenvironment such as pH, salt concentration or the nature of the ions present in the media, can alter the force contributions resulting in protein denaturalization.[16] Besides this unfolding propensity, proteins are really sensitive to the presence of proteolytic enzymes, which are enzymes capable to digest proteins and are abundant in living tissues. The presence of these proteolytic enzymes in plasma is one of the main responsible of their low half-life. Moreover, proteins can be rapidly removed from the bloodstream by kidneys which rapidly excrete smaller proteins, whereas the larger proteins such as glycoproteins and lipoproteins, are phagocytosed by mononuclear phagocytic system (MPS).[17] Moreover, the mayor part of the natural proteins are unable to enter inside the cells, due to electrostatic repulsions with the components of the cell membrane.[18] Even if they are introduced inside the cell using a nanocarrier or any other strategy, these macromolecules are usually degraded in the endosomes/lysosomes.[19]

For all these reasons, clinical use of proteins is severely hampered. There are numerous strategies to improve the protein stability and improve their delivery in human body. These strategies are collected in the Review "Nanotechnological Strategies for Protein Delivery" of the section Annex I. In this review, the description of each strategy is

detailed paying more attention of the use of polymeric nanocapsules which is one of most attractive strategies for delivering labile macromolecules.[20]

Polymeric nanocapsules able to house proteins inside have been proposed as suitable system for transporting labile macromolecules to the inner cellular space. These nanocapsules improve the thermal stability of the housed proteins providing protection of against external insults such as oxidative agents, extreme pH values and the presence of other proteolytic enzymes. This encapsulation strategy can increase the circulation times of the transported protein from hours to days,[21] reducing at the same time their immune response. For example, levels of white blood cells after urate oxidase administration are 2 fold higher that after its encapsulated form administration.[22] These properties induce that nanocapsules exhibit an improve and more sustained therapeutic effect of many enzymes.[22] All these properties make the protein nanocapsules a potent alternative to free enzyme administration and have demonstrated a better therapeutic effect in different applications as growth tumoral suppresion[23,24], hyperucemia[21] or hyperoxaluria[25] treatment, among others.

The polymeric nanocapsules can be designed as degradable or non-degradable systems depending of the type of hosted protein. For example, proteins that act on small substrates which are permeable to polymeric mesh can be encapsulated within non-degradable nanocapsules. These capsules are commonly synthesized employing non-degradable crosslinkers, as *N,N´*-methylene bisacrylamide (MBA).[26,27,28,29,30] Non-degradable nanocapsules have been employed in nanomedicine field.[31,32,22,33,21,27,28] For example, nanodevices loaded with Indole acetic (IAA), a non-toxic pro-drug, were externally decorated with Horseradish peroxidase (HRP), the enzyme responsible of prodrug activation.[34] This system generated cytotoxic species *in situ* once accumulated in the tumoral cell. Other application of non-degradable nanocapsules in a different and more

exotic field than nanomedicine is their use for improving the propulsion force of nanomachines. Commonly, nanomotors are fueled by the decomposition of hydrogen peroxide using both platinum or catalase, as catalysts.[35] Nanocapsules of catalase were able to protect the housed enzyme against oxidation and to improve its stability under high temperatures and in presence of proteases. As consequence, nanomotors equipped with catalase nanocapsules remained its propulsion capacity during several work cycles.[30]

When the transported protein must be released in order to guarantee its action, these nanocapsules are designed with a degradable behavior. Thus, these nanocapsules release the host enzyme under determined stimulus such as certain enzymes, changes in the redox potential or in pH (**Figure 3**).

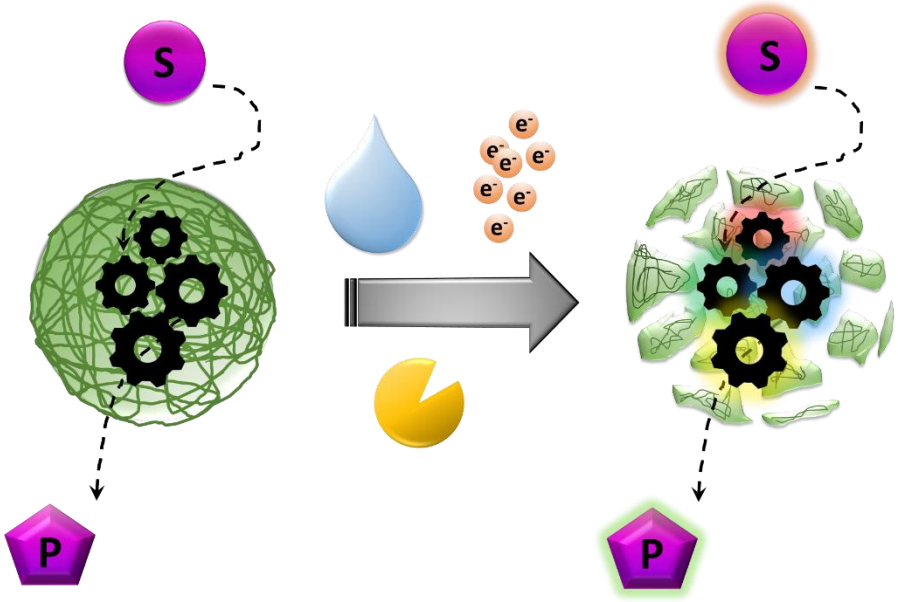

Figure 3. *Degradable capsules until different stimulus.*

This behavior can be provided by a planned choice of the crosslinker which conforms the polymeric mesh. As example, cytosol presents a lower redox potential than the extracellular media, due to a high concentration of glutathione (GSH) inside the cells. GSH is found at milimolar range in the inner cellular space, which is significantly higher

than the micromolar concentration found in the extracellular milieu. Thus, it is possible to design nanocapsules capable to release the hosted enzyme once it reaches the cytosol using crosslinkers which contains disulfide bonds breakable by the action of GSH.[36] These capsules exhibited a redox-responsive release of Caspase 3 (CP3) nanocapsules and demonstrated that they were be able to release the cargo in the cytosol. Other stimuli widely used is the presence of proteases which are usually more abundant in malignant tissues[37] or inside certain cells.[38] In order to exploit this stimulus, the crosslinker should be designed containing specific sequences recognized by the enzyme of interest. As example, Tang *et al.* designed nanocapsules which are disassembled upon cell endocytosis due to the presence of furin, an essential intracellular endoprotease, in order to avoid the protein degradation inside of lysosomes.[38] Finally, it is possible to design nanocapsules that suffer degradation in mild acidic conditions,[23] as for example the tumoral environment.[39] Nanocapsules crosslinked with ethyleneglycol dimethacrylate or glycerol dimethacrylate, which are pH-sensitive, have demonstrated to keep the protein unaltered at physiological pH and release the hosted protein at mild acid conditions (pH 5.5).[23,40]

Collagenase nanocapsules to improve nanocarriers penetration in tumoral tissues

As was mentioned above, the dense ECM is a herculean barrier for the drug nanocarriers penetration and therefore, this fact severely compromises the nanomedicine-based tumoral treatments. The scientific community has struggled with this restriction providing different alternatives in order to overwhelm this limitation, such as the administration of proteolytic enzymes or their attachment on the nanoparticle surface. However, the co-administration of these enzymes and nanodevices could increase tumoral cell dissemination due to the different action kinetic of each system and additionally, the labile nature of enzymes limits their efficacy.

In this section, the design of degradable nanocapsules capable to transport and release proteolytic enzymes and their use for improving the tumor penetration capacity of nanomedicines will be described. These nanocapsules have been designed to keep the housed enzyme within the polymer capsule and release it when the system reaches the acidic environment present in many solid tumors. Collagenase was chosen as proteolytic enzyme due to collagen is the main component of the tumoral ECM. Therefore, this enzyme specifically digest collagen that form the interconnected networking that support the tumoral tissue. For the construction of the polymeric nanocapsules, different monomers have been employed: Acrylamide (AAm) as structural monomer and 2-Aminoethyldimethacrylate hydrochloride (Am) as an extra structural monomer which provides, in this case, positive charges on the nanocapsules at physiological pH. These positive charges increase the colloidal stability of these systems in aqueous environment. Additionally, the presence of a positive charge on this monomer facilitates its adsorption onto the negatively charged protein which improves the efficacy of the encapsulation

process. The pH-sensitive behavior was provided by the incorporation of ethylene glycol dimethacrylate (EG) as crosslinker because this molecule is hydrolysable in mild acidic conditions.[23] The encapsulation process was carried out by free radical polymerization initiated by the addition of ammonium persulfate and *N,N,N´,N´*-tetramethylenediamine (TMEDA) which act as radical activators in aqueous solution at room temperature.

The resultant collagenase nanocapsules achieved a significant protection of the enzyme against proteolysis by proteases which can be present in living tissues, at the same time that provide pH-responsive behavior. These nanocapsules were anchored on the surface of mesoporous silica nanoparticles, chosen as nanoparticle model, in order to evaluate its efficacy as enhancer of the nanoparticle penetration in malignant tissues. MSN were selected as nanocarrier model due to their excellent properties such as, excellent biocompatibility, high cargo capacity and easy functionalization.

The evaluation of the penetration of these nanodevices was done employing 3D-collagen gels with tumoral cells embedded within the collagen matrix. This model tissue exhibits similar rheological properties that a real tumoral tissue.

The system which was decorated with collagenase nanocapsules exhibited more homogeneous and deeper distribution within the tissue than the naked particles (**Figure 4**). This result demonstrated that this strategy can be effectively applied for improving the penetration of nanomedicines in diseased tissues and therefore, it could significantly enhance the therapeutic efficacy of the therapies based on nanoparticles.

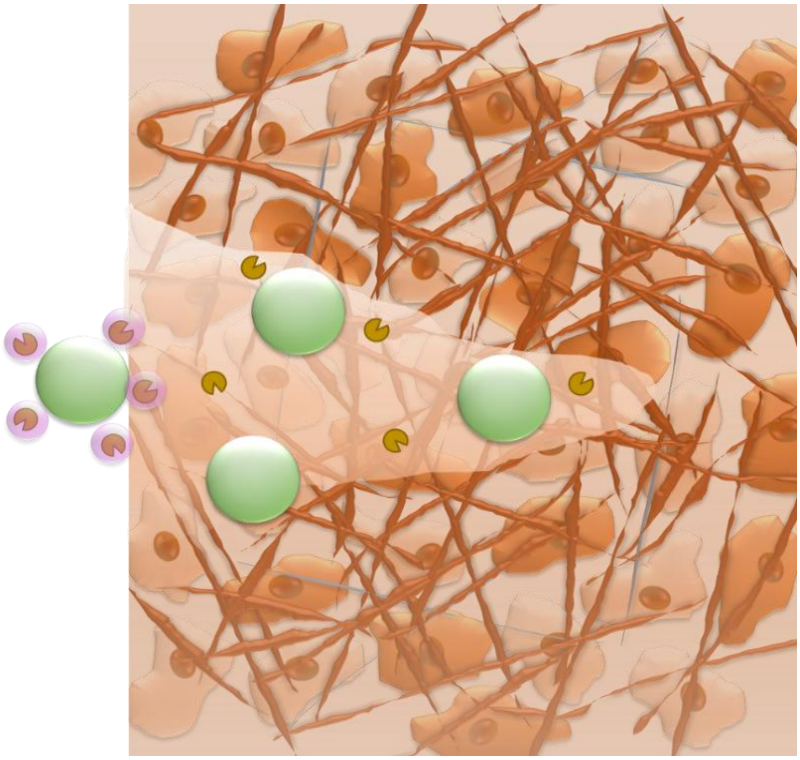

Figure 4. *Collagenase nanocapsules on nanocarrier surface and its penetration in a tumoral extracellular matrix (ECM)*

Once confirmed the protective function of the encapsulation of collagenase and the enhanced penetration capacity of nanoparticles decorated with these capsules, these nanocapsules were attached on a drug loaded nanoparticle in order to evaluate the full impact of this strategy. In this case, we have employed Protocells as nanocarrier model. Protocells are formed by mesoporous silica nanoparticles covered with a lipid bilayer. This class of system has been extensively studied[41,42,43,44] by the research group directed by Prof. Jeffrey Brinker in New Mexico University, in which a short research stay of 3 months was carried out during this thesis.

This class of systems are an interesting device that synergistically combine the advantageous nature of MSN with the interesting properties of liposomes. Thus, they exhibit beneficial characteristics of MSN such as robustness, controllable size and shape, ordered pore architecture and tunable diameter and high specific surface with the

characteristics of liposomes, as long circulation times and low inherent toxicity. Moreover, the presence of the lipid bilayer avoids the premature release of the drugs trapped within the silica matrix being able to encapsulate a wide type of cargos and combinations of them. Once the system reaches the inner cellular space, the cargo is released due to the mild acidic conditions present in endosomes.[44,45,46,47,48,49,43,50] There are several strategies to provide pH-reponsive lipid bilayers, such as use as pH-sensitive components as polyhistidine residues,[51,52] polymers with protonable groups[53,54] or cleavable bonds,[55,56,57] pH sensitive phospholipids as DOBAQ or DOPE based bilayers,[58,59] and the use of fusogenic peptide, being H5WYG an example.[43] Also, this type of devices have demonstrated passive and active targeting by EPR to solid tumors in vivo.[47,48,49,60]

In our work, the external surface of the lipid bilayer was decorated with an anti-EGFR antibody, whose receptors are overexpressed by lung cancer cells.[61,62] Thus, the nanodevices can be selectively engulfed by lung tumoral cells (A549). Finally, the external surface of the protocells was decorated with collagenase nanocapsules, which provide the capacity to digest the ECM. A potent cytotoxic agent (topotecan) was loaded in the MSN core (**Figure 5**). Topotecan was chosen because is a drug which exhibits a potent antitumoral effect but it suffers instability when is directly injected in the blood stream, losing its therapeutic effect in a few hours[63]. However, it is well-stablished that the encapsulation of this compound within nanocarrier improves its efficicacy.[64]

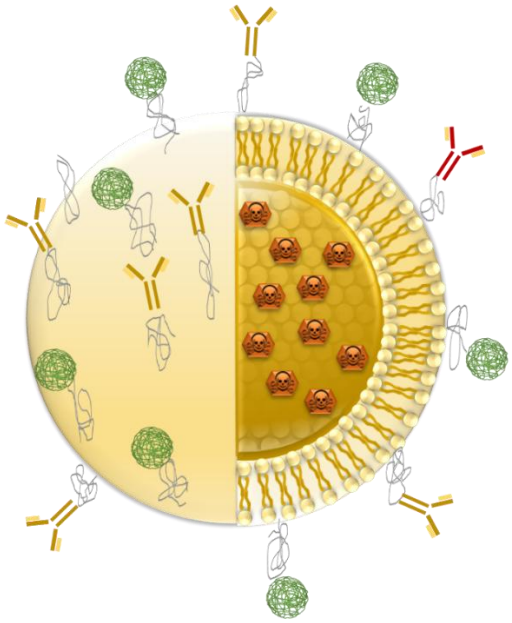

Figure 5. *Multifunctional protocell*.

The efficacy of the complete system was evaluated in a three dimensional tumoral tissue model. This model consisted in a cancerous cell monolayer covered with a collagen gel of 200 μm of thickness, also with tumoral cells embedded, in order to provide similar rheological parameters that a real tumoral tissue (**Figure 6**). This gel mimics the real barrier which a nanocarrier find once arrives to the malignant tissue.

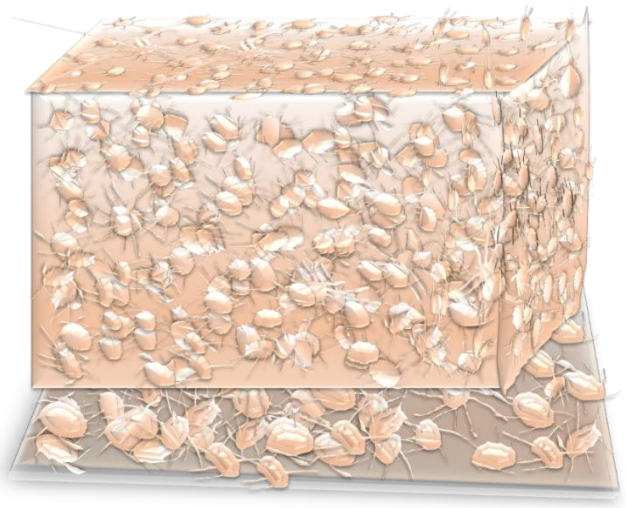

Figure 6. *Tumoral Extracellular Matrix model.*

In order to evaluate the full response of this system (improved penetration, enhanced cellular internalization and tumoral cell destruction) protocells, decorated or not with collagenase nanocapsules, were placed on the top of the collagen gel. The results confirmed that the collagen gel totally hampered the penetration of nanoparticles without collagenase nanocapsules whereas, the complete system was capable to reach the deep cell monolayer, causing their destruction. In conclusion, this nanocarrier exhibited a multitasking capacity being able to:

1)To reach deep tumoral zones.

2) To be selectively engulfed by tumoral cells.

3) To cause the eradication of these cells.

This multifunctional platform has demonstrated to be able to deliver selectively antitumoral drugs into deeper zones of malignant tissues. The application of this strategy can suppose an important advance in the design of future nanodevices which could achieve an improved therapeutic effect due to the homogenous distribution of them within the malignancy.

References:

(1) Coussios, C. C.; Roy, R. A. Applications of Acoustics and Cavitation to Noninvasive Therapy and Drug Delivery. *Annu. Rev. Fluid Mech.* **2008**, *40* (1), 395–420.

(2) Arvanitis, C. D.; Bazan-Peregrino, M.; Rifai, B.; Seymour, L. W.; Coussios, C. C. Cavitation-Enhanced Extravasation for Drug Delivery. *Ultrasound Med. Biol.* **2011**, *37* (11), 1838–1852.

(3) Paris, J. L.; Mannaris, C.; Cabañas, M. V.; Carlisle, R.; Manzano, M.; Vallet-Regí, M.; Coussios, C. C. Ultrasound-Mediated Cavitation-Enhanced Extravasation of Mesoporous Silica Nanoparticles for Controlled-Release Drug Delivery. *Chem. Eng. J.* **2017**.

(4) Kwan, J. J.; Graham, S.; Myers, R.; Carlisle, R.; Stride, E.; Coussios, C. C. Ultrasound-Induced Inertial Cavitation from Gas-Stabilizing Nanoparticles. *Phys. Rev. E - Stat. Nonlinear, Soft Matter Phys.* **2015**, *92* (2), 1–5.

(5) Kwan, J. J.; Myers, R.; Coviello, C. M.; Graham, S. M.; Shah, A. R.; Stride, E.; Carlisle, R. C.; Coussios, C. C. Ultrasound-Propelled Nanocups for Drug Delivery. *Small* **2015**, *11* (39), 5305–5314.

(6) Jain, R. K.; Stylianopoulos, T. Delivering Nanomedicine to Solid Tumors. *Nat. Rev. Clin. Oncol.* **2010**, *7* (11), 653–664.

(7) Jain, R. K. Normalizing Tumor Microenvironment to Treat Cancer: Bench to Bedside to Biomarkers. *J. Clin. Oncol.* **2013**, *31* (17), 2205–2218.

(8) Parodi, A.; Haddix, S. G.; Taghipour, N.; Scaria, S.; Taraballi, F.; Cevenini, A.;

Yazdi, I. K.; Corbo, C.; Palomba, R.; Khaled, S. Z.; Martinez, J. O.; Brown, B. S.; Isenhart, L.; Tasciotti, E. Bromelain Surface Modification Increases the Diffusion of Silica Nanoparticles in the Tumor Extracellular Matrix. *ACS Nano* **2014**, *8* (10), 9874–9883.

(9) Magzoub, M.; Jin, S.; Verkman, A. S. Enhanced Macromolecule Diffusion Deep in Tumors after Enzymatic Digestion of Extracellular Matrix Collagen and Its Associated Proteoglycan Decorin. *FASEB J.* **2007**, *22* (1), 276–284.

(10) Alexandrakis, G.; Brown, E. B.; Tong, R. T.; McKee, T. D.; Campbell, R. B.; Boucher, Y.; Jain, R. K. Two-Photon Fluorescence Correlation Microscopy Reveals the Two-Phase Nature of Transport in Tumors. *Nat. Med.* **2004**, *10* (2), 203–207.

(11) Netti, P. a; Berk, D. a; Swartz, M. a; Grodzinsky, a J.; Jain, R. K. Role of Extracellular Matrix Assembly in Interstitial Transport in Solid Tumors. *Cancer Res.* **2000**, *60* (9), 2497–2503.

(12) McKee, T. D.; Grandi, P.; Mok, W.; Alexandrakis, G.; Insin, N.; Zimmer, J. P.; Bawendi, M. G.; Boucher, Y.; Breakefield, X. O.; Jain, R. K. Degradation of Fibrillar Collagen in a Human Melanoma Xenograft Improves the Efficacy of an Oncolytic Herpes Simplex Virus Vector. *Cancer Res.* **2006**, *66* (5), 2509–2513.

(13) Mok, W.; Stylianopoulos, T.; Boucher, Y.; Jain, R. K. Mathematical Modeling of Herpes Simplex Virus Distribution in Solid Tumors: Implications for Cancer Gene Therapy. *Clin. Cancer Res.* **2009**, *15* (7), 2352–2360.

(14) Goodman, T. T.; Olive, P. L.; Pun, S. H. Increased Nanoparticle Penetration in Collagenase-Treated Multicellular Spheroids. *Int. J. Nanomedicine* **2007**, *2* (2),

265–274.

(15) Xu, X.; Wang, Y.; Chen, Z.; Sternlicht, M. D.; Hidalgo, M.; Steffensen, B. Matrix Metalloproteinase-2 Contributes to Cancer Cell Migration on Collagen. *Cancer Res.* **2005**, *65* (1), 130–136.

(16) Chi, E. Y.; Krishnan, S.; Randolph, T. W.; Carpenter, J. F. Physical Stability of Proteins in Aqueous Solution: Mechanism and Driving Forces in Nonnative Protein Aggregation. *Pharm. Res.* **2003**, *20* (9), 1325–1336.

(17) Aryasomayajula, B.; Torchilin, V. P. Nanoformulations. In *Nanobiomaterials in Cancer Therapy*; Elsevier, 2016; pp 307–330.

(18) Gu, Z.; Biswas, A.; Zhao, M.; Tang, Y. Tailoring Nanocarriers for Intracellular Protein Delivery. *Chem. Soc. Rev.* **2011**, *40* (7), 3638.

(19) van der Goot, F. G.; Gruenberg, J. Intra-Endosomal Membrane Traffic. *Trends Cell Biol.* **2006**, *16* (10), 514–521.

(20) Du, J.; Jin, J.; Yan, M.; Lu, Y. Synthetic Nanocarriers for Intracellular Protein Delivery. *Curr. Drug Metab.* **2012**, *13* (1), 82–92.

(21) Zhang, X.; Xu, D.; Jin, X.; Liu, G.; Liang, S.; Wang, H.; Chen, W.; Zhu, X.; Lu, Y. Nanocapsules of Therapeutic Proteins with Enhanced Stability and Long Blood Circulation for Hyperuricemia Management. *J. Control. Release* **2017**, *255*, 54–61.

(22) Zhang, X.; Chen, W.; Zhu, X.; Lu, Y. Encapsulating Therapeutic Proteins with Polyzwitterions for Lower Macrophage Nonspecific Uptake and Longer Circulation Time. *ACS Appl. Mater. Interfaces* **2017**, *9* (9), 7972–7978.

(23) Liu, C.; Wen, J.; Meng, Y.; Zhang, K.; Zhu, J.; Ren, Y.; Qian, X.; Yuan, X.; Lu, Y.; Kang, C. Efficient Delivery of Therapeutic miRNA Nanocapsules for Tumor Suppression. *Adv. Mater.* **2015**, *27* (2), 292–297.

(24) Zhao, M.; Hu, B.; Gu, Z.; Joo, K.; Wang, P.; Tang, Y. Degradable Polymeric Nanocapsul for Efficient Intracellular Delivery of a High Molecular Weight Tumor-Selective Protein Complex. *Nano Today* **2013**.

(25) Zhao, M.; Xu, D.; Wu, D.; Whittaker, J. W.; Terkeltaub, R.; Lu, Y. Nanocapsules of Oxalate Oxidase for Hyperoxaluria Treatment. **1898**, *1*, 8–11.

(26) Wei, W.; Du, J.; Li, J.; Yan, M.; Zhu, Q.; Jin, X.; Zhu, X.; Hu, Z.; Tang, Y.; Lu, Y. Construction of Robust Enzyme Nanocapsules for Effective Organophosphate Decontamination, Detoxification, and Protection. *Adv. Mater.* **2013**, *25* (15), 2212–2218.

(27) Li, J.; Jin, X.; Liu, Y.; Li, F.; Zhang, L.; Zhu, X.; Lu, Y. Robust Enzyme–silica Composites Made from Enzyme Nanocapsules. *Chem. Commun.* **2015**, *51* (47), 9628–9631.

(28) Liu, Y.; Du, J.; Yan, M.; Lau, M. Y.; Hu, J.; Han, H.; Yang, O. O.; Liang, S.; Wei, W.; Wang, H.; Li, J.; Zhu, X.; Shi, L.; Chen, W.; Ji, C.; Lu, Y. Biomimetic Enzyme Nanocomplexes and Their Use as Antidotes and Preventive Measures for Alcohol Intoxication. *Nat. Nanotechnol.* **2013**, *8* (3), 187–192.

(29) Yan, M.; Liang, M.; Wen, J.; Liu, Y.; Lu, Y.; Chen, I. S. Y. Single siRNA Nanocapsules for Enhanced RNAi Delivery. *J. Am. Chem. Soc.* **2012**, *134* (33), 13542–13545.

(30) Simmchen, J.; Baeza, A.; Ruiz-Molina, D.; Vallet-Regí, M. Improving Catalase-

Based Propelled Motor Endurance by Enzyme Encapsulation. *Nanoscale* **2014**, *6* (15), 8907–8913.

(31) Zhang, L.; Liu, Y.; Liu, G.; Xu, D.; Liang, S.; Zhu, X.; Lu, Y.; Wang, H. Prolonging the Plasma Circulation of Proteins by Nano-Encapsulation with Phosphorylcholine-Based Polymer. *Nano Res.* **2016**, *9* (8), 2424–2432.

(32) Liang, S.; Liu, Y.; Jin, X.; Liu, G.; Wen, J.; Zhang, L.; Li, J.; Yuan, X.; Chen, I. S. Y.; Chen, W.; Wang, H.; Shi, L.; Zhu, X.; Lu, Y. Phosphorylcholine Polymer Nanocapsules Prolong the Circulation Time and Reduce the Immunogenicity of Therapeutic Proteins. *Nano Res.* **2016**, *9* (4), 1022–1031.

(33) Zhao, M.; Xu, D.; Wu, D.; Whittaker, J. W.; Terkeltaub, R.; Lu, Y. Nanocapsules of Oxalate Oxidase for Hyperoxaluria Treatment. **2017**, *1*, 1–7.

(34) Baeza, A.; Guisasola, E.; Torres-Pardo, A.; González-Calbet, J. M.; Melen, G. J.; Ramirez, M.; Vallet-Regí, M. Hybrid Enzyme-Polymeric Capsules/Mesoporous Silica Nanodevice for In Situ Cytotoxic Agent Generation. *Adv. Funct. Mater.* **2014**, *24* (29), 4625–4633.

(35) Wang, W.; Duan, W.; Ahmed, S.; Mallouk, T. E.; Sen, A. Small Power: Autonomous Nano- and Micromotors Propelled by Self-Generated Gradients. *Nano Today* **2013**, *8* (5), 531–554.

(36) Zhao, M.; Biswas, A.; Hu, B.; Joo, K. Il; Wang, P.; Gu, Z.; Tang, Y. Redox-Responsive Nanocapsules for Intracellular Protein Delivery. *Biomaterials* **2011**, *32* (22), 5223–5230.

(37) Wen, J.; Yan, M.; Liu, Y.; Li, J.; Xie, Y.; Lu, Y.; Kamata, M.; Chen, I. S. Y. Specific Elimination of Latently HIV-1 Infected Cells Using HIV-1 Protease-

Sensitive Toxin Nanocapsules. *PLoS One* **2016**, *11* (4), 1–17.

(38) Biswas, A.; Joo, K.-I.; Liu, J.; Zhao, M.; Fan, G.; Wang, P.; Gu, Z.; Tang, Y. Endoprotease-Mediated Intracellular Protein Delivery Using Nanocapsules. *ACS Nano* **2011**, *5* (2), 1385–1394.

(39) Danhier, F.; Feron, O.; Préat, V. To Exploit the Tumor Microenvironment: Passive and Active Tumor Targeting of Nanocarriers for Anti-Cancer Drug Delivery. *J. Control. Release* **2010**, *148* (2), 135–146.

(40) Yan, M.; Du, J.; Gu, Z.; Liang, M.; Hu, Y.; Zhang, W.; Priceman, S.; Wu, L.; Zhou, Z. H.; Liu, Z.; Segura, T.; Tang, Y.; Lu, Y. A Novel Intracellular Protein Delivery Platform Based on Single-Protein Nanocapsules. *Nat. Nanotechnol.* **2010**, *5* (1), 48–53.

(41) Durfee, P. N.; Lin, Y. S.; Dunphy, D. R.; Mu??iz, A. J.; Butler, K. S.; Humphrey, K. R.; Lokke, A. J.; Agola, J. O.; Chou, S. S.; Chen, I. M.; Wharton, W.; Townson, J. L.; Willman, C. L.; Brinker, C. J. Mesoporous Silica Nanoparticle-Supported Lipid Bilayers (Protocells) for Active Targeting and Delivery to Individual Leukemia Cells. *ACS Nano* **2016**, *10* (9), 8325–8345.

(42) Butler, K. S.; Durfee, P. N.; Theron, C.; Ashley, C. E.; Carnes, E. C.; Brinker, C. J. Protocells: Modular Mesoporous Silica Nanoparticle-Supported Lipid Bilayers for Drug Delivery. *Small* **2016**, *12* (16), 2173–2185.

(43) Ashley, C. E.; Carnes, E. C.; Phillips, G. K.; Padilla, D.; Durfee, P. N.; Brown, P. a; Hanna, T. N.; Liu, J.; Phillips, B.; Carter, M. B.; Carroll, N. J.; Jiang, X.; Dunphy, D. R.; Willman, C. L.; Petsev, D. N.; Evans, D. G.; Parikh, A. N.; Chackerian, B.; Wharton, W.; Peabody, D. S.; Brinker, C. J. The Targeted Delivery

of Multicomponent Cargos to Cancer Cells by Nanoporous Particle-Supported Lipid Bilayers. *Nat. Mater.* **2011**, *10* (April), 389–397.

(44) Ashley, C. E.; Carnes, E. C.; Epler, K. E.; Padilla, D. P.; Phillips, G. K.; Castillo, R. E.; Wilkinson, D. C.; Wilkinson, B. S.; Burgard, C. a; Kalinich, R. M.; Townson, J. L.; Chackerian, B.; Willman, C. L.; Peabody, D. S.; Wharton, W.; Brinker, C. J. Delivery of Small Interfering RNA by Peptide-Targeted Mesoporous Silica Nanoparticle-Supported Lipid Bilayers. *ACS Nano* **2012**, *6* (3), 2174–2188.

(45) Epler, K.; Padilla, D.; Phillips, G.; Crowder, P.; Castillo, R.; Wilkinson, D.; Wilkinson, B.; Burgard, C.; Kalinich, R.; Townson, J.; Chackerian, B.; Willman, C.; Peabody, D.; Wharton, W.; Brinker, J. C.; Ashley, C.; Carnes, E. Delivery of Ricin Toxin A-Chain by Peptide-Targeted Mesoporous Silica Nanoparticle-Supported Lipid Bilayers. *Adv. Healthc. Mater.* **2012**, *1* (3), 348–353.

(46) Cauda, V.; Engelke, H.; Sauer, A.; Arcizet, D.; Bräuchle, C.; Rädler, J.; Bein, T. Colchicine-Loaded Lipid Bilayer-Coated 50 Nm Mesoporous Nanoparticles Efficiently Induce Microtubule Depolymerization upon Cell Uptake.

(47) Meng, H.; Wang, M.; Liu, H.; Liu, X.; Situ, A.; Wu, B.; Ji, Z.; Chang, C. H.; Nel, A. E. Use of a Lipid-Coated Mesoporous Silica Nanoparticle Platform for Synergistic Gemcitabine and Paclitaxel Delivery to Human Pancreatic Cancer in Mice. *ACS Nano* **2015**, *9* (4), 3540–3557.

(48) Wang, D.; Huang, J.; Wang, X.; Yu, Y.; Zhang, H.; Chen, Y.; Liu, J.; Sun, Z.; Zou, H.; Sun, D.; Zhou, G.; Zhang, G.; Lu, Y.; Zhong, Y. The Eradication of Breast Cancer Cells and Stem Cells by 8-Hydroxyquinoline-Loaded Hyaluronan Modified Mesoporous Silica Nanoparticle-Supported Lipid Bilayers Containing Docetaxel. *Biomaterials* **2013**, *34* (31), 7662–7673.

(49) Zhang, X.; Li, F.; Guo, S.; Chen, X.; Wang, X.; Li, J.; Gan, Y. Biofunctionalized Polymer-Lipid Supported Mesoporous Silica Nanoparticles for Release of Chemotherapeutics in Multidrug Resistant Cancer Cells. *Biomaterials* **2014**, *35* (11), 3650–3665.

(50) Han, N.; Zhao, Q.; Wan, L.; Wang, Y.; Gao, Y.; Wang, P.; Wang, Z.; Zhang, J.; Jiang, T.; Wang, S. Hybrid Lipid-Capped Mesoporous Silica for Stimuli-Responsive Drug Release and Overcoming Multidrug Resistance. *ACS Appl. Mater. Interfaces* **2015**, *7* (5), 3342–3351.

(51) Johnson, R. P.; Jeong, Y.-I.; John, J. V.; Chung, C.-W.; Choi, S. H.; Song, S. Y.; Kang, D. H.; Suh, H.; Kim, I. Lipo-Poly(L-Histidine) Hybrid Materials with pH-Sensitivity, Intracellular Delivery Efficiency, and Intrinsic Targetability to Cancer Cells. *Macromol. Rapid Commun.* **2014**, *35* (9), 888–894.

(52) Chiang, Y.-T.; Lo, C.-L. pH-Responsive Polymer-Liposomes for Intracellular Drug Delivery and Tumor Extracellular Matrix Switched-on Targeted Cancer Therapy. *Biomaterials* **2014**, *35*, 5414–5424.

(53) Watarai, S.; Iwase, T.; Tajima, T.; Yuba, E.; Kono, K.; Shikanov, A.; Tyan, Y.-C.; Yang, M.-H. Efficiency of pH-Sensitive Fusogenic Polymer-Modified Liposomes as a Vaccine Carrier. *Sci. World J.* **2013**, *7*.

(54) Bersani, S.; Vila-Caballer, M.; Brazzale, C.; Barattin, M.; Salmaso, S. pH-Sensitive Stearoyl-PEG-Poly(methacryloyl Sulfadimethoxine) Decorated Liposomes for the Delivery of Gemcitabine to Cancer Cells. *Eur. J. Pharm. Biopharm.* **2014**, *88*, 670–682.

(55) Sawant, R. M.; Hurley, J. P.; Salmaso, S.; Kale, A.; Tolcheva, E.; Levchenko, T.

S.; Torchilin, V. P. " SMART " DRUG DELIVERY SYSTEMS: DOUBLE-TARGETED pH- RESPONSIVE PHARMACEUTICAL NANOCARRIERS.

(56) Jiang, L.; Li, L.; He, X.; Yi, Q.; He, B.; Cao, J.; Pan, W.; Gu, Z. Overcoming Drug-Resistant Lung Cancer by Paclitaxel Loaded Dual-Functional Liposomes with Mitochondria Targeting and pH-Response. *Biomaterials* **2015**, *52*, 126–139.

(57) Xu, X.; Zhang, L.; Assanhou, A. G.; Wang, L.; Zhang, Y.; Li, W.; Xue, L.; Mo, R.; Zhang, C. Acid/redox Dual-Activated Liposomes for Tumor-Targeted Drug Delivery and Enhanced Therapeutic Efficacy. *RSC Adv.* **2015**, *5* (83), 67803–67808.

(58) Walsh, C. L.; Nguyen, J.; Szoka, F. C. Synthesis and Characterization of Novel Zwitterionic Lipids with pH-Responsive Biophysical Properties. *Chem. Commun.* **2012**, *48* (45), 5575.

(59) Ren Draffehn, S.; Kumke, M. U. Monitoring the Collapse of pH-Sensitive Liposomal Nanocarriers and Environmental pH Simultaneously: A Fluorescence-Based Approach.

(60) Liu, X.; Situ, A.; Kang, Y.; Villabroza, K. R.; Liao, Y.; Chang, C. H.; Donahue, T.; Nel, A. E.; Meng, H. Irinotecan Delivery by Lipid-Coated Mesoporous Silica Nanoparticles Shows Improved Efficacy and Safety over Liposomes for Pancreatic Cancer. *ACS Nano* **2016**, *10* (2), 2702–2715.

(61) Berger, M. S.; Gullick, W. J.; Greenfield, C.; Evans, S.; Addis, B. J.; Waterfield, M. D. Epidermal Growth Factor Receptors in Lung Tumours. *J. Pathol.* **1987**, *152* (4), 297–307.

(62) Noh, M. S.; Lee, S.; Kang, H.; Yang, J.-K.; Lee, H.; Hwang, D.; Lee, J. W.; Jeong, S.; Jang, Y.; Jun, B.-H.; Jeong, D. H.; Kim, S. K.; Lee, Y.-S.; Cho, M.-H. Target-Specific near-IR Induced Drug Release and Photothermal Therapy with Accumulated Au/Ag Hollow Nanoshells on Pulmonary Cancer Cell Membranes. *Biomaterials* **2015**, *45*, 81–92.

(63) Herben, V. M. M.; ten Bokkel Huinink, W. W.; Beijnen, J. H. Clinical Pharmacokinetics of Topotecan. *Clin. Pharmacokinet.* **1996**, *31* (2), 85–102.

(64) Drummond, D. C.; Noble, C. O.; Guo, Z.; Hayes, M. E.; Connolly-Ingram, C.; Gabriel, B. S.; Hann, B.; Liu, B.; Park, J. W.; Hong, K.; Benz, C. C.; Marks, J. D.; Kirpotin, D. B. Development of a Highly Stable and Targetable Nanoliposomal Formulation of Topotecan. *J. Control. Release* **2010**, *141* (1), 13–21.

III.I.I. Hybrid Collagenase Nanocapsules for Enhanced Nanocarrier Penetration in Tumoral Tissue

Villegas, M. R.; Baeza, A.; Vallet-Regí, M. Hybrid Collagenase Nanocapsules for Enhanced Nanocarrier Penetration in Tumoral Tissues. *ACS Appl. Mater. Interfaces* **2015**, *7*, 24075–24081, doi:10.1021/acsami.5b07116.

ACS APPLIED MATERIALS & INTERFACES

Research Article

www.acsami.org

Hybrid Collagenase Nanocapsules for Enhanced Nanocarrier Penetration in Tumoral Tissues

María Rocío Villegas,[†,‡] Alejandro Baeza,[*,‡,†] and María Vallet-Regí[*,†,‡]

[†]Departamento Química Inorgánica y Bioinorgánica, UCM, Instituto de Investigación Sanitaria Hospital 12 de Octubre i+12, Plaza Ramón y Cajal s/n, Madrid 28040, Spain

[‡]Centro de Investigación Biomédica en Red de Bioingeniería, Biomateriales y Nanomedicina (CIBER-BBN), Avenida Monforte de Lemos, 3-5, Madrid 28029, Spain

Supporting Information

ABSTRACT: Poor penetration of drug delivery nanocarriers within dense extracellular matrices constitutes one of the main liabilities of current nanomedicines. The conjugation of proteolytic enzymes on the nanoparticle surface constitutes an attractive alternative. However, the scarce resistance of these enzymes against the action of proteases or other aggressive agents present in the bloodstream strongly limits their application. Herein, a novel nanodevice able to transport proteolytic enzymes coated with an engineered pH-responsive polymeric is presented. This degradable coat protects the housed enzymes against proteolytic attack at the same time that it triggers their release under mild acidic conditions, usually present in many tumoral tissues. These enzyme nanocapsules have been attached on the surface of mesoporous silica nanoparticles, as nanocarrier model, showing a significatively higher penetration of the nanoparticles within 3D collagen matrices which housed human osteosarcoma cells (HOS). This strategy can improve the therapeutic efficacy of the current nanomedicines, allowing a more homogeneous and deeper distribution of the therapeutic nanosystems in cancerous tissues.

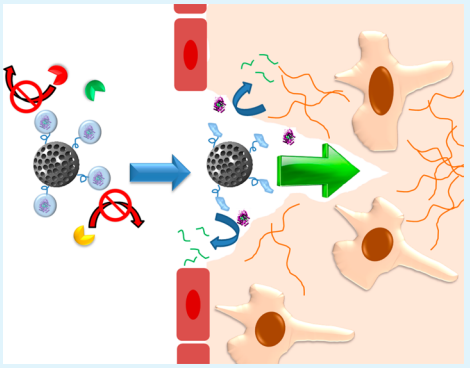

KEYWORDS: *tumoral tissue penetration, collagenase nanocapsules, nanomedicine, mesoporous silica nanodevices and hybrid nanocarriers*

INTRODUCTION

Nanoparticles have become a powerful weapon in the fight against cancer because of their passive accumulation within solid tumors (EPR effect).[1] This effect is caused by the distinctive tumoral blood vessels which present large pores and fenestrations of few hundred nanometers.[2] Thus, when the nanoparticles reach the tumoral zone, they are able to escape from these highly permeable blood vessels producing the accumulation in the diseased tissue.[3] Despite the huge importance of reaching the tumoral area, this is only the first step. The extravasated nanocarrier should be able to penetrate deeper into the solid tumor if a high therapeutic efficacy is pretended. Unfortunately, there are several physiological and physical barriers that should be overcome in order to achieve a homogeneous nanocarrier distribution in the entire malignant tissue.[4] Tumoral tissues exhibit elevated interstitial fluid pressure (IFP) which hampers the convective transport making diffusion the de facto sole transport mechanism for nanocarriers. Moreover, solid tumors usually present extracellular matrices (ECM) denser than healthy tissues, with higher collagen content that hinders even more the nanocarrier diffusion.[5] The lack of an efficient nanoparticle distribution throughout all the diseased tissue reduces considerably the therapeutic efficiency of the nanomedicines and is one of their main liabilities.[6] Different strategies have been postulated in order to overcome this limitation. Thus, the nanocarrier surface decoration with cell penetrating peptides (CPP) in combination with magnetic field guidance[7] and even the use of self-propelled devices have been described to achieve a higher penetration in 3D tissues.[8] A simpler approach consists in the local administration of proteolytic enzymes prior to the nanocarrier treatment, which has demonstrated a significant nanoparticle penetration enhancement within the tumoral tissue.[9] Different proteolytic enzymes such as collagenase or bromelain have been directly anchored on the nanoparticle surface improving their diffusion in comparison with nonfunctionalized particles.[10,11] However, enzymes are labile entities that can suffer a rapid degradation in living tissues by the action of proteases or other aggressive agents present in the bloodstream. Even the attachment method can compromise the enzymatic activity as a consequence of conformational changes or active site blockage.[12] Lu et al.[13,14] have reported an interesting strategy which consists in the enzyme encapsulation into polymeric nanocapsules in order to improve their resistance and to preserve their activity during

Received: August 3, 2015
Accepted: October 13, 2015
Published: October 13, 2015

DOI: 10.1021/acsami.5b07116
ACS Appl. Mater. Interfaces 2015, 7, 24075−24081

longer times. Our research group has described the attachment of enzyme nanocapsules onto the nanoparticle surface for the development of devices able to generate in situ cytotoxic compounds[15] and for the propulsion of nano- and micromotors.[16] Herein, we describe the design and attachment of hybrid collagenase-polymeric nanocapsules on the surface of mesoporous silica nanoparticles in order to improve their penetration within 3D collagen matrices with tumoral cells embedded within the network, which mimic tumoral tissues. These polymeric nanocapsules protect the enzyme against proteolytic degradation and hydrolysis during longer times improving enzyme performance while allowing higher matrix degradation and therefore, deeper penetration within the tissue (Scheme 1).

Scheme 1. Synthesis and Mechanism of pH-Responsive Polymeric Nanocapsules for Enhanced Extracellular Matrix Degradation and Tumoral Tissue Penetration

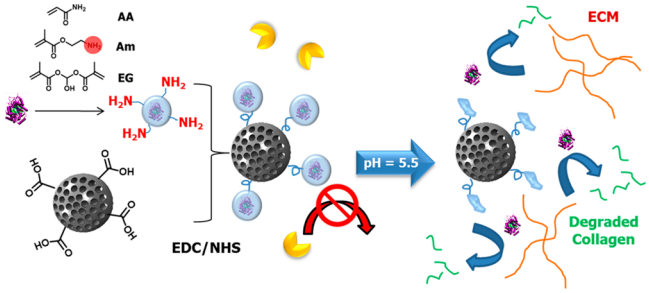

RESULTS AND DISCUSSION

Synthesis and Performance Evaluation of the Collagenase Nanocapsules. Collagen is the most abundant component of the extracellular matrix. Thus, collagenase is one of the most suitable enzymes for ECM degradation. As mentioned above, a polymeric coating was built around the enzyme in order to preserve the activity against aggressive agents. The enzyme substrate is a big molecule and therefore, the enzyme should be released from the capsule in order to be active for efficient collagen degradation. For this reason, a pH-responsive polymeric nanocapsule has been designed. This polymer coating undergoes slow degradation at physiological conditions (pH 7) but exhibits a rapid hydrolysis at mild acidic conditions (pH 5.5) which are naturally present in many tumoral tissues, as a consequence of their accelerated metabolism and the hypoxic environment.[17] Thus, the enzyme will stay in an inactive stage until the pH becomes acidic, which will trigger the enzyme release with the subsequent collagen matrix degradation.

Collagenase nanocapsules (Col-nc) were synthesized forming a polymeric coating around the native collagenase (Col) by radical polymerization employing a monomer mixture of acrylamide (AA) as structural monomer, hydrochloride salt of 2-aminoethyl methacrylate (Am) in order to provide amino groups on the capsule surface and ethylene glycol dimethacrylate (EG) as pH-cleavable cross-linker. Different conditions were tested until the following optimal capsule formation parameters were found: monomer/protein molar ratio of 1:2025 and AA:Am:EG ratio (7:6:2). Thus, homogeneous protein nanocapsules were obtained with a diameter size around 50 nm according to Dynamic Light Scattering (DLS) and Transmission Electron Microscopy (TEM). The spherical morphology and size of the capsules was confirmed by Atomic Force Microscopy (AFM) (Figure 1).

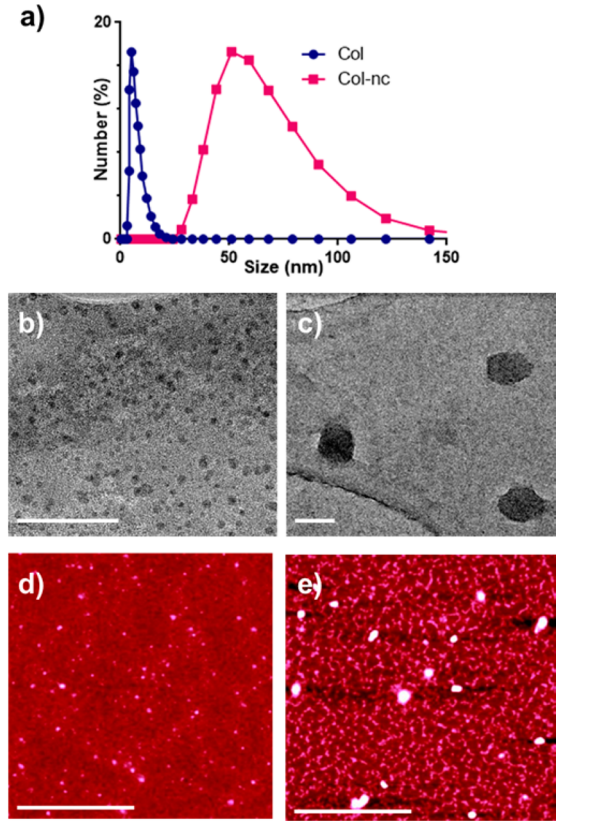

Figure 1. (a) DLS of Col and Col-nc, (b, c) TEM images of Col and Col-nc, respectively, stained with phosphotungstic acid as contrast agent (scale bars correspond to 50 nm) and (d, e) AFM of Col and Col-nc, respectively (scale bars correspond to 1 μm).

The presence of free amino groups on the capsule surface was confirmed by fluorescamine assay. The enzymatic activity of the capsules was determined using a commercial kit (EnzCheck Gellatinase/Collagenase, Molecular Probes), which is based in the measurement of the fluorescein released when fluorescently labeled gelatin was exposed to enzyme degradation. After the encapsulation process, the enzymatic activity suffers a drastic reduction of around 50% which indicates that the polymeric coating significatively hampers the collagen degradation by the encapsulated enzyme (Figure S1a).

This fact confirms that the enzyme should be released in order to achieve an efficient degradation of the collagen matrix, as it was mentioned above. For this reason, EG was employed as pH-cleavable cross-linker. This molecule exhibits rapid hydrolysis under mildly acidic conditions, compromising the stability of the whole capsule and hence releasing the housed enzyme. The pH-responsive nature of the capsule was evaluated by DLS suspending the capsules at different pH values, 7.0 and 5.5, respectively, during 2 h. After this time, the capsule exposed to acidic pH was completely broken showing the same hydrodynamic diameter by DLS as the native enzyme, whereas the capsule exposed to neutral pH did not suffer any size modification. Interestingly, the enzymatic activity was almost fully recovered after the acidic treatment but it was kept at 50% when the sample was maintained at pH 7. These results are

DOI: 10.1021/acsami.5b07116
ACS Appl. Mater. Interfaces 2015, 7, 24075−24081

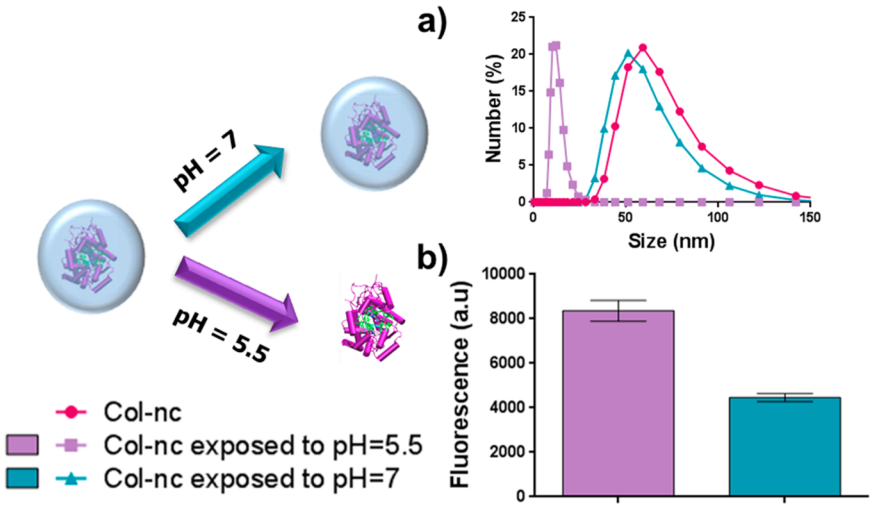

Figure 2. pH-responsive behavior of Col-nc: (a) DLS measurements of Col-nc exposed to pH 5.5 and 7 (purple and cyan lines, respectively) and (b) fluorescein released by a fluorescently labeled collagen matrix treated with Col-nc previously exposed to pH 5.5 and pH 7 (purple and cyan lines, respectively).

consistent with a complete release of the trapped enzyme (Figure 2).

Attachment of Collagenase Nanocapsules on the Nanocarrier Surface. Mesoporous silica nanoparticles (MSNs) have been chosen as nanomedicine model due to the excellent properties of this material such as high loading capacity and excellent biocompatibility, among others.[18,19] Thus, MSNs were synthesized following the modified Stöber method reported elsewhere.[20] According to DLS and TEM, the particles show a homogeneous size distribution centered around 140 nm which is convenient for their application as drug nanocarriers.[21] To provide anchoring points for the protein nanocapsules, the surface of the particles was decorated with carboxylic groups by condensation of 4-(trietoxisililetilene)succidimide with the silanol groups on the surface, followed by hydrolysis in acidic medium. The presence of carboxylic groups was confirmed by the apparition of the characteristic C═O band at 1710 cm^{-1} in the Fourier transform infrared (FT-IR) spectrum and by thermogravimetric analysis (TGA). According with the DLS measurements, the particle size was maintained during this functionalization process (Figure S2).

Enzyme nanocapsules were covalently grafted on the MSNs surface through the well-known carbodiimide chemistry. Thus, the carboxylic groups present on the MSN were transformed into activated esters through the reaction with *N*-(3-(dimethylamino)propyl)-*N*′-ethylcarbodiimide hydrochloride (EDC) and *N*-hydroxysuccidimide (NHS). Then, the presence of free amino groups on the capsule surface produces their attachment on the particle surface by the formation of highly stable amide bonds producing the complete material (MSN-Col-nc). The same reaction was carried out using native collagenase (MSN-Col) as control in order to compare the performance and stability of both systems. In both cases, FTIR spectra show a slight decrease in the carboxylic acid band at 1710 cm^{-1} and the appearance of two bands at 1650 and 1568 cm^{-1} that correspond to amide bond formation and the protein. DLS measurements showed a size increase of around 50 nm, which corresponds to a discrete attachment of enzyme nanocapsules instead of to a complete covering of the entire surface (Figure S2). The conjugation of Col and Col-nc on the surface was confirmed by TEM using phosphotungstic acid as staining agent in order to increase the electron opacity of the organic material. In these images, the presence of the native enzymes attached on the silica surface is clearly visible as dark spots (Figure 3b), which are not present in naked MSN (Figure 3a). In the case of mesoporous silica particles decorated with collagen nanocapsules (MSN-Col-nc) these enzyme capsules are clearly visible attached on the particle surface, even keeping their round shape morphology (Figure 3c, d). TGA measurements and Sulfur analysis of the MSN-Col and MSN-Col-nc did not exhibit significative differences between them, showing in both cases around 6−8% of grafted organic material. It is worth to note that MSN-Col-nc present high colloidal stability in aqueous media, being stable over time (Figure S3).

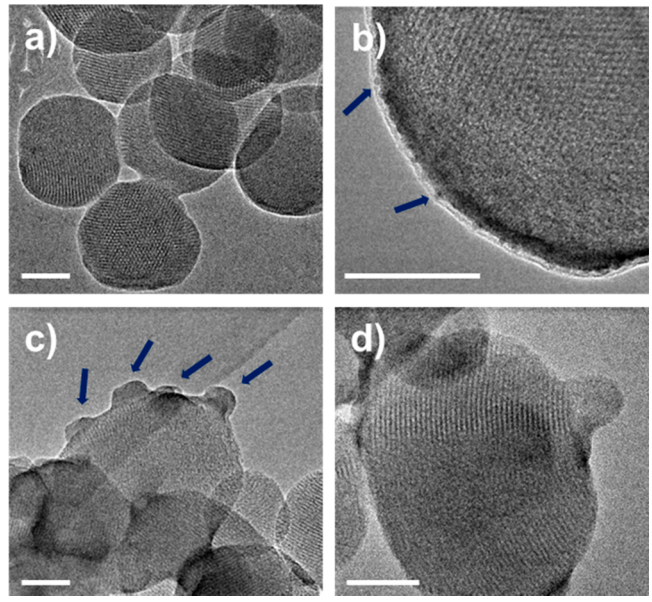

Figure 3. TEM images of (a) MSN, (b) MSN-Col, and (c, d) MSN-Col-nc. Scale bars correspond to 50 nm. Blue arrows point out the presence of Col and Col-nc. Because of the stochastic nature of the grafting procedure, the collagen nanocapsules are randomly distributed on the MSN surface.

DOI: 10.1021/acsami.5b07116
ACS Appl. Mater. Interfaces 2015, 7, 24075−24081

Stability of MSN-Col-nc. Obviously, MSN-Col initially presents higher enzymatic activity than MSN-Col-nc (Figure S1b) mainly by two reasons, first the absence of a polymeric coat as it has been mentioned above and second, the higher steric hindrance of the capsules which causes a lower enzyme nanocapsules grafting in comparison with the native protein attachment. However, despite this initial advantage, the enzymatic activity of MSN-Col decreases in a short period of time when the samples are suspended in a PBS buffer solution at pH 7 and 37 °C, whereas the activity increases to double its initial value in the case of MSN-Col-nc. This behavior proves that the polymeric coat which wraps the enzyme suffers hydrolysis and the housed enzymes are slowly released or exposed fully recovering their capacity to digest collagen after longer periods of time (Figure 4a). It is important to remark that a similar

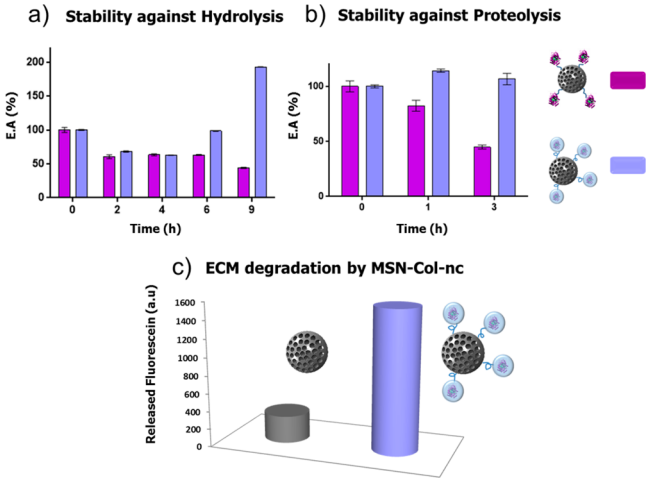

Figure 4. Stability test of MSN-Col and MSN-Col-nc against (a) hydrolysis and (b) proteolytic attack. (c) ECM degradation by MSN-Col-nc.

amount of free enzyme almost completely loses its activity after a short incubation time of 2 h in these conditions. One important role which should be played by the polymeric coat consists in the protection of the encapsulated enzyme against proteolytic attack, because the lack of stability against proteases is the main limitation on the use of proteins in clinical applications.[22] In order to compare the stability against proteases, samples MSN-Col and MSN-Col-nc were suspended at 37 °C in a solution of PBS (pH 7) which contains 1 mg mL^{-1} of protease from *Streptomyces griseus*. The results indicate that material with the uncoated enzyme lost more than 60% of its enzymatic activity after 3 h, whereas the sample with enzyme nanocapsules kept intact their activity (Figure 4b). All these experiments evidence the protective role of the polymeric nanocapsules.

EMC Degradation Capacity of MSN-Col-nc. The capacity of the protein capsules attached on the particle surface to degrade the extracellular matrix was initially tested using a 3D collagen matrix formed by MaxGelECM. This 3D matrix is composed by several human extracellular matrix components such as collagen, laminin, fibronectin, tenascin, elastin, and a number of proteoglycans and glycosaminoglycans which mimic the matrices present in human living tissues.[11] The proteins which form the 3D matrix were previously stained with fluorescein isothiocyanate (FITC) in order to monitorize the matrix degradation through the measurement of the fluorescein released after addition of the nanoparticles. Naked MSN, which shows negligible enzymatic activity (Figure S4) was used as control. A suspension of 1 mg mL^{-1} of MSN-Col-nc and MSN respectively, was carefully added on top of the fluorescent 3D gels and both samples were incubated at 37 °C during 24 h. After this time, a strong fluorescence was observed in the case of MSN-Col-nc, whereas a scarce fluorescence was observed in the case of naked MSN (Figure 4c). The particles decorated with collagenase nanocapsules present a 5-fold increase in the ECM degradation in comparison with the nonfunctionalized ones.

Penetration Capacity of MSN-Col-nc in 3D-Human Osteaosarcoma-Seeded Collagen Gels. A 3D tumoral tissue model was prepared in order to study the MSN-Col-nc performance in a more realistic model which takes into account the influence that could exert the presence of tumoral cells embedded within the matrix. To this end, we synthesized a 3D collagen gel that contains human osteosarcoma cells (HOS) following a slightly modified procedure reported elsewhere (Figure S5).[7] This matrix shows similar consistency to real human tissue and the presence of embedded tumoral cells provides a realistic environment for testing the penetration capacity of nanocarriers clothed with these enzyme capsules. To visualize the penetration of the nanoparticles within the collagen gel, we synthesized MSNs carrying fluorescein molecules covalently grafted within their structure following a procedure reported elsewhere.[26] The stability of the fluorescein molecules covalently grafted within the silica matrix was evaluated suspending a certain solution of fluorescent MSN in PBS buffer at pH 7 and 37 °C and measuring by fluorescence spectroscopy the fluorescein lixiviated in the supernatant and the fluorescence remained in the particles over time (Figure S6). The absence of lixiviated fluorescein confirms the stability of the FITC covalent grafting protocol. After this, collagenase nanocapsules were grafted on the fluorescent MSN surface through the same conjugation method employed for nonfluorescent MSN. A suspension of fluorescent MSN and MSN-Col-nc, respectively (25 μg mL^{-1}) was carefully placed on top of the 3D gels; the penetration capacity of each carrier was evaluated by confocal fluorescence microscopy after 24 h of incubation. The results indicated that the naked particles were not able to penetrate within the gel and remained fixed on the top layer, whereas MSN-Col-nc exhibited an improved penetration within the 3D-matrix (Figure 5a, b). It is worthy to point out that if the concentration

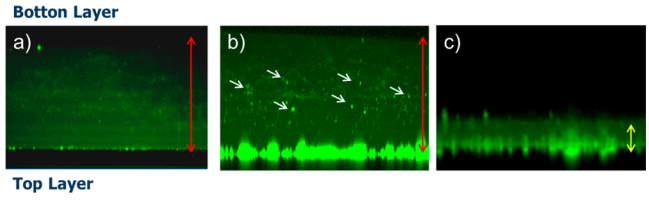

Figure 5. Penetration in 3D-HOS-seeded collagen gels of (a) MSN and(b) MSN-Col-nc using a particle concentration of 25 μg mL^{-1}, respectively (white arrows indicate the presence of clusters of MSN-Col-nc). (c) Penetration of MSN-Col-nc using a concentration of 50 μg mL^{-1}. Red arrows correspond to a gel thickness of 740 μm. Yellow arrow corresponds to a gel thickness of 280 μm.

of MSN-Col-nc was doubled, a drastic decrease of the matrix thickness was observed up to reach only one-third of the original size (Figure 5c). This fact indicates that the released collagenase diffuses throughout the matrix causing a higher collagen digestion as a consequence of their higher concentration in this case.

DOI: 10.1021/acsami.5b07116
ACS Appl. Mater. Interfaces 2015, 7, 24075−24081

Cytotoxicity Studies of MSN-Col-nc. It has been reported that collagenase, both alone or conjugated on the surface of different nanoparticles[23,24] causes very low toxicity in human cells. Additionally, MSN is also a biocompatible material.[25] However, our system is composed by a novel type of collagenase nanocapsules grafted on the MSN surface and its cytotoxicity should be evaluated. Thus, HOS cells were incubated in the presence of a fixed concentration of naked MSN and MSN-Col-nc (25 μg mL^{-1}, which is the optimal concentration for tissue penetration) during 24 h and their cell viability was evaluated measuring the Lactate deshydrogenase (LDH) released in the media. As shown in Figure 6a, the exposition to naked particles and particles decorated with the enzyme nanocapsules did not cause higher LDH release in comparison with the negative control which corresponds to untreated cells. In order to simulate a highly cytotoxic material, as positive control, the cells were exposed to a solution of Triton X (2%), which caused their complete destruction and a subsequent LDH increment of more than four times. The absence of cytotoxicity caused by the exposition to these materials was confirmed using the standardized cell viability test by MTS reduction that exhibit similar values in all systems (Figure 6b). These results indicate that neither of the materials provokes a substantial cell death.

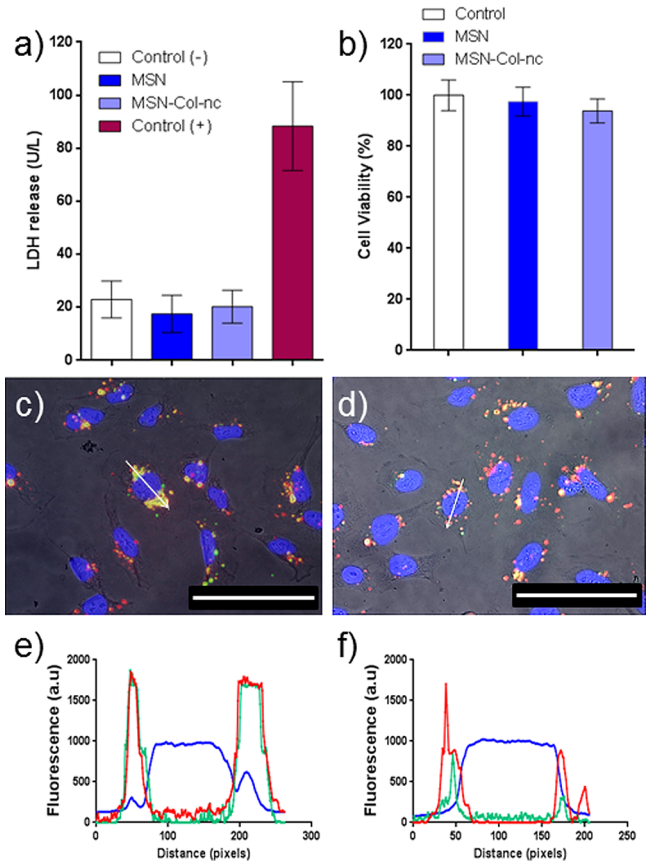

Figure 6. (a) LDH assay of MSN and MSN-Col-nc where Control (−) are cells without treated with particles and Control (+) are cells lysed with Triton X in order to simulate full cytotoxicity. (b) Cell viability assay by MTS test of MSN and MSN-Col-nc. (c, d) Merged microscopy images of HOS cells incubated with MSN and MSN-Col-nc labeled with fluorescein. Blue stain corresponds to cell nucleus, green stain corresponds to nanoparticles, and red stain corresponds to lysosomes (scale bar correspond to 100 μm). Each channel can be separately observed in Figure S7. (e, f) Fluorescence intensity of each fluorophore emission wavelength along the white arrow in images c and d (red pattern correspond to lysosomes, green pattern correspond to MSN and MSN-Col-nc, and blue pattern correspond to cell nuclei).

In order to visualize if the nanoparticles were internalized within the tumoral cells, the lysosomes were stained using Cell Navigator Lysosome Staining Kit showing that the nanoparticles were mainly located within these cell organelles (Figure 6c, d). Additionally, these results were confirmed measuring independently the fluorescence intensity of each fluorophore obtaining a clear pattern which shows that nanoparticles are mainly located in the same place than lysosomes and outside the cell nuclei (Figure 6e, f).

CONCLUSIONS

In conclusion, a novel strategy to transport collagenase attached on the surface of a nanocarrier and to release it in a controlled manner has been presented. This approach is based on the synthesis of hybrid enzyme-polymer nanocapsules which have been engineered to exhibit slow enzyme release at physiological conditions or faster if the pH drops to mild acidic values, which is characteristic of many tumoral tissues. Moreover, these capsules protect the enzymes against proteolytic attack by proteases, which is one of the main limitations of employing enzymes in living tissues, maintaining their activity during long times. Finally, the attachment of these enzyme capsules on the surface of a model nanocarrier has afforded a significant improvement of their penetration within a tumoral tissue model as a consequence of the abundant extracellular matrix degradation caused by the in situ released collagenase. These properties would be of paramount importance for clinical applications paving the way for the development of more efficient nanomedicines able to achieve deeper penetration and more homogeneous distribution within the tumoral tissues.

EXPERIMENTAL SECTION

Synthesis of Collagenase Capsule (Col-nc). Collagenase (3.1×10^{-5} mmol) was dissolved in 1 mL of $NaHCO_3$ buffer (0.01 M, pH 8.5), previously deoxygenated three times for freeze-vacum-N_2 cycles, at room temperature;. 0.035 mmol of acrylamide (AA), 0.026 mmol of 2-aminometacrylate hydrochloride (Am), and 0.01 mmol of ethylene glicol dimetacrylate (EG) were dissolved in 1 mL of deoxygenated $NaHCO_3$ (0.01 M pH 8.5) buffer and added to the solution of collagenase. This mixture was stirred at 300 rpm for 10 min under nitrogen atmosphere at room temperature. Then, 0.013 mmol of ammonium persulfate and 0.002 mmol of *N,N,N′,N′*-tetramethyl ethylenediamine (TMDA) dissolved in 1 mL of the deoxygenated $NaHCO_3$ buffer (0.01 M pH 8.5) were added. The solution was stirred at 300 rpm for 90 min at room temperature under inert atmosphere. After this time, the encapsulated enzyme was purified by centrifugal separation with 10 kDa cut-of filters (AMICON Ultra-2 mL 10KDa) and washed three times with $NaHCO_3$ buffer (0.01 M pH 8.5). The capsules of collagenase were preserved at 4 °C.

Synthesis of Mesoporus Silica Nanoparticles. Hexadecyltrimethylammonium bromide (CTAB, 2.74 mmol), 480 mL of water, and 7 mmol of NaOH were stirred at 600 rpm at 80 °C. Then, 22.4 mmol of tetraethylortosilicate (TEOS) was added slowly during 20 min and upon addition, the mixture was stirred during 2 h at 80 °C. Then, the particles were collected by centrifugation and washed three times with water and ethanol. The surfactant was removed placing the particles in 500 mL of a solution of 95% ethanol, 5% water, and 10 g NH_4NO_3 mL^{-1} at 80 °C during 2 h under intense stirring. The same cycle was repeated two times more in order to remove all the surfactant. The nanoparticles were dried under vacuum and preserved at room temperature.

For penetration studies within 3D gels, fluorescent nanoparticles were synthesized following an analogous protocol described elsewhere.[26] Briefly, FITC (1 mg) and APTES (2.2 μL) were dissolved in

DOI: 10.1021/acsami.5b07116
ACS Appl. Mater. Interfaces 2015, 7, 24075−24081

the minimum volume of EtOH and the mixture was stirred at room temperature for 2 h under a N_2 atmosphere. Then, this solution was mixed with 22.4 mmol of TEOS and the particles were synthesized following the same method mentioned above.

Synthesis of Acid-Funcionalized Silica Nanoparticles (MSN). Five hundred milligras of the particles obtained above and 1.34 mmol of anhydrous 4-(trietoxisililetilene)succidimide were suspended in 50 mL of dry toluene under an inert atmosphere at 110 °C under intense stirring overnight. Then, the nanoparticles were collected by centrifugation and washed with toluene, tetrahydrofuran, and finally with water, in order to hydrolyze the succinic anhydride providing the carboxylic acid groups. The particles were dried under vacuum and preserved at room temperature.

Attachment of Native Collagenase on Silica Nanoparticles (MSN-Col). A suspension of 50 mg of MSN in 2 mL of PBS (pH 7) was treated with 0.03 mmol of *N*-(3-(Dimethylamino)propyl)-*N*′-ethylcarbodiimide hydrochloride (EDC) and 0.04 mmol of *N*-Hydroxysuccidimide (NHS). The pH was fixed to pH 8.5 adding 0.06 mmol of sodium carbonate. The sample was placed in an orbital stirrer at 400 rpm during 10 min and after this time, 3.1×10^{-4} mmol of collagenase were added and the mixture was stirred during 4 h. The sample was collected by centrifugation and washed three times with PBS. The sample was preserved at 4 °C.

Attachment of Collagenase Nanocapsules on Silica Nanoparticles (MSN-Col-nc). A suspension of 50 mg of MSN in 2 mL of PBS (pH 7) was treated with 0.03 mmol of *N*-(3-(Dimethylamino)-propyl)-*N*′-ethylcarbodiimide hydrochloride (EDC) and 0.04 mmol of *N*-Hydroxysuccidimide (NHS). The pH was fixed to pH 8.5 adding 0.06 mmol of sodium carbonate. The sample was placed in an orbital stirrer at 400 rpm during 10 min and after this time, 10 mg of collagenase nanocapsules were added and the mixture was stirred during 4 h. The sample was collected by centrifugation and washed three times with PBS. The sample was preserved at 4 °C.

Enzymatic Activity Measurements. The enzymatic activity of all samples was evaluated using and following the protocol EnChekGelatinase/Collagenase Assay Kit. For this experiment, 80 μL of collagenase buffer 1×, 20 μL of Collagen-FITC, and 100 μL of each sample were used.

Study of pH Responsiveness of MSN-Col-nc. *Size Measurements by DLS.* One hundred microliters of the encapsulated collagenase (Col-nc) was dissolved in 2 mL of HPLC water. The initial hydrodynamic diameter of the capsules was characterized by DLS and it was compared with the size of the native collagenase (Col). One mL of this solution was placed into a pur-A-lyzer (6 kDa) which was submerged in a flask with 200 mL of PBS buffer pH 7.0 at 37 °C with magnetic stirring for 2 h. Another batch of 1 mL was similarly treated but in this case using a solution of 200 mL of PBS Buffer pH 5.5. After this time, the changes in the hydrodynamic diameter of both batches were evaluated by DLS.

Enzymatic Activity. One hundred fifty microliters of the encapsulated collagenase (Col-nc) was suspended in 1 mL of PBS buffer 0.01 M pH 7. One batch of 400 μL of this solution was placed into a pur-A-lyzer (6 kDa) submerged in 200 mL of the same buffer at 37 °C with magnetic stirring during 4h. Another batch was placed into a pur-A-lyzer (6 kDa) submerged in 200 mL of PBS Buffer pH 5.5 at 37 °C for 3 and 1 h more in PBS buffer 0.01 M pH 7 at 37 °C in order to equilibrate the pH before performing the enzymatic activity measurements. Thenboth batches were diluted 1:100 in PBS and then the enzymatic activity of the capsules solution was evaluated.

Study of the Enzymatic Activity of MSN-Col and MSN-Col-nc. *Stability during the Time.* Two milligrams of silica nanoparticles functionalized with native and encapsulated collagenase (Col and Col-nc, respectively) were suspended in PBS 0.01 M at pH 7 at 37 °C and their enzymatic activity was studied at different times.

Study Enzymatic Activity against Proteases. Two batches of 1 mg of the MSN-Col-nc and MSN-Col were suspended respectively in a solution of 1 mg mL^{-1} protease from *Streptomyces griseus* in PBS Buffer 0.01 M (pH 7). Both samples were incubated at 37 °C during the corresponding time and after this time, they were washed ten times with the same buffer in order to remove the proteases. Then, the enzymatic activity of the nanoparticles was measured using the protocol mentioned above.

ECM Degradation by MSN-Col-nc. MaxGelECM was diluted 1:2 in a cold solution of 0.0026 mmol/mL of Fluorescein isomer I (FITC) in PBS 0.01 M pH 7. Then the solution was pipetted into 96 well plates and incubated for 5h at 37 °C in order to promote the gelation. Once the gel was formed, the supernatant was removed and the gel was gently washed until the observation of neglictable fluorescence in the supernatant. Two hundred microliters of a suspension of 1 mg mL^{-1} of MSN and MSN-Col-nc in PBS 0.01 M pH 7 respectively, was pipetted on the ECM gel and incubated at 37 °C during 24 h. The fluorescence of supernatant was then analyzed.

Preparation of 3D-Human Osteaosarcoma-Seeded Collagen Gels. Two milliliters of rat tail collagen type I and 0.6 mL of complete medium (Dulbecco's modified eagle's medium complemented with 10% of FBS) were mixed in cold and 100 μL of sodium hydroxide were added to obtain a mixture of neutral pH. To this solution was added 0.5 mL of FBS, 0.5 mL of complete medium, and 0.5 mL of a solution of cells of concentration HOS $1:1 \times 10^6$ cell/mL, keeping the temperature at 0 °C. The mixture was pipetted into 12 well plates (0.5 mL/well) and incubated at 37 °C at 5% CO_2 atmospheric concentration for 1 h to promote gel formation. Then, 500 μL of complete medium was added in each well and the gel was incubated at 37 °C at 5% CO_2 atmospheric concentration overnight. After this time, a needle was run around the edge of each solid gel to detach it from the plastic and 0.5 mL of complete medium was added. Gels were used in experiments 4 days after detachment to allow full gel contraction.

Study of Penetration of MSN-Col-nc in HOS-Collagen Gels. To study the penetration of nanocarriers in 3D gels with cells HOS embedded, the medium, which cover the gels was removed and the corresponding amount of suspended MSN and MSN-Col-nc (1 mg mL^{-1}) was added on top of each gel. These samples were incubated at 37 °C at 5% CO_2 atmospheric concentration during 24h. Then, the supernatant was removed and the gel was fixed at 4 °C during 1 h with 0.5 mL of a solution of glutaraldehyde at 2.5% of concentration. Then, confocal fluorescence microscope (using 10× magnifications) was used to determine the penetration by *z*-stack images of each gel, composed of sequential images taken 2 μm apart. Each compressed *z*-stack was analyzed and used for statistical analysis and graphical representation.

Cell Viability Studies. The cytotoxicity of nanocarriers was evaluated using the standard LDH activity test and the MTS reduction assay protocol. For this study 20000 cells HOS cm^{-2} were seeded into each well of a 24-well plate, 0.5 mL of complete media was added to each well, and the cells were cultured at 37 °C at 5% CO_2 atmospheric concentration for 24 h. Then, the cells were incubated with the corresponding sample MSN and MSN-Col-nc, at 25 μg mL^{-1} or without particles in the case of controls (+) and (−), during 24 h at 37 °C at 5% CO_2 atmospheric concentration. In the case of control (+), a suspension of Triton X (2%) was added and the cells were incubated during 2 h. After this time, the supernatant was collected for measuring the extracellular LDH activity. The cells were washed with 0.5 mL of PBS twice and 0.3 mL of a solution of 2 mL of MTS in 10 mL of complete medium was added. The cell culture was incubated at 37 °C at 5% CO_2 atmospheric concentration for 4 h and then the supernatant was collected for the MTS assay.

Lactate Dehydrogenase (LDH) Assay. Extracellular LDH activity was measured using 33 μL of supernatant and 1000 μL of the kit for quantitative determination of LDH (Spinreact). The LDH activity was measured by spectrophotometer at 340 nm in the culture medium following the manufacturer protocol.

MTS Assay. The MTS (3-(4,5-dimethylthiazol-2-yl)-5-(3-carboxymethoxyphenyl)-2-(4-sulfophenyl)-2H-tetrazolium) reduction assay was performed using a commercial assay and following the manufacturer protocol (CellTiter aqueous one solution cell proliferation assay). The absorption of supernatant was measured at 490 nm using a microplate reader.

Fluorescence Microscopy Images of HOS Exposed to MSN and MSN-Col-nc. For this study, HOS cells were exposed during 24 h to the same nanoparticle concentration (25 μg mL^{-1}) of MSN and

DOI: 10.1021/acsami.5b07116
ACS Appl. Mater. Interfaces 2015, 7, 24075−24081

MSN-Col-nc covalently labeled with fluorescein as in the previously mentioned assays.

To visualize lysosomes, a staining kit (Cell Navigator Lysosome Staining Kit) was employed. Briefly, 20 μL of LisoBrite Red, 4.98 mL of live cell staining buffer, and 5 mL of complete media were mixed. 600 μLix hundred microliters of these dilutions were added into each well of a 24 well plate which contains the cells and they were incubated for 30 min at 37 °C. Then, the supernatant was removed and the cells were washed with 0.5 mL of PBS twice. To visualize the cells nuclei, we added 600 μL of 1 μg/mL DAPI in methanol into each well and the cells were incubated for 1 min at 37 °C. Finally, the supernatant was removed and the cells were washed with 0.5 mL of PBS twice.

■ ASSOCIATED CONTENT

Supporting Information

The Supporting Information is available free of charge on the ACS Publications website at DOI: 10.1021/acsami.5b07116.

Materials and instruments descriptions, enzymatic activity of Col and Col-nc, FTIR spectra, DLS, Z potential, TGA values, 3D-human osteaosarcoma-seeded collagen gel characterization, stability test of FITC on MSN, and fluorescence microscopy images of the cells (PDF)

■ AUTHOR INFORMATION

Corresponding Authors

*E-mail: abaezaga@ucm.es.

*E-mail: vallet@ucm.es.

Author Contributions

The manuscript was written through contributions of all authors. All authors have given approval to the final version of the manuscript.

Notes

The authors declare no competing financial interest.

■ ACKNOWLEDGMENTS

This work was supported by the Ministerio de Economía y Competitividad, through project MAT2012-35556, CSO2010-11384-E (Agening Network of Excellence). We also thank the X-ray Diffraction C.A.I. and the National Electron Microscopy Center, UCM.

■ REFERENCES

(1) Ediriwickrema, A.; Saltzman, W. M. Nanotherapy for Cancer: Targeting and Multifunctionality in the Future of Cancer Therapies. *ACS Biomater. Sci. Eng.* **2015**, *1*, 64−78.

(2) Maeda, H.; Nakamura, H.; Fang, J. The EPR Effect for Macromolecular Drug Delivery to Solid Tumors: Improvement of Tumor Uptake, Lowering of Systemic Toxicity, and Distinct Tumor Imaging in Vivo. *Adv. Drug Delivery Rev.* **2013**, *65*, 71−79.

(3) Jain, R. K.; Stylianopoulos, T. Delivering Nanomedicine to Solid Tumors. *Nat. Rev. Clin. Oncol.* **2010**, *7*, 653−664.

(4) Florence, A. T. Targeting" Nanoparticles: The Constraints of Physical Laws and Physical Barriers. *J. Controlled Release* **2012**, *164*, 115−124.

(5) Netti, P.; Berk, D.; Swartz, M.; Grodzinsky, J.; Jain, R. K. Role of Extracellular Matrix Assembly in Interstitial Transport in Solid Tumors. *Cancer Res.* **2000**, *60*, 2497−2503.

(6) Lammers, T.; Kiessling, F.; Hennink, W. E.; Storm, G. Drug Targeting to Tumors: Principles, Pitfalls and (pre-) Clinical Progress. *J. Controlled Release* **2012**, *161*, 175−187.

(7) Child, H. W.; Del Pino, P. a.; De La Fuente, J. M.; Hursthouse, A. S.; Stirling, D.; Mullen, M.; McPhee, G. M.; Nixon, C.; Jayawarna, V.; Berry, C. C. Working Together: The Combined Application of a Magnetic Field and Penetratin for the Delivery of Magnetic Nanoparticles to Cells in 3D. *ACS Nano* **2011**, *5*, 7910−7919.

(8) Kagan, D.; Benchimol, M. J.; Claussen, J. C.; Chuluun-Erdene, E.; Esener, S.; Wang, J. Acoustic Droplet Vaporization and Propulsion of Perfluorocarbon-Loaded Microbullets for Targeted Tissue Penetration and Deformation. *Angew. Chem., Int. Ed.* **2012**, *51*, 7519−7522.

(9) McKee, T. D.; Grandi, P.; Mok, W.; Alexandrakis, G.; Insin, N.; Zimmer, J. P.; Bawendi, M. G.; Boucher, Y.; Breakefield, X. O.; Jain, R. K. Degradation of Fibrillar Collagen in a Human Melanoma Xenograft Improves the Efficacy of an Oncolytic Herpes Simplex Virus Vector. *Cancer Res.* **2006**, *66*, 2509−2513.

(10) Kuhn, S. J.; Finch, S. K.; Hallahan, D. E.; Giorgio, T. D. Proteolytic Surface Functionalization Enhances in Vitro Magnetic Nanoparticle Mobility through Extracellular Matrix. *Nano Lett.* **2006**, *6*, 306−312.

(11) Parodi, A.; Haddix, X. S. G.; Taghipour, X. N.; Scaria, S.; Taraballi, F.; Cevenini, A.; Yazdi, I. K.; Corbo, C.; Palomba, R.; Khaled, S. Z.; Martinez, J. O.; Brown, B. S.; Isenhart, L.; Tasciotti, E. Bromelain Surface Modification Increases the Diffusion of Silica Nanoparticles in the Tumor Extracellular Matrix. *ACS Nano* **2014**, *8*, 9874−9883.

(12) Mateo, C.; Palomo, J. M.; Fernandez-Lorente, G.; Guisan, J. M.; Fernandez-Lafuente, R. Improvement of Enzyme Activity, Stability and Selectivity via Immobilization Techniques. *Enzyme Microb. Technol.* **2007**, *40*, 1451−1463.

(13) Yan, M.; Du, J.; Gu, Z.; Liang, M.; Hu, Y.; Zhang, W.; Priceman, S.; Wu, L.; Zhou, Z. H.; Liu, Z.; Segura, T.; Tang, Y.; Lu, Y. A Novel Intracellular Protein Delivery Platform Based on Single-Protein Nanocapsules. *Nat. Nanotechnol.* **2010**, *5*, 48−53.

(14) Liu, Y.; Du, J.; Yan, M.; Lau, M. Y.; Hu, J.; Han, H.; Yang, O. O.; Liang, S.; Wei, W.; Wang, H.; Li, J.; Zhu, X.; Shi, L.; Chen, W.; Ji, C.; Lu, Y. Biomimetic Enzyme Nanocomplexes: Use as Antidotes and Preventive Measures for Alcohol Intoxication. *Nat. Nanotechnol.* **2013**, *8*, 187−192.

(15) Baeza, A.; Guisasola, E.; Torres-Pardo, A.; González-Calbet, J. M.; Melen, G. J.; Ramirez, M.; Vallet-Regí, M. Hybrid Enzyme-Polymeric Capsules/Mesoporous Silica Nanodevice for In Situ Cytotoxic Agent Generation. *Adv. Funct. Mater.* **2014**, *24*, 4625−4633.

(16) Simmchen, J.; Baeza, A.; Ruiz-Molina, D.; Vallet-Regí, M. Improving Catalase-Based Propelled Motor Endurance by Enzyme Encapsulation. *Nanoscale* **2014**, *6*, 8907−8913.

(17) Danhier, F.; Feron, O.; Preat, V. To Exploit the Tumor Microenvironment: Passive and Active Tumor Targeting of Nanocarriers for Anti-Cancer Drug Delivery. *J. Controlled Release* **2010**, *148*, 135−146.

(18) Baeza, A.; Colilla, M.; Vallet-Regí, M. Advances in Mesoporous Silica Nanoparticles for Targeted Stimuli-Responsive Drug Delivery. *Expert Opin. Drug Delivery* **2015**, *12*, 319−337.

(19) Vallet-Regi, M.; Rámila, A.; del Real, R. P.; Pérez-Pariente, J. A New Property of MCM-41: Drug Delivery System. *Chem. Mater.* **2001**, *13*, 308−311.

(20) Hoffmann, F.; Cornelius, M.; Morell, J.; Froeba, M. Silica-Based Mesoporous Organic-Inorganic Hybrid Materials. *Angew. Chem., Int. Ed.* **2006**, *45*, 3216−3251.

(21) Mamaeva, V.; Sahlgren, C.; Linden, M. Mesoporous Silica Nanoparticles in Medicine-Recent Advances. *Adv. Drug Delivery Rev.* **2013**, *65*, 689−702.

(22) Fágáin, C. Ó. Understanding and Increasing Protein Stability. *Biochim. Biophys. Acta, Protein Struct. Mol. Enzymol.* **1995**, *1252*, 1−14.

(23) Khawar, I. A.; Kim, J. H.; Kuh, H.-J. Improving Drug Delivery to Solid Tumors: Priming the Tumor Microenvironment. *J. Controlled Release* **2015**, *201*, 78−89.

(24) Goodman, T. T.; Olive, P. L.; Pun, S. H. Increased Nanoparticle Penetration in Collagenase-Treated Multicellular Spheroids. *Int. J. Nanomedicine* **2007**, *2*, 265−274.

(25) Tang, F.; Li, L.; Chen, D. Mesoporous Silica Nanoparticles: Synthesis, Biocompatibility and Drug Delivery. *Adv. Mater.* **2012**, *24*, 1504−1534.

(26) Liong, M.; Lu, J.; Kovochich, M.; Xia, T.; Ruehm, S. G.; Nel, A. E.; Tamanoi, F.; Zink, J. I. Multifunctional Inorganic Nanoparticles for Imaging, Targeting and Drug Delivery. *ACS Nano* **2008**, *2*, 889−896.

DOI: 10.1021/acsami.5b07116
ACS Appl. Mater. Interfaces 2015, 7, 24075−24081

SUPPORTING INFORMATION

Hybrid Collagenase Nanocapsules for Enhanced Nanocarrier Penetration in Tumoral Tissues.

María Rocío Villegas[a,b], *Alejandro Baeza*[b,a]* *and María Vallet-Regí*[a,b]*

[a] Dpto. Química Inorgánica y Bioinorgánica. UCM. Instituto de Investigación Sanitaria Hospital 12 de Octubre i+12. Plaza Ramón y Cajal s/n, Madrid (28040), Spain.

[b] Centro de Investigación Biomédica en Red de Bioingeniería, Biomateriales y Nanomedicina (CIBER-BBN). Av Monforte de Lemos, 3-5, Madrid, Spain.

*Corresponding autor e-mail: abaezaga@ucm.es, vallet@ucm.es

Materials section:

The chemicals were bought to the corresponding supplier and they have been used without further purification: Sodium Phosphate tribasic pure anhydrous (Acros Organics); Collagenase Type I (Life Technologies); Acrylamide (Fluka); 2-Aminoethyl methacrylate hydrochloride (Sigma Aldrich); Ethylene glycol dimethacrylate (Sigma Aldrich); Ammonium persulfate (Sigma Aldrich); *N,N,N',N'*-Tetramethyl-ethylenediamine (Sigma Aldrich); Amicon®Ultra-2mL Centrifugal Filters Ultracel®-10K (Millipore); Hexadecyltrimethylammonium bromide (Sigma Aldrich); Sodium Hydroxyde (Sigma Aldrich); Tetraethylorthosilicate (Sigma Aldrich); Ammonium nitrate (Sigma Aldrich); Ethanol absolute 99,5% for Synthesis (AppliChem Panreac); 3-(Triethoxysilyl)propylsuccinic anhydride; Toluene anhydrous 99,8% (Sigma Aldrich); Tetrahydrofuran (Sigma Aldrich); Diethyl ether (Sigma Aldrich); *N*-(3-Dimethylaminopropyl)-*N'*-ethylcarbodiimide hydrochloride (Sigma Aldrich); *N*-Hydroxysuccidimide, (Sigma Aldrich); Fluorescein isothiocyanateisome I (Sigma Aldrich); 3-Aminopropyltietoxysilane; 97% (ABCR); Protease from *Streptomyces griseus* (Sigma Aldrich); EnChek®Gelatinase/Collagenase Assay Kit (Life Technologies); Pur-A-Lyzer™ Maxi 6000 Dialysis Kit (Sigma Aldrich); Fluorescamine (Sigma Aldrich);10X PBS Buffer pH=7.4 (Ambion) and MaxGel™ECM (Sigma Aldrich); Glurtaraldehyde solution (Sigma Aldrich); Dulbecco's modified eagle's medium (Sigma Aldrich); Rat tail collagen (type I) First Link (UK) Ltd; Cell Navigator™ Lysosome Staining Kit*:* Component A: LysoBrite™ Red (AAT Bioquest ®); Component B: Live Cell Staining Buffer (AAT Bioquest ®); Triton® X-100 (Aldrich®), DAPI (Sigma®).

Instrumental section:

Fourier Transform Infrared spectroscopy (FI-TR) in a Thermo Nicolet nexus equipped with a Goldengate attenuated total reflectance device. Thermogravimetry Analysis (TGA) were performed in a Perkin Elmer Pyris Diamond TG/DTA analyzer, with 5 ºC/min heating ramps, from room temperature to 600 ºC. The hydrodynamic size of mesoporous nanoparticles and protein capsules was measured by means of a Zetasizer Nano ZS (Malvern Instruments) equipped with a 633 nm "red" laser. Transmission Electron Microscopy (TEM) was carried out with a JEOL JEM 3000 instruments operated at 300kV, equipped with a CCD camera. Sample preparation was performed by dispersing in distilled water and subsequent deposition onto carbon-coated copper grids. A solution of 1% of phosphotungstic acid (PTA) pH 7.0 was employed as staining agent in order to visualize the protein capsules alone and attached on the mesoporous surface. Fluorescence was measure with Synergy 4, power supply for Biotek Laboratory Instrument 100-240VAC, 50/60Hz, 250W. Confocal microscope Leica SP-2 AOBS with digital camera Leica DFC 350 FX. Scanning electron microscopy (SEM) analyses were made on a JEOL **JSM 7600F** microscope (Electron Microscopy Centre, UCM).

FIGURES

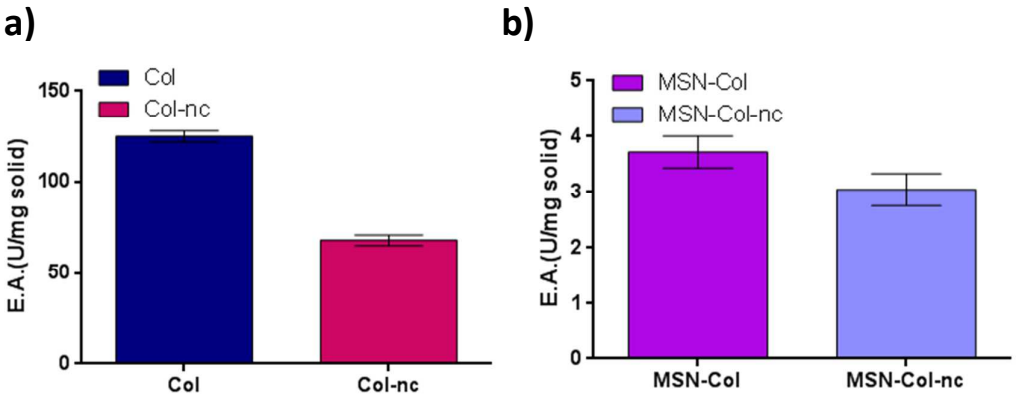

Figure S1. Enzymatic activity of a) Col and Col-nc b) MSN-Col and MSN-Col-nc.

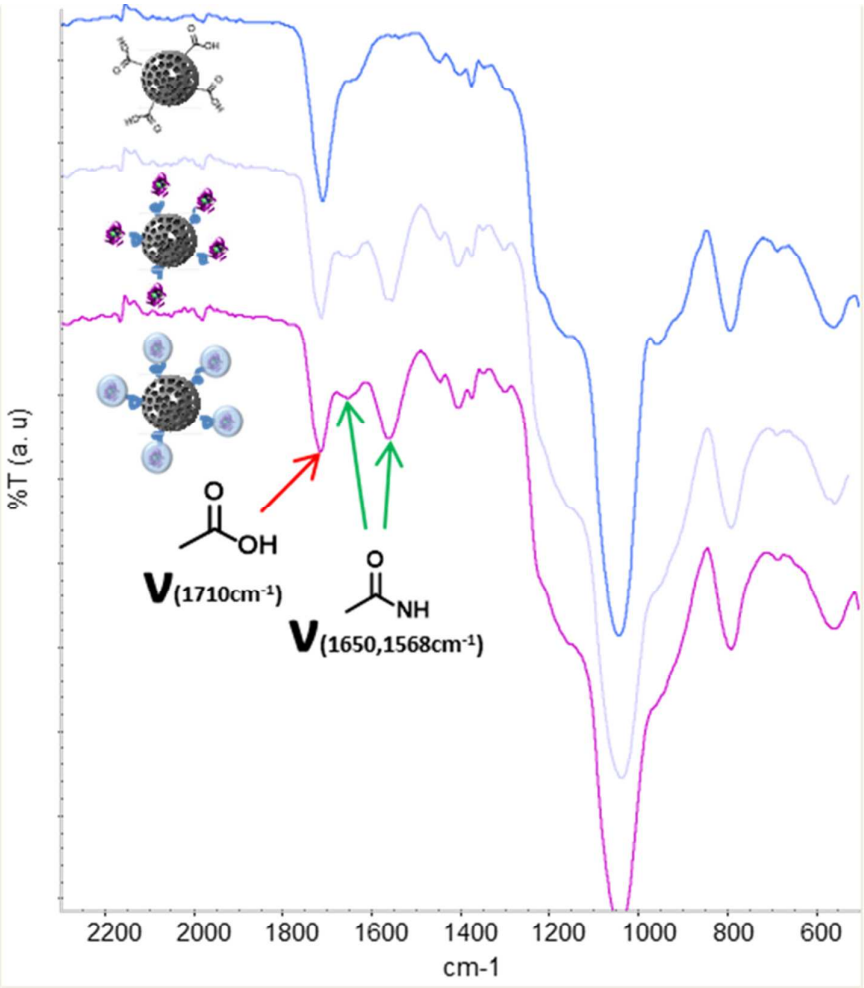

Sample	DLS (nm)	Z_{pot} (mV)	O.W. (%)	% [S]
MSN	141.8	-32.9	28	0.05
MSN-Col	220.2	-26.7	34	0.05
MSN-Col-nc	190.1	-33.1	36	0.08

Figure S2. Characterization of MSN, MSN-Col and MSN-Col-nc.

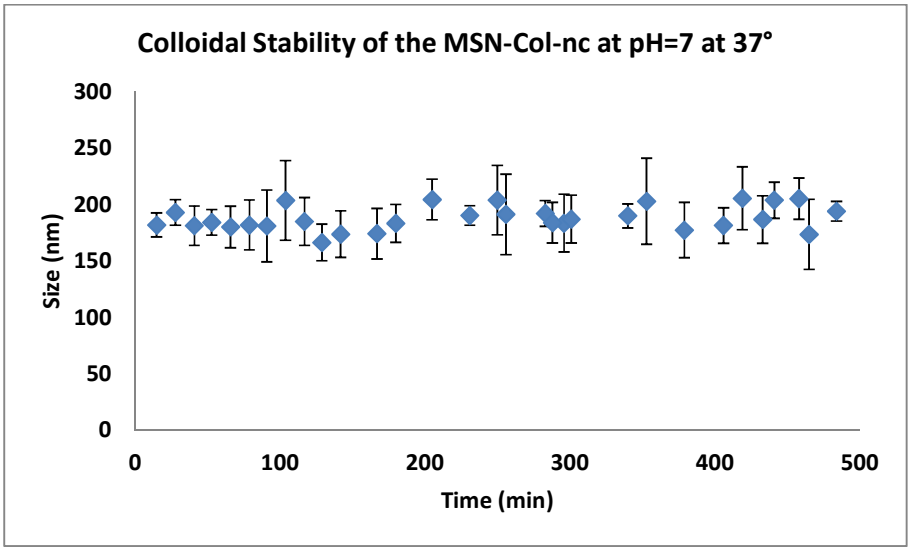

Figure S3. DLS measurements of MSN-Col-nc (0.1 mg/mL) suspended in PBS at pH = 7 and 37 ºC.

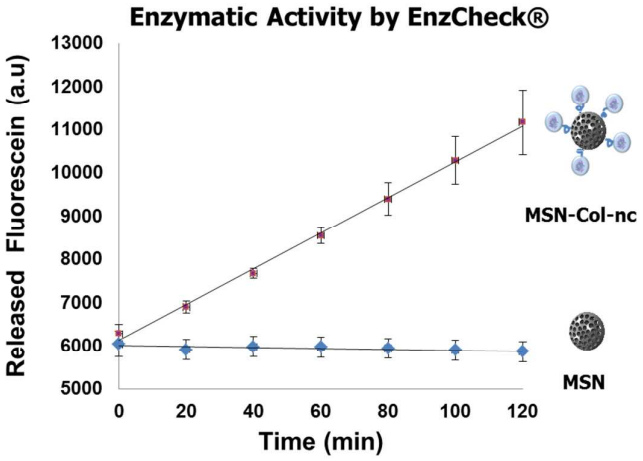

Figure S4. Enzymatic activity of MSN-Col-nc and MSN by EnzCheck®.

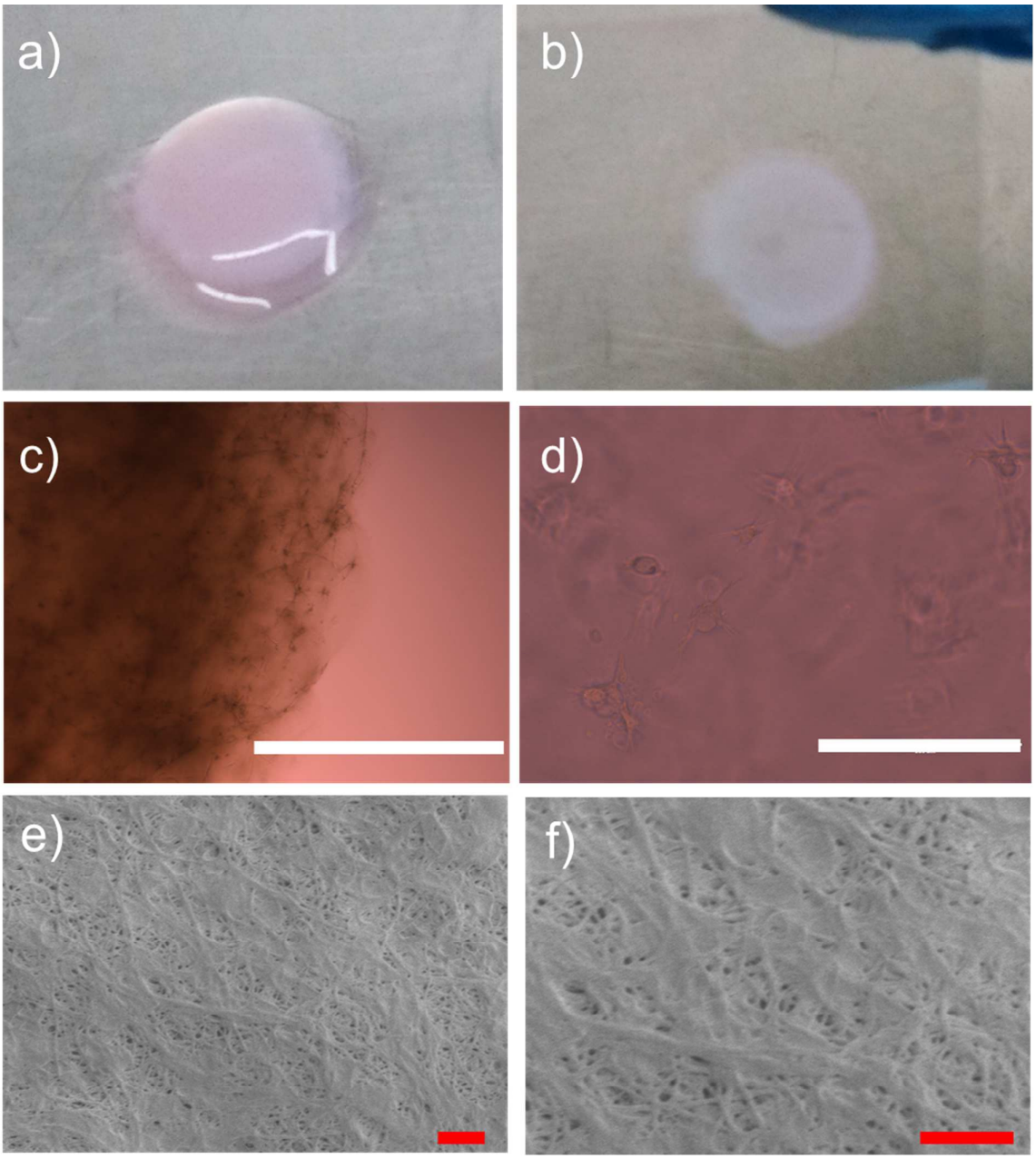

Figure S5. a) 3D-Human Osteosarcoma-seeded collagen gel b) Gel treated with glutaraldehyde during 25 min c) Optical Microscopy image of Gel (scale bar correspond to 1 mm) and d) Optical Microscopy image of the gel which shows the cells embedded within the matrix (White scale bar correspond 400 µm) e-f) Scaning electron microscopy of collagen gel (Red scale bar correspond to 1 µm).

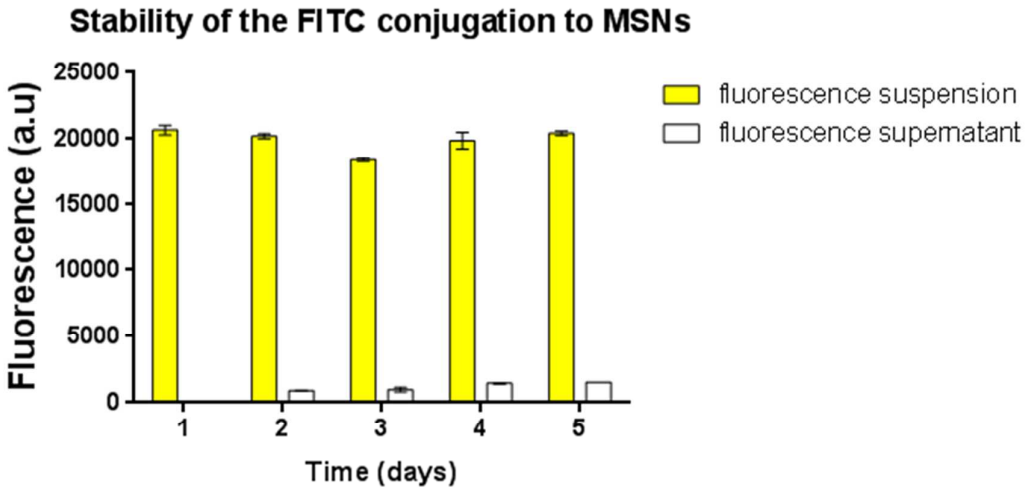

Figure S6. Stability over time of fluorescein conjugated within the silica matrix of fluorescent-MSN.

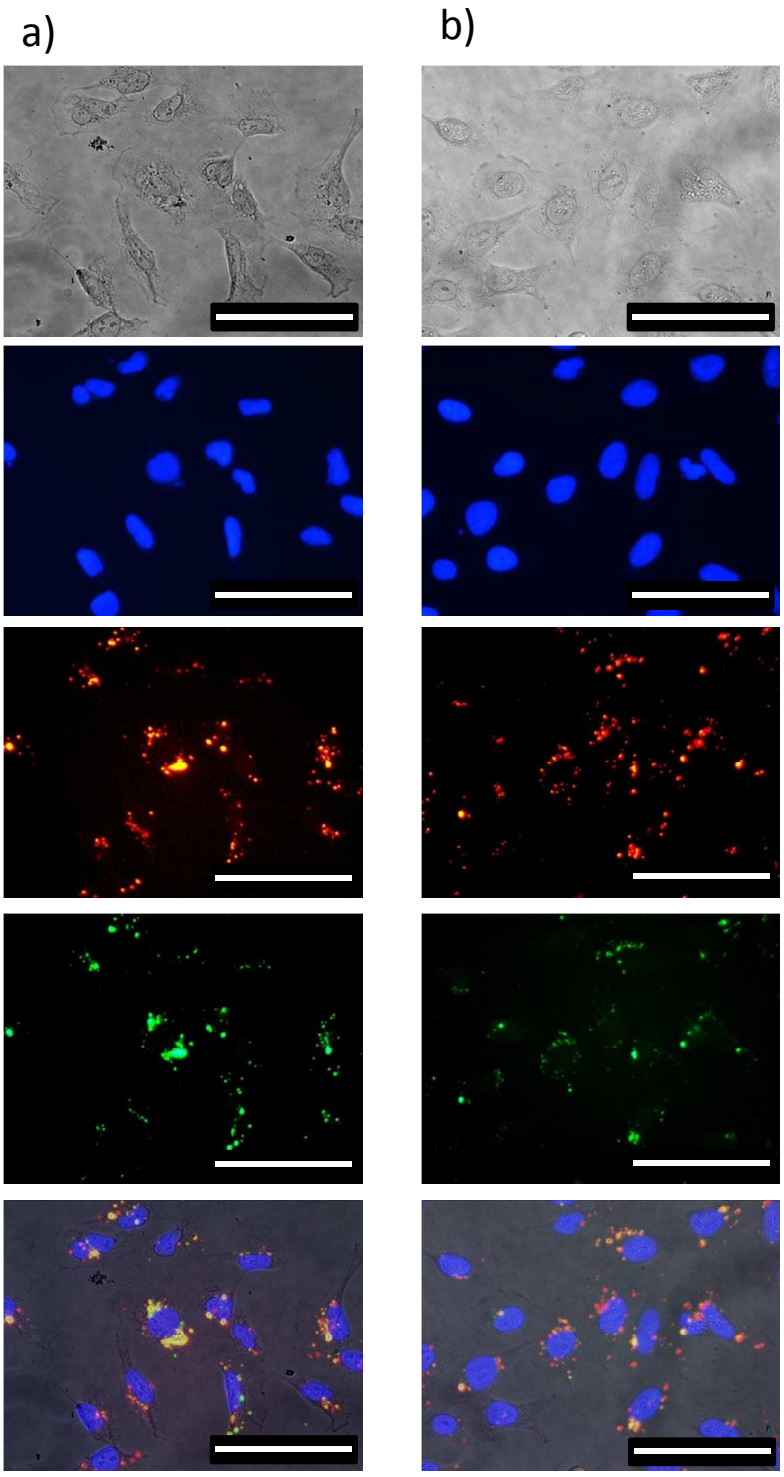

Figure S7. a) MSN and b) MSN-Col-nc. Fluorescence microscopy images of HOS cells incubated with MSN and MSN-Col-nc labeled with fluorescein. Blue stain corresponds to cell nucleus, red stain corresponds to lysosomes and green stain corresponds to nanoparticles. (Scale bar correspond to 100 µm).

III.I.II. Multifunctional Protocells for Enhanced Nanocarrier Penetration in 3D Extracellular Tumoral Matrices

Villegas, M. R.; Baeza, A.; Noureddine, A.; Durfee, P. N.; Butler, K. S.; Agola, J. O.; Brinker, C. J.; Vallet Regí, M. Multifunctional Protocells for Enhanced Penetration in 3D Extracellular Tumoral Matrices. *Chem. Mater.* **2017**, acs.chemmater.7b03128, doi:10.1021/acs.chemmater.7b03128.

CHEMISTRY OF MATERIALS
Cite This: Chem. Mater. 2018, 30, 112−120
Article
pubs.acs.org/cm

Multifunctional Protocells for Enhanced Penetration in 3D Extracellular Tumoral Matrices

María Rocío Villegas,[†,‡] Alejandro Baeza,[*,†,‡] Achraf Noureddine,[§] Paul N. Durfee,[§,⊥] Kimberly S. Butler,[§,⊥,#] Jacob Ongudi Agola,[§,⊥] C. Jeffrey Brinker,[*,§,⊥,¶,∥] and María Vallet-Regí[*,†,‡]

[†]Departamento de Química Inorgánica y Bioinorgánica, Facultad de Farmacia, Universidad Complutense de Madrid, 28040 Madrid, Spain

[‡]Networking Research Center on Bioengineering, Biomaterials and Nanomedicine (CIBER-BBN), 28029 Madrid, Spain

[§]Center for Micro-Engineered Materials, [⊥]Chemical and Biological Engineering, and [¶]Comprehensive Cancer Center, University of New Mexico, Albuquerque, New Mexico 87131, United States

[#]Nanobiology and [∥]Advanced Materials Laboratory, Sandia National Laboratories, Albuquerque, New Mexico 87123, United States

Supporting Information

ABSTRACT: The high density of the extracellular matrix in solid tumors is an important obstacle to nanocarriers for reaching deep tumor regions and has severely limited the efficacy of administrated nanotherapeutics. The use of proteolytic enzymes prior to nanoparticle administration or directly attached to the nanocarrier surface has been proposed to enhance their penetration, but the low *in vivo* stability of these macromolecules compromises their efficacy and strongly limits their application. Herein, we have designed a multifunctional nanocarrier able to transport cytotoxic drugs to deep areas of solid tumors and once there, to be engulfed by tumoral cells causing their destruction. This system is based on mesoporous silica nanocarriers encapsulated within supported lipid bilayers (SLBs). The SLB avoids premature release of the housed drug while providing high colloidal stability and an easy to functionalize surface. The tumor penetration property is provided by attachment of engineered polymeric nanocapsules that transport and controllably unveil and release the proteolytic enzymes that in turn digest the extracellular matrix, facilitating the nanocarrier diffusion through the matrix. Additionally, targeting properties were endowed by conjugating an antibody specific to the investigated tumoral cells to enhance binding, internalization, and drug delivery. This multifunctional design improves the therapeutic efficacy of the transported drug as a consequence of its more homogeneous distribution throughout the tumoral tissue.

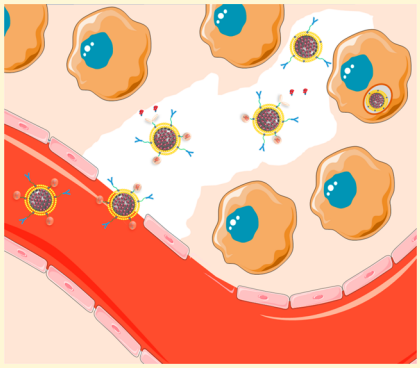

1. INTRODUCTION

Despite huge research efforts carried out in the last decades, cancer continues to be one of the leading causes of mortality worldwide.[1] Cancer cannot be considered as one simple disease. There are many different types of cancer depending on the type of malignant cell and the affected organ and even patient specific heterogeneity. Therefore, each of them presents its own set of particular features and therapeutic challenges. Moreover, even within the same tumor type, usually multiple tumor clonal cell populations coexist with different genetic alterations, which respond differently to the common administered therapeutic agents.[2] When it is not possible to remove the tumoral mass by surgery, the common treatment involves the administration of high energy radiation (radiotherapy) or the use of potent cytotoxic compounds (chemotherapy) to destroy dividing cells. However, the lack of selectivity of these therapies causes severe systemic toxicity on surrounding healthy tissues compromising not only the efficacy of the therapy, but also the patient's life or quality of life. Since Maeda and Matsumura's discovery in 1986 of passive accumulation of nanoparticles within tumoral masses,[3] the use of nanoparticles as drug carriers has been extensively studied in oncology.[4] This phenomenon, referred to as the enhanced permeation and retention effect (EPR), is caused by the unique blood vessel architecture present in solid tumors that presents pores with diameters up to a few hundred nanometers.[5] Thus, when nanoparticles reach the tumoral area, they are extravasated into the tumor passing through these pores, whereas they cannot cross the healthy blood vessel walls. The discovery of the EPR effect triggered the development of a multitude of nanocarriers with the aim to deliver the cytotoxic compounds directly to the diseased zone, without affecting the rest of the healthy tissues.[6] These nanodevices have been engineered to possess remarkable properties such as stimuli-responsive drug release,[7] invisibility to the immune system,[8] capacity to recognize the tumoral cells,[9] or even target to the tumor stem cells.[10] However, the clinical application of

Received: July 24, 2017
Revised: October 21, 2017
Published: December 15, 2017

DOI: 10.1021/acs.chemmater.7b03128
Chem. Mater. 2018, 30, 112−120

nanocarriers is still far from being a reality. A recent meta-study concluded that only 0.7% of the administered nanoparticles accumulate in the tumoral tissue, which could explain the low effectiveness of the nanotherapies observed in clinical trials.[11] One common problem in nanomedicine is the lack of system penetration into the tumoral tissue.[12] The extracellular matrix of tumoral tissues has usually a denser extracellular matrix than their healthy counterparts due to the higher presence of collagen which limits the penetration of carriers into the tissue.[13] Thus, the extravasated nanomedicine accumulates mainly on the periphery of the tumor where it can be easily flushed out of the tumor by intravasation after causing only local peripheral effects. The intratumoral administration of proteolytic enzymes such as collagenase or hyaluronidase prior to nanoparticle injection has been proposed to enhance the particle penetration.[14] These proteolytic enzymes have also been anchored on the nanocarrier surface resulting in improved particle penetration.[15] Recently, Villegas et al. reported the use of pH-responsive polymeric nanocapsules which contains collagenase for enhancing the particle penetration in 3D tumoral tissue models while protecting the proteolytic enzyme.[16] These nanocapsules were rapidly hydrolyzed under mild acidic conditions expected within hypoxic tumor tissue. In the mild acidic environment, the housed enzymes are released in 2 h, whereas nanocapsule hydrolysis requires longer times under normal physiological conditions. In addition to achieving higher penetration within the tumoral mass, an efficient nanocarrier should be able to fulfill other features such as the ability to selectively bind to the target tumoral cell within a myriad of different cell populations and retain the transported therapeutic payload until it reaches the intracellular space of the malignant cell.[17]

Herein, we report the synthesis and evaluation of a novel multifunctional nanocarrier able to penetrate deeply within a solid tumoral mass while retaining their payload and selectively bind and internalize into tumor cells where the triggered release of the cytotoxic cargo leads to destruction of the targeted tumor cell. This nanodevice is composed of a mesoporous silica nanoparticle (MSN) capable of loading high amounts of drugs due to its very high specific area and accessible interior pore volume. The MSN external surface is encapsulated within a supported lipid bilayer conjugated with proteolytic nanocapsules, targeting ligands, and polyethylene glycol (PEG) in a nanocarrier construct referred to as a protocell.[18,19]

The protocell SLB serves to protect and retain cargo within the MSN until pH triggered release within acidified endosomal environments.[19] It also confers unique properties to the system such as high colloidal stability, low immunogenicity, and long circulation times within the bloodstream. The SLB of the protocell was decorated with pH-responsive collagenase nanocapsules for enhancing tissue penetration and with EGFR-antibodies, able to selectively bind to cells that overexpress epidermal growth factor receptors (EGFR), to increase the internalization of the protocell into tumoral cells and ensuing drug delivery. The capacity of this novel multifunctional protocell to recognize EGFR-positive tumoral cells that are deeply located within a solid tumoral mass was tested employing an *in vitro* 3D cell culture model, showing significantly improved penetration, internalization and destruction capacity of the malignant cells relative to protocells prepared without collagenase nanocapsules.

2. RESULTS

2.1. Synthesis of Protocells. The protocell MSN core was designed with hexagonally arranged cylindrical pores of diameter 3−4 nm, which represents the optimal size for loading therapeutic agents based on small molecules,[20,21] as is the case for many conventional cytotoxic compounds employed in antitumoral chemotherapy.[22] MSNs were synthesized following a modified Stöber method reported elsewhere,[23] yielding monodisperse nanoparticles with an average diameter of 75−100 nm according to dynamic light scattering (DLS) measurements (Figure S1) and transmission electron microscopy (TEM) (Figure 1a). MSNs were covalently labeled with rhodamine B throughout the silica matrix to enable fluorescence imaging.

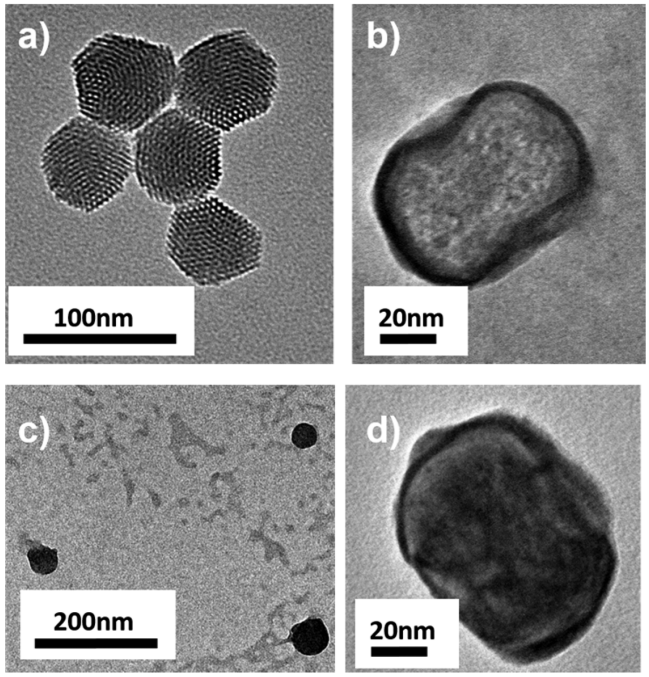

Figure 1. TEM images of (a) MSN, (b) PC−COOH13, (c) Col_{nc}, and (d) PC−COOH13-Col_{nc}.

MSNs were encapsulated within SLBs formed by fusion of zwitterionic lipid-based vesicles (Scheme 1). The zwitterionic lipid, 1,3-distearoyl-*sn*-glycero-3-phosphocholine (DSPC) was chosen as the main component to provide structural support to the liposome and cholesterol was added for controlling the fluidity of the SLB. To provide anchoring points for the further introduction of targeting moieties and collagenase nanocapsules, the functional PEGylated lipids, 1,2-distearoyl-*sn*-glycero-3-phosphoethanolamine-*N*-[carboxy(polyethylene glycol)-2000] (DSPE- PEG(2000)-COOH) providing a functional carboxylic group and 1,2-distearoyl-*sn*-glycero-3-phosphoethanolamine-*N*-[amino(polyethylene glycol)-2000] (DSPE-PEG(2000)-NH_2), providing a functional amine, were also employed in the vesicle formulation. Here the polyethylene glycol chain (2000 Da) intercalated between the phospholipid headgroup and the respective functional group serves to enhance the colloidal stability of the resulting vesicle, as well as the protocells once formed.[24] Moreover, it is well-established that the presence of PEG chains on the particle surface improves the circulation time of the nanocarriers within the bloodstream.[25] These polymeric chains hamper the adsorption of the immune proteins

DOI: 10.1021/acs.chemmater.7b03128
Chem. Mater. 2018, 30, 112−120

Scheme 1. Synthetic Pathway for the Production of Protocells

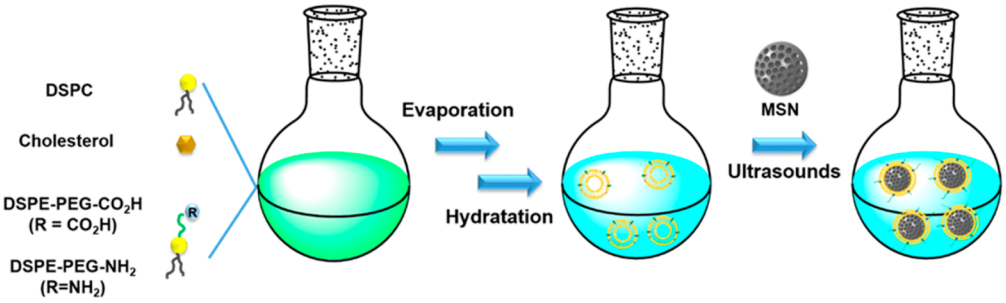

Scheme 2. Synthesis of Col_{nc} (Upper Scheme) And Attachment Pathway of Col_{nc} and Anti-EGFR-Biotin on PC Surface (Lower Scheme)

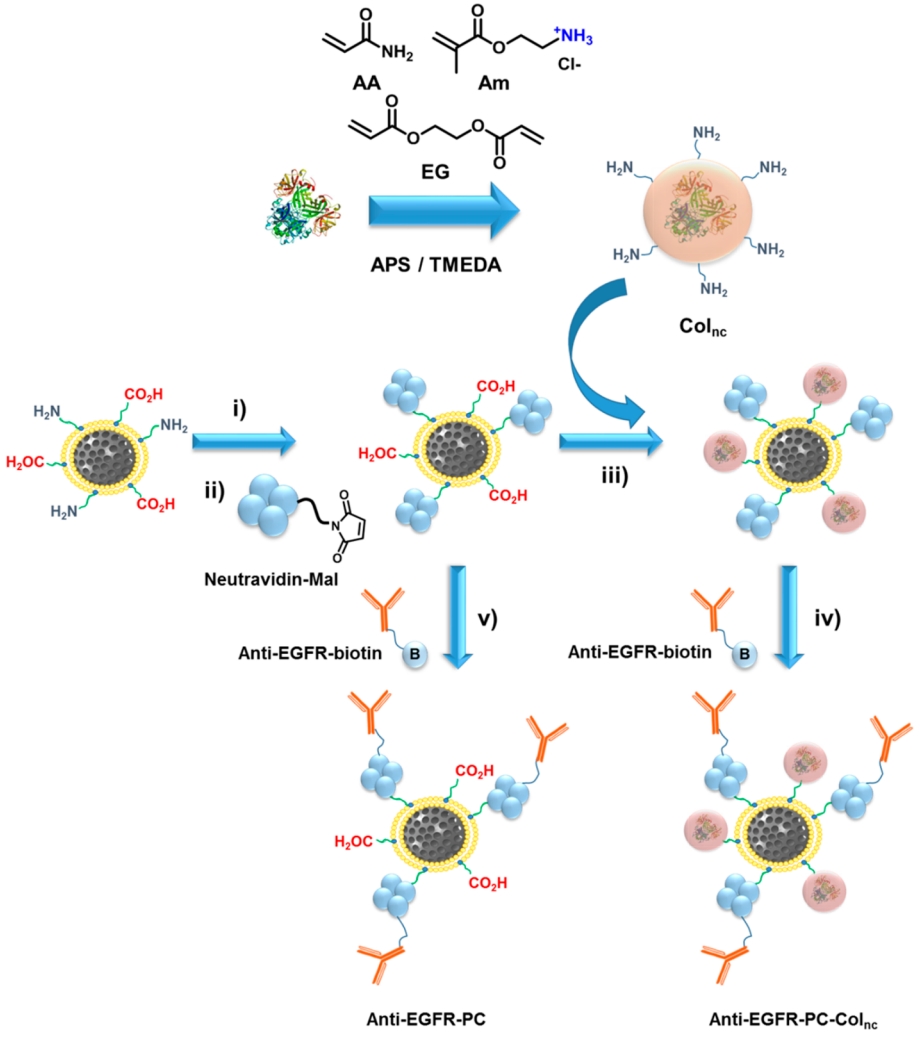

(opsonins) responsible for labeling foreign bodies for macrophage capture. Liposomes were synthesized following the thin-film hydration or Bangham method.[26] This method is based on the dissolution of various phospholipids in one organic phase followed by solvent evaporation, obtaining a lipid film. After that, the film is hydrated in a salt-rich aqueous medium under strong sonication, which results in the liposome formation. Two batches of vesicles were synthesized maintaining a fixed molar ratio of cholesterol to DSPE-PEG(2000)-NH_2 (20:2) and varying the molar ratio of DSPC and DSPE-PEG(2000)-COOH (65:13) and (48:30), respectively. The percentage of introduced amino groups was kept constant at 2% because this percentage is sufficient for the antibody attachment as previously reported.[18] Thus, the two batches present different concentrations of carboxylic groups to determine the effect of the concentration of collagenase nanocapsules on penetration. Both vesicle batches were extruded to yield a monodisperse size distribution centered at 100 nm according to DLS measurements (DLS of DSPE-PEG(2000)-COOH (65:13) shows in Figure S2 as an example).

Two batches of protocells were prepared by incubating an aqueous suspension of MSN with vesicles of the respective formulation under strong sonication for 20 s in phosphate

DOI: 10.1021/acs.chemmater.7b03128
Chem. Mater. 2018, 30, 112−120

buffered saline (PBS). Excess vesicles not fused to the silica surface were removed via centrifugation. Both protocell batches (PC−COOH13 and PC−COOH30, respectively) showed monodisperse sizes centered around 175 nm according to the DLS measurements (Figure S3). The presence of the lipid bilayer on the MSN surface was confirmed by TEM using phosphotungstic acid (PTA) as a staining agent (Figure 1b).[26] The thickness of the supported lipid bilayer was measured to be ∼4.7 nm on both batches (n = 20), which is in agreement with the values reported in the literature for 'protocell' systems.[18]

2.2. Synthesis of Collagenase Nanocapsules (Col_{nc}). As was mentioned in the introduction, tumor penetration is one of the most important challenges facing the field of nanomedicine. The diffusion of nanometric objects in a fluid is understood by the Stokes−Einstein equation ($D = KT/6\pi\eta r$), which indicates that the diffusion rate (D) is inversely proportional to the particle radius (r) and also to the viscosity of the media (η). Therefore, the diffusion of nanometric objects is clearly reduced by increasing particle size and the viscosity of the media. Many solid tumors exhibit overproduction of collagen, which accumulates within the extracellular matrix (ECM) and greatly impedes particle diffusion through the inner tumoral core. The intratumoral injection of proteolytic enzymes able to destroy these collagen accumulations partially alleviates this problem, but due to the labile nature of these enzymes, it is necessary to administer several dosages of them to achieve significant results. Our research group has reported the use of polymeric nanocapsules which contain enzymes encapsulated within an organic shell to preserve their catalytic function in the presence of aggressive agents such as temperature or other proteolytic enzymes.[27,28] Recently, collagenase has been encapsulated within pH-sensitive polymeric nanocapsules, which were designed to rapidly release the housed enzyme when the pH drops to the mild acidic conditions usually present in many tumoral tissues but retains the enzyme trapped within the polymeric matrix up to 24 h under normal physiological conditions.[16] Following the same methodology, collagenase polymeric nanocapsules were formed by a radical polymerization method which employs acrylamide (AA), as the main structural monomer, 2-aminoethyl methacrylate (Am) as the monomer that provides amino groups required for the further attachment on the protocell surface, and ethylenglycol dimethacrylate (EG) as pH-degradable cross-linker (Scheme 2).[29] In this process, monomer/protein molar ratios of 2419:1 and AA:Am:EG ratio (7:6:2) were employed.

The resulting nanocapsules were characterized by DLS measurements and TEM showing an average diameter of about 50 nm and a round-shaped morphology (Figure 1c). The employed polymer composition was selected to exhibit degradation by progressive hydrolysis over 24 h, which is accelerated in the mild-acidic conditions present in the tumor environment. The nanocapsule degradation at physiological pH was monitored by following decrease in hydrodynamic diameter over time. We observed that the collagenase nanocapsules initially of ∼50 nm in hydrodynamic diameter were progressively degraded until they reached a size of ∼7 nm, indicating the enzymes complete release after 24 h (Figure S4). The encapsulated collagenase retained its catalytic activity as was previously reported.[16]

2.3. Protocell Functionalization: Anchoring of Anti-EGFR and Collagenase Nanocapsules. To confer selectivity against tumoral cells, the nanoparticle surface was decorated with targeting moieties capable of being specifically recognized by cell membrane receptors overexpressed on the surface of cancerous cells. An EGFR antibody (anti-EGFR) was selected as a targeting ligand due to the common overexpression of EGFR in many human cancers, in particular lung cancer.[30,31] For this reason, A549 lung tumor cells were selected in this work as a cellular tumoral model. The anchoring of anti-EGFR and collagenase nanocapsules was carried out following a multistep synthetic process (Scheme 2).

The first step (i) was the conversion of the amino groups present on the protocell surface into thiol groups by the reaction with 2-iminothiolane hydrochloride (Traut's reagent). Then, these thiol groups were employed to anchor the maleimide-neutravidin moieties (ii). Thus, the protocells were ready for the antibody introduction employing biotinylated-Anti-EGFR (iv or (v). Because of the sensitive nature of antibodies, collagenase nanocapsules were anchored (iii) prior to the introduction of antibody to preserve the recognition capacity of this macromolecule. As was mentioned above, two protocell batches displaying different percentages of carboxylic groups were synthesized (PC−COOH13 and PC−COOH30) to find the optimal composition which resulted in a higher collagenase nanocapsule attachment. Thus, collagenase nanocapsules were anchored on both types of protocells, using well-known carbodiimide chemistry (iii). The presence of collagenase nanocapsules was confirmed by measuring the enzymatic activity of the PC−COOH13-Col_{nc} and PC−COOH30-Col_{nc} respectively, using EnChekGelatinase/Collagenase Assay Kit. Both samples exhibited similar enzymatic activity and therefore, an increase in the amount of carboxylic groups on the PC surface did not improve the Col_{nc} attachment (Figure S5). Additionally, the colloidal stability of PC−COOH13-Col_{nc} was significantly higher than PC−COOH30-Col_{nc}, showing that the particles remained well suspended in PBS for more than 15 days. For these reasons, PC−COOH13-Col_{nc} was selected as the best system for the further attachment of Anti-EGFR, which was carried out through the formation of a biotin-neutravidin bridge (iv and v).

2.4. *In Vitro* Evaluation of Protocell Targeting Capacity in 2D Model. As described above, Anti-EGFR was anchored on the protocell surface for improving the particle uptake within the tumoral cells. The capacity of these systems to selectively bind to tumoral cells was tested by employing 2D cultures of A549 lung cancer cells because these cells overexpress EGFR on their surface. A549 cells were exposed for 24 h to a fixed concentration of protocells (80 μg/mL) with and without the antibody anchored on their surface. After this time, the cells were gently washed with PBS to remove all noninternalized particles. The percentage of cells that had engulfed fluorescent nanoparticles was determined by flow cytometry thanks to the presence of rhodamine B covalently labeled within the silica matrix of the protocells (Figure 2).

The results confirmed the importance of the functionalization with the antibody because only 2% of the tumoral cells engulfed the protocells that did not present the antibody on their surface, whereas this value rose to over 90% when the antibody was present. In the complete system (Col_{nc}-PC-Anti-EGFR), collagenase nanocapsules were anchored prior to the antibody functionalization. This anchoring process requires carboxylic acid activation by carbodiimide chemistry, which could alter the neutravidin pockets due to the presence of carboxylic and amine groups in this protein and therefore could compromise the antibody conjugation. To evaluate this possibility, the cells were exposed to Col_{nc}-PC-Anti-EGFR and compared to the PC-Anti-

DOI: 10.1021/acs.chemmater.7b03128
Chem. Mater. 2018, 30, 112−120

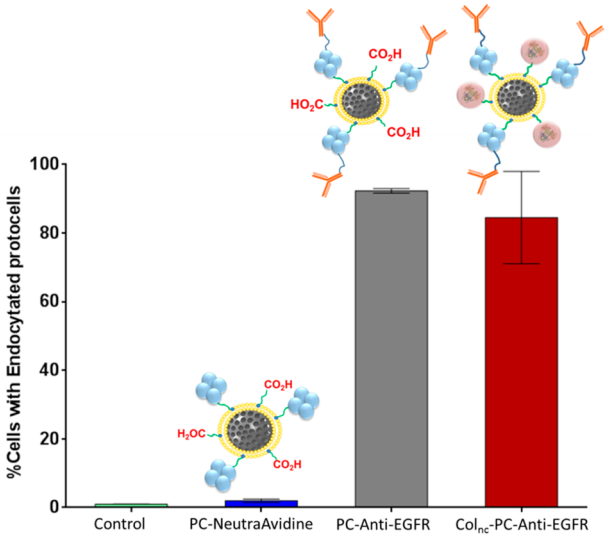

Figure 2. Cellular uptake of protocell with and without Anti-EGFR and Col$_{nc}$. Samples were performed in triplicate.

EGFR alone. Both the full construct, Col$_{nc}$-PC-Anti-EGFR, and PC-Anti-EGFR yielded similar uptake of 85% and >90%, respectively, confirming the suitability of this strategy for the synthesis of the complete nanodevice.

2.5. Evaluation of Penetration Capacity in 3D Tumoral Tissue Model. To evaluate the penetration capacity of these multifunctional protocells, a 3D tissue model that mimics the existing conditions in a solid tumoral mass was prepared. This model was based on the use of a 3D collagen gel containing embedded tumoral cells within its structure. This model presents similar consistency and rheological properties to human tumor tissue, and therefore, it can be employed as a simple substitute for a complex *in vivo* microenvironment.[32] Our model consisted of a monolayer of A549 cells on which a 3D collagen gel with embedded tumoral cells of 200 μm thickness was grown (Figure 3).

The gel mimics the ECM of the tumor and acts as barrier hindering the diffusion of protocells to the A549 monolayer. Thus, to test the enhanced penetration of the system decorated with collagenase nanocapsules, a suspension of fluorescent protocells (80 μg/mL) bearing the antibody and prepared with or without collagenase nanocapsules, was carefully placed on the top of the gel. After 24 h of incubation, the gels were gently washed with PBS to remove the protocells which were unable to penetrate within/into the collagen matrix. The capacity to reach the bottom cell monolayer was assessed in each case by fluorescence confocal microscopy. The cell nuclei were stained with DAPI (blue) and, with the aim to assess that protocells were truly engulfed within the cell cytoplasm thanks to the presence of the targeting moiety, actin filaments were stained with green phalloidin. The confocal images show that only protocells functionalized with nanocapsules were able to reach the bottom layer, as can be observed by the existence of perinuclear red dots which correspond to the rhodamine B labeled MSN cores of the protocells. This result confirms the capacity of Col$_{nc}$-PC-Anti-EGFR to overcome the collagen barrier and reach deep layers of the tissue model. In addition, these protocells were found within the tumoral cell cytosol, which confirms the enhanced internalization of these nanocapsule-bearing protocells inside malignant cells. On the contrary, PC-Anti-EGFR were not able to overcome the collagen barrier and they were likely removed in the washing step, as can be observed by the absence of red dots (labeled nanocapsule-free protocells) in the cell layer.

2.6. Evaluation of Cytotoxic Capacity of Drug-Loaded Protocells in 3D Tumoral Tissue Model. Having established the ability of Col$_{nc}$-PC-Anti-EGFR to reach deep areas within a 3D tumoral model and once there, to be selectively internalized by tumoral cells, the ability of the system to transport and deliver cytotoxic drugs capable of inducing cell death was studied. Topotecan (TOP) is a potent antitumoral therapeutic but it suffers significant instability in the bloodstream losing its activity in a few hours.[33] For this reason, repeated dosages are required to maintain its concentration in the blood, which leads to severe side effects. It has been reported that the encapsulation of TOP within a nanocarrier improves its therapeutic efficacy.[34] For these reasons, topotecan was selected as drug model for this system. Col$_{nc}$-PC-Anti-EGFR were loaded prior to the

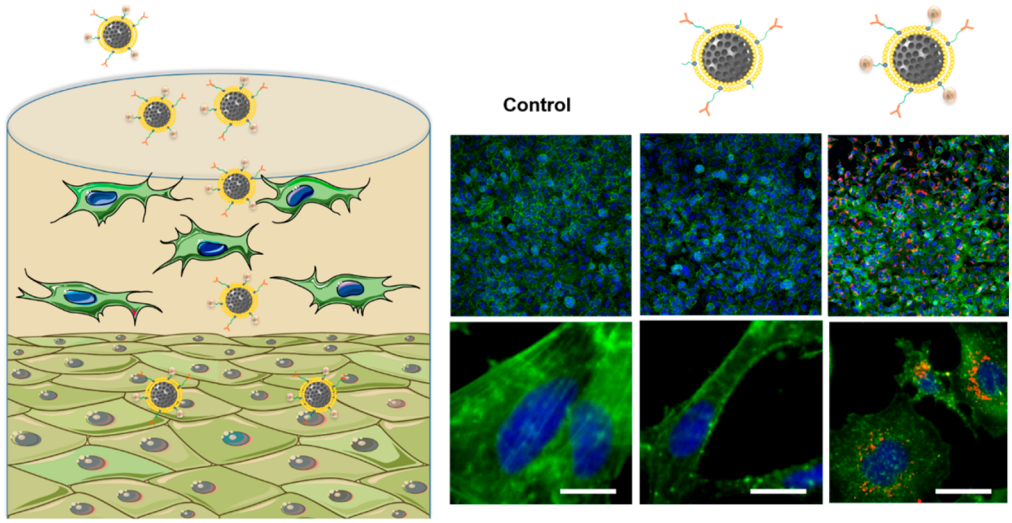

Figure 3. Evaluation of penetration and internalization capacity of PC-Anti-EGFR and Col$_{nc}$-PC-Anti-EGFR nanodevices, employing 3D tumoral tissue models. Cell nuclei are stained in blue, actin filaments were stained in green, and protocells were labeled in red (white bars correspond to 25 μm). Confocal fluorescent micrographs of each separate channel can be found in Supporting Information (Figure S6).

DOI: 10.1021/acs.chemmater.7b03128
Chem. Mater. 2018, 30, 112−120

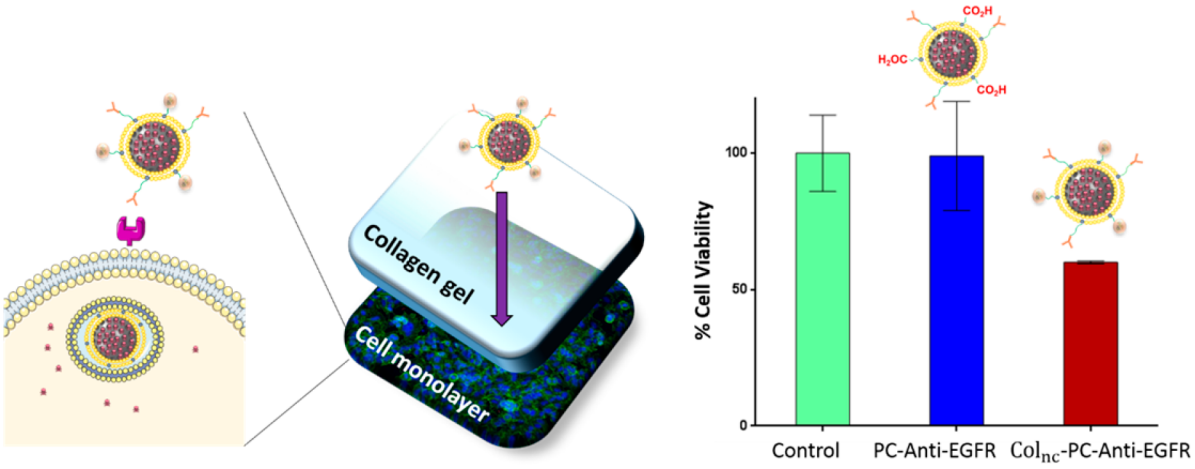

Figure 4. Cytotoxic capacity of Protocells in 3D tumoral tissue model after 24 h of incubation ($n = 3$, $p < 0.05$).

formation of the protocell by incubating the silica core for 24 h in an aqueous solution of topotecan (3 mg mL^{-1}). The loading capacity of the protocells was determined by differences in fluorescence between the topotecan solution, before and after the loading, yielding 0.6% (w:w) of cargo. A suspension of topotecan-loaded Col$_{nc}$-PC-Anti-EGFR was deposited on the surface of the 3D tumoral tissue model. PC-Anti-EGFR loaded with the same amount of topotecan was employed as a control to evaluate the cytotoxic capacity of protocells, which did not possess penetration capacity. After 24 and 48 h of incubation time, cell viability was evaluated by the Alamar blue viability assay. At 24 h, the results showed that topotecan-loaded Col$_{nc}$-PC-Anti-EGFR induced around 40% of cell mortality, whereas the system which did not contain the collagenase nanocapsules had negligible cytotoxicity (Figure 4). After 48 h, the cytotoxicity observed in the case of topotecan(TOP)-loaded Colnc-PC-Anti-EGFR reached up to 60% and PC-Anti-EGFR induced around 20% of cell destruction. The cytotoxicity provoked by this last nanodevice was probably caused by the small amount of TOP that leaks from protocells when they are exposed to physiological conditions over a relatively long timespan (Figure S7).[18] These results confirmed that the higher penetration capacity of collagenase nanocapsules results in significant improvements in the therapeutic efficacy of the cytotoxic compounds transported by these multifunctional protocells.

3. CONCLUSIONS

Herein, a multifunctional tumor-penetrating nanocarrier capable of selective delivery of antitumoral drugs to deep tumoral layers has been developed. This system is composed of mesoporous silica nanocarriers encapsulated within a supported lipid bilayer (aka protocell). The SLB of the protocell construct was modified with collagenase containing nanocapsules that serve to digest the highly dense tumoral extracellular matrix and enable protocell penetration. These collagenase nanocapsules were designed to protect the enzymatic activity of the collagenase until the target tissue is reached and then, to have pH-triggered (accelerated) release of collagenase within the tumoral area. Additionally, the "plug and play" feature of protocell surface allowed anchoring of EGFR antibodies, whose receptors are commonly overexpressed in human lung cancer cells, allowing a preferential internalization within tumoral cells. Thus, the system achieves highly efficient penetration within dense matrix, selective internalization by tumoral cells and successful and controlled delivery of cytotoxic anticancer drugs. The importance of this system was highlighted by employing a 3D tumoral tissue model that mimics the extracellular matrix present in diseased tissues. Therefore, this system has demonstrated the capability to overcome one of the major problems of current nanomedicine, which is the limited penetration of nanosystems. The application of this strategy would pave the way for the design of smarter nanoconstructs able to achieve more homogeneous drug distribution within solid tumors, which is an important advance toward their clinical applications.

4. MATERIALS AND METHODS

4.1. Materials. Rhodamine B isothiocyanate (RBITC) (Sigma-Aldrich); Ethanol (Dismadel); (3-aminopropyl)triethoxysilane (APTES) (ABCR); Hexadecyltrimethylammonium bromide (CTAB) (Sigma-Aldrich); ammonium hydroxide (NH4OH, 28−30%) (Fluka); Tetraethyl orthosilicate (TEOS) (Aldrich); Ammonium nitrate (Sigma-Aldrich); 1,3-distearoyl-*sn*-glycero-3-phosphocholine (DSPC) (Avanti Lipids); 1,2-distearoyl-*sn*-glycero-3-phosphoethanolamine-N-[amino(polyethylene glycol)-2000] (ammonium salt) (DSPE-PEG(2000)-NH2) (Avanti Lipids); 1,2-distearoyl-*sn*-glycero-3-phosphoethanolamine-N-[carboxy(polyethylene glycol)-2000] (ammonium salt) (DSPE- PEG(2000)-COOH) (Avanti Lipids); Cholesterol (Avanti Lipids); Traut's reagent (Aldrich); Maleimide activated netrAvidin (thermo Scientific); biotinlyated EGFR antibody (Abcam); Collagenase Type I (Life Technologies); Acrylamide (Fluka); 2-Aminoethyl methacrylate hydrochloride (Sigma-Aldrich); Ethylene glycol dimethacrylate (Sigma-Aldrich); Ammonium persulfate (Sigma-Aldrich); N,N,N′,N′-Tetramethylethylenediamine (Sigma-Aldrich); AmiconUltra-2 mL Centrifugal Filters Ultracel-10K (Millipore); N-(3- Dimethylaminopropyl)-N′-ethylcarbodiimide hydrochloride (Sigma-Aldrich); *N*-Sulfo-Hydroxysuccidimide, (Sigma-Aldrich); EnChekGelatinase/Collagenase Assay Kit (Life Technologies); 10X PBS Buffer pH = 7.4 (Ambion); Dulbecco's modified Eagle's medium (Sigma-Aldrich); Rat tail collagen (type I) First Link (UK) Ltd.; Bovine serum albumin (BSA) (Sigma); Paraformaldehyde (Sigma-Aldrich); Atto488 phalloidine (Sigma-Aldrich); Triton X-100 (Aldrich); DAPI (Sigma); Topotecan (Sigma-Aldrich); Alamar blue (Invitrogen).

4.2. Instrumental Section. The hydrodynamic size of mesoporous nanoparticles and protein capsules was measured by means of a Zetasizer Nano ZS (Malvern Instruments) equipped with a 633 nm "red" laser. Transmission electron microscopy (TEM) was carried out with a JEOL TEM 3000 instruments operated at 300 kV, equipped with a CCD camera. Sample preparation was performed by dispersing MSN or protocells in pure ethanol or in distilled water, respectively, and

DOI: 10.1021/acs.chemmater.7b03128
Chem. Mater. 2018, 30, 112−120

subsequent deposition onto holey carbon coated copper grids. A solution of 1% of phosphotungstic acid (PTA) pH 7.0 was employed as staining agent to visualize the protein capsules alone and attached on the mesoporous surface. Fluorescence was measured with Synergy 4, power supply for Biotek Laboratory Instrument 100−240VAC, 50/60 Hz, 250W. Confocal microscope Olympus FV1200 (Electron Microscopy Centre, UCM).

4.3. Synthesis of Mesoporous Silica Nanoparticles (MSN). To prepare dye-labeled mesoporous silica nanoparticles, 1.5 mg of Rhodamine B isothiocyanate (RBITC) was dissolved in 1 mL of ethanol and 1.5 μL of (3-aminopropyl)triethoxysilane (APTES) and the solution RBITC-APTES was keep at room temperature under magnetic stirring for 2 h. 0.290 g of hexadecyltrimethylammonium bromide (CTAB) was dissolved 150 g in ammonium hydroxide 0.32 M and the solution was incubated at 50 °C under magnetic stirring for 1 h in a 200 mL beaker sealed with parafilm. Then 3 mL of 0.88 M tetraethyl orthosilicate (TEOS) in ethanol and RBITC-APTES were added to the surfactant solution after adjusting the stirring speed to 650 rpm. The mixture was incubated at 50 °C under magnetic stirring for 1 h without parafilm, then the solution was aged at 50 °C overnight under static conditions. The next day, the particles were subjected to a hydrothermal treatment at 70 °C for 20 h before being collected by centrifugation and washed three times with water and ethanol. The surfactant was removed by placing the particles in 500 mL of a solution of 95% ethanol, 5% water, and 10 g of NH_4NO_3 mL^{-1} at 80 °C during 3 h with reflux and under stirring. The nanoparticles were washed with ethanol and were finally stored in pure ethanol.

4.4. Liposome Preparation. The lipids and cholesterol were solubilized in choloroform and were stored at −20 °C. To prepare liposomes, the corresponding lipids were mixed at mol % ratios: DSPC/Chol/DSPE-PEG(2000)-NH_2/DSPE- PEG(2000)-COOH = 65/20/2/13 and 48/20/2/30. The lipids were dried under vacuum to remove the organic solvent and obtain lipids film and were rehydrated in 1X PBS and bath sonicated for 1 h to obtain liposome solution. To obtain a monodispersed liposome solution, the liposomes were extruded using 0.05 μm polycarbonate filter membrane at least 21 times. Then monodispersed liposomes were obtained.

4.5. Synthesis of Protocells (PC−CO_2H13 and PC−CO_2H30). The silica nanoparticles were transferred to water at (2.5 mg/mL) from the ethanolic suspension by centrifugation (15 000 rpm, 10 min) and resuspension in water. To each batch of MSN, a suspension of liposomes 8×10^{-6} mol in 1.2 mL of PBS with 13% or 30% of carboxylic groups was added. The mixtures were sonicated for 20 s, and the excess of liposomes was removed by centrifugation (15 000 rpm, 10 min). The pelleted protocells were redispersed in PBS (1X) by sonication; this process was repeated two times. Finally, the protocells were stored in 1 mL of PBS (2.5 mg/mL).

4.6. Synthesis of Collagenase Capsule (Col_{nc}). First, the reaction buffer $NaHCO_3$ (0.01 M, pH 8.5) was deoxygenated by freeze-vacuum-N_2 cycles. Then collagenase (3.1×10^{-5} mmol) was dissolved in the freshly deoxygenated buffer. In a separated vial, 0.035 mmol of acrylamide (AA), 0.030 mmol of 2-aminoethyl metacrylate hydrochloride (Am), and 0.010 mmol of ethylene glycol dimetacrylate (EG) were dissolved in 1 mL of deoxygenated buffer and the monomer solution was added to the protein solution. This mixture was stirred at 300 rpm for 10 min under nitrogen atmosphere at room temperature. Then 0.013 mmol of ammonium persulfate and 0.02 mmol of *N*,*N*,*N*′,*N*′-tetramethyl ethylenediamine (TMDA) dissolved in 1 mL of the deoxygenated buffer was added. The solution was stirred at 300 rpm for 90 min at room temperature under inert atmosphere. Next, the encapsulated enzyme was purified by centrifugal separation with 10 kDa cutoff filters (AMICON Ultra-2 mL 10 kDa) and washed three times with $NaHCO_3$ buffer (0.01 M pH 8.5). The capsules of collagenase were preserved at 4 °C.

4.7. Protocells Functionalization with Anti-EGFR and Col_{nc}. *4.7.1. Conversion of NH_2 Groups into SH Groups.* A 125 μL sample of 250 mM Traut's reagent in PBS was added to the protocells. The reaction was kept for 2 h under stirring at room temperature. After this time, the excess of Traut's reagent was removed via centrifugation (15 000 rpm, 10 min) and the pellet of protocells was resuspended in PBS. This step was repeated twice. Finally, the thiol-functionalized protocells were stored in 1 mL of PBS (2.5 mg mL^{-1}).

4.7.2. Attachment of NeutrAvidin. A 0.5 mL sample of (1 mg mL^{-1} in water) maleimide-functionalized NeutrAvidin protein was added to 1 mL (2.5 mg mL^{-1}) of thiol-functionalized protocells. The reaction was incubated under stirring at room temperature during 12 h. After this time, the excess of maleimide-functionalized NeutrAvidin was removed via centrifugation (15 000 rpm, 10 min) and the protocells pellet was resuspended in 1X PBS. This step was carried out twice. PC-NeutrAvidin were stored in 1 mL of 1X PBS (2.5 mg mL^{-1}) at 4 °C.

4.7.3. Synthesis of Col_{nc}-PC. The carboxylic groups of PC-NeutrAvidin (0.6 mL of 2.5 mg.mL^{-1} in $NaHCO_3$ buffer (0.01 M, pH 8.5)) were activated by adding 2.5 mg of *N*-(3-(dimethylamino)-propyl)-*N*′-ethylcarbodiimide hydrochloride (EDC) and 2.5 mg of *N*-hydroxysulfosuccidimide (NHS). To maintain the basic conditions, 2.5 mg of $NaHCO_3$ was added to the mixture. The sample was placed in an orbital stirrer at 400 rpm during 10 min. After this time, 4 mg of collagenase nanocapsules was added, and the mixture was stirred during 4 h. Col_{nc}-PC-NeutrAvidin were collected by centrifugation and washed three times with PBS. Col_{nc}-PC-NeutrAvidin were stored at 4 °C.

4.7.4. Synthesis of Col_{nc}-PC-Anti-EGFR. Twenty-five micrograms of biotinlyated Anti-EGFR was mixed with 250 μg of PC-NeutrAvidin or Col_{nc}-PC-NeutrAvidin Protocells, respectively, during 1 h at room temperature. After this time, protocells were isolated by centrifugation (15 000 rpm, 10 min) and they were redispersed in 250 μL of PBS (1X) yielding PC-Anti-EGFR or Col_{nc}-PC-Anti-EGFR, respectively.

4.8. Cell Culture and Targeting Studies in 2D. Protocell selective uptake of each system were evaluated in 2D cell culture model and flow cytometry. For this study, 20 000 A549 cells cm^{-2} were seeded into each well of a 24-well plate. The cells were incubated with 80 μg of the corresponding protocell (PC-NetrAvidin or PC-Anti-EGFR) left untreated (control) during 24 h at 37 °C at 5% CO_2 atmospheric concentration. Then the cells were washed two times with PBS (1X) to remove the noninternalized protocells and then the cells were treated with trypsin and the percentages of cells that have internalized fluorescence protocells were measured by flow cytometry using a BD FACSCaliber flow cytometer. Samples were performed in triplicate, and 10 000 cells were assessed per sample. To calculate the percent of cells positive for the protocells, a gate was set to contain 1% of control cells. This gate was then applied to all other samples to determine the percent of cells positive for protocells.

4.9. Enzymatic Activity Measurements. The enzymatic activity of all samples were evaluated following the protocol EnChekGelatinase/Collagenase Assay Kit.

4.10. Preparation of 3D Tumoral Tissue Models Based on A549-Seeded Collagen Gels. For this study, 20 000 A549 cells cm^{-2} were seeded in 24-well plate. A 0.5 mL sample of complete media was added to each well, and the cells were cultured at 37 °C at 5% CO_2 atmospheric concentration for 24 h. Then the collagen gel with A549 cells embedded into the collagen matrix was directly prepared in contact with the cell monolayer. For this purpose, 5.32 mL of rat tail collagen type I (3 mg mL^{-1}) and 15.48 mL of complete medium (Dulbecco's modified Eagle's medium complemented with 10% of FBS) were mixed at 0 °C. Then 100 μL of sodium hydroxide was added to obtain a mixture with neutral pH. Five milliliters of FBS, 5 mL of complete medium, and 5 mL of a solution of cells of concentration A549 1.7×10^6 cell mL^{-1} were added to the neutral collagen solution, keeping the temperature at 0 °C. The mixture was pipetted into 24-well plates (0.25 mL per well) and incubated at 37 °C at 5% CO_2 atmospheric concentration for 1 day to promote gel formation. Then 250 μL of complete medium was added in each well, and the gel was incubated at 37 °C at 5% CO_2 atmospheric concentration overnight. These gels were used for the further experiments 2 days after gel formation.

4.11. Study of Penetration and Cell Internalization in A549-Seeded Collagen Gels. To study the penetration of nanocarriers in 3D tumoral tissue models, 80 μL of suspended PC-Anti-EGFR and Col_{nc}-PC-Anti-EGFR (1 mg mL^{-1}) was respectively added on top of each gel. These samples were incubated at 37 °C at 5% CO_2

DOI: 10.1021/acs.chemmater.7b03128
Chem. Mater. 2018, 30, 112−120

atmospheric concentration during 24 h. Then the supernatant was removed and the gel was washed twice with PBS. Then 0.5 mL of a solution 4% paraformaldehyde and 1% sucrose in PBS was added to each well and incubated for 20 min. After this time, the wells were washed two times with PBS 1X and 0.5 mL of a solution of 0.5% triton X-100 in PBS was added and the wells were incubated during 5 min at room temperature to permeate the cell membrane. Then the wells were washed with PBS and incubated for 20 min at 37 °C with a solution of BSA 1% in PBS. After this step, BSA was removed and 0.5 mL of a solution of 30 μL of ATTO488 phallloidine solution (1 mg mL^{-1} in methanol) in 1 mL of BSA1%, was added. The wells were incubated for 40 min and washed two times with PBS (1X). Then 0.5 mL of one solution of DAPI in PBS (0.1 μg/mL) was added, and the wells were incubated during 15 min at room temperature. Finally, the excess of DAPI was removed washing two times with PBS (1X). The samples were ready for observation by fluorescent confocal microscopy.

4.12. Topotecan Loading. One milliliter of ethanolic suspension of MSN (2.5 mg mL^{-1}) was washed two times with water and finally was resupended in 0.5 mL of an aqueous solution of topotecan (5 mg mL^{-1}) during 12 h. The excess of topotecan was removed by centrifugation (15 000 rpm, 10 min) and two washing steps in H_2O. The amount of topotecan housed in MSN was determined by the difference in fluorescence in the initial cargo solution and the resulting supernatant. These topotecan-loaded MSN were employed for the drug-loaded protocell following the method described above.

4.13. Cell Viability Studies. The cytotoxic capacity of these multifunctional protocells was evaluated using the same 3D tumoral tissue model mentioned above. Briefly, 80 μL of each drug-loaded protocell (1 mg mL^{-1}) was added on the top of 3D gels with cells A549 embedded. These gels were incubated at 37 °C at 5% CO_2 atmospheric concentration during 24 h. The supernatant was removed, and the gel was washed two times with PBS (1X). Then 0.5 mL of Alamar Blue solution (10%) in cell culture medium was added to each well, and the gels were incubated at 37 °C at 5% CO_2 atmospheric concentration during 1 h. Finally, the fluorescence of supernatant was measured using λ_{ex} = 570 nm and λ_{em} = 585 nm using a microplate reader.

■ ASSOCIATED CONTENT

Supporting Information

The Supporting Information is available free of charge on the ACS Publications website at DOI: 10.1021/acs.chemmater.7b03128.

Hydrodynamic diameter of mesoporous silica nanoparticles, liposomes, and protocells obtained by DLS, study of collagenase nanocapsules hydrolysis under physiological conditions, enzymatic activity of different types of protocells, and each separate channel of confocal fluorescent micrographs (PDF)

■ AUTHOR INFORMATION

Corresponding Authors

*E-mail: abaezaga@ucm.es.
*E-mail: cjbrink@sandia.gov.
*E-mail: vallet@ucm.es.

ORCID

Alejandro Baeza: 0000-0002-9042-8865
C. Jeffrey Brinker: 0000-0002-7145-9324

Author Contributions

The manuscript was written through contributions of all authors. All authors have given approval to the final version of the manuscript.

Notes

The authors declare no competing financial interest.

■ ACKNOWLEDGMENTS

This work was supported by the European Research Council (Advanced Grant VERDI; ERC-2015-AdG Proposal No. 694160) and the project MAT2015-64831-R. This work has been done thanks to the financial support provided by European Research Council (Advanced Grant VERDI; ERC-2015-AdG Proposal No. 694160) and the project MAT2015-64831-R. C.J.B., A.N., P.N.D., K.S.B., and J.O.A. acknowledge support from the Sandia National Laboratories (SNL) Laboratory-Directed Research Development program, the Leukemia and Lymphoma Society, and DTRA project IAA DTRA1002720595. SNL is a multimission laboratory managed and operated by National Technology and Engineering Solutions of Sandia, LLC., a wholly owned subsidiary of Honeywell International, Inc., for the U.S. Department of Energy's National Nuclear Security Administration under contract DE-NA-0003525.

■ REFERENCES

(1) Siegel, R. L.; Miller, K. D.; Jemal, A. Cancer Statistics. *Ca-Cancer J. Clin.* **2016**, *66*, 7−30.
(2) Hanahan, D.; Weinberg, R. A. Hallmarks of Cancer: The Next Generation. *Cell* **2011**, *144*, 646−674.
(3) Matsumura, Y.; Maeda, H. A New Concept for Macromolecular Therapeutics in Cancer-Chemotherapy - Mechanism of Tumoritropic Accumulation of Proteins and the Antitumor Agent Smancs. *Cancer Res.* **1986**, *46*, 6387−6392.
(4) Liu, D.; Auguste, D. T. Cancer Targeted Therapeutics: From Molecules to Drug Delivery Vehicles. *J. Controlled Release* **2015**, *219*, 632−643.
(5) Maeda, H. Toward a Full Understanding of the EPR Effect in Primary and Metastatic Tumors as Well as Issues Related to Its Heterogeneity. *Adv. Drug Delivery Rev.* **2015**, *91*, 3−6.
(6) Ediriwickrema, A.; Saltzman, W. M. Nanotherapy for Cancer: Targeting and Multifunctionality in the Future of Cancer Therapies. *ACS Biomater. Sci. Eng.* **2015**, *1*, 64−78.
(7) Mura, S.; Nicolas, J.; Couvreur, P. Stimuli-Responsive Nanocarriers for Drug Delivery. *Nat. Mater.* **2013**, *12*, 991−1003.
(8) Karakoti, A. S.; Das, S.; Thevuthasan, S.; Seal, S. PEGylated Inorganic Nanoparticles. *Angew. Chem., Int. Ed.* **2011**, *50*, 1980−1994.
(9) Xu, X.; Ho, W.; Zhang, X.; Bertrand, N.; Farokhzad, O. Cancer Nanomedicine: From Targeted Delivery to Combination Therapy. *Trends Mol. Med.* **2015**, *21*, 223−232.
(10) Sun, T.-M.; Wang, Y.-C.; Wang, F.; Du, J.-Z.; Mao, C.-Q.; Sun, C.-Y.; Tang, R.-Z.; Liu, Y.; Zhu, J.; Zhu, Y.-H.; et al. Cancer Stem Cell Therapy Using Doxorubicin Conjugated to Gold Nanoparticles via Hydrazone Bonds. *Biomaterials* **2014**, *35*, 836−845.
(11) Wilhelm, S.; Tavares, A. J.; Dai, Q.; Ohta, S.; Audet, J.; Dvorak, H. F.; Chan, W. C. W. Analysis of Nanoparticle Delivery to Tumours. *Nat. Rev. Mater.* **2016**, *1*, 16014.
(12) Florence, A. T. Targeting" Nanoparticles: The Constraints of Physical Laws and Physical Barriers. *J. Controlled Release* **2012**, *164*, 115−124.
(13) Netti, P. a; Berk, D. a; Swartz, M. a; Grodzinsky, a J.; Jain, R. K. Role of Extracellular Matrix Assembly in Interstitial Transport in Solid Tumors. *Cancer Res.* **2000**, *60*, 2497−2503.
(14) McKee, T. D.; Grandi, P.; Mok, W.; Alexandrakis, G.; Insin, N.; Zimmer, J. P.; Bawendi, M. G.; Boucher, Y.; Breakefield, X. O.; Jain, R. K. Degradation of Fibrillar Collagen in a Human Melanoma Xenograft Improves the Efficacy of an Oncolytic Herpes Simplex Virus Vector. *Cancer Res.* **2006**, *66*, 2509−2513.
(15) Parodi, A.; Haddix, S. G.; Taghipour, N.; Scaria, S.; Taraballi, F.; Cevenini, A.; Yazdi, I. K.; Corbo, C.; Palomba, R.; Khaled, S. Z.; et al. Bromelain Surface Modification Increases the Diffusion of Silica Nanoparticles in the Tumor Extracellular Matrix. *ACS Nano* **2014**, *8*, 9874−9883.

DOI: 10.1021/acs.chemmater.7b03128
Chem. Mater. 2018, 30, 112−120

(16) Villegas, M. R.; Baeza, A.; Vallet Regí, M. Hybrid Collagenase Nanocapsules for Enhanced Nanocarrier Penetration in Tumoral Tissues. *ACS Appl. Mater. Interfaces* **2015**, *7*, 24075−24081.
(17) Nguyen, K. T.; Zhao, Y. Engineered Hybrid Nanoparticles for On-Demand Diagnostics and Therapeutics. *Acc. Chem. Res.* **2015**, *48*, 3016−3025.
(18) Durfee, P. N.; Lin, Y.-S.; Dunphy, D. R.; Muñiz, A. J.; Butler, K. S.; Humphrey, K. R.; Lokke, A. J.; Agola, J. O.; Chou, S. S.; Chen, I.-M.; et al. Mesoporous Silica Nanoparticle-Supported Lipid Bilayers (Protocells) for Active Targeting and Delivery to Individual Leukemia Cells. *ACS Nano* **2016**, *10*, 8325−8345.
(19) Butler, K. S.; Durfee, P. N.; Theron, C.; Ashley, C. E.; Carnes, E. C.; Brinker, C. J. Protocells: Modular Mesoporous Silica Nanoparticle-Supported Lipid Bilayers for Drug Delivery. *Small* **2016**, *12*, 2173−2185.
(20) Ashley, C. E.; Carnes, E. C.; Epler, K. E.; Padilla, D. P.; Phillips, G. K.; Castillo, R. E.; Wilkinson, D. C.; Wilkinson, B. S.; Burgard, C. A.; Kalinich, R. M.; et al. Delivery of Small Interfering RNA by Peptide-Targeted Mesoporous Silica Nanoparticle-Supported Lipid Bilayers. *ACS Nano* **2012**, *6*, 2174−2188.
(21) Vallet-Regi, M.; Rámila, A.; del Real, R. P.; Pérez-Pariente, J. A New Property of MCM-41: Drug Delivery System. *Chem. Mater.* **2001**, *13*, 308−311.
(22) Vallet-Regi, M.; Balas, F.; Arcos, D. Mesoporous Materials for Drug Delivery. *Angew. Chem., Int. Ed.* **2007**, *46*, 7548−7558.
(23) Nussbaumer, S.; Bonnabry, P.; Veuthey, J.-L.; Fleury-Souverain, S. Analysis of Anticancer Drugs: A Review. *Talanta* **2011**, *85*, 2265−2289.
(24) Lin, Y.-S.; Haynes, C. L. Impacts of Mesoporous Silica Nanoparticle Size, Pore Ordering, and Pore Integrity on Hemolytic Activity. *J. Am. Chem. Soc.* **2010**, *132*, 4834−4842.
(25) He, Q.; Zhang, J.; Shi, J.; Zhu, Z.; Zhang, L.; Bu, W.; Guo, L.; Chen, Y. The Effect of PEGylation of Mesoporous Silica Nanoparticles on Nonspecific Binding of Serum Proteins and Cellular Responses. *Biomaterials* **2010**, *31*, 1085−1092.
(26) Bozzuto, G.; Molinari, A. Liposomes as Nanomedical Devices. *Int. J. Nanomed.* **2015**, *10*, 975.
(27) Bello, V.; Mattei, G.; Mazzoldi, P.; Vivenza, N.; Gasco, P.; Idee, J. M.; Robic, C.; Borsella, E. Transmission Electron Microscopy of Lipid Vesicles for Drug Delivery: Comparison between Positive and Negative Staining. *Microsc. Microanal.* **2010**, *16*, 456−461.
(28) Baeza, A.; Guisasola, E.; Torres-Pardo, A.; González-Calbet, J. M.; Melen, G. J.; Ramirez, M.; Vallet-Regí, M. Hybrid Enzyme-Polymeric Capsules/Mesoporous Silica Nanodevice for In Situ Cytotoxic Agent Generation. *Adv. Funct. Mater.* **2014**, *24*, 4625−4633.
(29) Simmchen, J.; Baeza, A.; Ruiz-Molina, D.; Vallet-Regí, M. Improving Catalase-Based Propelled Motor Endurance by Enzyme Encapsulation. *Nanoscale* **2014**, *6*, 8907−8913.
(30) Berger, M. S.; Gullick, W. J.; Greenfield, C.; Evans, S.; Addis, B. J.; Waterfield, M. D. Epidermal Growth Factor Receptors in Lung Tumours. *J. Pathol.* **1987**, *152*, 297−307.
(31) Noh, M. S.; Lee, S.; Kang, H.; Yang, J. K.; Lee, H.; Hwang, D.; Lee, J. W.; Jeong, S.; Jang, Y.; Jun, B.-H.; Jeong, D. H.; Kim, S. K.; Lee, Y.-S.; Cho, M.-H. Target-specific near-IR induced drug release and photothermal therapy with accumulated Au/Ag hollow nanoshells on pulmonary cancer cell membranes. *Biomaterials* **2015**, *45*, 81−92.
(32) Child, H. W.; Del Pino, P. a.; De La Fuente, J. M.; Hursthouse, A. S.; Stirling, D.; Mullen, M.; McPhee, G. M.; Nixon, C.; Jayawarna, V.; Berry, C. C. Working Together: The Combined Application of a Magnetic Field and Penetratin for the Delivery of Magnetic Nanoparticles to Cells in 3D. *ACS Nano* **2011**, *5*, 7910−7919.
(33) Herben, V. M.; ten Bokkel Huinink, W. W.; Beijnen, J. H. Clinical Pharmacokinetics of Topotecan. *Clin. Pharmacokinet.* **1996**, *31*, 85−102.
(34) Drummond, D. C.; Noble, C. O.; Guo, Z.; Hayes, M. E.; Connolly-Ingram, C.; Gabriel, B. S.; Hann, B.; Liu, B.; Park, J. W.; Hong, K. Development of a Highly Stable and Targetable Nano-liposomal Formulation of Topotecan. *J. Controlled Release* **2010**, *141*, 13−21.

DOI: 10.1021/acs.chemmater.7b03128
Chem. Mater. 2018, 30, 112−120

Supporting Information

Multifunctional Protocells for Enhanced Penetration in 3D Extracellular Tumoral Matrices.

María Rocío Villegas,[a,b] Alejandro Baeza,[a,b] Achraf Noureddine[c], Paul N. Durfee[c,d], Kimberly S. Butler,[c,d,e], Jacob Ongoudi Agola[c,d], C. Jeffrey Brinker[c,d,f,g]* and María Vallet-Regí.[a,b,]**

a. Departamento de Química Inorgánica y Bioinorgánica, Facultad de Farmacia, Universidad Complutense de Madrid, 28040 Madrid, Spain.

b. Networking Research Center on Bioengineering, Biomaterials and Nanomedicine (CIBER-BBN), Spain.

c. Center for Micro-Engineered Materials, University of New Mexico, Albuquerque, New Mexico 87131, USA

d. Chemical and Biological Engineering, University of New Mexico, Albuquerque, New Mexico 87131, USA

e. Nanobiology, Sandia National Laboratories, Albuquerque, New Mexico 87123, USA

f. Comprehensive Cancer Center, The University of New Mexico, Albuquerque, New Mexico 87131, USA

g. Advanced Materials Laboratory, Sandia National Laboratories, Albuquerque, New Mexico 87123, USA

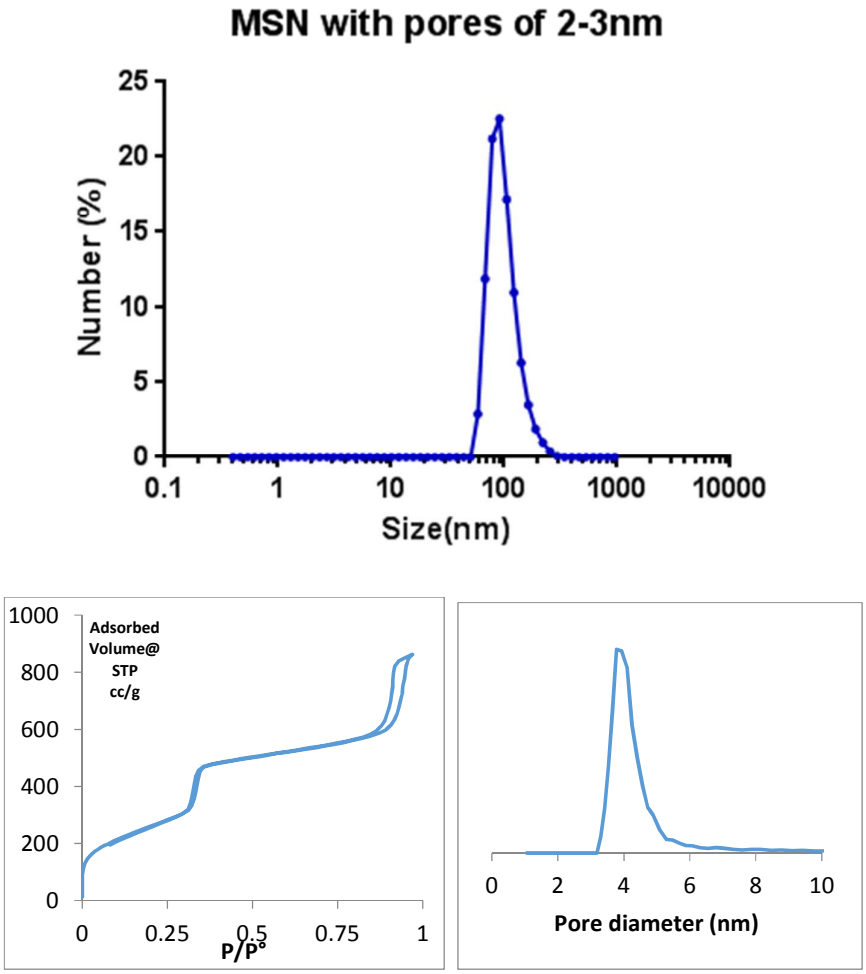

N_2 sorption isotherm (left) and DFT pore size distribution (right) of MSN

Textural properties of MSN	BET surface area	Pore volume	Average pore size (DFT)
	975 m^2/g	1.3 cc/g	3.7 nm

Figure S1. Hydrodynamic diameter obtained by dynamic light scattering (DLS) of MSN. N_2 physisorption isotherms of MSN. The shape of the isotherm is typical of a mesoporous material with a IUPAC's type IV adsorption branch. Indeed, the isotherms exhibit an inflexion of the N2 adsorbed amount typical for monolayer-multilayer adsorption process which ends by a plateau indicating the saturation of the mesoporosity. DFT pore size distribution indicates an average pore size of about 3.5 nm, slightly wider than MCM-41 like MSN presumably due to the insertion of RBITC and the other experimental conditions (ageing, hydrothermal treatment).

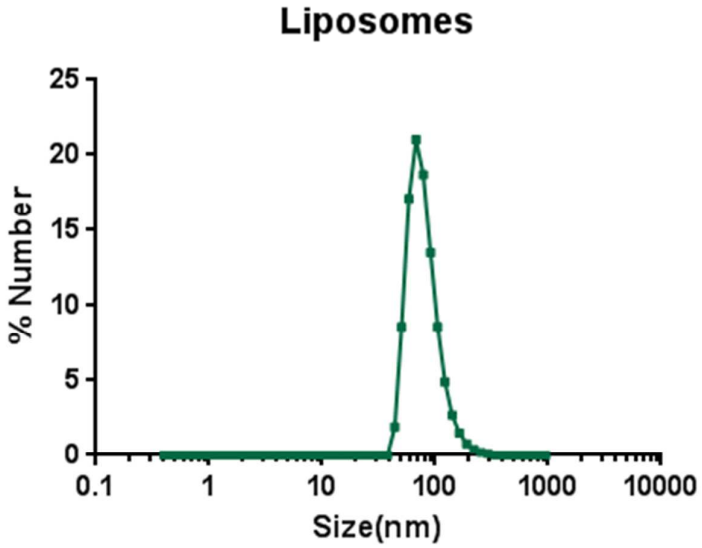

Figure S2. Hydrodynamic diameter obtained by dynamic light scattering (DLS) of DSPC and DSPE- PEG(2000)-COOH (65:13).

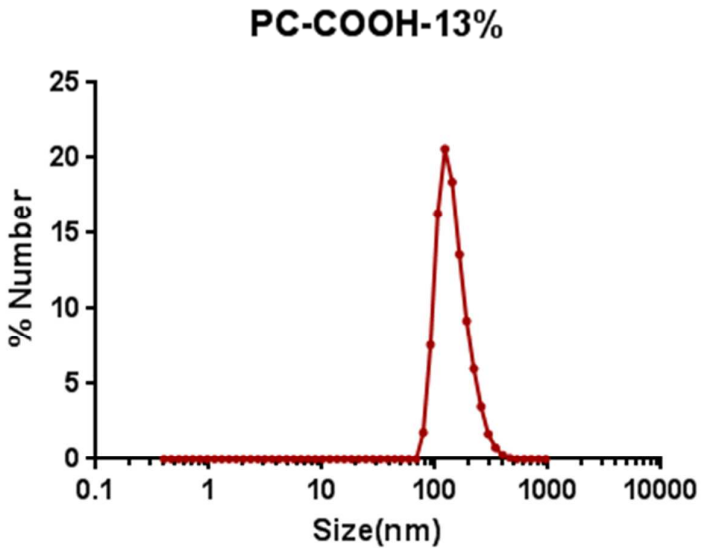

Figure S3. Hydrodynamic diameter obtained by dynamic light scattering (DLS) of PC DSPE-PEG(2000)-COOH (65:13).

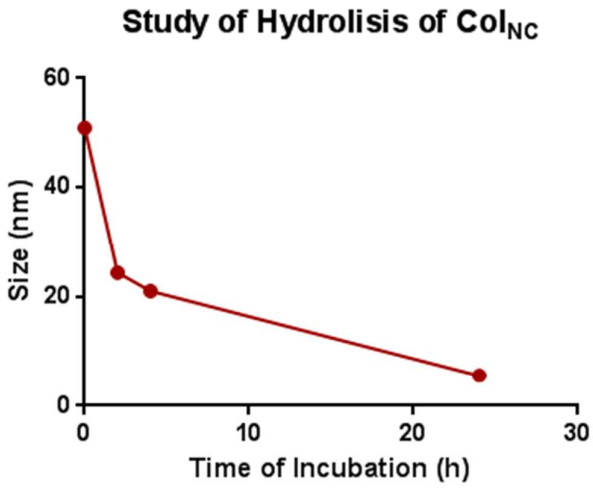

Figure S4. Hydrodynamic diameter change over time obtained by dynamic light scattering (DLS) of collagenase nanocapsules

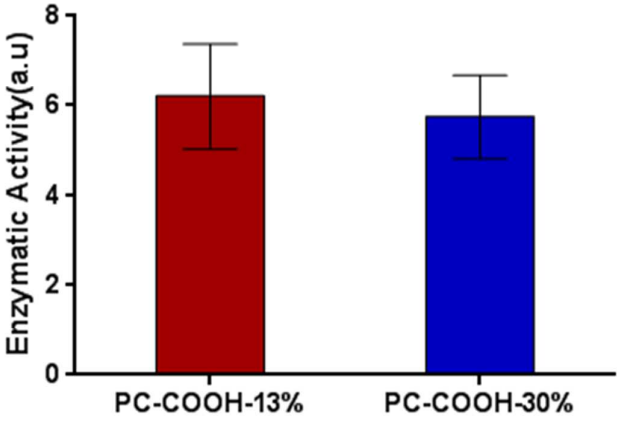

Figure S5. Enzymatic activity of each type of protocells (n = 3).

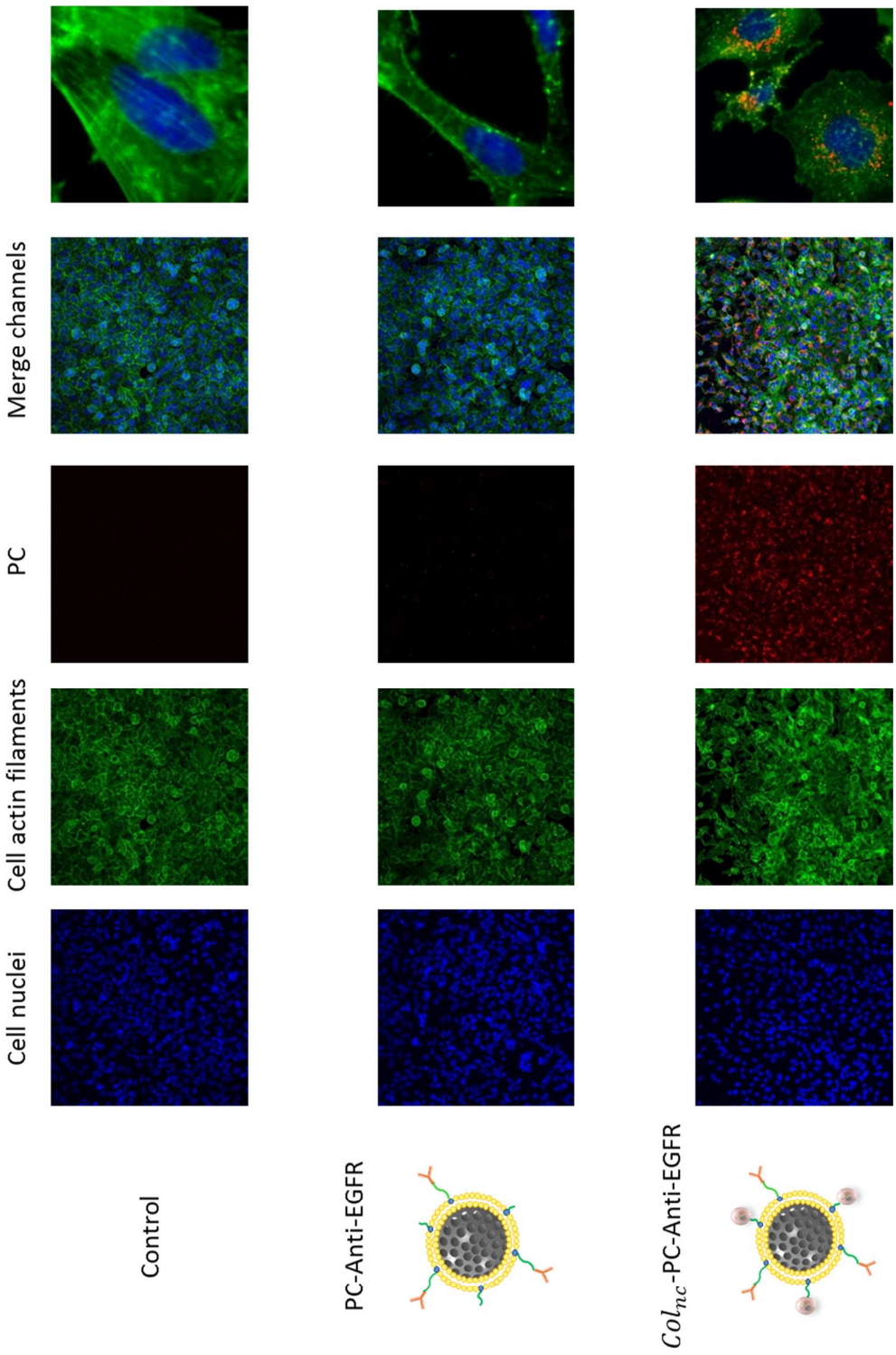

Figure S6. Confocal fluorescent micrographs of each separate channel of each type of protocell.

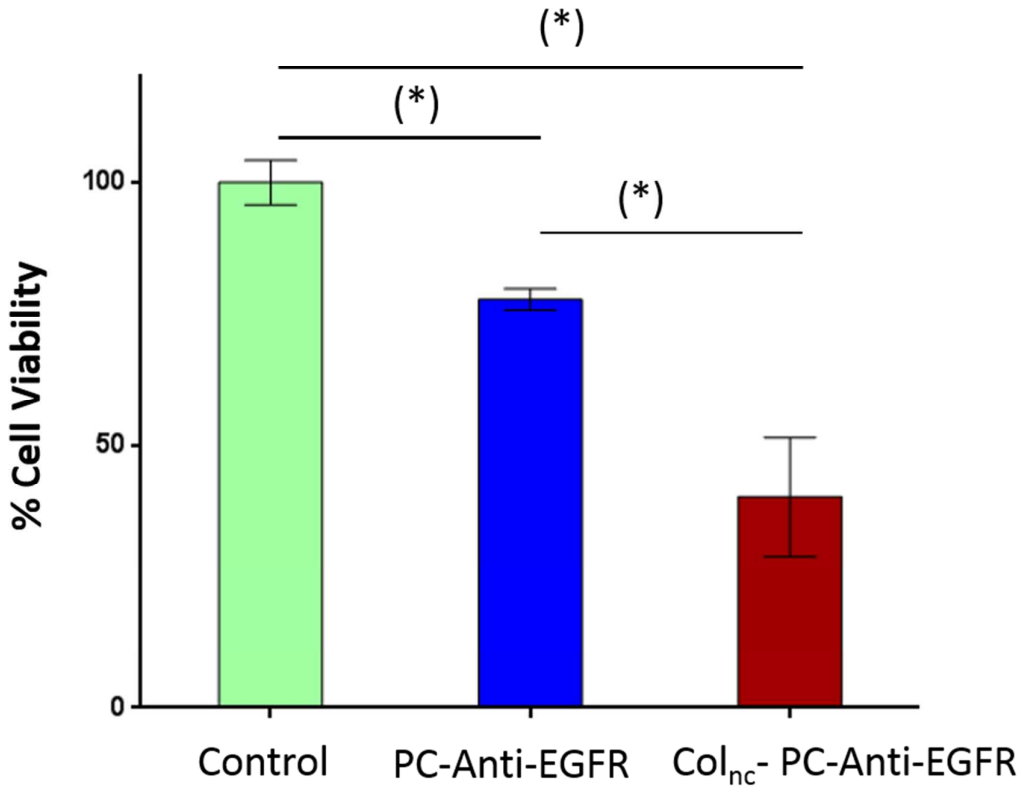

Figure S7. Cytotoxic capacity of Protocells in 3D tumoral tissue model after 48 hours of incubation (n =3, $p<0.05$).

Section III.II.

Asymmetric Nanoparticles as Elements of Dual Targeting Cell-Organelle

Conventional dual targeting systems in nanoparticles

It has been more than 30 years since the discovery of EPR (*Enhanced Permeation and Retention*) effect.[1] This finding supposed a paramount milestone in the development of nanomedicine because the scientific community glimpsed the opportunity to use nanodevices as drug carriers in order to treat selectively the malignant tissues. However, tumoral masses are not uniform sets of malignant cells but they are composed by a myriad of different cells, healthy and malignant cells.[2] Thus, it is necessary to provide of the nanocarriers of capacity to distinguish the tumoral cells from the rest of the cells that compose the tumoral tissue. One approach which has been widely employed with this aim is the decoration of nanovehicles surface with (bio)-moieties with high affinity for receptors overexpressed in tumoral cells. This affinity induces a strong binding of the nanoparticle with the cell membrane triggering its endocytosis and producing a significative destruction of the tumoral cell line. Nevertheless, due to the coexistence of several mutated tumoral cells which overexpress different receptors, the use of nanoparticles decorated with only one targeting agent can induce an undesirable growth of the other tumoral cells. This process resemble a Darwinian selection that push the mutated cells into an evolutive process which can complicate even more their complete elimination. Thus, in the last few years, the design of targeted vehicles has moved towards the development of nanocarriers with double specificity, *i.e.*, devices decorated with an array of targeting moieties specific to different cells or different levels of targeting.

One strategy for dual targeting is the combination of antivascular therapy with tumoral cell targeting. Angiogenesis is the physiological process responsible for the formation of blood vessels and is essential for tumor growth and metastasis so, one mode to suppress this growth consists in the blockage of this process. Traditionally, antiangiogenic therapy

has been often focused on targeting the endothelial cells which forms the blood vessels through the inhibition of the endothelial growth factor (VEGF) receptor inhibitor.[3] Despite the fact that anti-VEGF strategy has given rise to a higher patient survival in some tumors, the use of VEGF itself as a targeting moiety on nanocarrier-based therapy has been shown to be not enough to achieve tumor regression.[4] In order to overcome this issue, different strategies which involve the use of dual targeting have been developed. For instance, nanoparticles with simultaneous targeting to endothelial cells, *via* decoration with endothelial growth factor receptor (EGFR) inhibitor (AEE788), and ST1571 (PDGF receptor (PDGFR) inhibitor) to pericytes,[5] which are mesenchymal cells that wrap around the vessel and contribute to a normal stability and function of the microvasculature.[6] The simultaneous targeting to both types of cells resulted in a higher efficacy in tumor suppression of ovarian tumor growth of 69% to 84% whereas, the efficacy of the system which employed only AEE788 was 45-59% and the one that was decorated with STI571 alone, was not effective.

Another option is the use of nanoparticles with merges anti-angiogenesis and antitumoral therapy in one single treatment, *i.e.*, targeting the tumor cells and the neovasculature. In this sense, poly (ethyleneglycol)-poly(ε-caprolactone) (PEG-PCL) nanoparticles were decorated with interleukin-13, which targeted glioblastoma tumoral cells and RGD, that exhibit strong binding efficiency by $\alpha_v\beta_3$-integrins, which are overexpressed on tumoral vascular endothelial cells.[7] Moreover, these nanoparticles were loaded with docetaxel, a potent cytotoxic agent. The dual surface modification expanded median survival of orthotropic glioma bearing mice up to 35 days, that is significative higher than the results achieved with the nanoparticles decorated with only one targeting agent, in which the median survival expansion was up to 26.5 days.

Moreover, sequential dual targeting has been studied to treat amyloid plaques in the brain of Alzheimer´s disease mice.[8] Alzheimer is a neurodegenerative disease whose treatment is strongly limited by the poor permeable blood brain barrier (BBB). In order to overcome this restriction, PEG-PLGA nanoparticles were decorated with two targeting peptides: TGN, which specifically binds to the epithelial cells of BBB, and QSH, which present high affinity to $A\beta_{1-42}$, the predominant component of amyloid plaques. The evaluation of these dual targeted nanoparticles loaded with coumarin-6 was carried out employing an *in vivo* in mice model of Alzheimer´s disease yielding that, the dual modification resulted in a 1.75-2.89 times more uptake in hippocampus than mono-modified nanoparticles.

One potential problem of the combination of two targeting moieties in one nanoparticle is the fact that, the incorporation of the first targeting agent could compromise the attachment of the second one. In order to overcome this limitation, one ingenious strategy consists in the construction of one single moiety which contains both targeting moieties, being one of them encrypted into the structure.[9] Therefore, the hidden targeting moiety would be activated only in the diseased zone resulting in a hierarchical targeting strategy. As an example of this strategy, Villaverde *et al*. have described the use of a synthetic polypeptidic chain which contains the RGD pattern encrypted within a sequence sensitive to cathepsin K, an enzyme overexpressed on bone tumors.[10] A zoledronic acid derivative was attached at the end of this polypeptidic chain in order to provide binding capacity of the complete moiety for the exposed mineral part of the bone. Thus, nanoparticles decorated with this sequence will be strongly attached to the mineral part of the bone, which is more accessible in bone tumors than in healthy ones and once there, and only if the bone is affected by a tumor, the presence of cathepsin K will produce the particle release and cellular targeting activation at the same time. These type of dual targeting is

an interesting strategy to avoid the binding-site barrier, since the cell targeting is only exposed once the nanocarrier has arrived at the tumoral tissue. This system demonstrated a precise control of cell internalization because, in absence of cathepsin K the internalization was only of 10% in comparison with more than 90% achieved when this enzyme was present.

In addition to these strategies, available for targeting two different cell lines or also for the recognition of diseased tissues and cells, it is even possible to achieve a dual targeting effect of the tumoral cell and then, to certain organelles located inside. In this way, dual targeted nanocarriers can be able to achieve selective internalization within diseased cells and once there, be located close to important organelles, as nucleus or mitochondria, where the transported drugs induce a higher effect.[11] One example of this class of systems was developed by Chen *et al.* whose designed a novel-platform formed by gold nanoclusters functionalized with cyclic RGD, that specifically bind with αβ-integrins and AS1411 aptamer, that present high affinity to nucleus.[12] This system was predominantly found in nucleoplasm of the cells respect gold nanoclusters with RGD.

These systems have demonstrated an enhanced efficacy compared to their single-targeted counterparts. Unfortunately, in many cases, it has been found that the use of dual targeted nanodevices is not always capable to increase the delivery efficiency,[13] since the cross-interactions between both targeting moieties can compromise the binding capacity of each targeting moiety with the receptors located on the cell membrane. The importance of the distribution of the targeting moieties is crucial to achieve an effective treatment. Xia *et al.* studied the effect of the targeting moieties distribution on cellular uptake by a computer simulation study.[14] In this study, a cell membrane that over-expressed two types of receptors, R1 and R2, was modelled and the endocytosis process was examined employing nanoparticles decorated with one or two ligands (L1 and L2, respectively)

which were distributed according with different configurations (random or Janus-type, **Figure 1**). In this study, the authors found that the nanoparticle uptake was strongly related with the length which separate the targeting moieties from the particle surface (linker length). The cell membrane receptors have certain volume and therefore, when a ligand interacts with them, the binding process of another nearby ligand with a second receptor can be hindered by steric impediment. For this reason, it is required to optimize the suitable linker length in each case. Moreover, it was studied that when non-specific interactions were present, such as electrostatic interactions between targeting ligands, it resulted in a negative impact in the engulfment degree. Different distributions of the targeting moieties on the nanoparticle were studied, from the random decoration to asymmetric distribution of the targeting moieties in each hemisphere (Janus nanoparticles) observing that Janus configuration yielded the best results because the nanoparticle uptake in these systems are scarcely affected by the linker length and the physicochemical properties of the targeting agents.

Figure 1. *Nanoparticles with different targeting moieties distributions.*

Another example which point out the suitability of Janus configuration has been recently reported by Yi and co-workers.[15] In this work, the authors have demonstrated that it is

possible to avoid the capture of the nanoparticles by the macrophages through the decoration of only one hemisphere of the particle with PEG. The stealth properties achieved with this asymmetrical distribution of PEG was in the same magnitude that the one obtained with a complete PEG coating. The advantage of this strategy is that the other hemisphere is free for the introduction of any other functional group. In this case, the free hemisphere was decorated with anti-CD3, which is an antibody that specifically binds to membrane T cell receptors. Nanoparticles with targeting agents and PEG distributed in opposite hemispheres demonstrated higher targeting effect (26.4%) compared to the uniform distribution (4.2%).

Moreover, the enhanced endocytosis using Janus nanoparticles bearing two targeting moieties has been proved experimentally.[16] Nanoparticles with clusters of targeting ligands (anti-CD3 y anti-CD8) gave rise to a higher and more sustained T cell activation compared to the uniformly coated nanoparticles with the same number of targeting moieties. In this work, T cell activation was evaluated using three types of nanoparticles regarding the targeting distribution: Janus, patchy and randomly coated nanoparticles. It was found that Janus nanoparticles induced a more effective activation compared to random systems, and also more activation than patchy particles in which the number of targeting moieties is 7 times higher. This effect is due to an increase of the local concentration of ligands and the asymmetric distribution of them.

In conclusion, Janus nanoparticles constitute a promising system in which is possible the implementation of a dual-targeting strategies capable to provide a more controlled and effective distribution of the targeting moieties.

Asymmetric Nanoparticles as Elements of Dual Targeting Cell-Organelle.

This chapter is focused on the design of a dual-targeted nanoparticle able to improve the therapeutic effect of the transported drug. Janus nanoparticles were chosen as carriers due to their enhanced targeting effect with respect to the random distribution.

Several methods have been reported for the synthesis of Janus nanoparticles, including fluidic nanoprecipitation,[17]electrodinamic co-jetting[18], spattering or wax-in-water Pickering emulsions,[19,20] among others. In our case, the last strategy was chosen since, although this method yields nanoparticles which exhibit a lesser homogenous distribution of the targeting moieties than the physical methods as spattering, it allows to obtain Janus nanoparticles in a gram-scale, in an easy way.

As proof of concept, the possibility to introduce targeting agents able to act in two sequential levels have been studied. The selected targeting moieties have been folate, as cellular targeting agent, and a triphenylphospine derivative (TPP) able to target mitochondria. Folate receptors are overexpressed in many tumoral cell lines[21] and TPP is an excellent mitochondrial targeting agent, due to the electrostatic interactions between the cationic TPP and the negatively charged mitochondrial membrane (**Figure 2**).[22] Then, in a first study, the selective uptake by tumoral cells in comparison to healthy cells was tested.

In order to study if the dual system improve the therapeutic effect, the Janus nanoparticles were loaded with a potent antitumoral drug, topotecan (TOP). TOP is an inhibitor of DNA topoisomerase-I, an enzyme whose purpose is to reduce the strain in the DNA chains

during replication. The administration of this drug induces damage in the DNA located in the cell nucleus and also in the mitochondrial DNA causing the cell death.

Janus dual-targeted nanocarriers demonstrated an improved uptake in tumoral cells and an enhanced antitumoral effect. This strategy can be easily implemented in the other types of nanomedicines and could decrease the necessary doses required for achieving therapeutic efficacy.

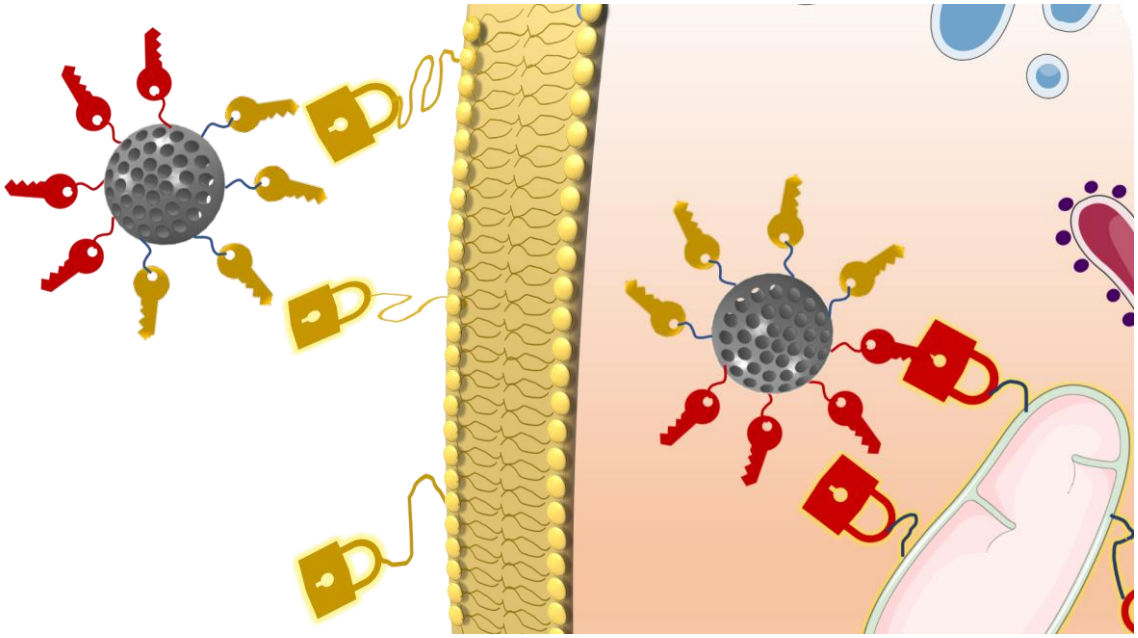

Figure 2. *Janus Dual-Targeted Nanoparticles for tumoral cell and mitochondria targeting.*

References:

(1) Maeda, H.; Nakamura, H.; Fang, J. The EPR Effect for Macromolecular Drug Delivery to Solid Tumors: Improvement of Tumor Uptake, Lowering of Systemic Toxicity, and Distinct Tumor Imaging in Vivo. *Adv. Drug Deliv. Rev.* **2013**, *65* (1), 71–79.

(2) DeBerardinis, R. J.; Lum, J. J.; Hatzivassiliou, G.; Thompson, C. B. The Biology of Cancer: Metabolic Reprogramming Fuels Cell Growth and Proliferation. *Cell Metab.* **2008**, *7* (1), 11–20.

(3) Fidler, I. J. The Organ Microenvironment and Cancer Metastasis. *Differentiation* **2002**, *70*, 498–505.

(4) Lu, C.; Kamat, A. A.; Lin, Y. G.; Merritt, W. M.; Landen, C. N.; Tae, J. K.; Spannuth, W.; Arumugam, T.; Han, L. Y.; Jennings, N. B.; Logsdon, C.; Jaffe, R. B.; Coleman, R. L.; Sood, A. K. Dual Targeting of Endothelial Cells and Pericytes in Antivascular Therapy for Ovarian Carcinoma. *Clin. Cancer Res.* **2007**, *13* (14), 4209–4217.

(5) Lu, C.; Kamat, A. A.; Lin, Y. G.; Merritt, W. M.; Landen, C. N.; Kim, T. J.; Spannuth, W.; Arumugam, T.; Han, L. Y.; Jennings, N. B.; Logsdon, C.; Jaffe, R. B.; Coleman, R. L.; Sood, A. K. Dual Targeting of Endothelial Cells and Pericytes in Antivascular Therapy for Ovarian Carcinoma. *Clin. Cancer Res.* **2007**, *13* (14), 4209–4217.

(6) Lu, C.; Sood, A. K. Role of Pericytes in Angiogenesis. In *Antiangiogenic Agents in Cancer Therapy*; Humana Press: Totowa, NJ, 2008; pp 117–132.

(7) Gao, H.; Yang, Z.; Cao, S.; Xiong, Y.; Zhang, S.; Pang, Z.; Jiang, X. Tumor Cells

and Neovasculature Dual Targeting Delivery for Glioblastoma Treatment. *Biomaterials* **2014**, *35* (7), 2374–2382.

(8) Zhang, C.; Wan, X.; Zheng, X.; Shao, X.; Liu, Q.; Zhang, Q.; Qian, Y. Dual-Functional Nanoparticles Targeting Amyloid Plaques in the Brains of Alzheimer's Disease Mice. **2014**.

(9) Wang, S.; Huang, P.; Chen, X. Hierarchical Targeting Strategy for Enhanced Tumor Tissue Accumulation/Retention and Cellular Internalization. *Adv. Mater.* **2016**, *28* (34), 7340–7364.

(10) Villaverde, G.; Nairi, V.; Baeza, A.; Vallet-Regí, M. Double Sequential Encrypted Targeting Sequence: A New Concept for Bone Cancer Treatment. *Chem. - A Eur. J.* **2017**, *23* (30), 7174–7179.

(11) Sakhrani, N. M.; Padh, H. Organelle Targeting: Third Level of Drug Targeting. *Drug Des. Devel. Ther.* **2013**, *7*, 585–599.

(12) Chen, D.; Li, B.; Cai, S.; Wang, P.; Peng, S.; Sheng, Y.; He, Y.; Gu, Y.; Chen, H. Dual Targeting Luminescent Gold Nanoclusters for Tumor Imaging and Deep Tissue Therapy. *Biomaterials* **2016**, *100*, 1–16.

(13) Sawant, R. R.; Jhaveri, A. M.; Koshkaryev, A.; Qureshi, F.; Torchilin, V. P. The Effect of Dual Ligand-Targeted Micelles on the Delivery and Efficacy of Poorly Soluble Drug for Cancer Therapy. *J. Drug Target.* **2013**, *21* (7), 630–638.

(14) Xia, Q.; Ding, H.; Ma, Y. Can Dual-Ligand Targeting Enhance Cellular Uptake of Nanoparticles? *Nanoscale* **2017**, *9* (26), 8982–8989.

(15) Yi, Y.; Sanchez, L.; Gao, Y.; Lee, K.; Yu, Y. Interrogating Cellular Functions with Designer Janus Particles. *Chem. Mater.* **2017**, *29* (4), 1448–1460.

(16) Lee, K.; Yu, Y. Janus Nanoparticles for T Cell Activation: Clustering Ligands to Enhance Stimulation. *J. Mater. Chem. B* **2017**, *5* (23), 4410–4415.

(17) Xie, H.; She, Z. G.; Wang, S.; Sharma, G.; Smith, J. W. One-Step Fabrication of Polymeric Janus Nanoparticles for Drug Delivery. *Langmuir* **2012**, *28* (9), 4459–4463.

(18) Misra, A. C.; Bhaskar, S.; Clay, N.; Lahann, J. Multicompartmental Particles for Combined Imaging and siRNA Delivery. *Adv. Mater.* **2012**, *24* (28), 3850–3856.

(19) Perro, A.; Meunier, F.; Schmitt, V.; Ravaine, S. Production of Large Quantities of "Janus" nanoparticles Using Wax-in-Water Emulsions. *Colloids Surfaces A Physicochem. Eng. Asp.* **2009**, *332* (1), 57–62.

(20) Simmchen, J.; Baeza, A.; Ruiz, D.; Esplandiu, M. J.; Vallet-Regí, M. Asymmetric Hybrid Silica Nanomotors for Capture and Cargo Transport: Towards a Novel Motion-Based DNA Sensor. *Small* **2012**, *8* (13), 2053–2059.

(21) Byrne, J. D.; Betancourt, T.; Brannon-Peppas, L. Active Targeting Schemes for Nanoparticle Systems in Cancer Therapeutics. *Adv. Drug Deliv. Rev.* **2008**, *60* (15), 1615–1626.

(22) Smith, R. A. J.; Porteous, C. M.; Gane, A. M.; Murphy, M. P. Delivery of Bioactive Molecules to Mitochondria in Vivo. *Proc. Natl. Acad. Sci.* **2003**, *100* (9), 5407–5412.

III.II.I. Janus Mesoporous Silica Nanoparticles for Dual Targeting of Tumor Cells and Mithocondria

López, V.; Villegas, M. R.; Rodríguez, V.; Villaverde, G.; Lozano, D.; Baeza, A.; Vallet-Regí, M. Janus Mesoporous Silica Nanoparticles for Dual Targeting of Tumor Cells and Mitochondria. *ACS Appl. Mater. Interfaces* **2017**, *9*, 26697–26706, doi:10.1021/acsami.7b06906.

ACS APPLIED MATERIALS & INTERFACES

Research Article

www.acsami.org

Janus Mesoporous Silica Nanoparticles for Dual Targeting of Tumor Cells and Mitochondria

Victoria López,[†] Maria Rocío Villegas,[†,‡] Verónica Rodríguez,[†] Gonzalo Villaverde,[†,‡] Daniel Lozano,[†,‡] Alejandro Baeza,[*,†,‡] and María Vallet-Regí[*,†,‡]

[†]Departamento de Química Inorgánica y Bioinorgánica, Facultad de Farmacia, Universidad Complutense de Madrid, 28040 Madrid, Spain

[‡]Networking Research Center on Bioengineering, Biomaterials and Nanomedicine, Avenida Monforte de Lemos, 3-5, 28029 Madrid, Spain

Supporting Information

ABSTRACT: The development of targeted nanocarriers able to be selectively internalized within tumor cells, and therefore to deliver anti-tumor drugs specifically to diseased cells, constitutes one of the most important goals in nano-oncology. Herein, the development of Janus mesoporous silica particles asymmetrically decorated with two targeting moieties, one of them selective for folate membrane cell receptors (folic acid) and the other one able to bind to mitochondria membrane (triphenylphosphine, TPP), is described in order to achieve sequential cell to organelle vectorization. The asymmetric decoration of each side of the particle allows fine control in the targeting attachment process in comparison with the use of symmetric nanocarriers. The presence of folic acid induces a higher increase in particle accumulation inside tumor cells, and once there, these nanocarriers are guided close to mitochondria by the action of the TPP moiety. This strategy can be applied for improving the therapeutic efficacy of current nanomedicines.

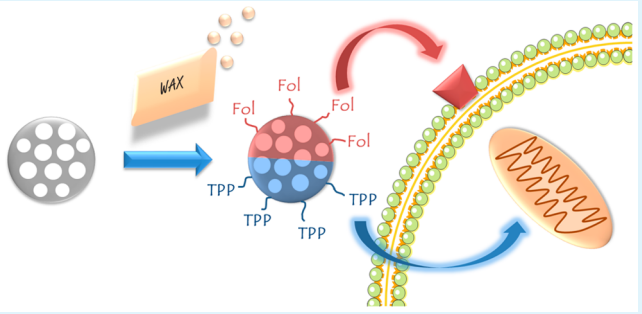

KEYWORDS: *Janus nanoparticles, targeted nanosystems, nano-oncology, mesoporous silica nanoparticles, mitochondria targeting*

INTRODUCTION

The paramount discovery made in 1986 by Matsumura and Maeda[1] about the natural tendency of nanometric systems to be passively accumulated within solid tumors triggered the race to design nanocarriers able to deliver anti-tumor agents specifically into diseased tissues.[2,3] Neoplastic tissues are irrigated by blood vessels, which have been built in a chaotic way so that they usually exhibit porous regions with diameters around a few hundred of nanometers.[4] Therefore, when the nanocarrier reaches the tumor area, it is able to pass through these pores to reach the tumor tissue, whereas it cannot cross the healthy vessel walls. Additionally, the rapid expansion of tumor cells compresses the nearby located lymphatic vessels, compromising the drainage, which enhances the accumulation time of nanocarriers into the diseased zone. This phenomenon, called the EPR (enhanced permeation and retention) effect, has also been described as primary targeting, being responsible for nanocarrier accumulation in tumor tissues. However, this effect alone is not enough to achieve an improved therapeutic response over conventional therapy. Tumor masses are incredibly complex tissues that are formed by a myriad of different cells (cancerous, supportive, and immune cells and so on)[5] Therefore, the capacity to distinguish between malignant and healthy cells is necessary for improving the effectiveness of nanomedicines. In order to acquire this property, the external surface of nanocarriers can be decorated with certain moieties such as antibodies,[6] aptamers,[7] vitamins,[8] peptides,[9] or synthetic molecules,[10] which are recognized by specific membrane cell receptors overexpressed by the tumor cells. The presence of these targeting agents (called secondary targeting) enhances accumulation within the tumor cell. Additionally, two targeting moieties can be anchored on the same nanocarrier in order to enhance even more the selectivity of the nanodevice.[11−13] It is also possible to control nanoparticle trafficking within the cell by placing targeting moieties able to recognize organelles such as mitochondria or cell nucleus (tertiary targeting).[14] Therefore, different tertiary targeting agents have been attached on drug-loaded nanoparticles to achieve significant improvements in the therapeutic efficacy of the transported payloads.[15] In light of these results, the possibility to design systems that combine these targeting capacities (tissue, cell, and organelle) has aroused great attention in the scientific community for improving even more the capacity to destroy tumor cells while limiting the side

Received: May 16, 2017
Accepted: July 31, 2017
Published: July 31, 2017

DOI: 10.1021/acsami.7b06906
ACS Appl. Mater. Interfaces 2017, 9, 26697−26706

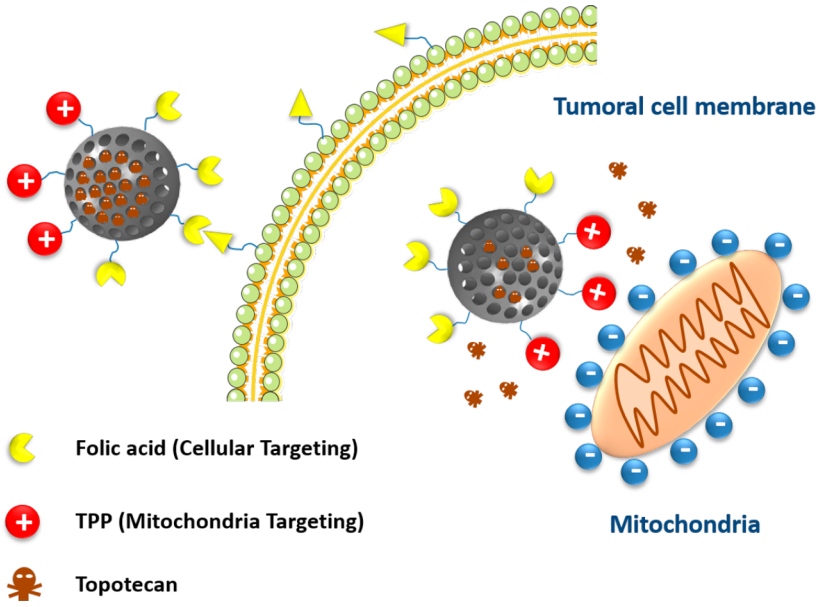

Figure 1. Mechanism of action of dual-targeted MSN: cellular and mitochondrial targeting.

effects and systemic toxicity of the therapy. Thus, there have been reports of engineered peptides that carry specific cell and organelle targeting devices,[16] nanoparticles doubly functionalized with both targeting agents,[17] and also nanocarriers functionalized with hierarchical targeting devices that recognize specific membrane cellular receptors and certain organelles following an activatable tandem mechanism.[18] However, in many cases, they lack precise control in the targeting ratio, have low transport capacity, or require the synthesis of complex moieties. Recently, Ma and co-workers[19] have carried out a computational study in order to determine the best configuration of the targeting moieties in dual-targeted nanocarriers. They concluded that Janus-type structures achieved the fastest engulfment by the cell membrane, regardless of physicochemical properties and separation between the targeting group and the carrier surface.

Herein, we describe an easy procedure for the synthesis of Janus mesoporous silica nanoparticles (J-MSN) that carry two different targeting moieties, for cells and organelles, each located in one hemisphere of the particle (Figure 1). Mesoporous silica nanoparticles (MSN) present great cargo capacity, excellent biocompatibility, and easy and cheap production.[20,21] In the approach presented here, one hemisphere of MSN was decorated with folic acid, which acts as a cellular targeting agent due to the fact that many tumor cell lines overexpress folate receptor.[22] On the other hemisphere, a triphenylphosphine derivative (TPP) was anchored for directing the nanocarrier to the mitochondrial membrane, exploiting the affinity of this positively charged group for the highly negative mitochondrial membrane.[23] The efficacy of this device has been evaluated by use of human prostate cancer cells (LNCaP), which present higher expression of folate-binding proteins on their membrane.[24,25] This system showed enhanced accumulation in tumor cells in comparison with a control line composed of healthy preosteoblastic cells (MC3T3-E1), which do not present overexpression of folate-binding proteins. Additionally, the presence of TPP on the particle surface leads to a selective accumulation of the nanoparticles close to mitochondria. Finally, when the carriers were loaded with topotecan (TOP), a potent DNA topoisomerase inhibitor that induces nuclear and mitochondria DNA damage,[26] the double-targeted device exhibit significantly higher toxicity in comparison with particles decorated with only one of the targeting moieties, which points out that the TOP effect is stronger when it is released close to mitochondria. These results indicate that the use of J-MSN decorated with cell and organelle targeting agents can significantly improve the efficacy of the transported drugs in anti-tumor therapies.

EXPERIMENTAL SECTION

Materials and Methods. The following compounds were purchased from Sigma−Aldrich Inc.: aminopropyltriethoxysilane (APTES), ammonium nitrate, cetyltrimethylammonium bromide (CTAB), tetraethyl orthosilicate (TEOS), dicyclohexylcarbodiimide (DCC), *N*-hydroxysuccinimide (NHS), *N*,*N*-diisopropylethylamine (DIPEA), fluorescein isothiocyanate (FITC), folic acid, succinic anhydride, (4-carboxybutyl)triphenylphosphonium bromide, topotecan hydrochloride hydrate (TOP, > 98%) and trifluoroacetic acid (TFA). All other chemicals [absolute ethanol, *N*,*N*-dimethylformamide (DMF), dimethyl sulfoxide (DMSO), acetone, ethyl ether, dichloromethane (DCM), heptane, dry solvents etc.] were commercially available and of best quality and they were employed as received.

Characterization Techniques. Fourier transform infrared spectroscopy (FTIR) was performed on a Thermo Nicolet nexus equipped with a Goldengate attenuated total reflectance device. The textural properties of the materials were determined by nitrogen sorption porosimetry on a Micromeritics ASAP2010 instrument. Prior to the N_2 measurements, the samples were degassed under vacuum for 24 h at room temperature. Thermogravimetric analysis (TGA) was performed on a PerkinElmer Pyris Diamond TG/DTA analyzer with a 5 °C·min^{-1} heating ramp from room temperature to 600 °C. The hydrodynamic size of the mesoporous nanoparticles was measured by means of a Zetasizer Nano ZS (Malvern Instruments) equipped with a 633 nm red laser. Mass spectra were acquired on a Voyager DE-STR Biospectrometry matrix-assisted laser desorption ionization time-of-flight (MALDI-TOF) mass spectrometer. Scanning electron microscopy (SEM) analyses were performed on a JEOL 6400-LINK AN10000 microscope (Electron Microscopy Centre, Universidad Complutense de Madrid). The samples underwent Au metallization prior to observation. Liquid NMR experiments were performed on a Bruker AV 250 MHz instrument.

Synthesis of (2,2-Dimethyl-4,15-dioxo-3,8,11-trioxa-5,14-diazanonadecan-19-yl)triphenylphosphonium Bromide (TPP-

DOI: 10.1021/acsami.7b06906
ACS Appl. Mater. Interfaces 2017, 9, 26697−26706

NH_2). To a solution of (4-carboxybutyl)triphenylphosphonium bromide (250 mg) and *N*-hydroxysuccinimide (130 mg, 2 equiv) in 3 mL of DMF were added *N*,*N*′-diisopropylcarbodiimide (DIC; 260 mg, 3 equiv) and DIPEA (1.2 mL, 6 equiv) under inert atmosphere. The mixture was stirred for 4 h at room temperature. When the acid activation was finished, a solution of *tert*-butyl {2-[2-(2-aminoethoxy)-ethoxy]ethyl}carbamate (303 mg, 1.1 equiv) was added dropwise. The mixture was stirred overnight. Crude product was precipitated in cool ether, and the filtered solid was purified by flash column chromatography (chloroform/MeOH 4:1). The resulting product was characterized by ^{1}H NMR (250 MHz, $CDCl_3$) δ 8.24 (t, J = 5.3 Hz, 1H, NH, amide), 7.89−7.76 (m, 9H, TPP), 7.76−7.63 (m, 6H, TPP), 5.18 (s, 1H, NH-Boc), 3.72 (dd, J = 14.0, 7.0 Hz, 2H), 3.59−3.47 (m, 8H), 3.40 (dd, J = 11.9, 6.2 Hz, 2H), 3.34−2.61 (m, 1H), 2.70−2.57 (m, 1H), 2.03−1.84 (m, 2H, CH_2), 1.80−1.55 (m, 6H, $3CH_2$), 1.42 (s, 9H, $3CH_3$, Boc).

The next step was removal of the *tert*-butyloxycarbonyl (Boc) protecting group, which was carried out by dissolving the product in 2 mL of DCM/TFA (1%) and stirring for 2 h. Crude product was precipitated in cool ether, and the filtered solid was purified by flash column chromatography (chloroform/MeOH 4:1). The resulting product was characterized by ^{1}H NMR (250 MHz, $CDCl_3$) δ 8.53 (br s, 2H, NH_2), 8.23 (s, 1H, NH, amide), 7.89−7.76 (m, 9H, TPP), 7.76−7.63 (m, 6H, TPP), 3.85 (br s, 2H), 3.59−3.47 (m, 8H), 3.40 (br s, 2H), 3.21 (br s, 1H), 2.70−2.57 (m, 1H), 1.94 (m, 2H, CH_2), 1.80−1.55 (m, 6H, $3CH_2$).

Synthesis of Fluorescent Mesoporous Silica Nanoparticles. In advance, FITC (1 mg) and APTES (2.2 μL) were dissolved in the minimum volume of EtOH, and the mixture was stirred at room temperature for 2 h under a N_2 atmosphere. The resulting solution was called solution 1.

MSN were synthesized as following: to a 1 L round-bottom flask were added 1 g of CTAB as a structure-directing agent, 480 mL of H_2O (Milli-Q), and 3.5 mL of NaOH (2 M). The mixture was heated to 80 °C and stirred at 600 rpm. When the reaction mixture was stabilized at 80 °C, 5 mL of TEOS was mixed with solution 1 and the resulting solution was added dropwise at 0.33 mL/min rate. The pale yellow suspension obtained was stirred for a further 2 h at 80 °C. The reaction mixture was filtered and washed 3 times with 100 mL of H_2O and then once with 50 mL of EtOH. Finally, the surfactant was removed via ion exchange by use of a solution of amonium nitrate (10 mg·mL^{-1}) in 400 mL of ethanol (95%) at 65 °C overnight with magnetic stirring under reflux. This procedure was repeated twice in order to eliminate the surfactant completely.

Synthesis of Aminated Mesoporous Silica Nanoparticles (MSN-NH_2). Dried MSN particles (200 mg) were vortexed for 80 s with a mixture of 1 g of molten paraffin in 11.6 mL of H_2O, 4.4 mL of EtOH, and 2 mg of CTAB at 70 °C. After this time, the suspension was immediately cooled down in order to solidify the paraffin. The obtained particles were filtered, washed, and subsequently dispensed in 14 mL of EtOH containing 1.5 mL of NH_3 (aqueous, 25%). After addition of 0.47 mL of APTES (2 mmol), the mixture was shaken overnight on an orbital shaker at room temperature. The solid was filtered and washed with heptane until there was no paraffin residue measured by FTIR.

Uniformly aminated MSN were synthesized as a control by the following synthetic procedure: TEOS (4.5 mL) and APTES (0.5 mL) were mixed and added dropwise to a solution of 1 g of CTAB, 480 mL of water, and 3.5 mL of 2 M NaOH at 80 °C. The final reaction mixture was stirred at 80 °C for 2 h. A white solid was filtered and washed with water and EtOH.

Synthesis of Carboxylic Acid-Functionalized Mesoporous Silica Nanoparticles (MSN-CO_2H). MSN-NH_2 particles (200 mg) were suspended in 10 mL of dry tetrahydrofuran (THF) under N_2 gas as inert atmosphere. To this solution, 40 mg of succinic acid was added and the mixture was stirred at room temperature overnight. The obtained particles were filtered and washed with THF.

Synthesis of Aminated/Carboxylic Acid-Functionalized Mesoporous Silica Nanoparticles (H_2N-MSN-CO_2H). MSN-CO_2H previously dried under vacuum (130 mg) was suspended in dry toluene under N_2 gas, and 0.15 mL of APTES was added. The mixture was refluxed at 110 °C overnight under inert atmosphere. The obtained particles were filtered and washed with toluene and ethyl ether.

Synthesis of Folic Acid/Carboxylic Acid-Functionalized Mesoporous Silica Nanoparticles (Folic-MSN-CO_2H). Folic acid (22 mg, 50 mmol) was dissolved in 2 mL of dry DMF/DMSO (4:1). To this solution were added 36 mg of DCC and 38 mg of NHS, and the mixture was stirred at room temperature for 30 min under N_2 atmosphere. After this time, the solution was added to a suspension of 50 mg of dried H_2N-MSN-CO_2H in 3 mL of DMF/DMSO (4:1). The resulting suspension was stirred under N_2 atmosphere overnight. The obtained particles were filtered and washed with DMF/DMSO (4:1), water, and acetone.

Synthesis of Aminated/Triphenylphosphine-Functionalized Mesoporous Silica Nanoparticles (H_2N-MSN-TPP). H_2N-MSN-CO_2H (100 mg) was suspended in 2 mL of dry DMF containing 12 mg of DCC and 13 mg of NHS. TPP derivative (41 mg) was dissolved in 1 mL of dry DMF containing 5 μL of DIPEA, and this solution was added to the particle suspension. The resulting mixture was stirred overnight under N_2 atmosphere. The obtained particles were filtered and washed with DMF, water, and acetone.

Synthesis of Folic Acid/Triphenylphosphine-Functionalized Mesoporous Silica Nanoparticles (Folic-MSN-TPP). Folic acid (22 mg, 50 mmol) was dissolved in 2 mL of dry DMF/DMSO (4:1). To this solution were added 36 mg of DCC and 38 mg of NHS, and the mixture was stirred at room temperature for 30 min under N_2 atmosphere. After this time, the solution was added to a suspension of 50 mg of dried H_2N-MSN-TPP in 3 mL of DMF/DMSO (4:1). The resulting suspension was stirred under N_2 atmosphere overnight. The obtained particles were filtered and washed with DMF/DMSO (4:1), water, and acetone.

Topotecan Loading within Mesoporous Silica Nanoparticles Derivatives. The desired MSN (NH_2-MSN-CO_2H, MSN-Fol, MSN-TPP, or Fol-MSN-TPP, 50 mg) was placed in a dark glass vial and dried at 80 °C under vacuum for 4 h. After this time, 5 mL of an aqueous solution of TOP (3 mg·mL^{-1}) were added and the suspension was stirred at room temperature for 48 h. The particles were filtered and the excess TOP was removed by washing three times with water. The amount of drug loaded in each system was determined from the difference between fluorescence measurements of the initial and recovered solutions (λ_{exc} = 400, λ_{em} = 540 nm). In all cases, the amount of TOP loaded was around 5% in weight.

Cell Culture. Cell culture studies were performed with mouse osteoblastic cell line MC3T3-E1 (subclone 4, CRL-2593; American Type Culture Collection, Manassas, VA) and androgen-sensitive LNCaP cells, a human prostate cancer cell line (CRL-1740; ATCC, Manassas, VA). The tested MSNs (6 μg/mL) were placed into each well of 6- or 24-well plates (CULTEK) after cell seeding. Cells were then plated at a density of 20 000 cells·cm^{-2} in 1 mL of α-minimum essential medium (for MC3T3-E1) or Dulbecco's modified Eagle's medium (DMEM, Sigma Chemical Co.; for LNCaP), containing 10% heat-inactivated fetal bovine serum and 1% penicillin (BioWhittaker Europe)−streptomycin (BioWhittaker Europe) at 37 °C in a humidified atmosphere of 5% CO_2, and incubated for different times. Some wells contained no MSN as controls.

Nanoparticle Uptake Studies by Flow Cytometry. After 24 h, the cells were incubated in the absence or presence of the tested MSNs (6 μg/mL) during 2 h. Cells were then washed twice with phosphate-buffered saline (PBS) and incubated at 37 °C with trypsin−ethylenediaminetetraacetic acid (EDTA) solution for cell detachment. The reaction was stopped with culture medium after 5 min, and cells were centrifuged at 1500 rpm for 10 min and resuspended in fresh medium. Then the surface fluorescence of the cells was quenched with trypan blue (0.4%) to confirm the presence of an intracellular, and therefore internalized, fluorescent signal. Flow cytometric measurements were performed at an excitation wavelength of 488 nm, and green fluorescence was measured at 530 nm. The trigger was set for the green fluorescence channel (FL1). The conditions for data acquisition and analysis were established by use of negative and

DOI: 10.1021/acsami.7b06906
ACS Appl. Mater. Interfaces 2017, 9, 26697−26706

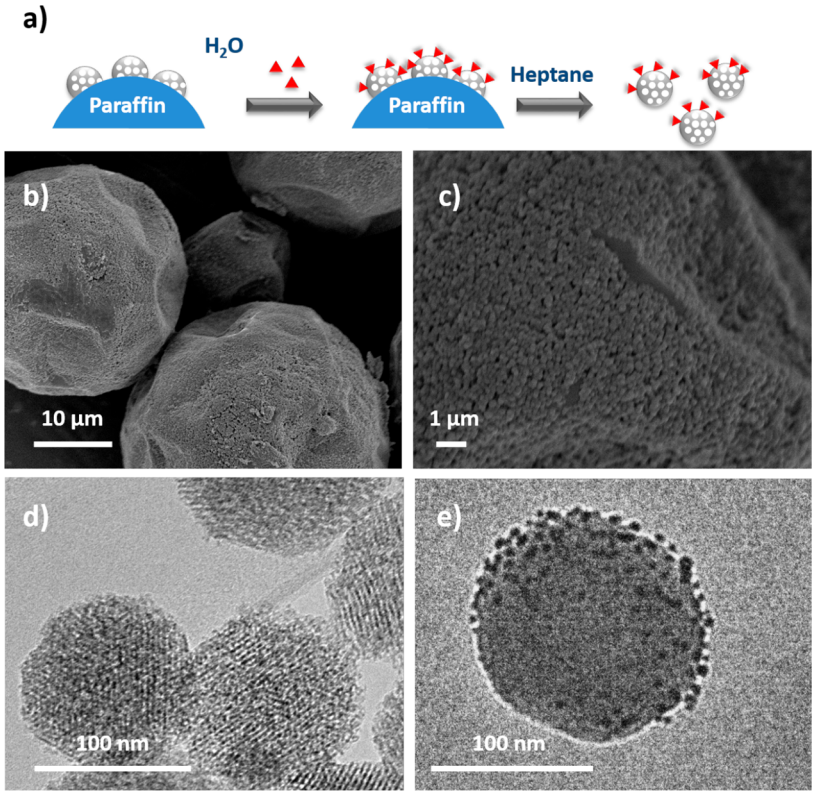

Figure 2. (a) Scheme of asymmetrization pathway of MSN (red triangles represent APTES, which is employed as amino source). (b, c) SEM images of paraffin beads with MSN embedded. (d) TEM image of MSN-NH_2. (e) TEM image of gold nanoparticles on one side of MSN-NH_2.

positive controls with the CellQuest Program of Becton, Dickinson and Company, and these conditions were maintained during all the experiments. Each experiment was carried out three times, and single representative experiments are displayed. For statistical significance, at least 10 000 cells were analyzed in each sample in a FACScan machine (Becton, Dickinson and Company) and the mean of the fluorescence emitted by these single cells was used.

Nanoparticle Uptake Studies by Fluorescence Microscopy. Cells were incubated with MSNs (6 μg/mL) for 2 h in serum-free culture medium. Then the medium was withdrawn and cells were washed with PBS three times. Cells were incubated for 45 min with MitoTracker to stain mitochondria. Cells were washed, fixed with ethanol for 2 min, and stained with DAPI (40, 60 diamidino-2-phenylindole) at 1 μg/mL. Fluorescence microscopic images were taken to evaluate MSNs. Green channel was used to locate MSNs, blue for cell nucleus, and red for mitochondria in a Evos FL cell imaging system equipped with three light-emitting diode (LED) light cubes (λ_{ex} [nm], λ_{em} [nm]): 4′,6-diamidino-2-phenylindole (DAPI; 357/44, 447/60), green fluorescent protein (GFP; 470/22, 525/50), and red fluorescent protein (RFP; 531/40, 593/40), from AMG (Advance Microscopy Group).

Cell Viability after Incubation with Topotecan-Loaded Mesoporous Silica Nanoparticles. Cell growth was analyzed by the CellTiter 96AQueous assay (Promega, Madison, WI), a colorimetric method for determining the number of living cells in culture. Briefly, both type of cells were cultured as described above without (control) or with the corresponding amount of functionalized MSNs (100 $\mu g \cdot mL^{-1}$, for 24 h) and TOP-loaded MSNs (6 $\mu g \cdot mL^{-1}$, for 6 h). In the case of empty MSN, the cells were analyzed after the incubation time. In the case of TOP-loaded MSN, after the 6 h incubation time, cells were gently washed two times with PBS and incubated in cell culture medium for 48 h more. CellTiter 96 AQueous one-solution reagent [40 μL, containing 3-(4,5-dimethythizol-2-yl)-5-(3-carboxymethoxyphenyl)-2-(4-sulfophenyl)-2*H*-tetrazolium salt (MTS) and an electron coupling reagent (phenazine ethosulfate) that allows its combination with MTS to form a stable solution) was added to each well, and plates were incubated for 4 h. The absorbance at 490 nm was then measured in a Unicam UV-500 UV−visible spectrophotometer.

RESULTS AND DISCUSSION

Mesoporous silica nanoparticles were prepared following a previously reported modified Stöber method that incorporates fluorescein covalently attached within the silica matrix.[27] The presence of this fluorophore is required in order to allow easy monitoring of nanoparticle cell uptake by fluorescence microscopic and cytometric techniques. There are different strategies for the asymmetric functionalization of this type of mesoporous material.[28] In our case, MSN were decorated with amino groups on one hemisphere following a two-step process that employs wax-in-water Pickering emulsions.[29,30] In this method, silica particles were added over a vigorously stirred aqueous emulsion of paraffin above the melting temperature of the wax (53−57 °C). After a short stirring time, the mixture was rapidly cooled at room temperature and the paraffin solidified, trapping the MSN particles on the surface (Figure 2b,c). The exposed MSN surface was functionalized with aminopropyltriethoxysilane (APTES), and finally the paraffin was removed by washing with heptane. Following this method, fluorescent round MSNs (MSN-NH_2) were obtained with size distribution centered on 190 nm, as can be observed by transmission electron microscopy (TEM) (Figure 2d). In order to study the asymmetrization process, MSN-NH_2 were mixed with gold nanoparticles (5 nm diameter) in aqueous solution for 12 h. After this time, the suspension was centrifuged under mild conditions (5000 rpm for 10 min) and the isolated particles were observed by TEM, which showed that the gold nanoparticles were mainly located on one side of MSN due to

DOI: 10.1021/acsami.7b06906
ACS Appl. Mater. Interfaces 2017, 9, 26697−26706

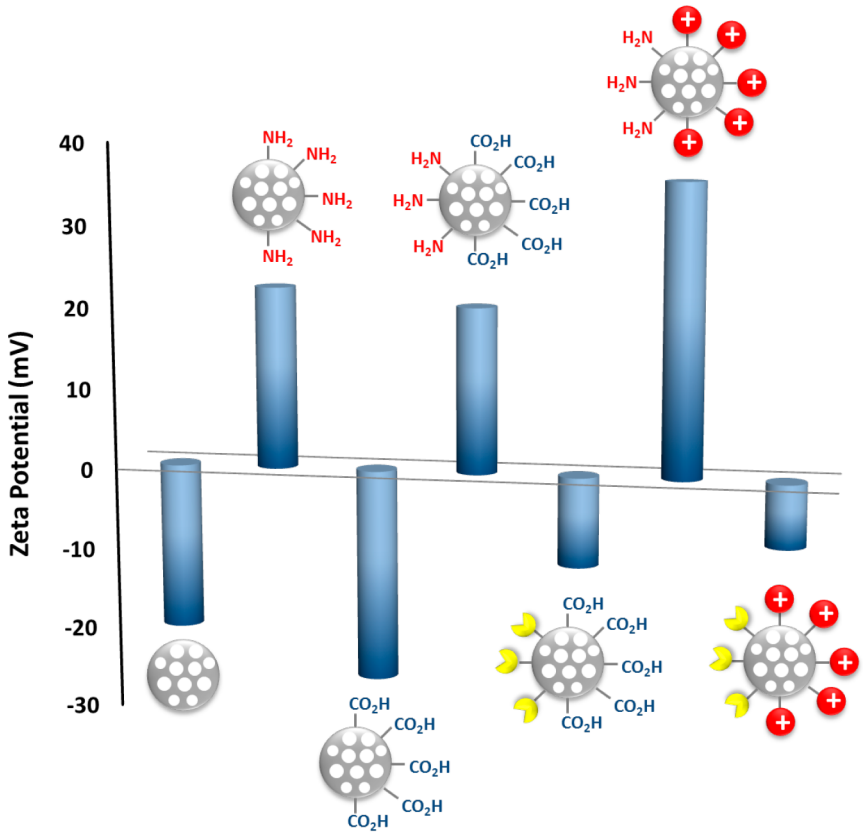

	MSN-Fol	MSN-TPP	TPP-MSN-Fol
$\%\Delta W_{\text{organic material}}$ *	8	3	12

Figure 3. (Top) ζ potential measurements of functionalized MSN derivatives. (Bottom) Increment in amount of organic material after the grafting step (*).

the affinity of gold for amino groups, which confirmed the asymmetric nanoparticle decoration (Figure 2e). When the same experiment was carried out with naked particles (MSN), the gold nanoparticles were not adsorbed on the silica surface remaining in the solution (Figure S1). Additionally, the percentage of nanoparticles that exhibited Janus structure was statistically determined by collecting several sets of TEM images, showing that around 66% of particles were asymmetrically functionalized with amino groups (Figure S2 and Table S1). MSN completely decorated with amino groups were synthesized and treated with gold nanoparticles in order employ them as control. In this case, the gold nanoparticles were uniformly distributed practically all around the MSN (96%) which indicated a uniform distribution of the amino groups (Figure S3 and Table S1). Finally, the asymmetrization process was also confirmed by the hydrophilicity change in the particles after introduction of amino groups, which was monitored by placing the particles in a vial that contains the same amount of an aqueous PBS solution (pH = 7.4) and dichloromethane. The particles uniformly functionalized with APTES, which are more hydrophobic, are located in the organic phase, whereas the hydrophilic naked particles are found in the aqueous phase. In the case of MSN-NH_2, they are mainly placed in the interphase, which proves the dual nature of these particles (Figure S4). All these data support the good performance of the asymmetrization process and are in agreement with previously reported works.[29,30]

The asymmetrization process did not alter the particle morphology, but it induced a slight hydrodynamic diameter increase (from 160 to 190 nm) according to dynamic light scattering (DLS; Figure S5). ζ potential measurement of the particles in phosphate-buffered saline solution (pH 7.2) showed a drastic change in surface charge, from a negative value (−20.5 mV) for naked particles to a positive one (+22.4 mV) for aminated nanoparticles (Figure 3). This change confirms the presence of amino groups on the particle surface, because they are protonated at physiological pH. The precise amount of amino groups was determined by quantitative fluorenylmethyloxycarbonyl (Fmoc) protocol[31] yielding a result of 100−130 μmol of amino groups/g of MSN-NH_2. In order to attach each targeting agents to one hemisphere of the particle, anchoring points with different reactivity should be incorporated on each side. Amino and carboxylic groups were selected because there are many synthetic procedures for grafting biomolecules to them.[32] Therefore, the amino groups present in MSN-NH_2 were derivatized to carboxylic acid by their reaction with succinic anhydride in organic solvent. Then the remained silanol groups present in the free hemisphere of MSN-CO_2H were react with APTES in order to introduce amino groups on the other side, yielding the asymmetrically functionalized NH_2-MSN-CO_2H (Scheme 1).

The complete synthetic process was monitored by ζ potential measurements (Figure 3). Transformation of the amino groups of MSN-NH_2 into carboxylic groups leads to a

DOI: 10.1021/acsami.7b06906
ACS Appl. Mater. Interfaces 2017, 9, 26697−26706

Scheme 1. Synthetic Pathway for Synthesis of Asymmetrically Functionalized MSN[a]

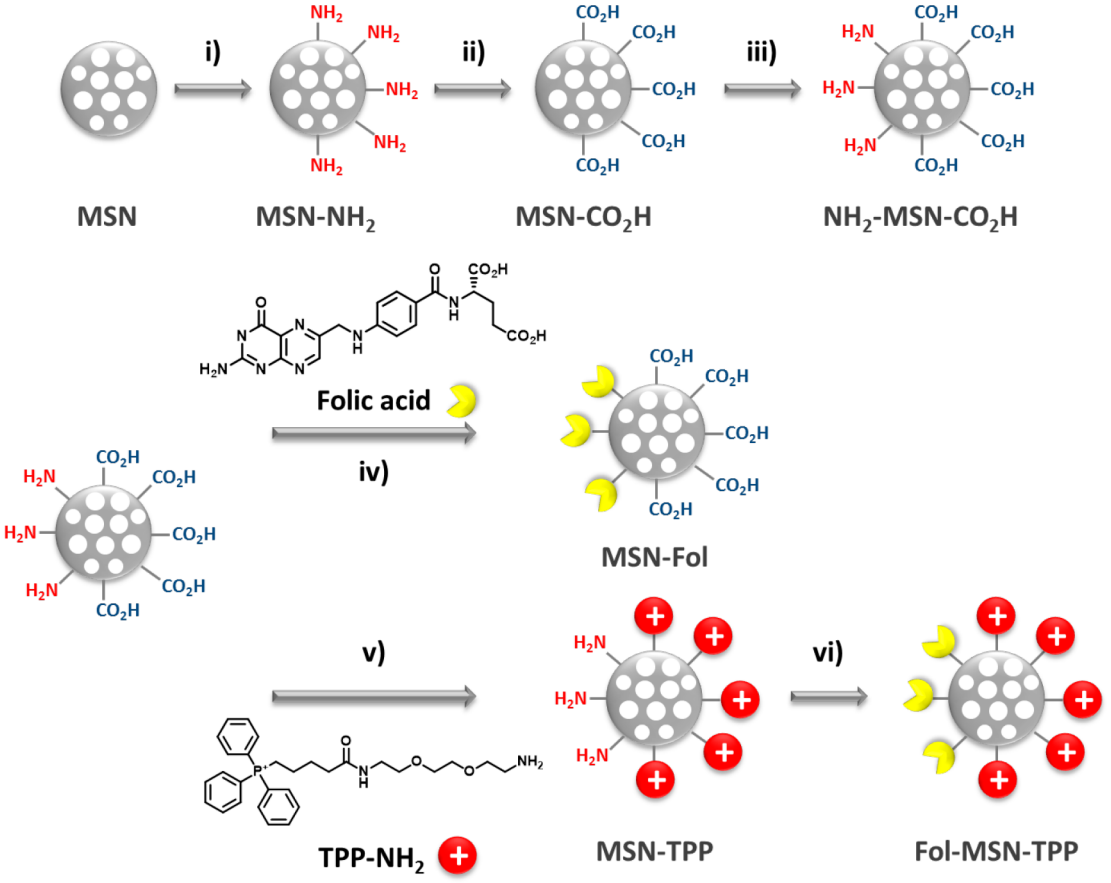

[a](i) Paraffin, CTAB, EtOH, H_2O, NH_3 (aq), APTES; (ii) succinic anhydride, THF; (iii) APTES, toluene, reflux; (iv) DMF, DMSO, DCC, NHS; (v) DMF, DCC, NHS, DIPEA; (vi) DMF, DMSO, DCC, NHS.

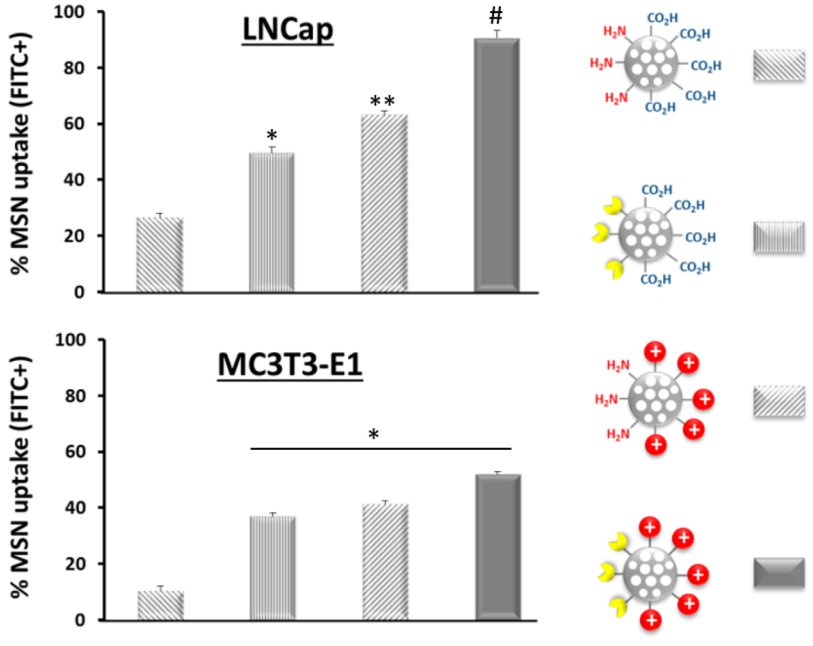

Figure 4. Comparative nanoparticle uptake of MSN derivatives in LNCaP and MC3T3-E1 cell lines, after 2 h of exposure time. Data are mean ± standard error of the mean of three independent experiments, performed at least in triplicate. *$p < 0.05$ vs NH_2-MSN-CO_2H; **$p < 0.05$ vs MSN-Fol and NH_2-MSN-CO_2H; #$p < 0.05$ vs all conditions (Student's t-test).

DOI: 10.1021/acsami.7b06906
ACS Appl. Mater. Interfaces 2017, 9, 26697−26706

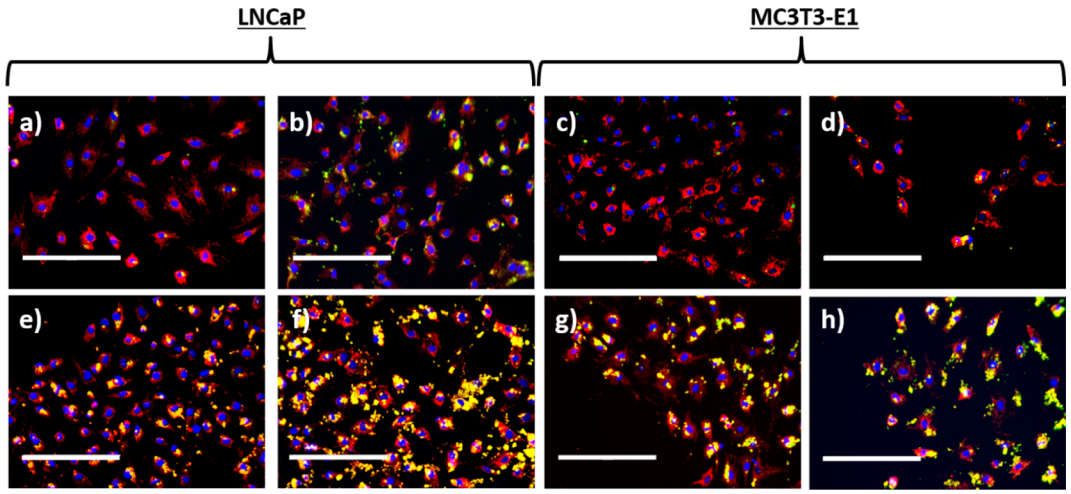

Figure 5. Fluorescence microscopic images of cells exposed to a fixed concentration of the following MSN derivatives: (a, c) NH_2-MSN-CO_2H, (b, d) MSN-Fol, (e, g) MSN-TPP, and (f, h) Fol-MSN-TPP. Blue corresponds to cell nuclei, obtained by use of blue DAPI staining agent; red corresponds to mitochondria, obtained by employing red MitoTracker; green dots correspond to MSN nanosystems due to the presence of fluorescein trapped within the silica matrix. White scale bars correspond to 200 μm.

strong decrease in the positive charge (MSN-CO_2H), which is partially re-established when new amino groups are introduced in the free hemisphere (NH_2-MSN-CO_2H). Attachment of folic acid was carried out on the NH_2 side by employing the well-known carbodiimide chemistry. The carboxylic group of the folic acid was activated by reaction with dicyclohexylcarbodiimide (DCC) and *N*-hydrosuccinimide (NHS), and then the resulting ester was directly added to a suspension of NH_2-MSN-CO_2H, yielding MSN-Fol. After this step, the surface charge of the particle changed back to a negative value, which is the consequence of reduction of free amino groups on the particle surface. In the case of the attachment of TPP moieties, a specific TPP analogue that carries one amino group at the end (TPP-NH_2) was synthesized (see Experimental Section for more details). These TPP moieties were introduced following a similar procedure but, in this case, through activation of the carboxylic groups of NH_2-MSN-CO_2H with DCC and NHS, followed by subsequent addition of TPP-NH_2. As expected, surface charge suffered a significant increase after this synthetic step due to the introduction of positive charges on the particle surface. Finally, folic acid was anchored to the free amino groups of MSN-TPP, leading to a dramatic reduction of the charge. Additionally, the introduction of each targeting agent was confirmed by measuring the amount of organic material by thermogravimetric analysis, before and after the grafting step (Figure 3, bottom) and also by FTIR spectroscopy, which shows the appearance of characteristic bands after each synthetic step (Figure S6).

Human prostate cancer cells (LNCaP) were selected as a tumor model cell line due to the overexpression of folate-binding receptors on their membranes.[24,25] In order to evaluate the capacity to enhance the particle uptake of each targeting agent, separately and asymmetrically combined in one single particle, LNCaP cells were exposed to a fixed concentration (6 $\mu g \cdot mL^{-1}$) of each type of fluorescently labeled (in green) nanoparticle, NH_2-MSN-CO_2H, MSN-Fol, MSN-TPP, and Fol-MSN-TPP, for 2 h. After this time, the cells were gently washed with PBS in order to remove noninternalized particles. The number of cells that had engulfed fluorescent nanoparticles was determined by flow cytometry. In order to discard the particles that are simply attached on the cell membrane and not internalized, the external fluorescence was quenched by adding trypan blue before cell counting. Thus, only the cells that have particles inside the inner space are counted as positive. The same experiment was carried out in parallel with healthy preosteoblastic cells (MC3T3-E1) as a model of cells that do not overexpress folate-binding proteins on their surfaces, in order to evaluate the capacity of these nanocarriers to distinguish between tumor cells and healthy ones. In the case of tumor cells, the uptake was around 25% when the particles did not present any targeting moiety (NH_2-MSN-CO_2H), whereas this value doubled when the particles were decorated with folic acid on one hemisphere (Figure 4). Interestingly, particles functionalized only with TPP (MSN-TPP) almost triple the uptake in comparison with the untargeted particles, showing than 63% of the tumor cell population engulfed these nanosystems, which is higher than the uptake achieved by particles decorated with folic acid. The reason could be that these nanoparticles presented the highest positive charge at physiological pH and therefore they present strong affinity for the negatively charged tumor cell membrane. In any case, nanoparticles decorated with both targeting moieties (Fol-MSN-TPP) showed the highest uptake value (more than 90%), which indicates that the presence of these groups significantly enhances the uptake in this tumor cell line. Regarding the nanoparticle uptake observed in healthy cells, only 10% of the untargeted MSNs were captured by these cells, while the uptake value was significantly higher for folic acid and TPP monofunctionalized MSN (Figure 4). Obviously, healthy cells also express folate receptors on their surface (although in lesser amount than tumor cells) because this vitamin is essential and it participates in many biochemical pathways such as amino acid metabolism and synthesis of RNA and DNA, among others. For this reason, the uptake of folic acid-functionalized MSN was higher than that of untargeted MSN but lower than in the case of tumor cells. Similar uptake was seen for MSN-TPP. This fact can be explained, as in the previous case, by electrostatic affinity between the positively charged nanoparticles and the negatively charged cell membrane. Finally, the uptake of dual-targeted MSN was slightly higher than that observed in monofunctionalized ones, but it was notably lower than the uptake achieved by tumor cells (52% in healthy cells

DOI: 10.1021/acsami.7b06906
ACS Appl. Mater. Interfaces 2017, 9, 26697−26706

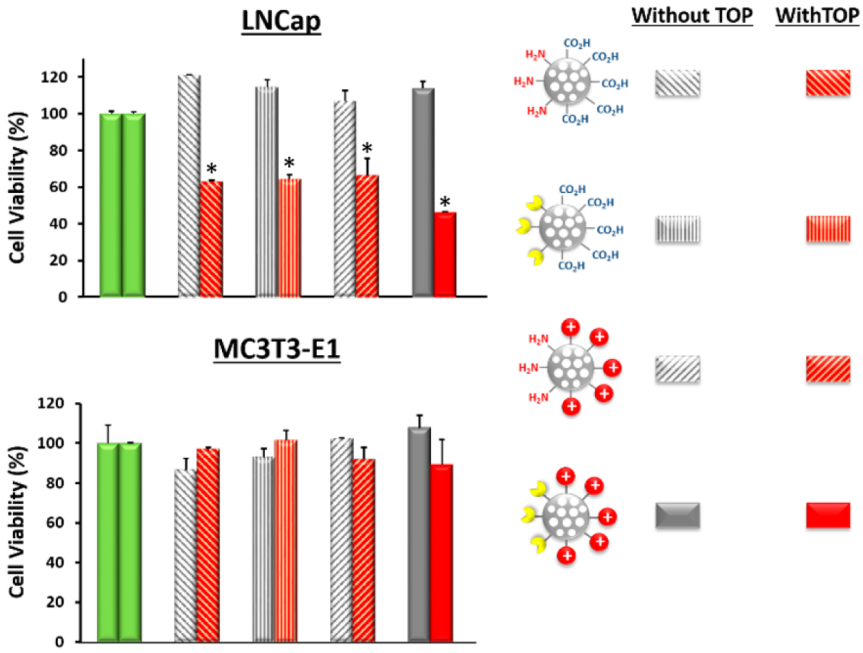

Figure 6. Cell viability studies, with and without TOP loaded within the MSN, for LNCaP and MC3T3-E1 cell lines and 48 h of exposure time. *p < 0.05 vs corresponding control without TOP (Student's t-test).

versus 91% in tumor cells). These results indicate the capacity of dual-targeted MSN to reach the inner space of tumor cells in a selective manner, which reflects its potential suitability for anti-tumor therapy.

To study in more detail the particle fate within the tumor cell, as well as the efficacy of the organelle targeting moiety, cells were incubated with each type of nanoparticle under the same conditions, and then they were stained with blue DAPI as a nuclear tracker and red Mitotracker for labeling mitochondria. This staining protocol allows qualitative determination by fluorescent microscopy of the particle location within the cells, detecting each fluorophore in separate channels, as has been reported elsewhere.[33] In both cell lines, untargeted MSN were barely taken up by the cells (Figure 5a,c). MSN-Fol showed higher uptake but significantly lower than the internalization achieved with MSN-TPP (Figure 5b,d versus e,g). Moreover, in the last case the presence of TPP on the particle surface caused that the nanoparticles were placed in close proximity with mitochondria, as can be observed by the overlapping between the green spots associated with the fluorescein of the nanoparticles and the red ones due to the mitochondria staining agent. Finally, dual-targeted MSN exhibited the highest accumulation and mitochondria localization in both cell lines (Figure 5f,h) being higher in the case of tumor cell line, which confirms the results obtained by flow cytometry.

The use of nanodevices as drug carriers for clinical applications requires that the designed material present excellent biocompatibility and absence of cytotoxicity. MSN is a biocompatible material that presents low toxicity and lack of immunogenicity and is degraded into nontoxic compounds (mainly silicic acid) in relatively short time periods.[34] Despite its lack of toxicity, the surface modification of this material could provoke the appearance of toxicity due to enhanced uptake within the cells. To evaluate toxicity, LNCaP and MC3T3-E1 cells were incubated with a significantly higher amount of functionalized MSNs (100 $\mu g \cdot mL^{-1}$) in cell culture medium for 24 h. After this time, cell viability was determined via the standard cell viability test by MTS reduction. The results showed that none of these empty materials exhibited cytotoxicity in either cell line (Figure 6).

In a parallel way, the capacity of these materials to deliver cytotoxic drugs in a selective manner to tumor cells was evaluated by employing MSN loaded with a cytotoxic compound, in this case topotecan (TOP). TOP is an inhibitor of DNA topoisomerase I, which is an enzyme that reduces the strain in DNA chains during replication. Administration of this drug induces damage to DNA located in the cell nucleus and also in mitochondria, causing cell death. This drug presents high anti-tumor activity but it is unstable at neutral and basic pH, losing its activity after a few hours.[35] Therefore, repeated dosages of this drug are needed in order to maintain its concentration in blood, which induces the appearance of systemic toxicity. For these reasons, TOP has been selected as a drug model for this system. Thus, TOP was loaded within MSN derivatives by soaking the particles in a saturated aqueous solution of TOP (3 $mg \cdot mL^{-1}$). The amount of loaded TOP was determined by the difference in fluorescence of the loading solution before and after MSN immersion, showing in all cases around 5% TOP by weight. LNCap and MC3T3-E1 cells were exposed to a fixed concentration of TOP-loaded MSN during 6 h. After this time, the cells were gently washed with PBS in order to remove the noninternalized particles, and they were incubated for 48 h more in cell culture medium. In the tumor cell line, when cells were exposed to untargeted MSN or monofunctionalized targeted MSN (MSN-Fol or MSN-TPP), cell viability decreased around 35−40% in all cases (Figure 6). Cell viability decrease was significantly higher in the case of dual-targeted MSN (Fol-MSN-TPP), which shows around 55% cell viability reduction. The higher toxicity can be attributed to the enhanced uptake observed and also to the close proximity of the nanocarrier to mitochondria, which could enhance the efficacy of the released TOP, as has been described in other systems.[36] It is important to point out that the particle concentration in all cases was very low (6 $\mu g \cdot mL^{-1}$) and the

DOI: 10.1021/acsami.7b06906
ACS Appl. Mater. Interfaces 2017, 9, 26697−26706

exposure time in each case was also short (6 h), which indicate the great cytotoxic capacity of these nanocarriers. In healthy cells, only a slight decrease in cell viability was observed in the case of dual-targeted MSN (11%). This fact can be attributed to the lower uptake observed in these cells in comparison with the tumor cell line and also to the higher resistance of healthy cells to cytotoxic drugs.

These data confirm the best performance of dual-targeted MSN in comparison with monofunctionalized ones, which indicates the excellent suitability of this strategy to enhance the efficacy of nanocarrier-based therapies.

CONCLUSIONS

In this work, a new strategy for the synthesis of asymmetrically functionalized dual-targeted MSN has been presented. This method, based on the formation of Pickering emulsions, allows one to obtain large amounts of J-MSN, which is a significant advantage compared with other reported procedures such as sputter-coating or microfluidic techniques. As a proof of concept, folic acid and a triphenylphosphine derivative have been chosen as cell and organelle targeting moieties, respectively, to study the effect of asymmetric introduction of these groups on the particle surface. The achieved results indicate that the combination of both targeting agents, each of them located in one hemisphere of the particle, enhances their uptake in tumor cells and induces localization of the nanocarrier close to mitochondria, which improves the efficacy of the transported drugs. This novel strategy can be easily adapted for the introduction of different targeting moieties on the MSN surface, which can improve the arsenal of nanomedicines in the fight against cancer.

ASSOCIATED CONTENT

Supporting Information

The Supporting Information is available free of charge on the ACS Publications website at DOI: 10.1021/acsami.7b06906.

Six figures showing images of precipitate and supernatant of naked or asymmetrically aminated MSN exposed to gold nanoparticles, location of MSN nanoparticles in a vial with two phases (organic and aqueous), hydrodynamic diameter measurements, and FTIR spectra of functionalized MSN; one table listing TEM statistical analysis (PDF)

AUTHOR INFORMATION

Corresponding Authors

*(A.B.) E-mail abaezaga@ucm.es.
*(M.V.-R.) E-mail vallet@ucm.es.

ORCID

Alejandro Baeza: 0000-0002-9042-8865

Author Contributions

All authors have given approval to the final version of the manuscript. The manuscript was written through contributions of all authors. V.R. optimized the MSN asymmetrization procedure. G.V. synthesized the TPP analog. D.L. carried out the cell viability evaluation. V.L. and M.R.V. contributed equally.

Notes

The authors declare no competing financial interest.

ACKNOWLEDGMENTS

This work was supported by the European Research Council (Advanced Grant VERDI; ERC-2015-AdG Proposal 694160) and Project MAT2015-64831-R.

REFERENCES

(1) Matsumura, Y.; Maeda, H. A New Concept for Macromolecular Therapeutics in Cancer-Chemotherapy - Mechanism of Tumoritropic Accumulation of Proteins and the Antitumor Agent Smancs. *Cancer Res.* **1986**, *46*, 6387−6392 (http://cancerres.aacrjournals.org/content/46/12_Part_1/6387.full-text.pdf).

(2) Nakamura, H.; Jun, F.; Maeda, H. Development of Next-Generation Macromolecular Drugs Based on the EPR Effect: Challenges and Pitfalls. *Expert Opin. Drug Delivery* **2015**, *12*, 53−64.

(3) Ediriwickrema, A.; Saltzman, W. M. Nanotherapy for Cancer: Targeting and Multifunctionality in the Future of Cancer Therapies. *ACS Biomater. Sci. Eng.* **2015**, *1*, 64−78.

(4) Jain, R. K.; Stylianopoulos, T. Delivering Nanomedicine to Solid Tumors. *Nat. Rev. Clin. Oncol.* **2010**, *7*, 653−664.

(5) Egeblad, M.; Nakasone, E. S.; Werb, Z. Tumors as Organs: Complex Tissues That Interface with the Entire Organism. *Dev. Cell* **2010**, *18*, 884−901.

(6) Vivek, R.; Thangam, R.; Nipunbabu, V.; Rejeeth, C.; Sivasubramanian, S.; Gunasekaran, P.; Muthuchelian, K.; Kannan, S. Multifunctional HER2-Antibody Conjugated Polymeric Nanocarrier-Based Drug Delivery System for Multi-Drug-Resistant Breast Cancer Therapy. *ACS Appl. Mater. Interfaces* **2014**, *6*, 6469−6480.

(7) Lao, Y.; Phua, K. K. L.; Leong, K. W. Aptamer Nanomedicine for Cancer Therapeutics: Barriers and Potential for Translation. *ACS Nano* **2015**, *9*, 2235−2254.

(8) Vlashi, E.; Kelderhouse, L. E.; Sturgis, J. E.; Low, P. S. Effect of Folate-Targeted Nanoparticle Size on Their Rates of Penetration into Solid Tumors. *ACS Nano* **2013**, *7*, 8573−8582.

(9) Field, L. D.; Delehanty, J. B.; Chen, Y.; Medintz, I. L. Peptides for Specifically Targeting Nanoparticles to Cellular Organelles: Quo Vadis? *Acc. Chem. Res.* **2015**, *48*, 1380−1390.

(10) Villaverde, G.; Baeza, A.; Melen, G. J.; Alfranca, A.; Ramirez, M.; Vallet-Regí, M. A New Targeting Agent for the Selective Drug Delivery of Nanocarriers for Treating Neuroblastoma. *J. Mater. Chem. B* **2015**, *3*, 4831−4842.

(11) Zhao, Y.; Jiang, Y.; Lv, W.; Wang, Z.; Lv, L.; Wang, B.; Liu, X.; Liu, Y.; Hu, Q.; Sun, W.; Xu, Q.; Xin, H.; Gu, Z. Dual Targeted Nanocarrier for Brain Ischemic Stroke Treatment. *J. Controlled Release* **2016**, *233*, 64−71.

(12) Li, Y.; He, H.; Jia, X.; Lu, W.-L.; Lou, J.; Wei, Y. A Dual-targeting Nanocarrier Based on Poly(amidoamine) Dendrimers Conjugated with Transferrin and Tamoxifen for Treating Brain Gliomas. *Biomaterials* **2012**, *33*, 3899−3908.

(13) Pan, W.; Yang, H.; Zhang, T.; Li, Y.; Li, N.; Tang, B. Dual-targeted Nanocarrier Based on Cell Surface Receptor and Intracellular mRNA: An Effective Strategy for Cancer Cell Imaging and Therapy. *Anal. Chem.* **2013**, *85*, 6930−6935.

(14) Kang, B. H.; Plescia, J.; Song, H. Y.; Meli, M.; Colombo, G.; Beebe, K.; Scroggins, B.; Neckers, L.; Altieri, D. C. Combinatorial Drug Design Targeting Multiple Cancer Signaling Networks Controlled by Mitochondrial Hsp90. *J. Clin. Invest.* **2009**, *119*, 454−464.

(15) Rajendran, L.; Knölker, H.-J.; Simons, K. Subcellular Targeting Strategies for Drug Design and Delivery. *Nat. Rev. Drug Discovery* **2010**, *9*, 29−42.

(16) Chen, W.-H.; Xu, X.-D.; Luo, G.-F.; Jia, H.-Z.; Lei, Q.; Cheng, S.-X.; Zhuo, R.-X.; Zhang, X.-Z. Dual-Targeting pro-Apoptotic Peptide for Programmed Cancer Cell Death via Specific Mitochondria Damage. *Sci. Rep.* **2013**, *3*, No. 3468.

(17) Pan, L.; Liu, J.; He, Q.; Shi, J. MSN-Mediated Sequential Vascular-to-Cell Nuclear-Targeted Drug Delivery for Efficient Tumor Regression. *Adv. Mater.* **2014**, *26*, 6742−6748.

(18) Chen, Z.; Zhang, L.; Song, Y.; He, J.; Wu, L.; Zhao, C.; Xiao, Y.; Li, W.; Cai, B.; Cheng, H.; Li, W. Hierarchical Targeted Hepatocyte Mitochondrial Multifunctional Chitosan Nanoparticles for Anticancer Drug Delivery. *Biomaterials* **2015**, *52*, 240−250.
(19) Xia, Q.-S.; Ding, H.-M.; Ma, Y.-Q. Can Dual Targeting Enhance Cellular Uptake of Nanoparticles? *Nanoscale* **2017**, *9*, 8982−8989.
(20) Vallet-Regi, M.; Rámila, A.; del Real, R. P.; Pérez-Pariente, J. A New Property of MCM-41: Drug Delivery System. *Chem. Mater.* **2001**, *13*, 308−311.
(21) Vallet-Regí, M.; Balas, F.; Arcos, D. Mesoporous Materials for Drug Delivery. *Angew. Chem., Int. Ed.* **2007**, *46*, 7548−7558.
(22) Byrne, J. D.; Betancourt, T.; Brannon-Peppas, L. Active Targeting Schemes for Nanoparticle Systems in Cancer Therapeutics. *Adv. Drug Delivery Rev.* **2008**, *60*, 1615−1626.
(23) Smith, R. a J.; Porteous, C. M.; Gane, A. M.; Murphy, M. P. Delivery of Bioactive Molecules to Mitochondria in Vivo. *Proc. Natl. Acad. Sci. U. S. A.* **2003**, *100*, 5407−5412.
(24) Hattori, Y.; Maitani, Y. Folate-Linked Nanoparticle-Mediated Suicide Gene Therapy in Human Prostate Cancer and Nasopharyngeal Cancer with Herpes Simplex Virus Thymidine Kinase. *Cancer Gene Ther.* **2005**, *12*, 796−809.
(25) Martínez-Carmona, M.; Lozano, D.; Colilla, M.; Vallet-Regí, M. Selective Topotecan Delivery to Cancer Cells by Targeted pH-Sensitive Mesoporous Silica Nanoparticles. *RSC Adv.* **2016**, *6*, 50923−50932.
(26) de la Loza, M. C. D.; Wellinger, R. E. A Novel Approach for Organelle-Specific DNA Damage Targeting Reveals Different Susceptibility of Mitochondrial DNA to the Anticancer Drugs Camptothecin and Topotecan. *Nucleic Acids Res.* **2009**, *37*, e26.
(27) Martínez-Carmona, M.; Baeza, A.; Rodriguez-Milla, M. a.; García-Castro, J.; Vallet-Regí, M. Mesoporous Silica Nanoparticles Grafted with a Light-Responsive Protein Shell for Highly Cytotoxic Antitumoral Therapy. *J. Mater. Chem. B* **2015**, *3*, 5746−5752.
(28) Ujiie, H.; Shimojima, A.; Kuroda, K. Synthesis of Colloidal Janus Nanoparticles by Asymmetric Capping of Mesoporous Silica with Phenylsilsesquioxane. *Chem. Commun.* **2015**, *51*, 3211−3214.
(29) Simmchen, J.; Baeza, A.; Ruiz, D.; Esplandiu, M. J.; Vallet-Regí, M. Asymmetric Hybrid Silica Nanomotors for Capture and Cargo Transport: Towards a Novel Motion-Based DNA Sensor. *Small* **2012**, *8*, 2053−2059.
(30) Perro, A.; Meunier, F.; Schmitt, V.; Ravaine, S. Production of Large Quantities of "Janus" Nanoparticles Using Wax-in-Water Emulsions. *Colloids Surf., A* **2009**, *332*, 57−62.
(31) Yoon, T. J.; Yu, K. N.; Kim, E.; Kim, J. S.; Kim, B. G.; Yun, S. H.; Sohn, B. H.; Cho, M. H.; Lee, J. K.; Park, S. B. Specific Targeting, Cell Sorting, and Bioimaging with Smart Magnetic Silica Core-Shell Nanomaterials. *Small* **2006**, *2*, 209−215.
(32) Sapsford, K. E.; Algar, W. R.; Berti, L.; Gemmill, K. B.; Casey, B. J.; Oh, E.; Stewart, M. H.; Medintz, I. L. Functionalizing Nanoparticles with Biological Molecules: Developing Chemistries That Facilitate Nanotechnology. *Chem. Rev.* **2013**, *113*, 1904−2074.
(33) Zhang, Y.; Shen, Y.; Teng, X.; Yan, M.; Bi, H.; Morais, P. C. Mitochondria-targeting Nanoplatform with Fluorescent Carbon Dots for Long Time Imaging and Magnetic Field-Enhanced Cellular Uptake. *ACS Appl. Mater. Interfaces* **2015**, *7*, 10201−10212.
(34) Lu, J.; Liong, M.; Li, Z.; Zink, J. I.; Tamanoi, F. Biocompatibility, Biodistribution, and Drug-Delivery Efficiency of Mesoporous Silica Nanoparticles for Cancer Therapy in Animals. *Small* **2010**, *6*, 1794−1805.
(35) Herben, V. M.; ten Bokkel Huinink, W. W.; Beijnen, J. H. Clinical Pharmacokinetics of Topotecan. *Clin. Pharmacokinet.* **1996**, *31*, 85−102.
(36) Luo, G.-F.; Chen, W.-H.; Liu, Y.; Lei, Q.; Zhuo, R.-X.; Zhang, X.-Z. Multifunctional Enveloped Mesoporous Silica Nanoparticles for Subcellular Co-Delivery of Drug and Therapeutic Peptide. *Sci. Rep.* **2015**, *4*, No. 6064.

DOI: 10.1021/acsami.7b06906
ACS Appl. Mater. Interfaces 2017, 9, 26697−26706

Supporting Information

Janus Mesoporous Silica Nanoparticles for Dual-Targeting for Tumoral Cells and Mitochondria.

Victoria López,[a,†] *Maria Rocío Villegas,*[a,b,†] *Verónica Rodríguez,*[a] *Gonzalo Villaverde,*[a,b] *Daniel Lozano,*[a,b] *Alejandro Baeza**[a,b] *and María Vallet-Regí**[a,b]

a. Departamento de Química Inorgánica y Bioinorgánica, Facultad de Farmacia, Universidad Complutense de Madrid, 28040 Madrid, Spain.

b. Networking Research Center on Bioengineering, Biomaterials and Nanomedicine (CIBER-BBN), Av. Monforte de Lemos, 3-5. 28029 Madrid, Spain.

*Alejandro Baeza, abaezaga@ucm.es; *María Vallet-Regí, vallet@ucm.es

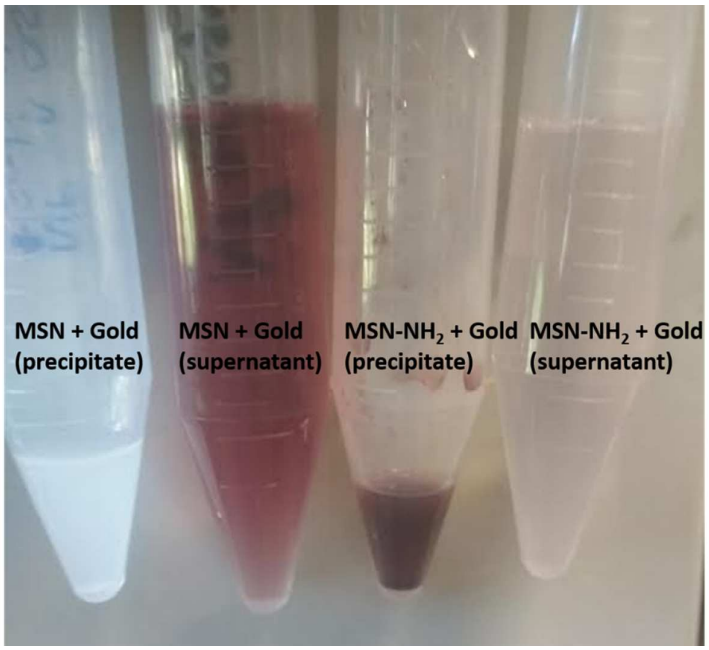

Figure S1. MSN and MSN-NH2 nanoparticles exposed to gold nanoparticles during 12 hours and centrifuged during 10 min at 5000 rpm.

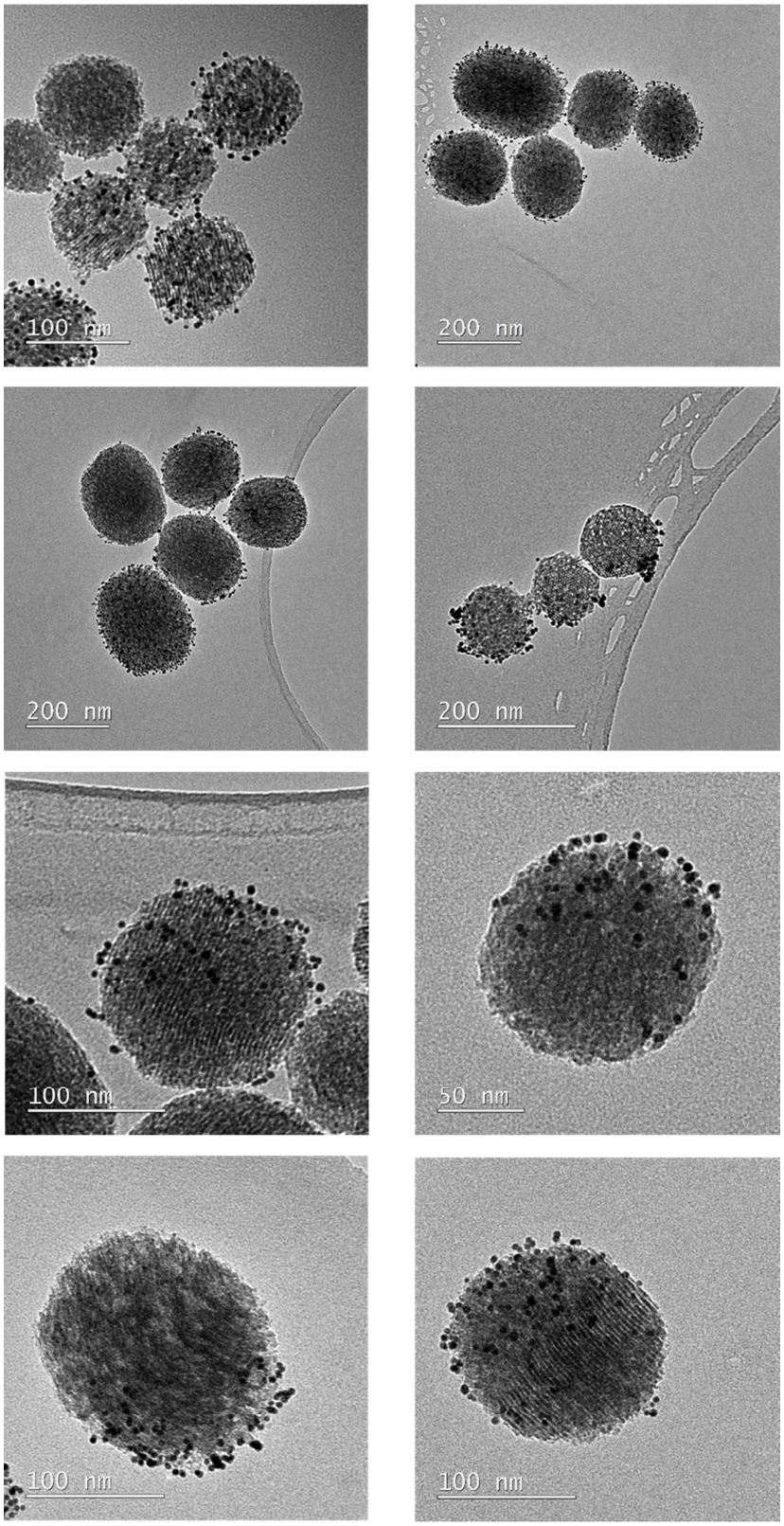

Figure S2. TEM micrographs of Janus MSN-NH2 nanoparticles exposed to gold nanoparticles.

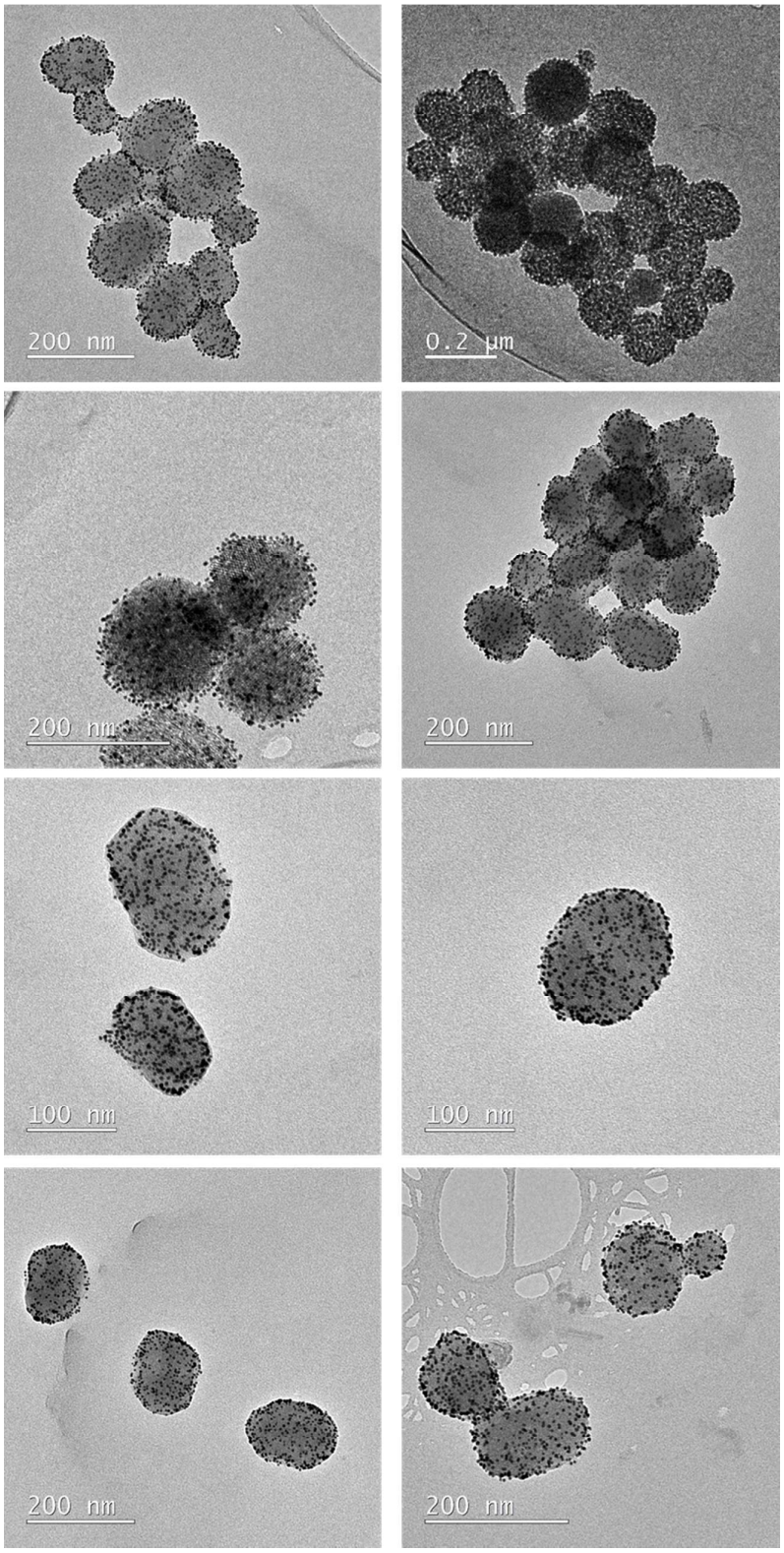

Figure S3. TEM micrographs of Uniform MSN-NH2 nanoparticles exposed to gold nanoparticles.

TEM Statistical Analysis			
Sample	Configuration Percentage (Total Nanoparticles Number=53)		
	Janus†	Uniform‡	Naked§
Janus MSN-NH_2	66	19	15
Uniform MSN-NH_2	0	96	4

Table S1. TEM statistical analysis of Janus MSN-NH_2 and Uniform MSN-NH_2 nanoparticles exposed to gold nanoparticles. † Percentage of nanoparticles asymmetrically functionalized, ‡ Percentage of particles which showed an uniform functionalization and § Percentage of nanoparticles which did not show functional groups.

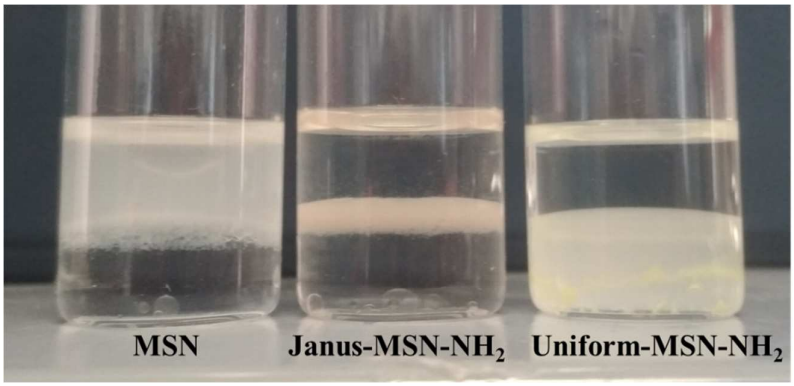

Figure S4. Location of each type of particles in a vial with PBS (pH = 7.4) (upper phase) and dichloromethane (bottom phase).

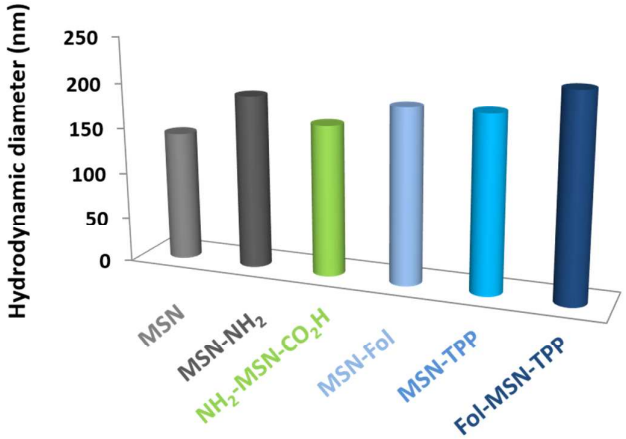

Figure S5. Hydrodynamic diameter obtained by dynamic light scattering (DLS) of each type of MSN

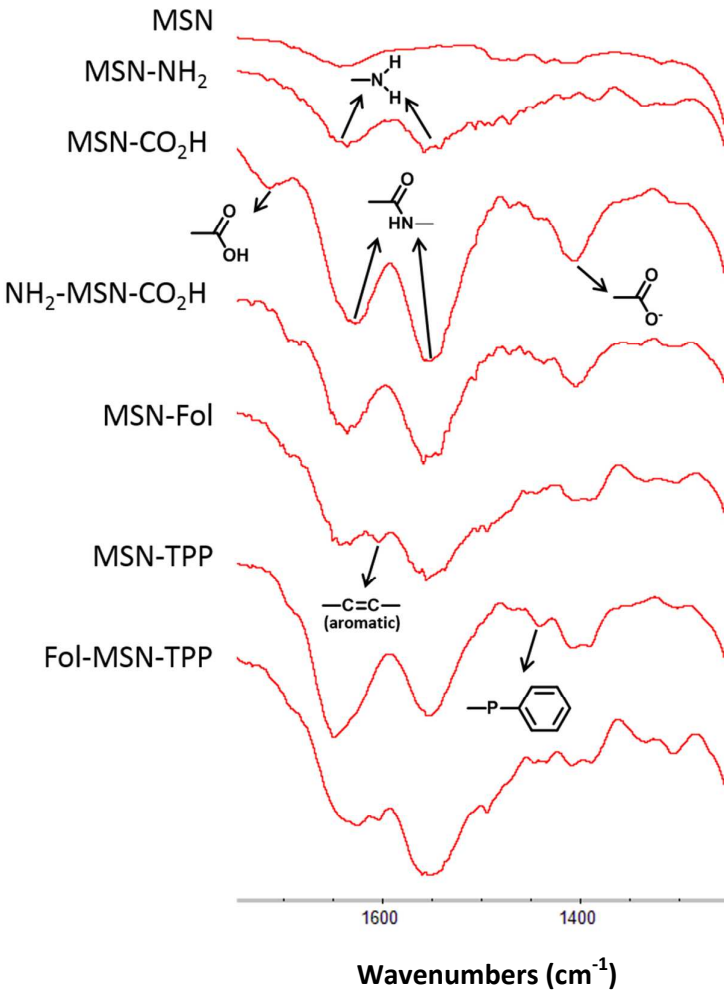

Figure S6. FTIR transmittance spectra of each functionalized MSN.

Section III.III.

Use of Collagenase Nanocapsules to Treat Fibrotic Lesions

Introduction to fibrotic pathologies

Extracellular matrix (ECM) is defined as the interconnected meshwork of macromolecules that surrounds cells in solid tissues which provide them of structural and mechanical properties.[1,2] The correct dynamic ECM remodeling is essential to wound healing process and maintain the normal organ homeostasis. The excessive or uncontrolled ECM remodeling plays an important role in cancer, since it promotes the tumorigenesis and metastatic progression, as well as, can leads to fibrotic lesions.

Fibrosis is a common lesion in several diseases and can be defined as a pathological state characterized by the excessive development of connective fibrotic tissue in organs or a tissue. These connective fibrotic tissues are characterized by an excess of collagen, among other structural proteins, that can lead to permanent scarring, organs dysfunction and, in certain cases, the death.[3,4] The principal mediators in fibrosis are myofribloblasts that are the principal collagen producer when they are activated.[5] The process of fibrotic lesions formation can occur systematically as systemic sclerosis, which is a chronic multisystem disorder characterized by high deposition of collagen in skin and internal organs[6] or locally, as for example by local deposition of collagen in the tunica albuginea of penis (Peyronie disease),[7] in the hand (Dupuytren disease)[8] and keloids[9] and hypertrophic scars[10] and local scleroderma[11] diseases.

Fibrotic diseases have a significant incidence in the population. For instance, systemic sclerosis has an incidence of 4.4 case per 100.000,[12,13] localized scleroderma (Morphea) has an annual incidence around 3 cases per 100.000,[11] idiopathic pulmonary fibrosis have an incidence of 4 per 100.000 persons, in age range from18 to 34 years and 227.2 persons per 100.000 for over 75 years,[14] liver fibrosis affect to more than ten millions of person in all world and can lead to cirrhosis.[15] Dupuytren affects about 5-15% of males older

than 50y.[16,17] Prevalence of Peyronie disease among 1.5-6.9% of men.[18] Moreover, fibrotic diseases such as systemic sclerosis, pulmonary fibrosis, liver cirrhosis and cardiovascular diseases lead to over 45% of deaths in the developed world.

The actual treatments for fibrosis diseases are surgery, immunosupressor treatments and collagenase administration. Traditionally, fibrotic lesions have been treated through the cord excision by surgery.[19,7,20] Unfortunately, surgical procedures often carry important complications and can produce serious adverse effects such as nerve and artery injuries, neupraxia, complex regional pain, tendon injury[21,22] neurovascular injury, penile shorting and erectile dysfunction[23] or not produce a significant benefit.[24] In addition, these interventions are invasive techniques that require long recovery times until the patient can return to normal life. Additionally, patients with other medical complications or that cannot tolerate anesthesia, surgery or postoperative are not suitable for drastic surgical interventions.

The high potential morbidities of surgery treatments lead to the necessity to develop other type of treatments such as radiotherapy, oral administration of vitamin E (Tocopherol) or injection of corticosteroids between others, but these approaches have not demonstrated significant improvements.[25,19,7]

On the other hand, treatments based on immunosupressor drugs have moderate efficacy and often cause the apparence of severe side effects due to its lack of selectivity.

The administration of Collagenase Clostridium Histolyticum (CCH) has emerged as a promising alterative to fibrotic surgery treatments. CCH is a matrix metalloproteinase able to cleave collagens I and III, which are the most abundant collagen types in fibrotic tissues. Moreover, CCH does not cleavable collagen type IV with is present in nerve and

blood vessel basement membranes.[25,26] Thus, the clinical use of CCH is safe and have not demonstrated important side effects in these tissues.[27]

The use of collagenase for the treatment of Dupuytren and Peyronie was approved by Food Drug Administration (FDA) in 2010[25] and 2013,[28] respectively. Additionally, CCH has been widely used to other type of pathologies such as wound healing and burns, keloids, debridement[29] and cellulite[30] uterine fibroids[31] nipple pain[32] ,to detach of human retained placenta.[33] Collagenase is also used to treat eye diseases such as glaucoma[34] or to remove fibroproliferative tissues in certain vitrectomy cases.[35]

These treatments require several administrations of CCH in order to achieve a therapeutic effect. The current treatment of Peyronie consist in a 4 cycles of collagenase injections during 24 weeks. In each cycle is necessary two injections. The current treatment for Dupuytren consists in its administration 3 times per cord in intervals of 4 weeks.[36]

Collagenase is partially inhibited in serum medium which leads to the necessity to employ high and repetitive doses in order to achieve an operative therapeutic effect.[26] This type of repetitive treatments supposes an important alteration in the normal life of the patient. Moreover, it has been demonstrated that it presents side effects, usually after of second injection of collagenase. As example, in the case of Peyronie, corporal ruptures generally occurred after second intralesional collagenase injection of each cycle.[37]

One of the reasons why several repetitions of collagenase injections are needed is the short half-life of this enzyme, which lost its effect once administered after only a few hours.[38] Thus, the development of a nanosystem able to provide a sustained and prolonged collagenase release constitutes a real necessity which can increase the patient quality of life and its probabilities to overcome this type of diseases.

Use of Collagenase Nanocapsules to Treat Fibrotic Lesions

This chapter deals with the development of nanocapsules capable to exhibit prolonged and sustained collagenase release in order to improve the therapeutic effect of collagenase-based treatments for fibrotic diseases.

As it has been mentioned above, the enzyme-based treatments for fibrotic diseases require several cycles of collagenase administration. These repetitions often lead to appearance of several adverse effects. Then, the idea to produce a nanodevice able to provide a continuous and sustained collagenase release, at the same time that maintains their catalytic activity, results highly encouraging.

In the chapter 3.1, a polymeric nanocapsule was designed in order to release collagenase when the system reached the mild acidic tumoral environment, at the same time that kept its activity unaltered in the presence of common insults present in living tissues (proteases, temperature, among others). These capsules also released the enzyme at physiological conditions, although showing slower kinetics (around 1 day). Thus, the aim of this chapter was to redesign the polymeric mesh composition in order to increase the degradation time and to achieve a prolonged collagenase release during long periods of time. As first approach, the amount of degradable crosslinker (EG) was reduced to a half, keeping constant the protein-monomers ratio. It was expected that, a decrease in the amount of degradable crosslinker would induce an important increase in the time required for the capsule disassembly. However, the obtained results with this strategy were unsuccessful, observing that collagenase was completely released after 2 days, which was not enough to guarantee an improvement in the therapeutic efficacy. A higher reduction

in the amount of degradable crosslinker was discarded since the presence of this crosslinker is necessary to make a robust and protective capsule. Therefore, the design of nanocapsules was addressed from other point of view. Our idea was to add a second crosslinker to the monomer composition, in this time, a non-degradable crosslinker, *N*,*N´*-methylenebisacrylamide (MBA). This approach would lead to a reduction in the hydrolizable points of the polymeric mesh increasing its degradation time, without compromising its formation. MBA was chosen as non-degradable crosslinker because it has been widely employed in many radical polymerization processes and its use has provided stable nanocapsules at physiological conditions.[39] The combination of these crosslinkers yielded collagenase nanocapsules that exhibited a sustained release during more than 7 days, which is a convenient time for the treatment of fibrotic lesions. The efficacy of these collagenase nanocapsules was evaluated in a fibrotic mouse model in comparison with the administration of free enzymes, which is the current treatment for these diseases, showing a significantly improved efficacy.

References

(1) Batzios, S. P.; Zafeiriou, D. I.; Papakonstantinou, E. Extracellular Matrix Components: An Intricate Network of Possible Biomarkers for Lysosomal Storage Disorders? *FEBS Lett.* **2013**, *587* (8), 1258–1267.

(2) Cox, T. R.; Erler, J. T. Remodeling and Homeostasis of the Extracellular Matrix: Implications for Fibrotic Diseases and Cancer. *Dis. Model. Mech.* **2011**, *4* (2), 165–178.

(3) Bataller, R.; Brenner, D. Liver Fibrosis. *J. Clin. Invest.* **2005**, *115* (2), 209–218.

(4) Wynn, T. A. Integrating Mechanisms of Pulmonary Fibrosis. *J. Exp. Med.* **2011**, *208* (7), 1339–1350.

(5) Wynn, T. A.; Ramalingam, T. R. Mechanisms of Fibrosis: Therapeutic Translation for Fibrotic Disease. *Nat. Med.* **2012**, *18* (7), 1028–1040.

(6) Barnes, J.; Mayes, M. D. Epidemiology of Systemic Sclerosis. *Curr. Opin. Rheumatol.* **2012**, *24* (2), 165–170.

(7) Bilgutay, A. N.; Pastuszak, A. W. Peyronie's Disease: A Review of Etiology, Diagnosis, and Management. *Curr. Sex. Heal. Reports* **2015**, *7* (2), 117–131.

(8) Desai, S. S.; Hentz, V. R.; Orthopedic, N.; Beach, N.; Hand, R. A. C.; Limb, U. The Treatment of Dupuytren Disease. *YJHSU* **2011**, *36* (5), 936–942.

(9) Robles, D. T.; Berg, D. Abnormal Wound Healing: Keloids. *Clin. Dermatol.* **2007**, *25* (1), 26–32.

(10) Kang, N.; Sivakumar, B.; Sanders, R.; Nduka, C.; Gault, D. Intra-Lesional Injections of Collagenase Are Ineffective in the Treatment of Keloid and

Hypertrophic Scars. *J. Plast. Reconstr. Aesthetic Surg.* **2006**, *59* (7), 693–699.

(11) Sehgal, V. N.; Srivastava, G.; Aggarwal, A. K.; Behl, P. N.; Choudhary, M.; Bajaj, P. Localized Scleroderma/morphea. *Int. J. Dermatol.* **2002**, *41* (8), 467–475.

(12) Walker, U. A.; Tyndall, A.; Czirják, L.; Denton, C. P.; Farge-Bancel, D.; Kowal-Bielecka, O.; Müller-Ladner, U.; Matucci-Cerinic, M.; EUSTAR co-authors, and the E. Geographical Variation of Disease Manifestations in Systemic Sclerosis: A Report from the EULAR Scleroderma Trials and Research (EUSTAR) Group Database. *Ann. Rheum. Dis.* **2009**, *68* (6), 856–862.

(13) Cooper, G. S.; Stroehla, B. C. The Epidemiology of Autoimmune Diseases. *Autoimmun. Rev.* **2003**, *2* (3), 119–125.

(14) Raghu, G.; Weycker, D.; Edelsberg, J.; Bradford, W. Z.; Oster, G. Incidence and Prevalence of Idiopathic Pulmonary Fibrosis. *Am. J. Respir. Crit. Care Med.* **2006**, *174* (7), 810–816.

(15) Balsano, C.; Alisi, A.; Nobili, V. Liver Fibrosis and Therapeutic Strategies: The Goal for Improving Metabolism.

(16) Ross, D. C. Epidemiology of Dupuytren's Disease. *Hand Clin.* **1999**, *15* (1), 53–62, vi.

(17) Anthony, S. G.; Lozano-Calderon, S. A.; Simmons, B. P.; Jupiter, J. B. Gender Ratio of Dupuytren's Disease in the Modern U.S. Population. *Hand (N. Y).* **2008**, *3* (2), 87–90.

(18) Schwarzer, U.; Sommer, F.; Klotz, T.; Braun, M.; Reifenrath, B.; Engelmann, U. The Prevalence of Peyronie's Disease: Results of a Large Survey. *BJU Int.* **2001**, *88* (7), 727–730.

(19) Gokce, A.; Wang, J. C.; Powers, M. K.; Hellstrom, W. J. Current and Emerging Treatment Options for Peyronie's Disease. *Res. reports Urol.* **2013**, *5*, 17–27.

(20) Alkatout, I. Surgical Treatment of Fibroids. *Curr. Obstet. Gynecol. Rep.* **2014**, 207–215.

(21) Smeraglia, F.; Del Buono, A.; Maffulli, N. Collagenase Clostridium Histolyticum in Dupuytren's Contracture: A Systematic Review. *Br. Med. Bull.* **2016**, *118* (1), 157–166.

(22) Bulstrode, N. W.; Jemec, B.; Smith, P. J. The Complications of Dupuytren's Contracture Surgery. *J. Hand Surg. Am.* **2005**, *30* (5), 1021–1025.

(23) Gelbard, M.; Goldstein, I.; Hellstrom, W. J. G.; McMahon, C. G.; Smith, T.; Tursi, J.; Jones, N.; Kaufman, G. J.; Carson, C. C. Clinical Efficacy, Safety and Tolerability of Collagenase Clostridium Histolyticum for the Treatment of Peyronie Disease in 2 Large Double-Blind, Randomized, Placebo Controlled Phase 3 Studies. *J. Urol.* **2013**, *190* (1), 199–207.

(24) Masonna, D.; Isaacson, G.; Rosenfeld, R. M.; Panitch, H. Effect of Sinus Surgery on Pulmonary Function in Patients With Cystic Fibrosis. *Laryngoscope* **1997**, *107*, 328–331.

(25) Bayat, A.; Thomas, A. The Emerging Role of Clostridium Histolyticum Collagenase in the Treatment of Dupuytren Disease. *Ther. Clin. Risk Manag.* **2010**, *Volume 6*, 557–572.

(26) Badalamente, M. A.; Hurst, L. C. Efficacy and Safety of Injectable Mixed Collagenase Subtypes in the Treatment of Dupuytren's Contracture. *J. Hand Surg. Am.* **2007**, *32* (6), 767–774.

(27) Levine, L. A.; Schmid, T. M.; Hart, S. G. E.; Tittelbach, T.; Mclane, M. P.; Tursi, J. P. COLLAGENASE CLOSTRIDIUM HISTOLYTICUM DEGRADES TYPE I AND III COLLAGEN WHILE SPARING TYPE IV COLLAGEN IN VITRO IN PEYRONIE'S PLAQUE EXPLANTS: PD22-03. *J. Urol.* **2014**, *191* (4), e672–e673.

(28) Levine, L. A.; Larsen, S. M. Surgical Correction of Persistent Peyronie's Disease Following Collagenase Clostridium Histolyticum Treatment. *J. Sex. Med.* **2015**, *12* (1), 259–264.

(29) Ramundo, J.; Gray, M. Collagenase for Enzymatic Debridement. *J. Wound, Ostomy Cont. Nurs.* **2009**, *36* (Supplement), S4–S11.

(30) Alipour, H.; Raz, A.; Zakeri, S.; Dinparast Djadid, N. Therapeutic Applications of Collagenase (Metalloproteases): A Review. *Asian Pac. J. Trop. Biomed.* **2016**, *6* (11), 975–981.

(31) Brunengraber, L. N.; Jayes, F. L.; Leppert, P. C. Injectable Clostridium Histolyticum Collagenase as a Potential Treatment for Uterine Fibroids. *Reprod. Sci.* **2014**, *21* (12), 1452–1459.

(32) Morland-Schultz, K.; Hill, P. D. Prevention of and Therapies for Nipple Pain: A Systematic Review. *J. Obstet. Gynecol. Neonatal Nurs.* **2005**, *34* (4), 428–437.

(33) Fecteau, K. A.; Haffner, J. C.; Eiler, H. The Potential of Collagenase as a New Therapy for Separation of Human Retained Placenta: Hydrolytic Potency on Human, Equine and Bovine Placentae. *Placenta* **1998**, *19* (5–6), 379–383.

(34) Honkanen, R. "Use of Collagenase to Treat Glaucoma."

(35) Moorhead, C.; Kirkpatrick, D. S.; Kretzer, F. Collagenase With Proposed Adjunct

to Vitrectomy.

(36) No Title Xiaflex Prescribing Information. **2010**, 1–42.

(37) Yan, S.; Yap, T.; Minhas, S. Collagenase Clostridium Histolyticum Intralesional Injections for the Treatment of Peyronie ' S Disease : A Safety Profile. **2017**, *6* (3), 123–126.

(38) Kuhn, S. J.; Finch, S. K.; Hallahan, D. E.; Giorgio, T. D. Proteolytic Surface Functionalization Enhances in Vitro Magnetic Nanoparticle Mobility through Extracellular Matrix. *Nano Lett.* **2006**, *6* (2), 306–312.

(39) Simmchen, J.; Baeza, A.; Ruiz-Molina, D.; Vallet-Regí, M. Improving Catalase-Based Propelled Motor Endurance by Enzyme Encapsulation. *Nanoscale* **2014**, *6* (15), 8907–8913.

III.III.I. Collagenase Nanocapsules: A Approach for Fibrosis Treatment

Villegas, M. R.; Baeza, A.; Usategui, A.; Ortiz-romero, P. L.; Pablos, J. L.; Vallet-regí, M. Collagenase Nanocapsules : An Approach to Fibrosis Treatment. *Acta Biomater.* **2018**, doi:10.1016/j.actbio.2018.05.007.

Acta Biomaterialia xxx (2018) xxx–xxx

Contents lists available at ScienceDirect

Acta Biomaterialia

journal homepage: www.elsevier.com/locate/actabiomat

Full length article

Collagenase nanocapsules: An approach to fibrosis treatment

M. Rocío Villegas [a,b], Alejandro Baeza [a,b,*], Alicia Usategui [c], Pablo L Ortiz-Romero [d], José L. Pablos [c], María Vallet-Regí [a,b,*]

[a] Departamento de Química en Ciencias Farmaceúticas, Facultad de Farmacia, Universidad Complutense de Madrid, 28040 Madrid, Spain
[b] Networking Research Center on Bioengineering, Biomaterials and Nanomedicine (CIBER-BBN), Spain
[c] Servicio de Reumatología, Instituto de Investigación Hospital 12 de Octubre (I+12 Medical School), Universidad Complutense de Madrid, Spain
[d] Servicio de Dermatología, Instituto de Investigación Hospital 12 de Octubre (I+12 Medical School), Universidad Complutense de Madrid, Spain

ARTICLE INFO

Article history:
Received 5 February 2018
Received in revised form 19 April 2018
Accepted 3 May 2018
Available online xxxx

Keywords:
Fibrosis
Collagenase
Polymeric nanocapsules
Enzymatic injection

ABSTRACT

Fibrosis is a common lesion in different pathologic diseases and defined by the excessive accumulation of collagen. Different approaches have been used to treat different conditions characterized by fibrosis. The FDA and EMA approved the use of collagenase to treat palmar fibromatosis (Dupuytren's contracture). The EMA approved additionally its use in severe Peyronie's disease, but it has been used off label in other conditions [1,2]. The approved treatment includes up to three (in palmar fibromatosis) or up to eight (in penile fibromatosis) injections followed by finger extension or penile modeling procedures, typically causing severe pain. Frequent single injections are adequate to treat palmar fibromatosis [3]. The need to repeatedly inject doses of this enzyme can be due to the labile nature of collagenase, which exhibits a complete activity loss after a short period of time. This study presents a novel strategy to manage this enzyme based on the synthesis of polymeric nanocapsules that contain collagenase encapsulated within their matrix. These nanocapsules have been engineered for achieving a gradual release of the encapsulated enzyme for a longer time, which can be up to ten days. The efficacy of these nanocapsules has been tested in a murine model of local dermal fibrosis, and the results demonstrate a reduction in fibrosis greater than that with the injection of free enzyme; this type of treatment showed a significant improvement compared to conventional therapy of free collagenase.

Statement of Significance

The use of proteins as therapeutic molecules has recently attracted great interest. Collagenase injection is the current treatment for fibrotic diseases. Unfortunately, proteins have a low stability and presume several repetition cycles to obtain an effective treatment. This article describes a novel treatment for these types of diseases using collagenase nanocapsules designed to exhibit a sustainable release of the encapsulated enzyme, which maintains the enzymatic activity for a long period of time. The therapeutic effect of nanocapsules was tested in a murine mouse model of local dermal fibrosis, and the results showed an important improved effect compared to the effect of the administration of free enzyme. These results indicate a high potential for this novel system to improve the current treatment for fibrotic diseases.

1. Introduction

Collagen is the most abundant protein in the body of mammals (approximately 30% of all proteins) and is a major structural component in the extracellular matrix (ECM) [4]. There are different diseases associated with excess collagen. The overproduction of collagen is due to fibroblast hyperproliferation or ECM remodeling imbalance, among other reasons [5]. The accumulation of this excess collagen within a tissue can lead to fibrosis, which compromises the tissue function, thereby resulting in physiological disorders and organ malfunction [6,7]. Fibrosis occurs in multiple conditions. For example, in superficial fibromatosis such as Dupuytren's contracture, which consists in formation of a fibrotic cord in the hand, thus resulting in hand dysfunction. In Peyronie's disease, penile involvement includes penile deviation, which makes sexual relationships difficult or even impossible. Keloids

* Corresponding authors at: Departamento de Química en Ciencias Farmaceúticas, Facultad de Farmacia, Universidad Complutense de Madrid, 28040 Madrid, Spain.
E-mail addresses: abaezaga@ucm.es (A. Baeza), vallet@ucm.es (M. Vallet-Regí).

https://doi.org/10.1016/j.actbio.2018.05.007
1742-7061/

or hypertrophic scars are consequences of abnormal scarring. Some autoimmune diseases such as scleroderma characteristically present fibrotic/sclerous plaques on localized areas (morphea), generalized on the skin or even systemic (e.g., pulmonary involvement with lung fibrosis, resulting in high mortality rate).

Fibromatosis has been traditionally treated by surgery to remove the collagen deposition [6,8]. Unfortunately, surgical procedures often carry important complications, thereby producing serious adverse effects in many cases. In addition, the invasive nature of this type of intervention avoids the general application of surgical treatments, especially in fragile patients owing to a long postoperative recovery period [9]. The high prevalence of associated morbidity in surgical treatments has led to the development of other types of treatments such as radiotherapy, oral administration of vitamin E (tocopherol), or injection of corticosteroids, among others. However, these nonsurgical treatments have not demonstrated significant improvement in many cases [4,10,11].

The administration of injections of collagenase *Clostridium histolyticum* (CCH) has emerged as a promising nonsurgical alternative for the treatment of fibrotic diseases because it is minimally invasive and cost-effective as well as presents lower complications and adverse side effects [7,9,12]. CCH is a matrix metalloproteinase mixture of two synergistic microbial collagenases, AUX-I and AUX-II, which act in combination and cleave the peptide bond of the collagen fibers between repeated sequences of Glycine–Proline–X (X being hydroxyproline or proline in the most effective cases) [4]. Collagenase is capable of lysing type 1 and type 3 collagens, which are the most abundant collagen types in fibrotic diseases. This enzyme shows a high specificity for collagen fibrils, whereas it does not produce any remarkable alteration in elastic fibers, vascular smooth muscle, and axonal myelin sheaths [10]. Thus, this enzyme has been tested in the treatment of a wide number of pathologies that course with an abnormal high regulation of formation and/or accumulation of collagen such as intervertebral disc herniation, [13] vitrectomy, [14] burns, [15] wound healing process, keloid, [1,16] and even in the treatment of solid tumors [17]. In the last application, the intratumoral injection of collagenase previous to the treatment with chemotherapeutic agents, both conventional drugs or nanoparticulated agents, allows a more homogeneous distribution of these therapeutic compounds along the tumoral tissue as a consequence of an improved diffusion of the molecules within a less dense ECM [18].

Owing to its probed effectiveness in some of these pathologies, CCH has been approved as an enzymatic treatment by the Food and Drug Administration in the USA in 2 February 2010 and by the European Agency for the Evaluation of Medicinal Products (EMEA) in January 2011, and it has been marketed under the name Xiaflex (Endo Pharmaceuticals, Inc) for the treatment of Dupuytren's contracture, a palmar fibromatosis [4]; in December 2013, it has been approved for the treatment of Peyronie's disease, a fibrosis that affects the tunica albuginea of the penis [2,19]. Label recommendations for the treatment of Dupuytren's contracture include up to three injections followed by finger extension 24–48 h after injection, which is usually a painful procedure. However, majority of the cases need only one injection on the fibrotic lesion [3]. Peyronie's disease requires up to eight collagenase injections followed by penile remodeling [20]. The need to apply repeated administration could be due to the low physico-chemical stability of collagenase, which suffers rapid proteolysis when it is exposed to the proteases present in tissues and also to relatively rapid denaturalization by oxidation or hydrolysis, among others. Thus, at physiological pH, collagenase in solution practically lost all its activity after 24 h, which indicates the labile nature of this macromolecule. Owing to the short half-life of collagenase, enzymatic activity is rapidly lost and efficacy is limited. Repeated injections followed by finger extension or penile remodeling are time consuming and very painful for patients as well as increase the risk of adverse events. For example, corporal ruptures of the penis have been reported to occur relatively frequent five days after the second injection of each cycle [21].

In view of these data, it is reasonable to think that injecting collagenase with long half-life could increase its efficacy, reduce the number of injections, spare working time of health professionals, and decrease the apparition of adverse events. Several alternatives have been evaluated to prolong the circulation time of these proteins, such as their transport immobilized on the surface of nanocarriers [22] or their encapsulation within polymeric shells [17]. However, these types of alternatives do not show a sustained release of the enzyme for a long time. This study presents a novel polymeric nanocapsule that contains collagenase encapsulated inside a matrix and is capable of releasing the enzyme with a controlled kinetics, thereby achieving a prolonged and sustained effect over time. Moreover, these nanocapsules protect the encapsulated collagenase against external aggressions, thus maintaining its catalytic activity for a long time. The efficacy of these nanocapsules has been tested using a mouse model of localized dermal fibrosis (scleroderma) induced by repeated dermal injection of bleomycin; these nanocapsules demonstrated a significant reduction in the fibrotic lesion compared to the conventional administration of free collagenase. These results could pave the way for the clinical use of these nanocapsules to treat localized fibrotic diseases. As an additional advantage, the highly versatile nature of the presented methodology can be easily applied for the encapsulation of different proteins, thus providing interesting alternatives of protein-based diseases.

2. Experimental section

2.1. Materials

Collagenase Type I (Life Technologies); Acrylamide (AA) (Fluka); 2-Aminoethyl methacrylate hydrochloride (Am) (Sigma-Aldrich); Ethylene glycol dimethacrylate (EG) (Sigma-Aldrich); N,N'-Methylenebis(acrylamide) (MBA) (Sigma-Aldrich); Ammonium persulfate (AP) (Sigma-Aldrich); N,N,N',N'-Tetramethylethylenediamine (TMDA) (Sigma-Aldrich); Amicon® Ultra-2 mL Centrifugal Filters Ultracel® 10 K (Millipore); EnChek® Gelatinase/Collagenase Assay Kit (Life Technologies); 10X phosphate-buffered saline (PBS), buffer pH = 7.4 (Ambion).

2.2. Instrumentation section

The hydrodynamic size of protein capsules was measured by means of a Zetasizer Nano ZS (Malvern Instruments) equipped with a 633-nm "red" laser. Analysis using transmission electron microscopy (TEM) was carried out with a JEOL TEM 3000 instrument operated at 300 kV, equipped with a charge-coupled device (CCD) camera. Sample preparation was performed by dispersing these protein capsules in distilled water and subsequent deposition onto carbon-coated copper grids. A solution of 1% phosphotungstic acid (PTA), pH 7.0, was employed as the staining agent to visualize the protein capsules. Fluorescence was measured using Synergy 4; power supply for Biotek Laboratory Instrument was 100–240 VAC, 50/60 Hz, and 250 W.

2.3. Synthesis of collagenase nanocapsules

First, the reaction buffer $NaHCO_3$ (0.01 M, pH 8.5) was deoxygenated by freeze-vacuum-N_2 cycles. Then, collagenase (3.1×10^{-5} mmol) was dissolved in 1 mL of deoxygenated buffer. AA, Am, EG, and MBA, the proportions of which are required in each case,

Please cite this article in press as: M.R. Villegas et al., Collagenase nanocapsules: An approach to fibrosis treatment, Acta Biomater. (2018), https://doi.org/10.1016/j.actbio.2018.05.007

were dissolved in 1 mL of deoxygenated buffer in a vial, and the solution containing monomers was added to the protein solution. This mixture was stirred at 300 rpm for 10 min under nitrogen atmosphere at room temperature. Further, 0.013 mmol of AP and 0.02 mmol of TMDA dissolved in 1 mL of the deoxygenated buffer were added to the mixture. This solution was stirred at 300 rpm for 90 min at room temperature under inert atmosphere. Furthermore, the encapsulated enzyme was purified by centrifugal separation with 10-KDa cut-off filters (AMICON Ultra-2 mL 10 KDa) and washed three times with $NaHCO_3$ buffer (0.01 M, pH 8.5). The capsules of collagenase were preserved at 4 °C.

2.4. Enzymatic activity assay

The samples were incubated using the same collagenase concentration (measured by absorbance at 280 nm) in PBS with physiological pH = 7.4 and at 37 °C under stirring. The encapsulation process does not affect the absorbance because the monomers and polymers created do not have absorbance at this wavelength. At certain times, an aliquot of this solution was removed and its enzymatic activity was evaluated using the commercial kit (EnzChekGelatinase/Collagenase Assay Kit). The kit provides a fluorimetric method, and its protocol consists in mixing the collagenase sample with commercial buffer, which contains calcium and fluorescent-labeled gelatin. The fluorescence signal is quenched until gelatin digestion. Then, the enzymatic activity of the collagenase sample was determined by fluorescence release.

2.5. Hydrolysis assay

Collagenase nanocapsules were incubated in PBS with physiological pH = 7.4 and at 37 °C under stirring. At certain times, an aliquot was removed from the solution and stained with 1% phosphotungstic acid; these nanocapsules were then observed by TEM.

2.6. Mouse model of scleroderma

Female 6-week-old C3H/HeNHse mice were purchased from Envigo (Valencia, Spain). Dermal fibrosis was induced by subcutaneous injections of 100 μg of bleomycin (1 $mg{\cdot}ml^{-1}$; Mylan Pharmaceuticals, Barcelona, Spain) or 0.9% saline control into the shaved skin at the back every day for 4 weeks as previously described [23]. To analyze the effect of collagenase administration in this model after fibrosis induction, 10 mice in each group were administered with 300 μg of collagenase (Life Technologies), either as a single subcutaneous injection of free collagenase or encapsulated nanocapsules, in the bleomycin-injected skin area and maintained for 10 days. To ensure that the amount of injected free and encapsulated collagenase is the same, the total protein content was determined by absorbance at 280 nm. The study was approved by Animal Care and Use Committee of Hospital 12 de Octubre with protocol reference number PROEX 407/15, and this was carried out in accordance with the institutional guidelines.

The treated skin was harvested, and paraffin was embedded for histological evaluation of the collagen dermal area by using the Masson's trichrome staining kit (Sigma-Aldrich, St. Louis, USA). Masson-stained full-thickness skin sections were photographed and digitalized using an AxioCam ERc 5S camera and ZEN lite 2012 software (Zeiss, Jena, Germany). The blue-stained collagen fractional area was quantified using ImageJ software (http://rsb.info.nih.gov/ij). The collagen area of each individual mouse was calculated as the mean area of several (three to five) sections of the central part of the excised skin piece.

2.7. Statistical analyses

Data were analyzed using Prism software (GraphPad Software, San Diego, CA, USA). Results are expressed as mean ± standard deviation (SD), and quantitative data were analyzed by the Mann–Whitney *U* test. P values < 0.05 were considered significant.

3. Results and discussion

In this work, a protective polymer capsule is designed around the collagenase whose function is to release the encapsulated enzyme in a controlled sustained manner for a long period of time. In this way, the polymeric nanocapsule acts as collagenase reservoir that presents a slow and tunable kinetic release capable of providing a prolonged effect, thus avoiding the need for important and repeat doses.

Protein nanocapsules have been widely studied to obtain a controllable delivery system that also protects the cargo at the same time. In this sense, the development of a protein carrier based in its encapsulation within the polymeric mesh has received increasing attention in the last few years [24]. This type of system has demonstrated its capacity to trigger the protein release in response to different stimuli, for example, enzymes present in the target site, according to local environment or specific cellular events [25]. In addition, these protein nanocapsules have been designed to achieve a sequential release of multiple proteins, so that the release of the first protein triggers the release of the rest in a tandem sequence [26]. As an added value, polymeric nanocapsules act as a protective coating for the encapsulated enzyme against external stresses that can compromise its structure and, therefore, its catalytic activity [17].

Thus, with the objective to obtain a collagenase nanocapsule that provides a sustained release, a polymeric mesh was designed to coat the protein. Our nanocapsules have been synthesized by free radical polymerization of two types of monomers, i.e., a neutral monomer, AA, and Am. AA is widely used as a structural monomer, whereas Am presents the capacity to adsorb around negative proteins by electrostatic affinity owing to its positive charge in the aqueous phase. Thus, the enrichment of monomers around the proteins is favored by electrostatic bonding. Additionally, once the nanocapsule is formed, the presence of these amino groups on the surface avoids capsule aggregation by repulsion charge, thereby enhancing the colloidal stability of the system. Finally, EG was chosen as a degradable crosslinker to form the polymeric shell [27].

First, the monomers and protein are allowed to come in contact in an aqueous solution free of oxygen. The protein and monomer mixture was kept under stirring for 10 min to allow the adsorption of the monomers on the negative surface of protein through intermolecular interactions. Then the protein surface could be enriched with monomers in such a way that the polymerization occurs around the protein. Oxygen, which can terminate the radical polymerization process, is removed from the buffer reaction previous to the addition of radical initiators. This first stage is followed by a polymerization step. The polymerization is initiated by the addition of AP in the presence of TMDA, and this forms free radicals of oxygen in the aqueous solution at room temperature through a basic catalysis mechanism. AP is the initiator of free radical generation and this is catalyzed by TMDA, which promotes the decomposition of AP into free radicals, thereby decreasing the activation energy of polymerization [28]. In this way, the addition of TMDA allows the free radical polymerization process to occur at room temperature. The free radical process leads to polymerization of acryloyl groups of monomers and crosslinker, thus yielding a polymeric mesh that coats the protein (Scheme 1). The mixture

Please cite this article in press as: M.R. Villegas et al., Collagenase nanocapsules: An approach to fibrosis treatment, Acta Biomater. (2018), https://doi.org/10.1016/j.actbio.2018.05.007

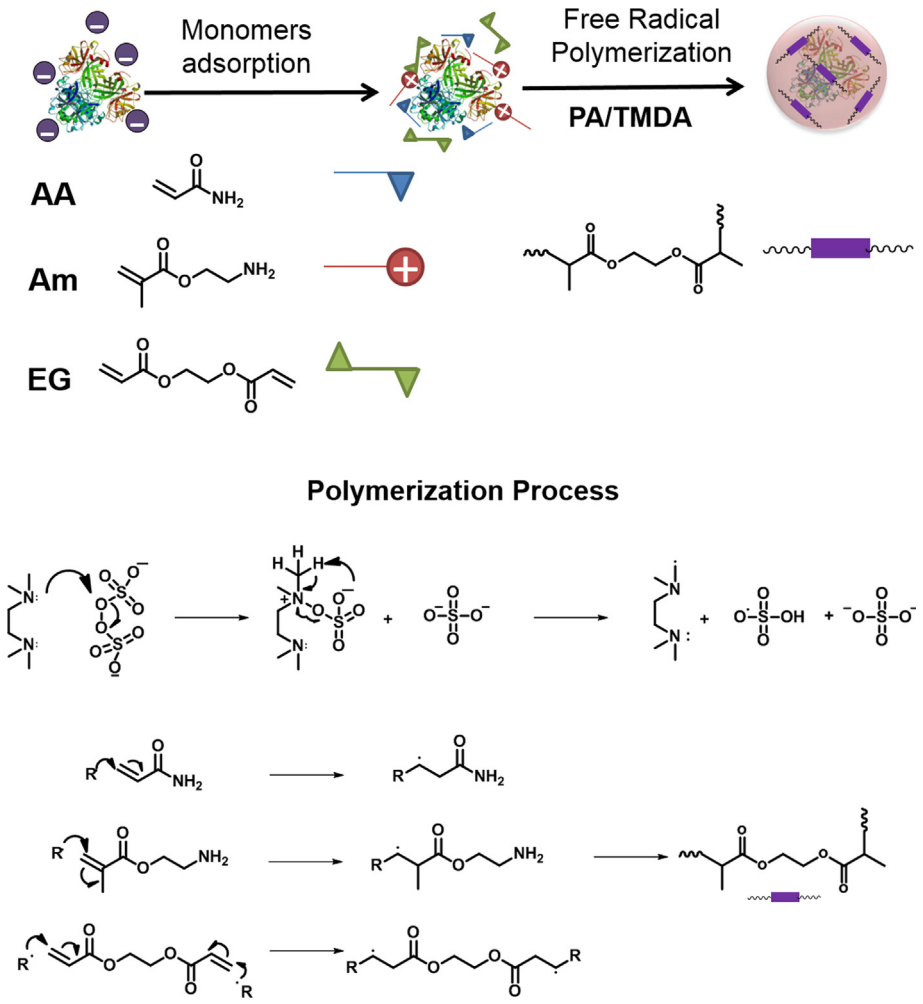

Scheme 1. Synthesis of collagenase nanocapsule by free radical polymerization. AA, Am, EG, PA/TMDA are referred to acrylamide, 2-Aminoethylmethacrylate hydrochloride, ethylene glycol dimethacrylate, ammonium persulfate/ N, N, N′, N′, tetramethylenediamine respectively.

was kept at room temperature for 90 min, and collagenase nanocapsules were isolated by centrifugal separation with 10-KDa cut-off filters to remove the excess monomer. Collagenase acts on large substrates (collagen fibers), and therefore, it is necessary to consider its release to facilitate its catalytic activity. To provide a controlled release mechanism, EG was chosen as a pH-responsive crosslinker. Thus, the obtained nanocapsules would be degradable by hydrolysis. The collagenase release mechanism is shown in Scheme 2. In the aqueous medium, water molecules act as nucleophiles that attack the carbonyl group of the crosslinker, which results in the hydrolysis of the ester bonds. This crosslinker degradation is catalyzed in acidic environments because of an interaction of protons with the oxygen atom of the carbonyl group, thus increasing the polarity of the covalent bond and favoring the nucleophilic attack by water.

3.1. Optimization of collagenase synthesis for sustained release

3.1.1. Previous work

Our research group recently reported the encapsulation of collagenase inside degradable polymeric nanocapsules using a protein-to-monomer ratio of 1:2025 and AA-to-Am-to-EG monomer ratio of 7:6:2 [17]. These conditions favored the nanocapsules to release the encapsulated enzyme in <12 h under physiological conditions. This presumes a high improvement in the stability of the enzyme, and this relatively rapid release is suitable for certain clinical applications such as in the case of fibrotic disease, a longer release time is required as mentioned.

3.1.2. Strategies to achieve a sustained and prolonged release

Based on the previous work, different strategies have been performed to achieve a prolonged and sustained release. In this way, it is hoped that the collagenase nanocapsules can act a depot of the proteolytic enzyme and improve the temporal window by enhancing its therapeutic effect. Two strategies were developed to achieve this goal; first, the degradable crosslinker ratio was reduced to reduce the hydrolyzable attack points in the polymeric mesh, and second, obtaining collagenase nanocapsules with sustained release was addressed from another point of view, that is, the addition of an additional nondegradable crosslinker; in this way, the polymeric mesh would become more robust and the collagenase release rate would decrease.

3.1.2.1. Decrease in the proportion of degradable crosslinker. To decrease the hydrolysis rate of the collagenase nanocapsules, the amount of degradable crosslinker was reduced to half with regard to a previous work [17]. The protein-to-monomer ratio was maintained constant because a significant alteration in this ratio can lead to poor protein encapsulation. The capacity to provide a sustained enzymatic activity of these nanocapsules for a long time was evaluated by incubating the nanocapsules in an aqueous solution at physiological pH and temperature under orbitalic soft stir-

Please cite this article in press as: M.R. Villegas et al., Collagenase nanocapsules: An approach to fibrosis treatment, Acta Biomater. (2018), https://doi.org/10.1016/j.actbio.2018.05.007

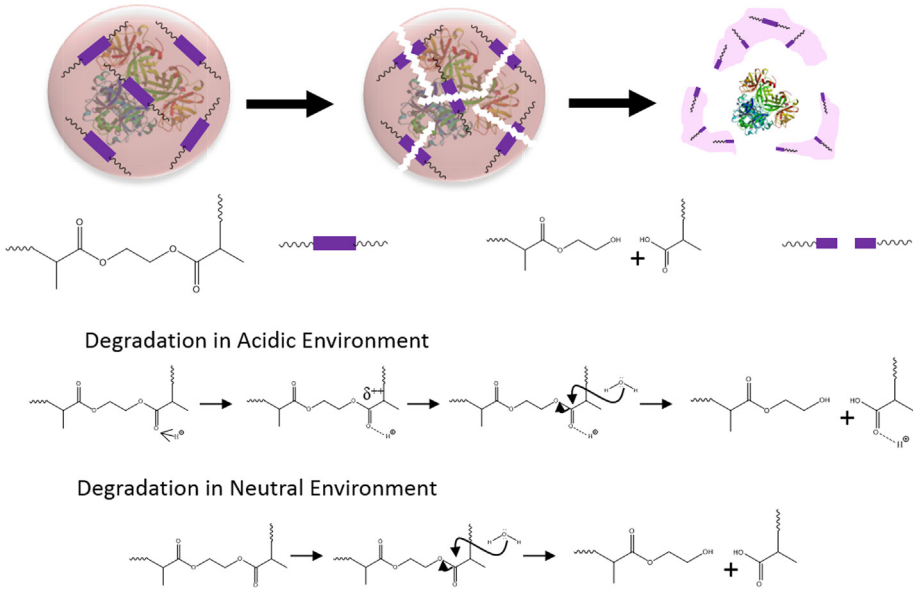

Scheme 2. Degradation mechanism of the collagense nanocapsules.

ring. Then, at certain times, an aliquot of this solution was removed, and the enzymatic activity was measured using a commercial kit protocol. The nanocapsules retain more than 50% of the catalytic capacity initially for 2 days, which is a significant improvement compared to the free enzyme, which lost more than 80% of its capacity after 1 day. The encapsulation efficacy is also dependent on the capacity of the monomers to get adsorbed on the protein surface, and this capacity is related to the intermolec-

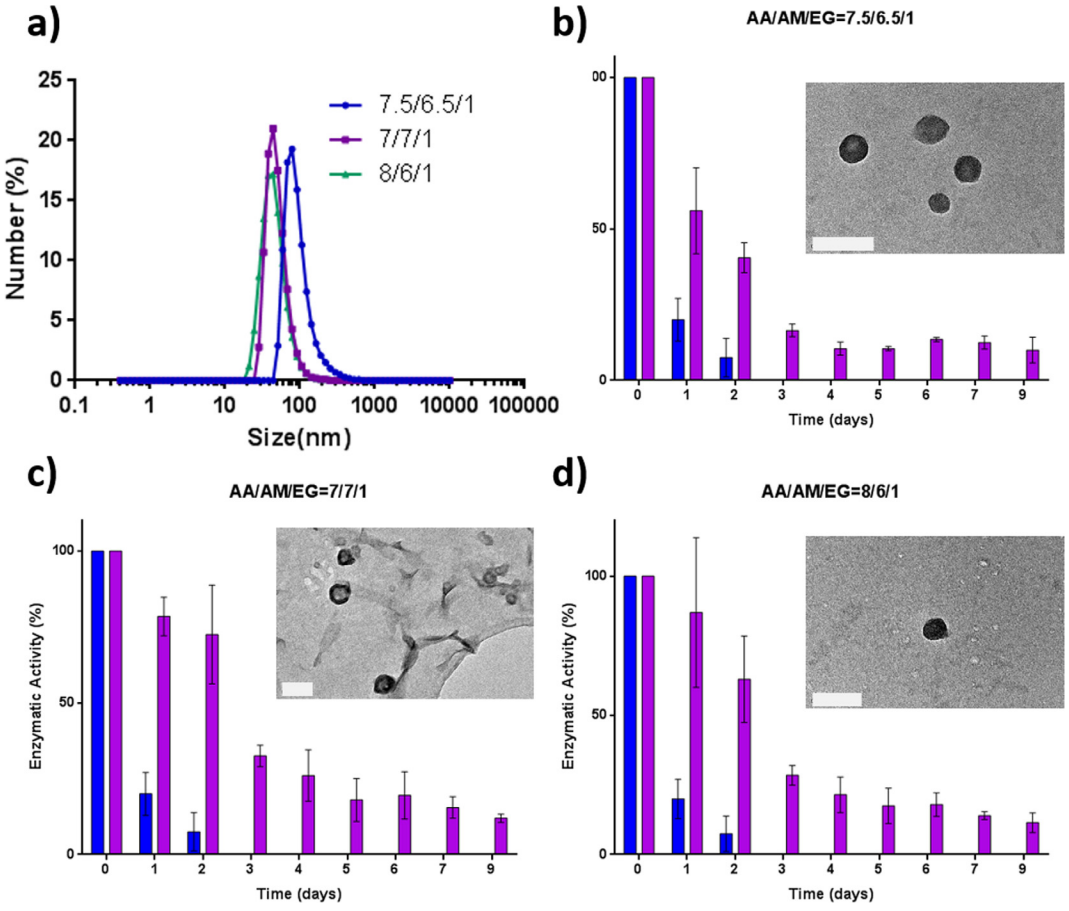

Fig. 1. (a) Study of Dynamic Light Scaterring (DLS) of collagenase nanocapsules with different AA/Am ratios. Study of stability of collagenase nanocapusules with different ratios AA/Am (purple). Micrograph by transmission Electron Microscopy (b) AA/Am/EG = 7.5/6.5/1, (c) AA/Am/EG = 7/7/1 and (d) AA/Am/EG = 8/6/1 (white scale bar correspond to 100 nm). Study of free collagenase was represented in blue.

Please cite this article in press as: M.R. Villegas et al., Collagenase nanocapsules: An approach to fibrosis treatment, Acta Biomater. (2018), https://doi.org/10.1016/j.actbio.2018.05.007

ular interactions between both systems. To evaluate whether the AA-to-Am monomer ratio could play a role in this process, two different monomer ratios were also evaluated, i.e., AA-to-Am-to-EG ratios of 7:7:1 and 8:6:1, respectively. Neither of these cases provided a significant improvement in the catalytic activity during time, thus losing more than 50% of their capacity after 2 days, similar to the results of the previous work (Fig. 1).

The presence of a crosslinker is strictly needed to obtain a dense and protective mesh around the protein. Although a high decrease in the crosslinker ratio could be an option to extend the release time, it could result in an inappropriate capsule formation. For this reason, the possibility to reduce its amount even more was discarded and the other strategy was addressed.

3.1.2.2. Introduction of a nondegradable crosslinker. Instead of reducing the crosslinker ratio, a novel strategy that consists in the introduction of an additional nondegradable crosslinker, MBA, was employed. The introduction of this crosslinker should not alter the nanocapsule formation because the crosslinker-to-monomer ratio was maintained and could increase the degradation time of the nanocapsule, thus allowing a sustained release for a longer time. Although the addition of a nondegradable crosslinker can result in incomplete collagenase release, this strategy decreases the hydrolyzable points in the polymeric mesh without altering the crosslinker ratio. Thus, with the protein-to-monomer ratio as 1:2025 and AA-to-Am-to-crosslinker ratio as 7:6:2, which provided a good encapsulation capacity, different ratios of both degradable and nondegradable crosslinkers were studied. The addition of the new crosslinker did not alter the size and morphology of the nanocapsules in all cases. The results indicate that employing a 1:1 ratio of degradable and nondegradable crosslinkers enables the system to maintain the enzymatic activity for a really long time. This sample shows a sustained release of around 50% of its initial activity lasting for 10 days and maintaining 15% of its activity for 12 days (Fig. 2). Surprisingly, for unknown reasons, when different ratios of the two crosslinkers are employed, the capacity to maintain the catalytic activity reduces to values even lower than those of the previous systems that carry only the degradable crosslinker, i.e., when the nondegradable crosslinker is employed both in a higher ratio and in a lower ratio. In any case, the system that employs a 1:1 ratio exhibits excellent properties. The hydrolysis of this sample was observed in the micrographs obtained by TEM (Fig. 3). It can be observed that the collagenase nanocapsules progressively lost their integrity as is expected because they are degradable nanocapsules. Owing to their sustained release, a sample with an EG-to-MBA ratio as 1:1 was chosen for in vivo evaluation in comparison with the current treatment.

Therefore, two strategies were evaluated to achieve a sustained and prolonged release of collagenase. Both approaches demonstrated an increase in the collagenase release time with regard to our previous work. In the first study, a decrease in degradable crosslinker ratio in the synthesis of collagenase nanocapsules was evaluated. This strategy was based on the idea that decreasing the degradable crosslinker ratio led to a reduction in the hydrolyzable attack points. Although the stability of the collagenase nanocapsules was higher than that of the free enzyme, the results were not satisfactory because the collagenase release was not sustained, losing almost completely the enzymatic activity after 3 days. The idea to continue reducing the crosslinker ratio was dis-

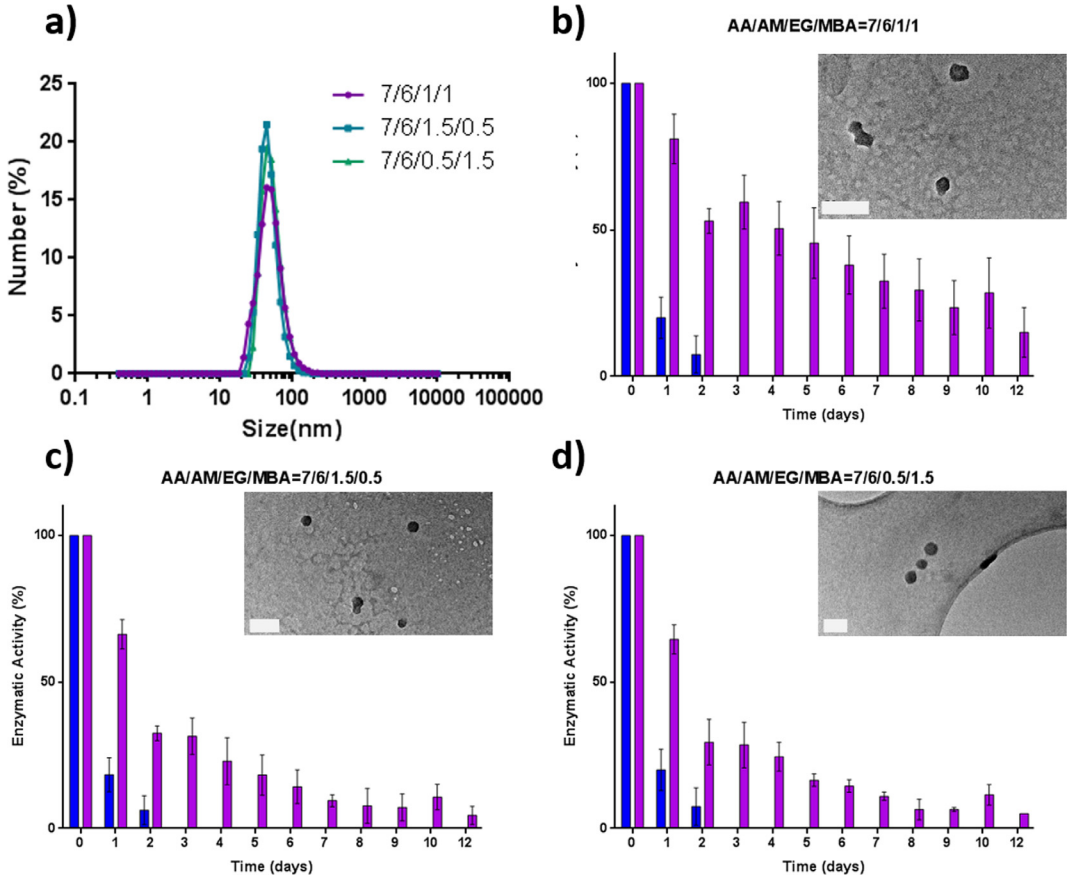

Fig. 2. (a) Study of Dynamic Light Scaterring (DLS) of collagenase nanocapsules with different EG/MBA ratios. Study of stability of collagenase nanocpasules with different ratios EG/MBA (purple). Micrograph by transmission Electron Microscopy (b) AA/Am/EG/MBA = 7/6/1/1, (c) AA/Am/EG/MBA = 7/6/1.5/0.5 and (d) AA/Am/EG/MBA = 7/6/0.5/1.5 (white scale bars correspond to 100 nm). Study of free collagenase was represented in blue.

Please cite this article in press as: M.R. Villegas et al., Collagenase nanocapsules: An approach to fibrosis treatment, Acta Biomater. (2018), https://doi.org/10.1016/j.actbio.2018.05.007

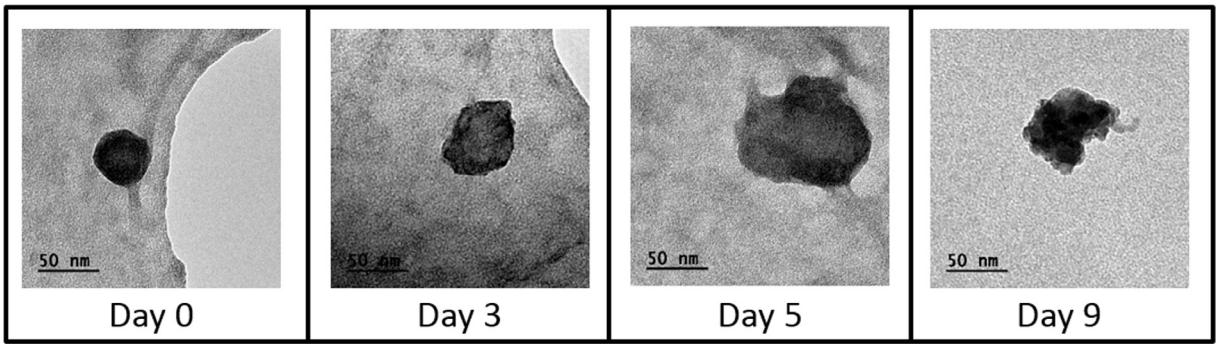

Fig. 3. TEM micrographs of collagenase nanocapsules incubated at physiological conditions at different times.

carded because the presence of crosslinker is necessary to obtain a robust polymeric coating. Thus, the problem was addressed from the other point of view, by the introduction of an additional nondegradable crosslinker. Despite the fact that the addition of a nondegradable crosslinker presented a potential liability regarding the possibility to lead to an incomplete collagenase release, it decreased the hydrolysis-sensitive points in the nanocapsules without altering the crosslinker ratio. This approach yielded the nanocapsules with excellent properties for the treatment of fibrotic lesions because they exhibited a sustained and prolonged collagenase release for up to 10 days. Once the synthetic conditions for the formation of collagenase nanocapsules with desired properties are optimized, the suitability to treat fibrotic lesions with this nanodevice was evaluated in a mice model as proof of concept in comparison with the conventional free enzyme administration.

3.2. In vivo cytotoxicity test of collagenase nanocapsules

To check the biocompatibility of the collagenases nanocapsules in vivo, a fixed amount of nanocapsules or free collagenase was injected subcutaneously into the shaved skin at the back of healthy mice. After 10 days, the animals were sacrificed and histological analysis of collagenase-injected skin showed a normal structure of all skin layers and absence of inflammatory cell infiltration (Fig. 4). Dermal collagen area and structure did not show changes compared to the normal (uninjected) skin (Normal skin *vs.* free collagenase, $p = 0.7$; normal skin *vs.* nanocapsules, $p = 0.99$; and free collagenase *vs.* nanocapsules, $p = 0.628$).

3.3. In vivo evaluation of the efficacy of collagenase nanocapsules

To study the efficacy of collagenase nanocapsules on bleomycin-induced skin fibrosis, we evaluated changes in the fibrotic area induced by bleomycin for 4 weeks, after injection of either free collagenase or collagenase nanocapsules. We found a marked increase in the dermal collagen area of the dermis after bleomycin injection compared to control (saline-injected) group (Fig. 5).

The fibrotic area, evaluated as the fractional collagen-stained area (blue-stained area) of the dermis, was significantly reduced

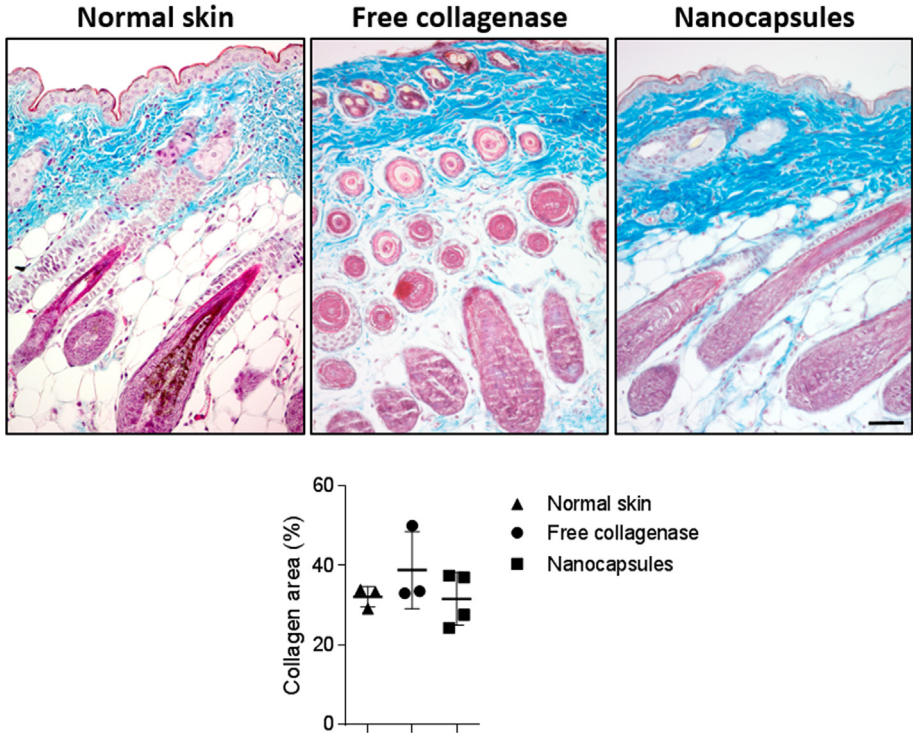

Fig 4. Study of biocompatibility of nanocapsules. Mice received a single subcutaneous injection with a fixed amount of nanocapsules or free collagenase. Skin was stained by Masson's trichrome (collagen fibers are stained in blue). Data are representative of one experiment with three-four mice per group. Bar 50 μm.

Please cite this article in press as: M.R. Villegas et al., Collagenase nanocapsules: An approach to fibrosis treatment, Acta Biomater. (2018), https://doi.org/10.1016/j.actbio.2018.05.007

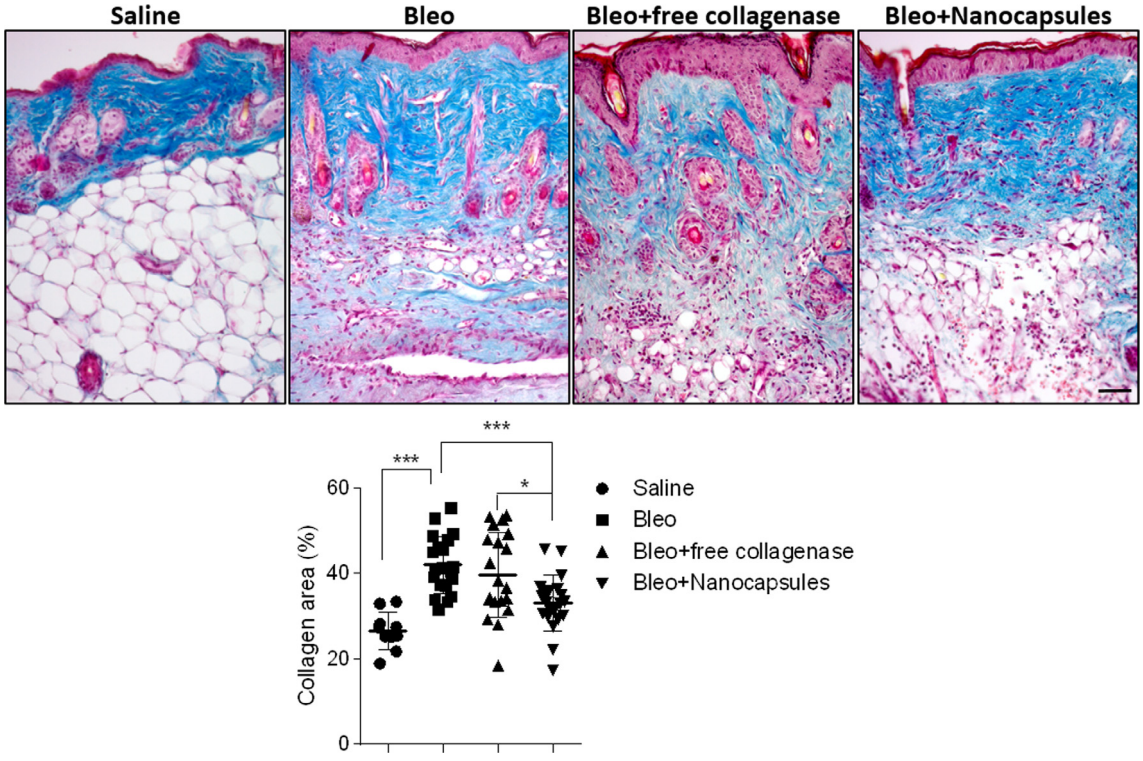

Fig 5. Effect of collagenase nanocapsules in bleomycin induced skin fibrosis. C3H mice received daily subcutaneous injections of bleomycin and were treated with free collagenase or nanocapsules. Control mice were daily injected with saline. Fibrosis was quantified as the collagen area (blue-stained area as stained by Masson trichrome), expressed as a fraction of the total skin area. Data are representative of two independent experiments with 10 mice per group. Bar 50 μm.

bleomycin-injected, collagenase nanocapsule–treated mice compared to those in bleomycin-injected mice ($p < 0.0001$) and bleomycin-injected, free collagenase–treated mice ($p = 0.026$). There were no significant differences between bleomycin-injected, free collagenase–treated and bleomycin-injected groups ($p = 0.457$; Fig. 5). Therefore, administration of a single dose of encapsulated collagenase nanocapsules significantly decreased the collagen area, whereas the same dose of collagenase without encapsulation (free collagenase) was insufficient to reduce the collagen area.

The fact that a single injection of collagenase nanocapsules results in a significant decrease in the collagen area with regard to free enzyme could presume an important advance the treatment for fibrotic lesions. In the future, preclinical studies should be organized to conduct clinical trials in humans.

4. Conclusion

This study presents a novel collagenase nanocapsule capable of a sustained release and delivery of the proteolytic enzyme. These collagenase nanocapsules were designed to protect the activity of the collagenase enzyme and release with controllable kinetics for long and modular periods of time. These polymeric nanocapsules presume a delivery system of collagenase capable of releasing the enzyme under physiological conditions for 10 days.

This type of release is highly beneficial in enzymatic treatments because a prolonged effect of the required enzyme over time is obtained, thus allowing the use of lower doses and/or reducing the number of injections necessary to achieve acceptable results. The high stability conferred by this coating composition coupled with the sustained release profile results in a promising advance in the stabilization of the enzyme and makes it possible to improve the current clinical treatment. It has been observed in fibrotic models that the encapsulated collagenase showed a high efficacy of degradation compared to that of free enzyme, which is the actual treatment. The application of this strategy would pave way for the proteins to get delivered in a more sustained release, which would provide an important advance in their clinical applications.

5. Acknowledgments

The authors acknowledge the financial support provided by European Research Council (Advanced Grant VERDI; ERC-2015-AdG Proposal No. 694160) and the project MAT2015-64831-R. In addition, this work was supported by grants from the Instituto de Salud Carlos III (Ministerio de Economía y Competitividad, Spain) PI 12/439 and RIER (Red de Investigación en Inflamación y Enfermedades Reumáticas) to AU and JLP as well as cofinanced by FEDER (European Union).

References

[1] Y.-S.C. Bae-Harboe, J.E. Harboe-Schmidt, E. Graber, B.A. Gilchrest, Collagenase Followed by Compression for the Treatment of Earlobe Keloids, Dermatologic Surg. 40 (2014) 519–524, https://doi.org/10.1111/dsu.12465.
[2] J. Akerman, J.R. Kovac, Treatment of Peyronie's disease via preoperative intralesional collagenase clostridium histolyticum followed by placement of an inflatable penile prosthesis: the new standard of care?, Transl Androl. Urol. 6 (2017) S822–S823, https://doi.org/10.21037/tau.2017.11.04.
[3] D.J. Warwick, D. Graham, P. Worsley, New insights into the immediate outcome of collagenase injections for Dupuytren's contracture, J. Hand Surg. European 41 (2016) 583–588. doi:10.1177/1753193415600670.
[4] A. Bayat, A. Thomas, The emerging role of Clostridium histolyticum collagenase in the treatment of Dupuytren disease, Ther. Clin. Risk Manag. 6 (2010) 557–572, https://doi.org/10.2147/TCRM.S8591.
[5] T.R. Cox, J.T. Erler, Remodeling and homeostasis of the extracellular matrix: implications for fibrotic diseases and cancer, Dis. Model. Mech. 4 (2011) 165–178, https://doi.org/10.1242/dmm.004077.
[6] N.W. Bulstrode, B. Jemec, P.J. Smith, The complications of Dupuytren's contracture surgery, J. Hand Surg. Am. 30 (2005) 1021–1025, https://doi.org/10.1016/j.jhsa.2005.05.008.

Please cite this article in press as: M.R. Villegas et al., Collagenase nanocapsules: An approach to fibrosis treatment, Acta Biomater. (2018), https://doi.org/10.1016/j.actbio.2018.05.007

[7] M. Gelbard, I. Goldstein, W.J.G. Hellstrom, C.G. McMahon, T. Smith, J. Tursi, N. Jones, G.J. Kaufman, C.C. Carson, Clinical efficacy, safety and tolerability of collagenase clostridium histolyticum for the treatment of peyronie disease in 2 large double-blind, randomized, placebo controlled phase 3 studies, J. Urol. 190 (2013) 199–207, https://doi.org/10.1016/j.juro.2013.01.087.

[8] S.S. Desai, V.R. Hentz, N. Orthopedic, N. Beach, R.A.C. Hand, U. Limb, The Treatment of Dupuytren Disease, YJHSU. 36 (2011) 936–942, https://doi.org/10.1016/j.jhsa.2011.03.002.

[9] F. Smeraglia, A. Del Buono, N. Maffulli, Collagenase clostridium histolyticum in Dupuytren's contracture: a systematic review (2016) 1–10, https://doi.org/10.1093/bmb/ldw020.

[10] A. Gokce, J.C. Wang, M.K. Powers, W.J. Hellstrom, Current and emerging treatment options for Peyronie's disease, Res. Reports Urol. 5 (2013) 17–27, https://doi.org/10.2147/RRU.S24609.

[11] A.N. Bilgutay, A.W. Pastuszak, Peyronie's Disease: A Review of Etiology, Diagnosis, and Management, Curr. Sex. Heal. Rep. 7 (2015) 117–131, https://doi.org/10.1007/s11930-015-0045-y.

[12] R. Arora, P. Kaiser, T.-J. Kastenberger, G. Schmiedle, S. Erhart, M. Gabl, Injectable collagenase Clostridium histolyticum as a nonsurgical treatment for Dupuytren?s disease, Oper. Orthop?die Und Traumatol. 28 (2016) 30–37. doi:10.1007/s00064-015-0434-4.

[13] D. Zhang, Y. Zhang, Z. Wang, X. Zhang, M. Sheng, Target radiofrequency combined with collagenase chemonucleolysis in the treatment of lumbar intervertebral disc herniation, Int. J. Clin. Exp. Med. 8 (2015) 526–532.

[14] C. Moorhead, D.S. Kirkpatrick, F. Kretzer, Collagenase With Proposed Adjunct to Vitrectomy (n.d.). doi:10.1001/archopht.1980.01020040681018.

[15] N.E. Sharp, P. Aguayo, D.J. Marx, R.N.E.E. Polak, D.E. Rash, P.C. Shawn, D.S. Peter, D.J. Ostlie, D. Juang, Nursing Preference of Topical Silver Sulfadiazine Versus Collagenase Ointment for Treatment of Partial Thickness Burns, Children (2014) 253–257, https://doi.org/10.1097/JTN.0000000000000073.

[16] N. Kang, B. Sivakumar, R. Sanders, C. Nduka, D. Gault, Intra-lesional injections of collagenase are ineffective in the treatment of keloid and hypertrophic scars, J. Plast. Reconstr. Aesthetic Surg. 59 (2006) 693–699, https://doi.org/10.1016/j.bjps.2005.11.022.

[17] M.R. Villegas, A. Baeza, M. Vallet, Regí, Hybrid Collagenase Nanocapsules for Enhanced Nanocarrier Penetration in Tumoral Tissues, ACS Appl. Mater. Interfaces 7 (2015) 24075–24081, https://doi.org/10.1021/acsami.5b07116.

[18] T.D. McKee, P. Grandi, W. Mok, G. Alexandrakis, N. Insin, J.P. Zimmer, M.G. Bawendi, Y. Boucher, X.O. Breakefield, R.K. Jain, Degradation of fibrillar collagen in a human melanoma xenograft improves the efficacy of an oncolytic herpes simplex virus vector, Cancer Res. 66 (2006) 2509–2513, https://doi.org/10.1158/0008-5472.CAN-05-2242.

[19] L.A. Levine, S.M. Larsen, Surgical Correction of Persistent Peyronie's Disease Following Collagenase Clostridium Histolyticum Treatment, J. Sex. Med. 12 (2015) 259–264, https://doi.org/10.1111/jsm.12721.

[20] Xiaflex (Collagenase Clostridium Histolyticum), Prescribing Information Malvern, PA: Auxilim Pharmaceuticals, 2010, pp. 1–42.

[21] S. Yan, T. Yap, S. Minhas, Collagenase clostridium histolyticum intralesional injections for the treatment of Peyronie's disease: a safety profile 6 (2017) 123–126, https://doi.org/10.21037/tau.2016.12.08.

[22] S.J. Kuhn, S.K. Finch, D.E. Hallahan, T.D. Giorgio, Proteolytic surface functionalization enhances in vitro magnetic nanoparticle mobility through extracellular matrix, Nano Lett. 6 (2006) 306–312, https://doi.org/10.1021/nl052241g.

[23] B. Santiago, I. Gutierrez-Cañas, J. Dotor, G. Palao, J.J. Lasarte, J. Ruiz, J. Prieto, F. Borrás-Cuesta, J.L. Pablos, Topical application of a peptide inhibitor of transforming growth factor-β1 ameliorates bleomycin-induced skin fibrosis, J. Invest. Dermatol. 125 (2005) 450–455, https://doi.org/10.1111/j.0022-202X.2005.23859.x.

[24] Y. Lu, W. Sun, Z. Gu, Stimuli-responsive nanomaterials for therapeutic protein delivery, J. Control. Release 194 (2014) 1–19, https://doi.org/10.1016/j.jconrel.2014.08.015.

[25] J. Wen, S.M. Anderson, J. Du, M. Yan, J. Wang, M. Shen, Y. Lu, T. Segura, Controlled protein delivery based on enzyme-responsive nanocapsules, Adv. Mater. 23 (2011) 4549–4553, https://doi.org/10.1002/adma.201101771.

[26] S. Zhu, L. Nih, S.T. Carmichael, Y. Lu, T. Segura, Enzyme-Responsive Delivery of Multiple Proteins with Spatiotemporal Control, Adv. Mater. 27 (2015) 3620–3625, https://doi.org/10.1002/adma.201500417.

[27] C. Liu, J. Wen, Y. Meng, K. Zhang, J. Zhu, Y. Ren, X. Qian, X. Yuan, Y. Lu, C. Kang, Efficient delivery of therapeutic miRNA nanocapsules for tumor suppression, Adv. Mater. 27 (2015) 292–297, https://doi.org/10.1002/adma.201403387.

[28] B. Strachota, L. Matějka, A. Zhigunov, R. Konefał, J.í Spěváček, J.í Dybal, R. Puffr, Poly(N-isopropylacrylamide)–clay based hydrogels controlled by the initiating conditions: evolution of structure and gel formation (n.d.). doi:10.1039/c5sm01996f.

Please cite this article in press as: M.R. Villegas et al., Collagenase nanocapsules: An approach to fibrosis treatment, Acta Biomater. (2018), https://doi.org/10.1016/j.actbio.2018.05.007

Chaper IV

Conclusions

IV. Conclusions

This doctoral thesis has been focused on the development of nanosystems suitable for the treatment of two types of diseases: Cancer and Fibrosis.

- Polymeric nanocapsules able to house collagenase maintaining unaltered the catalytic capacity of the enzyme was produced.

- These capsules were designed with pH-responsive behavior in order to release the enzyme in tumoral tissues.

- Nanocarriers decorated with these nanocapsules were able to achieve homogeneous distribution in 3D model tumoral tissues, as consequence of the higher penetration provided by the released collagenase.

- Nanocarriers decorated with three different gadgets (Multifunctional Protocells): a lipid bilayer which avoids the drug premature release, collagenase nanocapsules for enhancing their penetration and targeting moieties for tumoral cell recognition, have been produced.

- Multifunctional Protocells achieved an astonishing performance being able to pass through a thick collagen barrier and to destroy the tumoral cells located in deep zones of the model tissue.

- Nanocarriers asymmetrically decorated with two targeting moieties in order to provide a sequential capacity to recognize tumoral cells and then, the inner mitochondria were produced.

- These Janus dual-targeted nanoparticles strengthened the effect of the transported drugs due to their controlled release close to mitochondria.

- Finally, the treatment of fibrotic lesions with collagenase nanocapsules was addressed. This fact required the design of a nanocapsules able to provide a prolonged and sustained collagenase release during more than 1 week.

- The simple injection of these collagenase nanocapsules showed a produced therapeutic effect while the conventional treatment barely produced any effect. These nanocapsules has been protected by a European Patent and their clinical application is under study nowadays.

IV. Conclusiones

Esta tesis doctoral se ha centrado en el desarrollo de sistemas para el tratamiento de dos tipos de enfermedades: Cáncer y Fibrosis.

- Se sintetizaron nanocápsulas poliméricas capaces de albergar colagenasa manteniendo inalterada la capacidad catalítica de la enzima.

- Estas cápsulas fueron diseñadas con un comportamiento sensible al pH para liberar la enzima en los tejidos tumorales.

- Los nanotransportadores decorados con estas nanocápsulas lograron una distribución homogénea en los tejidos tumorales modelo 3D, como consecuencia de la mayor penetración proporcionada por la colagenasa liberada.

- Se han producido nanotransportadores decorados con tres herramientas diferentes (Protocelulas Multifuncionales): una bicapa lipídica que evita la liberación prematura del fármaco, nanocápsulas de colagenasa para mejorar su penetración y agentes de vectorización para el reconocimiento de células tumorales.

- Las Protocélulas Multifuncionales lograron un rendimiento asombroso al poder atravesar una gruesa barrera de colágeno y destruir las células tumorales ubicadas en zonas profundas del tejido modelo.

-Fueron sintetizados nanotransportadores decorados asimétricamente con dos elementos de vectorización con el fin de proporcionar una capacidad secuencial para reconocer las células tumorales y, a continuación, las mitocondrias.

- Estas nanopartículas Janus de doble objetivo reforzaron el efecto de las drogas transportadas debido a su liberación controlada cerca de las mitocondrias.

-Finalmente, se abordó el tratamiento de las lesiones fibróticas con nanocápsulas de colagenasa. Este hecho requirió el diseño de una nanocápsula capaz de proporcionar una liberación prolongada y sostenida de colagenasa durante más de una semana.

-La simple inyección de estas nanocápsulas de colagenasa mostró un efecto terapéutico mientras que el tratamiento convencional apenas produjo ningún efecto. Estas nanocápsulas han sido protegidas por una Patente Europea y su aplicación clínica está en estudio en la actualidad.

Anexo I. Nanotechnological Strategies for Protein Delivery

Villegas, M. R.; Baeza, A.;Vallet-Regí. M. Nanotechnological Strategies for Protein Delivery. **2018**, 1–21, doi:10.3390/molecules23051008.

molecules

MDPI

Review

Nanotechnological Strategies for Protein Delivery

María Rocío Villegas [1,2], Alejandro Baeza [1,2,*] and María Vallet-Regí [1,2,*]

1 Departamento de Química en Ciencias Farmacéuticas, Facultad de Farmacia, UCM, 28040 Madrid, Spain; mr.villegas@ucm.es

2 Centro de Investigación Biomédica en Red de Bioingeniería, Biomateriales y Nanomedicina (CIBER-BBN), 28029 Madrid, Spain

* Correspondence: abaezaga@ucm.es (A.B.); vallet@ucm.es (M.V.-R.); Tel.: +34-91-394-1843 (M.V.-R.); Fax: +34-91-394-1786 (M.V.-R.)

Received: 9 April 2018; Accepted: 22 April 2018; Published: 25 April 2018

Abstract: The use of therapeutic proteins plays a fundamental role in the treatment of numerous diseases. The low physico-chemical stability of proteins in physiological conditions put their function at risk in the human body until they reach their target. Moreover, several proteins are unable to cross the cell membrane. All these facts strongly hinder their therapeutic effect. Nanomedicine has emerged as a powerful tool which can provide solutions to solve these limitations and improve the efficacy of treatments based on protein administration. This review discusses the advantages and limitations of different types of strategies employed for protein delivery, such as PEGylation, transport within liposomes or inorganic nanoparticles or their in situ encapsulation.

Keywords: protein delivery system; PEGylation; liposomes; nanoparticles; polymeric nanocapsules; protein therapy

1. Introduction

The transition of a prebiotic to a biotic Earth was determined by the appearance of self-sustained, self-replicating and self-assembled life. Living organisms are complex bioreactor systems, where numerous biochemical reactions occur simultaneously, allowing their structures to self-assemble, replicate itself and be transmitted. One example of structures that self-assemble with precision and fidelity are proteins. All human cells have the same genetic information, which is contained in its deoxyribonucleic acid (DNA) and encodes proteins.

Proteins are aminoacid strands which are folded in characteristic three-dimensional structures determined by the aminoacid sequence and the microenvironment. These chains form a secondary structure characterized by alpha helices and beta sheets stabilized by intramolecular hydrogen bonds. The secondary structure is then folded into a tertiary structure governed by hydrophobic and hydrophilic interactions so that hydrophobic zones of the protein are in its core and the hydrophilic parts remain exposed to the aqueous medium on the protein surface. The highly specific structures produced by protein folding and their precise amino acid sequences determine protein function. The huge variety of highly-specific chemical processes needed for life is obtained by the great versatility of potential protein structures and conformations.

Proteins performed essential functions, such as catalyzing biochemical reactions [1], signal transduction [2], defensive functions [3], regulatory functions [4,5], controlling cell fates [6], providing cellular and tissue structure [7,8], as molecule carriers [9–11], and maintaining a fine balance between cell survival and programmed death. For this reason, proteins are called the "engines of life".

Eukaryotic cells contain thousands of proteins that participate in the normal cellular function [12]. Their correct function is vital to maintain homeostasis in the body. Protein dysfunction is related to

numerous diseases such as diabetes, which consists of unbalanced regulation of insulin, hemophilia which is a defect in coagulation protein levels, neurological disorders (Alzheimer's [13] and Parkinson's disease [14]), cystic fibrosis which is related to a defective folding and export of proteins from the endoplasmic reticulum [15] and cancer (about 50% of all human tumors have a mutant p53 protein) among others [16].

Consequently, the use of proteins as therapeutic molecules appears as an attractive and promising therapy for cancer [17], autoimmunity/inflammation [18], infection [19] and genetic disorders and it has shown high efficacy for the treatment of numerous diseases [20,21]. Protein therapeutics include antibodies, cytokines, transcription factors and enzymes, among others.

Although proteins hold great potential as therapeutics, their clinical application is limited due to their labile nature. The functional conformation of a protein is only slightly more stable (5–20 kcal/mol in free energy) than unfolded conformations (the term unfolded is used to refer to any non-functional conformation resulting from an unfolding process). This means that the process of protein folding until functional conformation presents a negative increment of Gibbs free energy [22–25]. From an entropic point of view, this is an unfavorable process. Entropy acts at a local level, that involves translational, rotational and vibrational degrees of liberty at the molecule scale, and non-local level, which include volume and chain configurational freedom [23]. The resulting negative increment of Gibbs free energy is due to a negative increment of enthalpy in the folding process. The forces that stabilize the structure are hydrophobic interactions, electrostatic forces, local peptide interactions, hydrogen bonding and Van der Waals forces [23]. The balance between forces that mantain the functional three-dimensional structure of folding is fragile and can be destabilized under small changes in temperature, pH, type and salts concentration, concentration of serum proteases, solvent or external microenvironment can induce protein unfolding leading to biologically inactive conformations [22].

Moreover, proteins can suffer from proteolysis by proteases present in the bloodstream and in living tissues, which induce an irreversible change in their structure and, therefore, a loss of biological function. In addition to the low stability of proteins, protein delivery presents additional problems. Foreign proteins administered intravenously can often be recognized by opsonins and many scavenger receptors. Opsonization with lipoproteins results in their accumulation in hepatocytes and other tissues rich in lipoprotein receptors. Moreover, attachment of complement proteins leads to an immediate clearance from the bloodstream by macrophages which form the macrophage phagocytic system (MPS) [26,27]. Thus, administered proteins are often cleared out rapidly by spleen, liver or kidney, where they can be accumulated undesirably and activate immune responses.

Clinical uses of proteins are limited by their low stability [22] against temperature, solvent changes, changes in pH, serum proteases, freezing cycles and storage. In addition, proteins are usually unable to cross cell membranes [28], they can activate immune responses and be accumulated in tissues and they show fast clearance after intravenous administration [29]. All of these problems have given rise to the development of recombinant proteins, which try to palliate these limitations. Recombinant insulin was the first commercially available recombinant protein approved by the US FDA in 1982 [30–34]. In recent years, between 2011–2016 the Food and Drug Administration Center for Drug Evaluation and Review (CDER) and the Center for Biologics Evaluation and Review (CBER) have approved 62 therapeutic proteins [35].

Therapeutic proteins represent a fast-growing proportion of marketed drugs. Nevertheless, such "biodrugs" have important hurdles that hamper their application. As mentioned above, proteins exhibit unfavorable intrinsic properties. Nanomedicine has emerged as powerful tool to try to overcome these strong limitations. The scientific community have done vast efforts to design versatile, protective and functional protein delivery systems to achieve an improved therapeutic effect. Important efforts in this area had been focused in the conjugation of proteins with polymeric chains in order to increase their size and block recognition zones. Another strategy has been their transport attached onto the surface of nanocarriers or inside their structure, which has often been employed to allow proteins to enter inside cells. As another option, proteins have been entrapped in the aqueous core of lipidic

vesicles for prolonging their circulation time within the blood stream. However, in the ultimate years, nanomedicine has centered its efforts in the development of encapsulation methodology that allows wrapping of proteins into polymeric nanocapsules. This class of materials allow design of robust and flexible protein-coating and engineer it as non-degradable or degradable in function of the biomedical application. Some of the most important approaches are collected in this review and shown schematically in Figure 1.

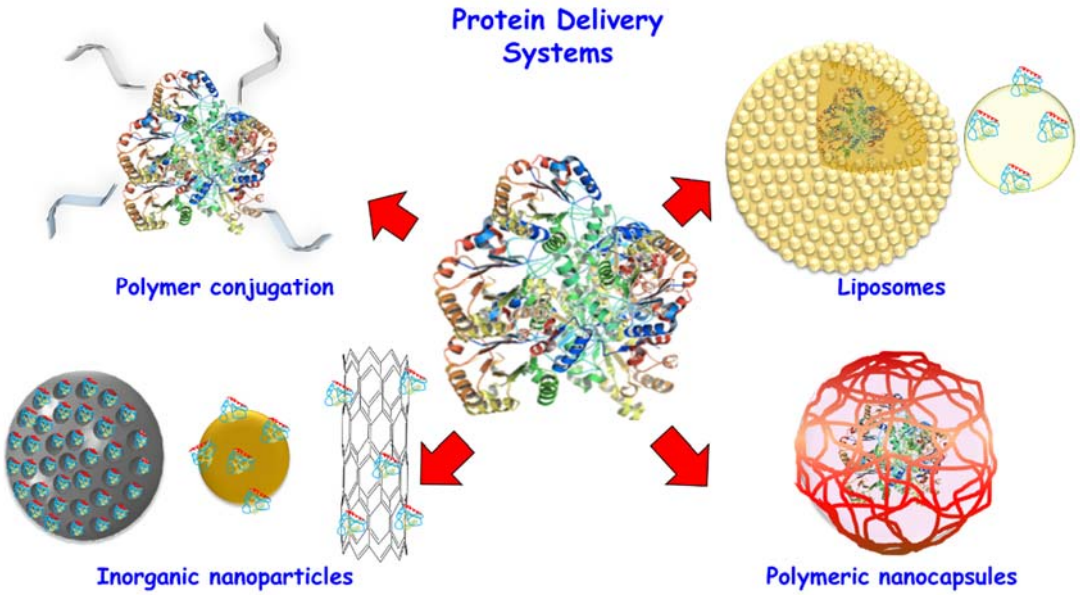

Figure 1. Scheme of different protein delivery systems.

2. PEGylation

The most common strategy to increase the circulation times of protein in the bloodstream is the covalent conjugation of polymers on the protein surface, being the most popular poly(ethylene glycol) (PEG). Protein conjugation with PEG is often achieved by its reaction with free amine groups from lysine residues on the protein surface [36]. PEG is a polymer approved by FDA as "generally recognized as safe" [37] and is known to be able to coordinate with water molecules that create a hydrophilic corona around the protein via hydrogen bonding. As a result of this hydration layer and the high flexibility of the PEG chains, PEGylation increases the hydrodynamic radius of the PEGylated protein facilitating its solubility and hindering its renal clearance [38,39]. PEGylation produces a steric impediment to opsonization, improving the plasma half-life of proteins and avoiding the clearance by MPS [40–42]. PEG acts as a hindrance to proteases and therefore, make the proteins more resistant to proteolytic degradation. In this way, PEGylation can preserve the protein structure and therefore, its function. Moreover, PEGylation can hide antigenic zones of foreign proteins which avoids the formation of specific antibodies against them decreasing their immunogenicity. The first evidence of the advantages of protein PEGylation was reported by Abuchowski et al. in 1977 [43,44]. Later, in 1990, adenosine deaminase was the first PEGylated protein approved by FDA and commercialized for the treatment of immunodeficiency diseases [45]. Since then, different conjugates have been approved [46] and marketed such as, for example, PEGylated interferon α2b y α2a for the treatment of hepatitis C [47], granulated stimulating factor for treatment of neutrophenia caused by chemotherapy [48,49], and epotein-β protein for the treatment of chronic renal failure [50], among others.

Unfortunately, it has been found that approximately 25% of patients present or develop anti-PEG antibodies previously or immediately after the first administration of PEG-protein conjugates [42,51,52]. This fact implies the rapid clearance from blood of the administered proteins and nullifies their efficacy for systemic treatments.

Another hydrophilic polymer used to prepare enzyme conjugates is poly(vinylpyrolidone) (PVP). After its use as plasma expander during Second War World [53], PVP was the first polymer reported to form polymer-drug conjugates [54]. PVP is considered a harmless compound [55] and it also improves the circulation time of enzymes [56]. Unfortunately, PVP conjugates can increase antigenicity compared to free enzymes, as is the case for uricase [57]. As an alternative to hydrophilic polymers, zwitterionic polymers have also been used for their capacity to coordinate water molecules via hydrogen bonding. Zwitterionic polymer conjugates have shown similar pharmacokinetic profiles to PEGylated systems [58]. Another option is the conjugation with dextran, which is a polysaccharide that also extends the circulation time in blood [59]. However, intravenous administration of dextran can produce life-threatening anaphylaxis [60,61].

Since polymer conjugation is a simple and popular method, it is employed for many commercial formulations. However, polymer conjugation often blocks the active sites of enzymes. Thus, the enzyme partially or completely loses its catalytic activity [62]. This fact, along with those above mentioned, constitute strong limitations of polymer-protein conjugates.

As an example, of commercial method to protein delivery are the so called chariot systems. These consist of a 2843 Da peptide able to form a non-covalent complex with the protein that allows the transport of biologically active proteins into the cells with an efficiency of 60–95% [63].

3. Liposomes

One interesting approach for protein delivery involves their transport in liposomes. Liposomes consist of concentric lipid bilayer vesicles surrounding aqueous compartments. The vesicles are formed by phospholipids and their structure is similar to that of the cellular membrane. Proteins can be carried inside the aqueous core of the liposome or can be grafted on the lipid surface.

The protein functionalized liposome techniques include loading the liposome into the core and on the surface. As examples, Szoka et al. [64] reported a technical procedure to prepare liposomes with large aqueous spaces. This method allowed them to encapsulate water-soluble materials, such as proteins, with high efficiency. This process consists in the formation of lipid vesicles when aqueous buffer was introduced into a mixture of phospholipids in organic solvents. The authors reported that, in spite of the fact the organic solvent produced protein denaturalization, an appreciable amount of activity (41%) was retained. On the other hand, loading of proteins on the liposome surface have been widely reported. Shao et al. [65] synthesized liposomes including a porphyin-phospholipid. This phospholipid, which is able to chelate cobalt, allowed the effective capture of His-tagged proteins As an additional example, Blenke et al. [66] develop liposomes able to conjugate azide-protein by "click chemistry" which allows more control at the conjugation site than commonly used coupling chemistries.

The cell-like nature of lipid systems eases the translocation of the protein carried into the cytoplasm or lysosomes inside the cells. Uptake of liposomes by cells is produced by an initial liposome adsorbtion onto the cell membrane, followed by an endocytosis step [67]. Liposomes possess excellent characteristics for protein delivery, including biocompatibility, the capacity to maintain an aqueous environment around the protein and modulable size and charge which can be obtained by selection of phospholipids [68,69]. The composition of the phospholipids that form the liposomes determines their characteristics. For example, cationic liposomes facilitate the adsorption and endocytosis processes by interaction with negatively-charged phospholipids on the cell membrane. Moreover, they disrupt the enodosome by the proton sponge effect allowing the cargo release to the cytosol [70]. As an example, cationic liposomes were used to carry β-galactosidase and caspases [71]. However cationic liposomes present low stability in the presence of serum proteins and poor stability in vivo [72]. Also, these systems produce a certain toxicity due to apoptosis induced by their cationic moieties [73]. Neutral liposomes have demonstrated a good ability to enter into the cell, but the protein cargo is often trapped within lysosomes and, therefore, the transported proteins are digested in the lysosome due to their inability to escape from endosomes.

Additionally, a potential problem of liposomes as protein carriers is their rapid clearance by the MPS [74]. This problem can be partially palliated by conjugation with PEG chains on the lipid surface. In fact, liposome PEGylation has been shown to extend their circulation half-life from 30 min to 5 h [75]. This long circulation time is due to the increase in the hydrodynamic volume of the system and the capacity of PEG to avoid the immune response by steric impediment. However, a high degree of functionalization with PEG produces a reduction in the melting temperature of the liposomes, which entails their destabilization, whereas a low functionalization decreases the achievable circulation time [76]. Moreover, a repeated administration of PEGylated liposomes results in an accelerated blood clearance [77]. In addition, the nature of liposomes limits their clinical use, since liposomes are not robust and can release the cargo protein when are in an environment with a high concentration of lipoproteins, as is the case in the bloodstream [67,78,79].

In spite of all these limitations, there are commercial kits for protein delivery based on liposomes, as is the case of lipofectamine, which is a cationic liposome able to carried DNA, siRNA and proteins into the cells in a fast, simple, and reproducible method [80].

4. Inorganic Nanoparticles

Inorganic nanoparticles have been explored as interesting nanodevices due to the fact they are robust and easily modulable. The proteins can be carried on the nanocarrier surface or inside their structures, in the case of porous nanoparticles. The applications of such materials however, require chemical and/or biological modification to satisfy the requirements for cellular delivery, such as biocompatibility and long circulation times [81].

4.1. Mesoporous Silica Nanoparticles

An example of inorganic nanoparticles is mesoporous silica nanoparticles (MSN). These nanoparticles have also been investigated as protein carriers. They are characterized by a high surface area and tunable pore size [82], that provide a high cargo-loading capacity and allow delivering a wide variety of proteins [83]. Tu and coworkers [84] have recently proposed this type of nanoparticles to deliver proteins with different molecular weights (12.4–250 kDa), size ($2.3 \times 2.6 \times 4$ to $7 \times 8 \times 10$ nm) and isoelectric points (4.5–11.35). Functionalization or not of the pores of nanoparticles with amine groups favors the electrostatic interaction with proteins bearing negatively or positively charged groups. Moreover, their surface can be easily modified with nickel moieties to chelate polyhistidine-tagged proteasomes. Cells treated with exogenous proteasomes are able to significantly degrade tau aggregates, a pathological hallmark of Alzheimer´s disease, compared to the free proteasomes [85]. These nanoparticles have improved the intracellular delivery of membrane-impermeable proteins [83]. As example, MSNs demonstrated be able to intracellularly deliver cytochrome C in human cervical cancer cells (HeLa), an induce a significant cell death [86,87].

4.2. Gold Nanoparticles

Gold nanoparticles have been studied as protein delivery systems for their unique optical properties, low toxicity, bio-inertness and easily funcionalizable surface via thiol groups [88–92]. The first intracellular protein delivery system using gold nanoparticles was reported in 2004 [93]. In that work, BSA was previously modified with CPP and was adsorbed onto gold nanoparticles. Protein adsorption on the surface of gold nanoparticles allowed its delivery into the cell cytoplasm, followed by nuclear localization mediated by CPP. Gold nanoparticles have been functionalized with positively-charged moieties which allow the adsorption of anionic proteins via electrostatic interactions. Additionally, the adsorption on the gold surface inhibits the protein activity until it is released in the cytosol as consequence of its exposure to the glutathione present in this environment [94]. As an additional example, gold nanocarriers were also studied to carry vascular endothelial growth factor (VEGF) [95]. VEGF was attached on the gold nanoparticle surface via the thiol groups of cysteine residues in VEGF. The conjugation with VEGF produced a recovery of blood perfusion to values

of normal tissue in hind-limb ischemia mice, as opposed to administration of free VEGF that did not produce significant changes compared to the control group. β-Galactosidase was also adsorbed in its activated form onto gold nanoparticles coated with short peptide in order to improve its cell internalization presumably via an endocytic pathway (Figure 2) [28].

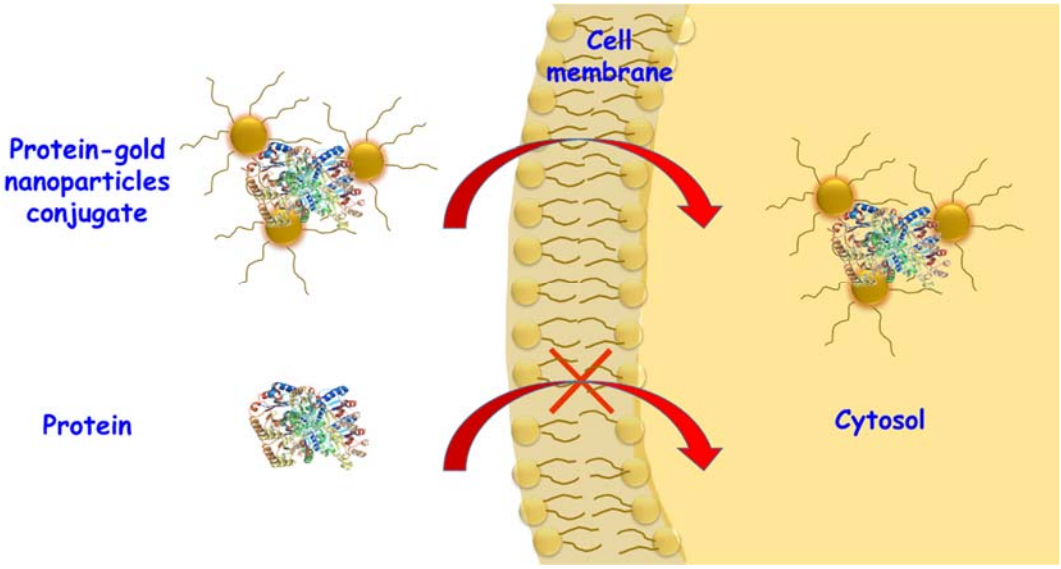

Figure 2. Scheme of protein adsorbed onto peptide coated gold nanoparticles to improve cell internalization by endocytic pathway.

4.3. Carbon Nanotubes

Carbon nanotubes are rolled sheets of graphene formed from sp^2-hybridized carbon atoms. This class of materials is used for biomedical imaging due to their unique near-infrared (NIR) photoluminescence. Moreover, carbon nanotubes have been explored to shuttle different molecular cargos inside of cells, including short peptides, nucleic acids and proteins [96–103]. Carbon nanotubes are also used as protein delivery systems and have demonstrated to be a polyvalent system able to adsorb a widely variety of proteins on its surface, such as streptavidin, BSA, protein A and cytochrome C for their intracellular delivery by adherent (HeLa and NIH-3T3) and no adherent cell lines (HL60 and Jurkat) [96]. As an example, fluorescent carbon nanotubes were biotinated and subsequently incubated with streptavidin. The carbon nanotube conjugate allowed the intracellular delivery of streptavidin, which is well known for its inability to cross the cell membrane, and induce a dose-dependent effect in HL60 cells.

5. Polymeric Nanocapsules

While traditionally protein delivery has been addressed by their conjugation with polymers or delivery in inorganic nanoparticles or liposomes, a new approach has recently emerged. This new strategy consists of the in situ formation of polymeric coatings around the protein (nanocapsules). These nanodevices have demonstrated promising characteristics compared to traditional systems since they combine the flexibility and cell-like properties of liposomes with the sturdiness of inorganic nanoparticles. As will be discussed in the following sections, the polymeric matrix serves as a protective shield and are highly adaptable to the objective pursued.

Typically, the encapsulation process comprises three steps (Figure 3). Firstly, the protein is functionalized with acroyl groups in order to introduce polymerizable groups on the protein surface facilitating the polymer coating around the macromolecule. This process is usually carried out by the addition of *N*-acryloxysuccinimide (NAS), which can react with amino groups of the lysine

residues and the terminal NH_2 of the protein. Secondly, the acroylated protein is mixed with the monomers in a deoxygenated buffer. The reason for the use of buffers without oxygen is that the presence of this molecule stops the polymerization due to the radical scavenger behavior of triplet oxygen. In this step, the monomers are adsorbed on the protein surface by electrostatic interactions forming a dynamic monomer layer around it. Finally, the third step is the in situ polymerization which is initiated by the addition of radical initiators such as ammonium persulfate (APS) and *N*,*N*,*N*′,*N*′-tetramethylenediamine (TMEDA). APS forms reactive oxygen species in aqueous solution by basic catalysis, and TMEDA acts as the base that allows the process to take place at room temperature [104]. In the case of the formation of stimuli-responsive nanocapsules capable of releasing the housed protein if certain stimuli are present, the acroylation step can be ignored in order to achieve a complete protein departure when the capsule are broken. In order to facilitate the understanding by the reader, the description of the different polymeric nanocapsules will be carried out in two separated groups: non-degradable nanocapsules, which are especially useful for enzyme encapsulation, and degradable nanocapsules suitable for the transportation of therapeutic proteins or enzymes.

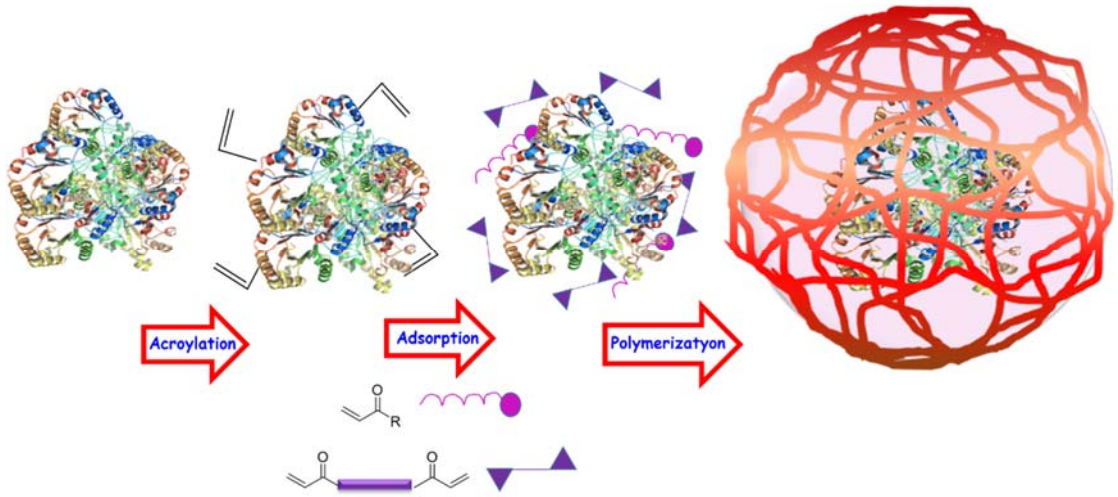

Figure 3. Scheme of the encapsulation process.

5.1. Non-Degradable Nanocapsules

This is an appropriate strategy to encapsulate enzymes for which the substrate is a small molecule and the coating is permeable to it. In this sense, the crosslinker responsible for the formation of the polymer matrix must be non-degradable. The most studied non-degradable crosslinker is *N*,*N*′-methylene bisacrylamide (MBA). Using this crosslinker, different types of non-degradable nanocapsules have been developed.

5.1.1. Acrylamide-Based Nanocapsules

Different research groups have studied the use of acrylamide as a structural monomer. This monomer is used in combination with positively-charged and neutral monomers in order to favor the encapsulation process via electrostatic interactions with the protein surface. Lu et al. [105] have developed different nanosystems based on this idea. One of them consisted of the encapsulation of organophosphorus hydrolase (OPH) inside polymeric nanocapsules. Organophosphates are highly toxic and are widely used as pesticides, insecticides and even chemical warfare agents [106]. The use organophosphorus hydrolase (OPH) has been proposed for the destruction of these compounds but, unfortunately, this enzyme has a labile nature. In this work, OPH was coated by a polymeric shell produced using acrylamide (AAm) as a structural monomer, *N*-(3-aminopropyl)methacrylamide hydrochloride (APm) as positively-charged monomer and MBA as crosslinker. As a result of the

coating process, the encapsulated enzyme exhibited a higher enzymatic activity with compared with free enzyme in a pH range of 7.5–10. This effect was especially pronounced at a neutral pH. The authors demonstrated that this peculiarity was caused by the basic environment which affect the enzyme when it is inside the capsule. The catalytic activity of OPH is higher under basic conditions and, being APm a basic monomer (pKa = 10) its presence around the enzyme provides a local basic pH which enhances its activity. Moreover, protein encapsulation within these polymeric shells conferred thermal stability, since the free enzyme lost all of its activity after 90 min at 65 °C while the encapsulated enzyme retained 60% of the initial activity under the same conditions. This improvement in thermal stability was demonstrated to be a result of the acroylation process of the enzyme prior to its encapsulation. Nanocapsules obtained after the acroylation process which employed a ratio of NAS:enzyme = 50:1 retained 100% of their enzymatic activity after thermal treatment. Conversely, when the ratio was 10:1, the enzymatic activity after the thermal treatment dropped to 10%. The increase in the thermal stability is the result of the multiple covalent bonds that link the enzyme with the polymeric mesh, which hinder any conformational changes. Also, the encapsulation process improves the enzyme stability in the presence of organic solvents. Encapsulated enzymes retained 50% of their activity in a medium with 30% DMSO in comparison with free enzyme that only showed 10% activity under the same conditions [105]. Polar organic solvents are harmful to proteins because they compete with them in forming hydrogen bonds with water. This leads to changes in their structure resulting in a loss of function. Encapsulation creates a hydrophilic microenvironment around the protein that overcome this limitation. Additionally, enzyme encapsulation eased their storage, since nanocapsules showed 80% activity after five freeze-thaw cycles while free enzymes only maintained 15% of their activity [105]. The encapsulation of OPH in acrylamide-based nanocapsules has also demonstrated to solve the loss of enzymatic activity when embedding or adsorbing enzymes in mesoporous OPH-silica scaffolds [107] and enhanced results obtained with OPH mutants [108] grafted to solid matrices like silica [109], and carbon nanotubes [110].

Encapsulated OPH also showed better results with respect to its naked homolog in in vivo experiments. These experiments consisted of the administration of OPH and OPH nanocapsules in mice that were also administered the organophosphorus compound paraoxon 5 min later. Non-treated mice died 5 min after the paraoxon injection and only two out of three mice with OPH treatment survived, although all of them presented serious toxic effects. Mice treated with encapsulated OPH survived without serious toxic symptoms, validating its therapeutic efficacy.

The encapsulation process has also been studied to coat more than one enzyme so that they can work as an enzymatic tandem [111]. The joint encapsulation of catalase (Cat) and alcohol oxidase (AOx) has demonstrated to decrease alcohol levels in blood in a much more efficient way than the co-administration of the same enzymes encapsulated separately. Moreover, this strategy was demonstrated to be more effective that the use of liposomes loaded with both enzymes. The injection of co-encapsulated AOx and Cat reduced the alcohol levels by 20% in 5 h whereas a liposomal injection did not result in a significant reduction

This class of systems have been applied in other less conventional investigation fields such as nanomotors. Nanomotors are self-propelled tiny machines able to perform useful tasks which are normally fueled by the decomposition of peroxide either by platinum or by catalase [112]. In the case of catalase, it has little resistance to oxidation, in such a way, is unable to retain its enzymatic activity during several work cycles. Acrylamide-based encapsulation of catalase has been developed in order to solve this limitation [113]. Catalase capsules demonstrated improved thermal stability of the enzyme and its stability against proteases. After 1 h of incubation at 60 °C the encapsulated enzyme kept more than 50% of its activity whereas its native form only kept 20%. On the other hand, the native enzyme lost all of its activity when it was incubated in the presence of proteases whereas its encapsulated form retained more than 90% of the activity. Additionally, the encapsulation allowed increase the turnover of the enzyme up to more than 10 cycles (Figure 4).

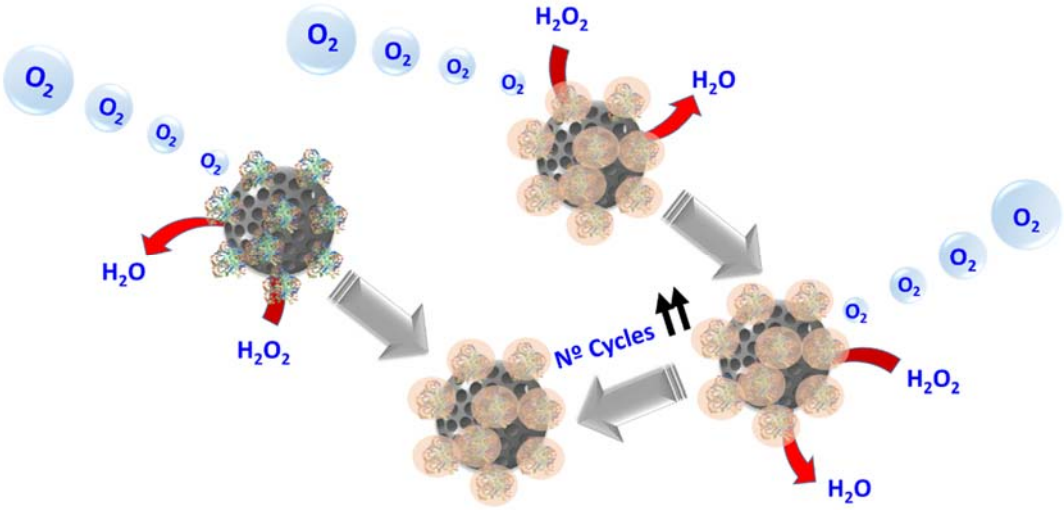

Figure 4. Scheme of nanomotors of mesoporous silica nanoparticles with catalase nanocapsules.

5.1.2. Phosphorylcholine Nanocapsules

One widely used monomer for protein encapsulation is 2-methacryloyloxyethylphosphorylcholine (MPC). MPC has been used as monomer in combination with MBA as a non-degradable crosslinker to obtain a polymeric network of polyMPC (PMPC) by free radical polymerization. This method has been explored to encapsulate horseradish peroxidase (HRP), glucose oxidase (GOx), uricase (UOx) and alcohol oxidase (AOx) among others [114]. These enzymes were previously acroylated with *N*-hydroxysuccinimide ester and subsequently put in contact with the monomers, crosslinker and radical initiators. The formation of the polymeric coating was shown to preserve 75% of the enzymatic activity of the native form and provided them with thermal stability and protection against proteolysis. In this sense, it was proven that the encapsulated UOx retained 85% of its activity after 5 days of incubation at physiological temperature compared to 50% for the native enzyme. In addition, the UOx nanocapsules retained 95% of their activity after 90 min of incubation in a trypsin solution whereas the activity of the native enzyme decreased to 0% after 40 min. These data showed the protective properties of the polymeric layer.

As mentioned in the Introduction, in addition to their protective function, protein delivery systems must be able to avoid the opsonization in serum in order to evade internalization by phagocityc cells, prolonging their plasmatic half-life. PMPC-nanocapsules were demonstrated to fulfill both requirements. Thus, PMPC-nanocapsules were shown to avoid fagocitation by J744A mouse macrophages, with or without previous incubation with mouse serum, while native enzymes were completely uptaken by the macrophages.

Finally, PMPC nanocapsules were shown to evade the adaptive immune system in mice. These data demonstrated the capacity of nanocapsules to avoid the opsonization, phagocytosis and stimulated adaptive immune system. These properties allow a prolonged circulation time of the enzyme and circumvent undesirable accumulation in the liver, kidney and spleen.

In another work it was demonstrated that the capacity of avoiding protein adsorption, which is the main requirement to prolong the circulation time, is due to phosphorylcholine [114,115]. In order to prove this, bovine serum albumin (BSA) encapsulation was done inside four different types of nanocapsules. One of them was synthesized using MPC that resulted in a nanocapsule with a Z potential value of −2.76 mV. Another was synthesized using a combination of AAm and *N*-(3-aminopropyl) methacrylamide (APM) and a last one employing succinic anhydride. This combination allows one to obtain nanocapsules with neutral charge similar to PMP capsules (−2.26 mV), positive charge (+5.28 mV) and negative charge (−15.37 mV), respectively. All of them presented a size of approximately 10 nm during 8 days in phosphate buffer saline (PBS)

under physiological conditions. Only positively-charged nanocapsules showed opsonization when they were incubated in the presence of serum proteins and produced a considerable decrease of the cell viability to 75% when they were incubated with HeLa cells at high concentrations (1600 nM). Positively-charged nanocapsules were phagocytosed by J744A.1 mouse macrophages, while neutral and negatively-charged nanocapsules were significantly less engulfed by macrophages and, finally, negligible phagocythosis was found in macrophages incubated with PMPC-nBSA. These results indicated that PMPC was responsible for avoiding endocytosis by macrophages. In vivo studies showed that positively-charged BSA nanocapsules were removed from the bloodstream and accumulated in liver and kidney. Similar results, although no so pronounced, were obtained for negatively-charged capsules. The fast clearance from the bloodstream was caused by interactions between positively-charged nanocapsules and serum proteins, which results in aggregates of proteins being easily withdrawn by liver fenestra and kidney glomeruli. Moreover, highly-charged surfaces (both positively and negatively) activated the complement system, leading to a formation of immune complexes that are easily recognized by Kupffer cells and accumulate in the liver. Neutral acrylamide-BSA nanocapsules showed much slower blood clearance than charged systems. Finally, PMPC-nanocapsules maintain 70% of their enzymatic activity after being in circulation for 8 day.

In regard to pharmacokinetics, it has been studied that PMPC-nanocapsules show an 8-fold increase in their plasmatic circulation time compared to native enzyme ($t_{1/2}$ = 48.92 h vs 6.43 h of native UOx), with clearance rate 169 times lower (11.01 mL/h vs 0.065 mL/h) [116]. Furthermore, the distribution volume of the native enzyme was 22 times higher than for the encapsulated form, what indicates that PMPC nanocapsules stay in the bloodstream whereas the non-encapsulated enzyme invaded the surrounding tissues.

PMPC nanocapsules have also been investigated for the treatment of high urate levels [116]. In order to study their efficacy, native UOx or PMPC-UOx nanocapsules were injected intravenously. The administration of the native enzyme induced a reduction of serum urate from 227 μmol/L to 56 μmol/L in the 5 first hours after the administration. This reduction was followed by an abrupt increase to 293 μmol/L at 24 h, and after that, it slowly decreased to normal values (227 μmol/L) at longer times. The injection of nanocapsules, instead, produced a more sustained and prolonged therapeutic effect, maintaining the serum urate levels below to 150 μmol/L for 5 days. Moreover, repeated administrations of native enzyme induced more immunogenic response, and twice higher levels of white blood cells (WBC) and lymphocytes. PMPC nanocapsules have therefore been proven to be effective for the treatment of hyperoxaluria [29].

Thus PMPC-nanocapsules have been demonstrated to be an extraordinary strategy to encapsulate enzymes. PMPC nanocapsules protect the host enzymes against temperature and proteolysis. Additionally, the polymeric coating prevents their opsonization and phagocytosis by macrophages, allowing longer circulation times and a more sustained and prolonged therapeutic effect.

5.1.3. *N*-Vinylpyrrolidone Nanocapsules

Another type of non-degradable polymeric capsules is based on the use of *N*-vinylpyrrolidone (NVP) as monomer and MBA as crosslinker [117]. Nanocapsules obtained with these monomers display improved thermal, pH and proteolysis stability in comparison to free enzymes. As an example, UOx encapsulated with this monomer maintained 100% of its activity after 3 h whereas the free enzyme retained less than 50%. Also, UOx exhibited activity at pH 4.4–9.4 whereas UOx only had enzymatic activity at physiological pH. With respect to stability against proteolysis, nUOx kept the initial activity after 20 min of incubation with trypsin whereas the native form lost more than 80% of its function after just 5 min. Encapsulation of UOx also avoided the uptake by macrophages, decreasing the internalization percentage from 98% after 1 h (native UOx) to less the 20% after 5 h (encapsulated UOx). Regarding its pharmacokinetic profile, free enzyme clearance rate was 25 times faster than its encapsulated form, with twice the distribution volume. PNVP nanocapsules were evaluated for the treatment of high urate levels. UOx reduced the serum uric acid from normal levels

(58.5 µmol/L) to 25.7 µmol/L, but after that, there was a rapid increase up to 91.95 µmol/L after 72 h, followed by a slow reduction to normal levels during 18 days. Administration of encapsulated UOx resulted in constant level of 20 µmol/L during the first 5 days followed by a progressive increase to normal levels, reached after 10 days. Finally, polymer excretion was also studied, showing that 90% of the administrated dose was recovered in urine after 24 h.

5.2. Degradable Nanocapsules

When the substrate on which the enzyme acts is so large that the polymeric mesh is not permeable to it or the transportation of a therapeutic protein is intended, nanocapsules must be designed in order to release the host protein when certain stimuli is present (Figure 5). Thus, degradable nanocapsules allow an on-demand release of the housed protein and, therefore, a precise control of the protein administration. Different stimuli have been explored to trigger the nanocapsules disassembly as a function of the pursued purpose and therefore, different crosslinker have been explored. In all of this type of systems, acrylamide (AAm) was employed as structural monomer in combination with other charged monomer to facilitate the absorption of monomers on the surface of the protein or provide anchor points to the resulting capsules.

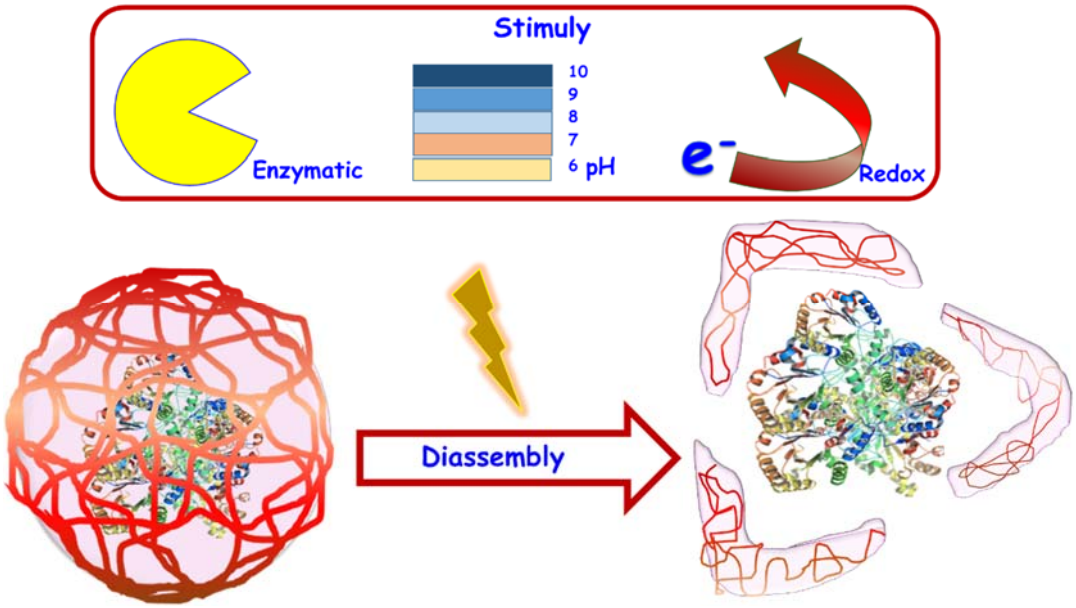

Figure 5. "Stimulation" and "diassembly" of degradable nanocapsules.

5.2.1. pH-Respondive Nanocapsules

One widely used strategy is the design of pH-responsive nanocapsules. Acidic conditions are present in different pathologies as solid tumors, which present a mild-acidic environment as a consequence of their accelerated metabolism and hypoxic conditions [118]. Therefore, it is possible to release the enzyme once it has reached the tumor tissue providing pH-responsiveness to the polymeric coating.

An interesting use of the proteins in nanomedicine consist of degrade the extracellular matrix allowing the drug loaded nanocarrier to homogenous distribution inside tumoral mass. Tumoral mass often present denser extracellular matrix than healthy tumors. This fact hinders the penetration of nanodevices and, therefore, limits the therapeutic efficacy of drug carried to a peripheral effect [119]. Proteolytic enzymes have been attached onto nanoparticle surface in order to degrade the tumoral extracellular matrix and allow that the nanocarrier reaches deeper zones of the tumor [120]. However, as have been extensively commented, enzymes have strong limitations. Then, in order to obtain a

system able to protect the proteolytic enzyme and provide the nanocarriers to penetration capacity until they reach the tumor zone, acid-degradable nanocapsules of collagenase were developed (Figure 6) [121]. These nanocapsules were formed using ethyleneglycol dimethacrylate (EGDMA) as the pH-degradable crosslinker. The enzymatic activity was blocked as a consequence of the encapsulation process until exposed to an acidic environment, where it exhibited its activity. This effect is due to the polymeric mesh providing a steric impediment for the enzyme to act on its substrate, but once the mesh is degraded in the presence of the stimulus, the enzyme is exposed.

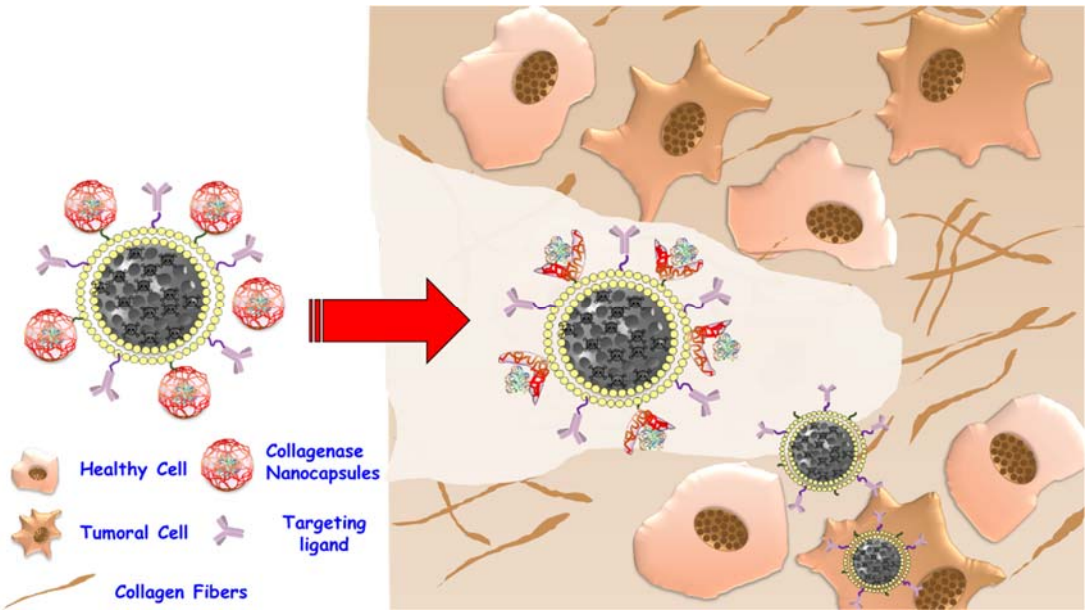

Figure 6. Collagenase nanocapsules to improve the penetration of drug loaded nanocarriers inside tumors.

Besides pH-responsiveness, the authors investigated the protective function of the polymeric coating against the proteases which are present in the bloodstream. Nanocapsules and free enzyme were exposed to proteases, being observed that the encapsulated enzyme retained 100% of its activity after 3 h whereas the catalytic activity of the free enzyme was reduced by more than 50%.

On the other hand, it is well known that endosomes present acid pH values. Thus, a pH-responsive polymeric mesh can be degraded in the endosomes, upon intracellular entrance, releasing the protein into the cytoplasm. This strategy has been employed in order to avoid the problem of degradation of proteins in lysosomes. In a recent study, pH-sensitive protein nanocapsules have been demonstrated to escape from the endosomes [122]. In this case, glycerol dimethacrylate was employed as pH-responsive crosslinker. The endosomal escape was investigated by the incubation of rhodamine-labelled HRP nanocapsules with HeLa cells and a posterior labeling of early endosomes and late lysosomes. The staining reveals that nanocapsules co-localized with early endosomes and lysosomes at short times, following a gradual release of their cargo inside the cytosol. Also, cells treatment with EGFP nanocapsules was demonstrated to be more effective than treatment with EFGP and TAT-EGFP conjugates. As comparison, protein encapsulation inside liposomes can allow the translocation of the cargo to the cell cytosol, but with lower efficiency [123]. The advantage of pH-responsive nanocapsules over liposomes was shown in a recent publication. In this work, pH-responsive miRNA nanocapsules were developed in order to achieve tumor suppression. The capsules were synthesized using (EGDMA) as the pH-degradable crosslinker. The obtained nanocapsules were able to knock down the expression of mir-21 to 11.5% of the control. This system was demonstrated to be much more effective than miRNA carried inside of liposomes, which only led to a knockdown of 46.2% of control. In addition, nanocapsule endocytosis was five times greater than for the analogous liposomes.

5.2.2. Enzyme Responsive Nanocapsules

Polymeric nanocapsules can be designed to be protease-sensitive. A creative example can be found in the construction of polymeric nanocapsules crosslinked with peptides sensitive to the own loaded enzyme. In this way, the capsule can be degraded from its core by the host enzyme [124]. Caspase 3, an apoptotic protease, was encapsulated using a crosslinker sensitive to this enzyme. The obtained capsule was totally degraded after 200 min at physiological temperature whereas it remained intact at 4 °C, what would enable its storage. This system was shown to induce CP3-mediated apoptosis in HeLa cells in a dose-dependent manner. CP3 cleaves the caspase-activate-deoxyribonuclease inhibitor (ICAD), leading to nucleosome fragmentation and, therefore causing apoptosis. Additionally, in order to allow spatiotemporal control protease release, a degradable crosslinker which contains a photolabile moiety (*o*-nitrobenzyl ester) was incorporated to the nanocapsule composition in such a way that only after ultraviolet exposure the nanocapsule would start to be degraded by CP3 and induced the apoptotic effect. The last example is an ingenious method since it is the own host enzyme which acts to degrade the polymeric nanocapsule, however, in order to deliver another type of proteins, others crosslinker have been explored. A way to obtain nanocapsules with more general and, at the same time, specific mechanism for enzymatic degradation, is to exploit the existence of endoproteases that are expressed in many mammalian cells as triggers. Thus, Tang et al. [125] designed nanocapsules able to specifically degrade by incubation with furin, which is a endoprotease present in several intracellular localizations. Due to is degradability the obtained nanocapsules were able to carry proteins to the cell cytosol or, when the protein was loaded in combination with a localization signal, be localizated in the nucleus. Other proteases have been investigated to trigger the degradation of nanocapsules, such as plasmin and metalloproteinases (MMP) [126]. Plasmin is a serine protease present in the blood and often secreted by tissue cells during new blood vessel formation. On the other hand, MMP are proteases that have an important role in tissue remodeling. Bovine serum albumin (BSA) nanocapsules were obtained using a plamin-cleavable crosslinker (-KNRVK-), or an MMP-cleavable crosslinker (-KLGPAK-) [127]. Specific degradation was studied by incubating the nanocapsules with plasmin or collagenase, obtaining a specific response to the corresponding protease. Another interesting approach for nanocapsules is their use in hydrogels. The formation of hydrogels in the presence of proteins often results in a loss of their structure and activity. Moreover, hydrogels must present big pores in order to achieve a diffusion of nutrients and cell growth. Unfortunately, this also favors a rapid release of the proteins. The encapsulation of proteins and their subsequent addition to hydrogels during consolidation has been demonstrated to be a good strategy to protect the enzyme during hydrogel formation and to avoid protein leaching [126].

Another interesting design is the use of a crosslinker with protease-cleavable specific sequences using aminoacids with different chirality [127]. Peptides formed with L- or D-chiral forms in the same sequence of aminoacids exhibit the same specificity for a determined enzyme but different cleavage kinetics. The rupture kinetic of the sequence NRV formed by D-chiral forms of aminoacids is 10 times slower than the corresponding to the L-form. Using combinations of these crosslinkers, it is possible to achieve different kinetics to obtain nanocapsules with specific and controlled release. This was studied in a recent publication where multiple proteins were encapsulated using this method [127].

5.2.3. Redox-Responsive Nanocapsules

The cell cytosol exhibits lower redox potential than the external intracellular media due to the high concentration of reduced glutathione (GSH). GSH is found in milimolar concentrations inside the cell, whereas it is in the micromolar range in the extracellular medium [128]. Thus, one interesting option is to design nanocapsules able to undergo disassembly exploiting this gradient. Crosslinkers that contain disulfide bonds are redox-sensitive and therefore, their use allow the preparation of nanocapsules that undergo degradation when the system reaches the cell cytosol.

An interesting piece of work reported [129] the synthesis of nanocapsules formed with *N*,*N*′-bis(acryloyl) cystamine as a redox-responsive crosslinker. Capsules designed with the sensitive

crosslinker were completely degraded when they were incubated with 2 mM GSH for 2 h at 37 °C. Also, the encapsulation allowed the endocytosis of the protein whereas the native protein was not able to enter the cell. The endocytosed nanocapsules were localized in the early endosomes for 1 to 2 h after incubation, but no co-localization with late endosomes was found, so it was concluded that the protein was released to the cytosol. The treatment of different cell lines with caspase 3 (CP3) in its native form and encapsulated in non-degradable (using MBA as a non degradable crosslinker) or in redox-sensitive nanocapsules demonstrated that only the last system induced apoptosis (which was also dose-dependent). Using the same monomers and crosslinker, Tang et al. [130] developed redox-responsive apoptin nanocapsules. Apoptin is a protein able to go to the nucleus and induce p53-independent apoptosis in tumoral cells without affecting healthy cells, due to a tumor-specific phosphorylation of Thr108 that lead to its accumulation. Mice with MCF-7 breast cancers were treated with apoptin capsules, BSA nanocapsules and PBS, and the treatment with apoptin nanocapsules resulted in a reduction of tumor growth rate, demonstrating its therapeutic effect.

p53 plays an important role in tumoral cell sensitivity against radio- and chemotherapy but also promotes their apoptosis. Since approximately the 50% of all human tumors presents mutations in p53 proteins, it is the most frequent mutant gene [131]. Then, transport of non-mutant p53 copies appears as an interesting strategy. Unfortunately, p53 has a tetrameric structure which is prone to aggregation and therefore, to loss of function [132]. On the basis of this fact, Tang et al. [16] designed protein nanocapsules of p53 using *N*,*N*′-methylenebis(acroyl)cystamine as redox-sensible crosslinker. Also, they included *N*-azidodeca(ethyleneglycol) ethylacrylamide in the polymeric composition in order to avoid the non-selective uptake by the cells due to electrostatic interactions between positive charges provided from the positively-charged monomer in the polymeric mesh with negative charges of phospholipids on the cell membrane. The azide groups of the neutral monomer also allowed the anchorage of targeting moieties by orthogonal chemistry in order to achieve selective endocytosis. Nanocapsules were successfully decorated with a specific targeting peptide, LHRH for which receptors are overexpressed in many breast and prostate cancers, in such a way that nanocapsules were selectively endocytated by cells after 12 h of incubation. Moreover, when they had been formed with a degradable croosslinker, p53 was localized in the nuclei inducing cytotoxicity.

Another type of redox sensitive protein nanocapsules was developed by Thayumanavan et al. [133], who used *p*(PEGMA-co-*p*-nitrophenylcarbonate) as a polymer that contains disulfide bonds and ethylenediamine (ED) or tetraethylene oxide bisamine (PEG-bid-amine) as crosslinkers. The polymer was conjugated to the protein surface via reaction between amino groups of lysine residues on the protein surface with *p*-nitrophenylcarbonate (NPC). The remaining NPCs groups were reacted with the respective bis-amine crosslinker, forming a polymeric shell around the protein. It is important to note that the disulfide bonds are in β-position with respect to the carbamate oxygen, in such a way that under reducing environments, as the cell cytosol, the disulfide bonds are broken, which results in carbamate cleavage, releasing the amino groups of the native protein. The most successful encapsulation was achieved with the crosslinker ED which gave rise to an encapsulation efficiency of 64–67% compared to the 5–7% achieved with the bisamine PEG. The obtained capsule preserved the activity of the enzyme against proteases and was only degraded in the presence of dithiothreitol (DTT), which induced a reducing environment, releasing the host enzyme in its functional structure. This system was demonstrated be able to traffic the protein across the cellular membrane and release it in the cytosol.

6. Conclusions

Nanomedicine has developed different systems for delivery and protection of proteins. Their conjugation with polymeric chains allows increased circulation times due to an increase in their size but has limited efficacy to protect them against proteases. Other alternatives are their loading inside liposomes or inorganic systems and onto their surface. These strategies have been demonstrated to protect proteins against external agents. However, liposomes have low physicochemical stability

in vivo and inorganic nanoparticles are more sturdy systems but often must be functionalized to be biocompatible. The development of platform nanotechnology for protein delivery based on encapsulation for free radical polymerization has been demonstrated be a widely applicable strategy to encapsulate an extensive range of proteins combining the flexibility of liposomes and the sturdiness of inorganic nanoparticles. All these strategies are summarized in Table 1.

Table 1. Summary of Protein Delivery Systems.

	Strategies for Protein Delivery
Pegylation	This strategy consists in the conjugation of polymeric chains on protein surface. This allow increase significally the times of circulation of proteins in bloodstream, however has a limited efficacy to protect against proteases attack.
Liposomes	Liposomes are biocompatible and cell-like nanodevices. Proteins can be delivered inside the aqueous core of liposomes or attached on their surface. Liposomes are characterized by high flexibility but their use are limited by small stability in human body.
Inorganic nanoparticles	Mesoporous silica nanoparticles, gold nanoparticles and carbon nanotubes allow the delivery of proteins on their surface or inside them. They are characterized by a high sturdiness but have a poor flexibility.
Polymeric nanocapsules	This strategy consist in a polymerization in situ around the protein making a polymeric coating. This strategy can be used to a large number of proteins and allow the design of nanocapsules both degradable and non-degradable. This class of systems combine the sturdiness of inorganic nanoparticles with flexibility of liposomes

As conclusion, several conditions must be fulfilled in order to achieve an efficient protein delivery system: (1) the transported protein must keep its functional structure during the encapsulation process; (2) the carrier must present high loading capacity; (3) the protein should be protected against enzyme degradation, proteolysis or thermic denaturalization, among others; (4) the nanocapsules must allow hide the protein activity until the nanodevice reaches the target site. Moreover, depending of the enzyme work on large or impermeable substrate to the polymeric coating, the enzyme nanocapsule should be designed to dissemble in response to certain stimuli releasing the transported protein with their function intact. Finally, (5) nanocapsules should avoid opsonization and increase the half-life of the enzyme.

As it has been extensively described along this review, polymeric nanocapsules have shown be able to comply all of these requirements by a specific selection of the monomers and crosslinkers that conform to them. This technique has been demonstrated to improve the abovementioned aspects in comparison with liposome encapsulation, polymer protein conjugation and loading in inorganic nanoparticles which have been traditionally employed. Thus, the protein encapsulation strategy has emerged as an approach with high potential to develop the next generation of protein treatments.

Author Contributions: All authors have contributed equally.

Acknowledgments: This work has been done thanks to the financial support provided by European Research Council (Advanced Grant VERDI; ERC-2015-AdG Proposal No. 694160) and the project MAT2015-64831-R.

Conflicts of Interest: The authors declare no conflict of interest.

References

1. Nitiss, J.L. DNA topoisomerase II and its growing repertoire of biological functions. *Nat. Rev. Cancer* **2009**, *9*, 327–337. [CrossRef] [PubMed]
2. Newton, A.C. Protein kinase C: Structure, function, and regulation. *J. Biol. Chem.* **1995**, *270*, 28495–28498. [CrossRef] [PubMed]
3. Childers, N.K.; Bruce, M.G.; McGhee, J.R. Molecular Mechanisms of Immunoglobulin a Defense. *Annu. Rev. Microbiol.* **1989**, *43*, 503–536. [CrossRef] [PubMed]

4. Puigserver, P.; Rhee, J.; Donovan, J.; Walkey, C.J.; Yoon, J.C.; Oriente, F.; Kitamura, Y.; Altomonte, J.; Dong, H.; Accili, D.; et al. Insulin-regulated hepatic gluconeogenesis through FOXO1–PGC-1α interaction. *Nature* **2003**, *423*, 550–555. [CrossRef] [PubMed]
5. Vassart, G.; Dumont, J.E. The Thyrotropin Receptor and the Regulation of Thyrocyte Function and Growth. *Endocr. Rev.* **1992**, *13*, 596–611. [CrossRef] [PubMed]
6. Bartkova, J.; Lukas, J.; Müller, H.; Lützhøt, D.; Strauss, M.; Bartek, J. Cyclin D1 protein expression and function in human breast cancer. *Int. J. Cancer* **1994**, *57*, 353–361. [CrossRef] [PubMed]
7. Gelse, K.; Pöschl, E.; Aigner, T. Collagens—Structure, function, and biosynthesis. *Adv. Drug Deliv. Rev.* **2003**, *55*, 1531–1546. [CrossRef] [PubMed]
8. McKittrick, J.; Chen, P.-Y.; Bodde, S.G.; Yang, W.; Novitskaya, E.E.; Meyers, M.A. The Structure, Functions, and Mechanical Properties of Keratin. *JOM* **2012**, *64*, 449–468. [CrossRef]
9. Aas, F.E.; Li, X.; Edwards, J.; Hongrø Solbakken, M.; Deeudom, M.; Vik, Å.; Moir, J.; Koomey, M.; Aspholm, M. Cytochrome *c*-based domain modularity governs genus-level diversification of electron transfer to dissimilatory nitrite reduction. *Environ. Microbiol.* **2015**, *17*, 2114–2132. [CrossRef] [PubMed]
10. Zhang, R.; Hess, D.T.; Qian, Z.; Hausladen, A.; Fonseca, F.; Chaube, R.; Reynolds, J.D.; Stamler, J.S. Hemoglobin βCys93 is essential for cardiovascular function and integrated response to hypoxia. *Proc. Natl. Acad. Sci. USA* **2015**, *112*, 6425–6430. [CrossRef] [PubMed]
11. Hoffman, B.M.; Petering, D.H. Coboglobins: Oxygen-Carrying Cobalt-Reconstituted Hemoglobin and Myoglobin. *Proc. Natl. Acad. Sci. USA* **1970**, *67*, 637–643. [CrossRef] [PubMed]
12. Zhang, J.; Du, J.; Yan, M.; Dhaliwal, A.; Wen, J.; Liu, F.; Segura, T.; Lu, Y. Synthesis of protein nano-conjugates for cancer therapy. *Nano Res.* **2011**, *4*, 425–433. [CrossRef]
13. Strittmatter, W.J.; Weisgraber, K.H.; Goedert, M.; Saunders, A.M.; Huang, D.; Corder, E.H.; Dong, L.-M.; Jakes, R.; Alberts, M.J.; Gilbert, J.R.; et al. Hypothesis: Microtubule Instability and Paired Helical Filament Formation in the Alzheimer Disease Brain Are Related to Apolipoprotein E Genotype. *Exp. Neurol.* **1994**, *125*, 163–171. [CrossRef] [PubMed]
14. Selkoe, D.J. Cell biology of protein misfolding: The examples of Alzheimer's and Parkinson's diseases. *Nat. Cell Biol.* **2004**, *6*, 1054–1061. [CrossRef] [PubMed]
15. Wang, X.; Venable, J.; LaPointe, P.; Hutt, D.M.; Koulov, A.V.; Coppinger, J.; Gurkan, C.; Kellner, W.; Matteson, J.; Plutner, H.; et al. Hsp90 Cochaperone Aha1 Downregulation Rescues Misfolding of CFTR in Cystic Fibrosis. *Cell* **2006**, *127*, 803–815. [CrossRef] [PubMed]
16. Zhao, M.; Liu, Y.; Hsieh, R.S.; Wang, N.; Tai, W.; Joo, K.I.; Wang, P.; Gu, Z.; Tang, Y. Clickable protein nanocapsules for targeted delivery of recombinant p53 protein. *J. Am. Chem. Soc.* **2014**, *136*, 15319–15325. [CrossRef] [PubMed]
17. Fong, S.; Debs, R.J.; Desprez, P.-Y. Id genes and proteins as promising targets in cancer therapy. *Trends Mol. Med.* **2004**, *10*, 387–392. [CrossRef] [PubMed]
18. Patterson, H.; Nibbs, R.; McInnes, I.; Siebert, S. Protein kinase inhibitors in the treatment of inflammatory and autoimmune diseases. *Clin. Exp. Immunol.* **2014**, *176*, 1–10. [CrossRef] [PubMed]
19. Nikles, D.; Bach, P.; Boller, K.; Merten, C.A.; Montrasio, F.; Heppner, F.L.; Aguzzi, A.; Cichutek, K.; Kalinke, U.; Buchholz, C.J. Circumventing tolerance to the prion protein (PrP): Vaccination with PrP-displaying retrovirus particles induces humoral immune responses against the native form of cellular PrP. *J. Virol.* **2005**, *79*, 4033–4042. [CrossRef] [PubMed]
20. Lagassé, H.A.D.; Alexaki, A.; Simhadri, V.L.; Katagiri, N.H.; Jankowski, W.; Sauna, Z.E.; Kimchi-Sarfaty, C. Recent advances in (therapeutic protein) drug development. *F1000Research* **2017**, *6*, 113. [CrossRef] [PubMed]
21. Leader, B.; Baca, Q.J.; Golan, D.E. Protein therapeutics: A summary and pharmacological classification. *Nat. Rev. Drug Discov.* **2008**, *7*, 21–39. [CrossRef] [PubMed]
22. Chi, E.Y.; Krishnan, S.; Randolph, T.W.; Carpenter, J.F. Physical stability of proteins in aqueous solution: Mechanism and driving forces in nonnative protein aggregation. *Pharm. Res.* **2003**, *20*, 1325–1336. [CrossRef] [PubMed]
23. Dill, K.A. Dominant forces in protein folding. *Biochemistry* **1990**, *29*, 7133–7155. [CrossRef] [PubMed]
24. Pace, C.N.; Shirley, B.A.; McNutt, M.; Gajiwala, K. Forces contributing to the conformational stability of proteins. *FASEB J.* **1996**, *10*, 75–83. [CrossRef] [PubMed]
25. Jaenicke, R. Protein folding: Local structures, domains, subunits, and assemblies. *Biochemistry* **1991**, *30*, 3147–3161. [CrossRef] [PubMed]

26. Ruddy, S.; Gigli, I.; Austen, K.F. The Complement System of Man. *N. Engl. J. Med.* **1972**, *287*, 489–495. [CrossRef] [PubMed]
27. Müller-Eberhard, H.J. Molecular Organization and Function of the Complement System. *Annu. Rev. Biochem.* **1988**, *57*, 321–347. [CrossRef] [PubMed]
28. Ghosh, P.; Yang, X.; Arvizo, R.; Zhu, Z.-J.; Agasti, S.S.; Mo, Z.; Rotello, V.M. Intracellular Delivery of a Membrane-Impermeable Enzyme in Active Form Using Functionalized Gold Nanoparticles. *J. Am. Chem. Soc.* **2010**, *132*, 2642–2645. [CrossRef] [PubMed]
29. Zhao, M.; Xu, D.; Wu, D.; Whittaker, J.W.; Terkeltaub, R.; Lu, Y. Nanocapsules of oxalate oxidase for hyperoxaluria treatment. *Nano Res.* **1898**, *1*, 8–11. [CrossRef]
30. Banting, F.G.; Best, C.H.; Collip, J.B.; Campbell, W.R.; Fletcher, A.A. Pancreatic Extracts in the Treatment of Diabetes Mellitus. *Can. Med. Assoc. J.* **1922**, *12*, 141–146. [PubMed]
31. Goeddel, D.V.; Kleid, D.G.; Bolivar, F.; Heyneker, H.L.; Yansura, D.G.; Crea, R.; Hirose, T.; Kraszewski, A.; Itakura, K.; Riggs, A.D. Expression in *Escherichia coli* of chemically synthesized genes for human insulin. *Proc. Natl. Acad. Sci. USA* **1979**, *76*, 106–110. [CrossRef] [PubMed]
32. Clark, A.J.; Adeniyi-Jones, R.O.; Knight, G.; Leiper, J.M.; Wiles, P.G.; Jones, R.H.; Keen, H.; MacCuish, A.C.; Ward, J.D.; Watkins, P.J.; et al. Biosynthetic human insulin in the treatment of diabetes. A double-blind crossover trial in established diabetic patients. *Lancet* **1982**, *2*, 354–357. [CrossRef]
33. Keen, H.; Glynne, A.; Pickup, J.C.; Viberti, G.C.; Bilous, R.W.; Jarrett, R.J.; Marsden, R. Human insulin produced by recombinant DNA technology: Safety and hypoglycaemic potency in healthy men. *Lancet* **1980**, *2*, 398–401. [CrossRef]
34. Richter, B.; Neises, G. "Human" insulin versus animal insulin in people with diabetes mellitus. In *The Cochrane Database of Systematic Reviews (Protocol)*; John Wiley & Sons, Ltd.: Chichester, UK, 2003; p. CD003816.
35. Pensions, D.B.; Risk, U. *The Purple Book*; Pension Protection Fund: Wymondham, UK, 2014; pp. 1–2.
36. Fee, C.J.; Van Alstine, J.M. PEG-proteins: Reaction engineering and separation issues. *Chem. Eng. Sci.* **2006**, *61*, 924–939. [CrossRef]
37. Pasut, G.; Veronese, F.M. Polymer–drug conjugation, recent achievements and general strategies. *Prog. Polym. Sci.* **2007**, *32*, 933–961. [CrossRef]
38. Knauf, M.J.; Bell, D.P.; Hirtzer, P.; Luo, Z.P.; Young, J.D.; Katre, N.V. Relationship of effective molecular size to systemic clearance in rats of recombinant interleukin-2 chemically modified with water-soluble polymers. *J. Biol. Chem.* **1988**, *263*, 15064–15070. [PubMed]
39. Bhat, R.; Timasheff, S.N. Steric exclusion is the principal source of the preferential hydration of proteins in the presence of polyethylene glycols. *Protein Sci.* **1992**, *1*, 1133–1143. [CrossRef] [PubMed]
40. Harris, J.M.; Chess, R.B. Effect of pegylation on pharmaceuticals. *Nat. Rev. Drug Discov.* **2003**, *2*, 214–221. [CrossRef] [PubMed]
41. Knop, K.; Hoogenboom, R.; Fischer, D.; Schubert, U.S. Poly(ethylene glycol) in drug delivery: Pros and cons as well as potential alternatives. *Angew. Chem. Int. Ed.* **2010**, *49*, 6288–6308. [CrossRef] [PubMed]
42. Veronese, F.M. Peptide and protein PEGylation: A review of problems and solutions. *Biomaterials* **2001**, *22*, 405–417. [CrossRef]
43. Abuchowski, A.; van Es, T.; Palczuk, N.C.; Davis, F.F. Alteration of Immunological properties of bovine serum albumin by covalent attachment of polyethylene glycol. *J. Biol. Chem.* **1977**, *252*, 3578–3581. [PubMed]
44. Abuchowski, A.; Mccoy, J.R.; Palczuk, N.C.; Es, T.V.A.N.; Davis, F.F. Effect of covalent attachment of polyethylene glycol on immunogenicity and circulating life of bovine liver catalase. *J. Biol. Chem.* **1977**, *252*, 3582–3586. [PubMed]
45. Levy, Y.; Hershfield, M.S.; Fernandez-Mejia, C.; Polmar, S.H.; Scudiery, D.; Berger, M.; Sorensen, R.U. Adenosine deaminase deficiency with late onset of recurrent infections: Response to treatment with polyethylene glycol-modified adenosine deaminase. *J. Pediatr.* **1988**, *113*, 312–317. [CrossRef]
46. Alconcel, S.N.S.; Baas, A.S.; Maynard, H.D. FDA-approved poly(ethylene glycol)–protein conjugate drugs. *Polym. Chem.* **2011**, *2*, 1442–1448. [CrossRef]
47. Rajender Reddy, K.; Modi, M.W.; Pedder, S. Use of peginterferon alfa-2a (40 KD) (Pegasys®) for the treatment of hepatitis C. *Adv. Drug Deliv. Rev.* **2002**, *54*, 571–586. [CrossRef]
48. Bennett, C.L.; Djulbegovic, B.; Norris, L.B.; Armitage, J.O. Colony-Stimulating Factors for Febrile Neutropenia during Cancer Therapy. *N. Engl. J. Med.* **2013**, *368*, 1131–1139. [CrossRef] [PubMed]

49. Romero-Weaver, A.L.; Wan, X.S.; Diffenderfer, E.S.; Lin, L.; Kennedy, A.R. Kinetics of Neutrophils in Mice Exposed to Radiation and/or Granulocyte Colony-Stimulating Factor Treatment. *Radiat. Res.* **2013**, *180*, 177–188. [CrossRef] [PubMed]
50. Locatelli, F.; Villa, G.; de Francisco, A.L.M.; Albertazzi, A.; Adrogue, H.J.; Dougherty, F.C.; Beyer, U. Effect of a continuous erythropoietin receptor activator (CERA) on stable haemoglobin in patients with CKD on dialysis: Once monthly administration. *Curr. Med. Res. Opin.* **2007**, *23*, 969–979. [CrossRef] [PubMed]
51. Armstrong, J.K.; Hempel, G.; Koling, S.; Chan, L.S.; Fisher, T.; Meiselman, H.J.; Garratty, G. Antibody against poly(ethylene glycol) adversely affects PEG-asparaginase therapy in acute lymphoblastic leukemia patients. *Cancer* **2007**, *110*, 103–111. [CrossRef] [PubMed]
52. Ishihara, T.; Takeda, M.; Sakamoto, H.; Kimoto, A.; Kobayashi, C.; Takasaki, N.; Yuki, K.; Tanaka, K.; Takenaga, M.; Igarashi, R.; et al. Accelerated Blood Clearance Phenomenon upon Repeated Injection of PEG-modified PLA-nanoparticles. *Pharm. Res.* **2009**, *26*, 2270–2279. [CrossRef] [PubMed]
53. Ravin, H.A.; Seligman, A.M.; Fine, J. Polyvinyl Pyrrolidone as a Plasma Expander. *N. Engl. J. Med.* **1952**, *247*, 921–929. [CrossRef] [PubMed]
54. Duncan, R. Polymer conjugates as anticancer nanomedicines. *Nat. Rev. Cancer* **2006**, *6*, 688–701. [CrossRef] [PubMed]
55. Haaf, F.; Sanner, A.; Straub, F. Polymers of *N*-Vinylpyrrolidone: Synthesis, Characterization and Uses. *Polym. J.* **1985**, *17*, 143–152. [CrossRef]
56. Caliceti, P.; Schiavon, O.; Morpurgo, M.; Veronese, F.M.; Sartore, L.; Ranucci, E.; Ferruti, P. Physico-Chemical and Biological Properties of Monofunctional Hydroxy Teriminating Poly(*N*-Vinylpyrrolidone) Conjugated Superoxide Dismutase. *J. Bioact. Compat. Polym.* **1995**, *10*, 103–120. [CrossRef]
57. Caliceti, P.; Schiavon, O.; Veronese, F.M. Immunological properties of uricase conjugated to neutral soluble polymers. *Bioconjug. Chem.* **2001**, *12*, 515–522. [CrossRef] [PubMed]
58. Lewis, A.; Tang, Y.; Brocchini, S.; Choi, J.; Godwin, A. Poly(2-methacryloyloxyethyl phosphorylcholine) for Protein Conjugation. *Bioconjug. Chem.* **2008**, *19*, 2144–2155. [CrossRef] [PubMed]
59. Wileman, T.E.; Foster, R.L.; Elliott, P.N.C. Soluble asparaginase-dextran conjugates show increased circulatory persistence and lowered antigen reactivity. *J. Pharm. Pharmacol.* **1986**, *38*, 264–271. [CrossRef] [PubMed]
60. Zinderman, C.E.; Landow, L.L.; Wise, R.P. Anaphylactoid Reactions to Dextran 40 and 70: Reports to the US Food and Drug Administration (FDA): 246. *Pharmacoepidemiol. Drug Saf.* **2006**, *15*, S115–S116.
61. Zinderman, C.E.; Landow, L.; Wise, R.P. Anaphylactoid reactions to Dextran 40 and 70: Reports to the United States Food and Drug Administration, 1969 to 2004. *J. Vasc. Surg.* **2006**, *43*, 1004–1009. [CrossRef] [PubMed]
62. Jevševar, S.; Kunstelj, M.; Porekar, V.G. PEGylation of therapeutic proteins. *Biotechnol. J.* **2010**, *5*, 113–128. [CrossRef] [PubMed]
63. Chariot^{TM}. Simple, Efficient Protein Delivery. Available online: https://www.activemotif.com/catalog/37/chariot-protein-delivery-reagent (accessed on 25 April 2018).
64. Szoka, F.; Papahadjopoulos, D. Biochemistry Procedure for preparation of liposomes with large internal aqueous space and high capture by reverse-phase evaporation (drug delivery/encapsulation/lipid vesicles/encapsulated macromolecules). *Proc. Natl. Acad. Sci. USA* **1978**, *75*, 4194–4198. [CrossRef] [PubMed]
65. Shao, S.; Geng, J.; Ah Yi, H.; Gogia, S.; Neelamegham, S.; Jacobs, A.; Lovell, J.F. Functionalization of cobalt porphyrin–phospholipid bilayers with his-tagged ligands and antigens. *Nat. Chem.* **2015**, *7*, 438–446. [CrossRef] [PubMed]
66. Oude Blenke, E.; Klaasse, G.; Merten, H.; Plückthun, A.; Mastrobattista, E.; Martin, N.I. Liposome functionalization with copper-free "click chemistry". *J. Control. Release* **2015**, *202*, 14–20. [CrossRef] [PubMed]
67. Bozzuto, G. Liposomes as nanomedical devices. *Int. J. Nanomed.* **2015**, *10*, 975–999. [CrossRef] [PubMed]
68. Reto, A. Schwendener Liposomes as vaccine delivery systems: A review of the recent advances. *Ther. Adv. Vaccines* **2014**, *2*, 159–182. [CrossRef]
69. Li, J.; Wang, X.; Zhang, T.; Wang, C.; Huang, Z.; Luo, X.; Deng, Y. A review on phospholipids and their main applications in drug delivery systems. *Asian J. Pharm. Sci.* **2015**, *10*, 81–98. [CrossRef]
70. Varkouhi, A.K.; Scholte, M.; Storm, G.; Haisma, H.J. Endosomal escape pathways for delivery of biologicals. *J. Control. Release* **2011**, *151*, 220–228. [CrossRef] [PubMed]
71. Zelphati, O.; Wang, Y.; Kitada, S.; Reed, J.C.; Felgner, P.L.; Corbeil, J. Intracellular delivery of proteins with a new lipid-mediated delivery system. *J. Biol. Chem.* **2001**, *276*, 35103–35110. [CrossRef] [PubMed]

72. Du, J.; Jin, J.; Yan, M.; Lu, Y. Synthetic Nanocarriers for Intracellular Protein Delivery. *Curr. Drug Metab.* **2012**, *13*, 82–92. [CrossRef] [PubMed]
73. Iwaoka, S.; Nakamura, T.; Takano, S.; Tsuchiya, S.; Aramaki, Y. Cationic liposomes induce apoptosis through p38 MAP kinase-caspase-8-Bid pathway in macrophage-like RAW264.7 cells. *J. Leukoc. Biol.* **2006**, *79*, 184–191. [CrossRef] [PubMed]
74. Scherphof, G.L.; Dijkstra, J.; Spanjer, H.H.; Derksen, J.T.P.; Roerdink, F.H. Uptake and Intracellular Processing of Targeted and Nontargeted Liposomes by Rat Kupffer Cells In Vivo and In Vitro. *Ann. N. Y. Acad. Sci.* **1985**, *446*, 368–384. [CrossRef] [PubMed]
75. Klibanov, A.L.; Maruyama, K.; Torchilin, V.P.; Huang, L. Amphipathic polyethyleneglycols effectively prolong the circulation time of liposomes. *FEBS Lett.* **1990**, *268*, 235–237. [CrossRef]
76. Liu, Y.; Li, J.; Lu, Y. Enzyme therapeutics for systemic detoxification. *Adv. Drug Deliv. Rev.* **2015**, *90*, 24–39. [CrossRef] [PubMed]
77. Ishida, T.; Kiwada, H. Accelerated blood clearance (ABC) phenomenon upon repeated injection of PEGylated liposomes. *Int. J. Pharm.* **2008**, *354*, 56–62. [CrossRef] [PubMed]
78. Scherphof, G.; Roerdink, F.; Waite, M.; Parks, J. Disintegration of phosphatidylcholine liposomes in plasma as a result of interaction with high-density lipoproteins. *Biochim. Biophys. Acta* **1978**, *542*, 296–307. [CrossRef]
79. Fanciullino, R.; Ciccolini, J. Liposome-Encapsulated Anticancer Drugs: Still Waiting for the Magic Bullet? *Curr. Med. Chem.* **2009**, *16*, 4361–4373. [CrossRef] [PubMed]
80. Yan, M.; Liang, M.; Wen, J.; Liu, Y.; Lu, Y.; Chen, I.S.Y. Single siRNA nanocapsules for enhanced RNAi delivery. *J. Am. Chem. Soc.* **2012**, *134*, 13542–13545. [CrossRef] [PubMed]
81. Xu, Z.P.; Zeng, Q.H.; Lu, G.Q.; Yu, A.B. Inorganic nanoparticles as carriers for efficient cellular delivery. *Chem. Eng. Sci.* **2006**, *61*, 1027–1040. [CrossRef]
82. Baeza, A.; Colilla, M.; Vallet-Regí, M. Advances in mesoporous silica nanoparticles for targeted stimuli-responsive drug delivery. *Expert Opin. Drug Deliv.* **2015**, *12*, 319–337. [CrossRef] [PubMed]
83. Yu, M.; Gu, Z.; Ottewell, T.; Yu, C. Silica-based nanoparticles for therapeutic protein delivery. *J. Mater. Chem. B* **2017**, *5*, 3241–3252. [CrossRef]
84. Tu, J.; Boyle, A.L.; Friedrich, H.; Bomans, P.H.H.; Bussmann, J.; Sommerdijk, N.A.J.M.; Jiskoot, W.; Kros, A. Mesoporous Silica Nanoparticles with Large Pores for the Encapsulation and Release of Proteins. *ACS Appl. Mater. Interfaces* **2016**, *8*, 32211–32219. [CrossRef] [PubMed]
85. Hoon Han, D.; Na, H.-K.; Hoon Choi, W.; Hoon Lee, J.; Kyung Kim, Y.; Won, C.; Lee, S.-H.; Pyo Kim, K.; Kuret, J.; Min, D.-H.; et al. Direct cellular delivery of human proteasomes to delay tau aggregation. *Nat. Commun.* **2014**, *5*, 5633. [CrossRef] [PubMed]
86. Slowing, I.I.; Trewyn, B.G.; Lin, V.S.Y. Mesoporous silica nanoparticles for intracellular delivery of membrane-impermeable proteins. *J. Am. Chem. Soc.* **2007**, *129*, 8845–8849. [CrossRef] [PubMed]
87. Huang, W.Y.; Davies, G.L.; Davis, J.J. Engineering cytochrome-modified silica nanoparticles to induce programmed cell death. *Chem. Eur. J.* **2013**, *19*, 17891–17898. [CrossRef] [PubMed]
88. Bhattacharya, R.; Mukherjee, P. Biological properties of "naked" metal nanoparticles. *Adv. Drug Deliv. Rev.* **2008**, *17*, 1289–1306. [CrossRef] [PubMed]
89. Ghosh, P.; Han, G.; De, M.; Kim, C.K.; Rotello, V.M. Gold nanoparticles in delivery applications. *Adv. Drug Deliv. Rev.* **2008**, *60*, 1307–1315. [CrossRef] [PubMed]
90. De, M.; Ghosh, P.S.; Rotello, V.M. Applications of Nanoparticles in Biology. *Adv. Mater.* **2008**, *20*, 4225–4241. [CrossRef]
91. Nativo, P.; Prior, I.A.; Brust, M. Uptake and Intracellular Fate of Surface-Modified Gold Nanoparticles. *ACS Nano* **2008**, *2*, 1639–1644. [CrossRef] [PubMed]
92. Pujals, S.; Bastús, N.G.; Pereiro, E.; López-Iglesias, C.; Puntes, V.F.; Kogan, M.J.; Giralt, E. Shuttling Gold Nanoparticles into Tumoral Cells with an Amphipathic Proline-Rich Peptide. *ChemBioChem* **2009**, *10*, 1025–1031. [CrossRef] [PubMed]
93. Tkachenko, A.G.; Xie, H.; Liu, Y.; Coleman, D.; Ryan, J.; Glomm, W.R.; Shipton, M.K.; Franzen, S.; Feldheim, D.L. Cellular Trajectories of Peptide-Modified Gold Particle Complexes: Comparison of Nuclear Localization Signals and Peptide Transduction Domains. *Bioconjug. Chem.* **2004**, *15*, 482–490. [CrossRef] [PubMed]

94. Verma, A.; Simard, J.M.; Worrall, J.W.E.; Rotello, V.M. Tunable reactivation of nanoparticle-inhibited β-galactosidase by glutathione at intracellular concentrations. *J. Am. Chem. Soc.* **2004**, *126*, 13987–13991. [CrossRef] [PubMed]
95. Kim, J.; Cao, L.; Shvartsman, D.; Silva, E.A.; Mooney, D.J. Targeted delivery of nanoparticles to ischemic muscle for imaging and therapeutic angiogenesis. *Nano Lett.* **2010**, *11*, 694–700. [CrossRef] [PubMed]
96. Kam, N.W.S.; Dai, H. Carbon nanotubes as intracellular protein transporters: Generality and biological functionality. *J. Am. Chem. Soc.* **2005**, *127*, 6021. [CrossRef] [PubMed]
97. Kam, N.W.S.; Jessop, T.C.; Wender, P.A.; Dai, H. Nanotube molecular transporters: Internalization of carbon nanotube-protein conjugates into mammalian cells. *J. Am. Chem. Soc.* **2004**, *126*, 6850–6851. [CrossRef] [PubMed]
98. Lu, Q.; Moore, J.M.; Huang, G.; Mount, A.S.; Rao, A.M.; Larcom, L.L.; Ke, P.C. RNA polymer translocation with single-walled carbon nanotubes. *Nano Lett.* **2004**, *4*, 2473–2477. [CrossRef]
99. Bianco, A.; Hoebeke, J.; Godefroy, S.; Chaloin, O.; Pantarotto, D.; Briand, J.P.; Muller, S.; Prato, M.; Partidos, C.D. Cationic carbon nanotubes bind to CpG oligodeoxynucleotides and enhance their immunostimulatory properties. *J. Am. Chem. Soc.* **2005**, *127*, 58–59. [CrossRef] [PubMed]
100. Pantarotto, D.; Briand, J.-P.; Prato, M.; Bianco, A. Translocation of bioactive peptides across cell membranes by carbon nanotubes. *Chem. Commun.* **2004**, *1*, 16–17. [CrossRef] [PubMed]
101. Pantarotto, D.; Singh, R.; McCarthy, D.; Erhardt, M.; Briand, J.-P.; Prato, M.; Kostarelos, K.; Bianco, A. Functionalized Carbon Nanotubes for Plasmid DNA Gene Delivery. *Angew. Chem.* **2004**, *116*, 5354–5358. [CrossRef]
102. Shi Kam, N.W.; O'Connell, M.; Wisdom, J.A.; Dai, H. Carbon nanotubes as multifunctional biological transporters and near-infrared agents for selective cancer cell destruction. *Proc. Natl. Acad. Sci. USA* **2005**, *102*, 11600–11605. [CrossRef] [PubMed]
103. Kam, N.W.S.; Liu, Z.; Dai, H. Functionalization of carbon nanotubes via cleavable disulfide bonds for efficient intracellular delivery of siRNA and potent gene silencing. *J. Am. Chem. Soc.* **2005**, *127*, 12492–12493. [CrossRef] [PubMed]
104. Strachota, B.; Matějka, L.; Zhigunov, A.; Konefał, R.; Spěváček, J.; Dybal, J.; Puffr, R. Poly(*N*-isopropylacrylamide)–clay based hydrogels controlled by the initiating conditions: Evolution of structure and gel formation. *Soft Matter* **2015**, *11*, 9291–9306. [CrossRef] [PubMed]
105. Wei, W.; Du, J.; Li, J.; Yan, M.; Zhu, Q.; Jin, X.; Zhu, X.; Hu, Z.; Tang, Y.; Lu, Y. Construction of robust enzyme nanocapsules for effective organophosphate decontamination, detoxification, and protection. *Adv. Mater.* **2013**, *25*, 2212–2218. [CrossRef] [PubMed]
106. Donarski, W.J.; Dumas, D.P.; Heitmeyer, D.P.; Lewis, V.E.; Raushel, F.M. Structure-Activity Relationships in the Hydrolysis of Substrates by the Phosphotriesterase from *Pseudomonas diminutat*. *Biochemistry* **1989**, *28*, 4650–4655. [CrossRef] [PubMed]
107. Li, J.; Jin, X.; Liu, Y.; Li, F.; Zhang, L.; Zhu, X.; Lu, Y. Robust enzyme–silica composites made from enzyme nanocapsules. *Chem. Commun.* **2015**, *51*, 9628–9631. [CrossRef] [PubMed]
108. Cai, J.; Liu, S.; Feng, J.; Kimura, S.; Wada, M.; Kuga, S.; Zhang, L. Cellulose-Silica Nanocomposite Aerogels by In Situ Formation of Silica in Cellulose Gel. *Angew. Chem.* **2012**, *124*, 2118–2121. [CrossRef]
109. Ramanathan, M.; Luckarift, H.R.; Sarsenova, A.; Wild, J.R.; Ramanculov, E.K.; Olsen, E.V.; Simonian, A.L. Lysozyme-mediated formation of protein–silica nano-composites for biosensing applications. *Colloids Surf. B Biointerfaces* **2009**, *73*, 58–64. [CrossRef] [PubMed]
110. Pedrosa, V.A.; Paliwal, S.; Balasubramanian, S.; Nepal, D.; Davis, V.; Wild, J.; Ramanculov, E.; Simonian, A. Enhanced stability of enzyme organophosphate hydrolase interfaced on the carbon nanotubes. *Colloids Surf. B Biointerfaces* **2010**, *77*, 69–74. [CrossRef] [PubMed]
111. Liu, Y.; Du, J.; Yan, M.; Lau, M.Y.; Hu, J.; Han, H.; Yang, O.O.; Liang, S.; Wei, W.; Wang, H.; et al. Biomimetic enzyme nanocomplexes and their use as antidotes and preventive measures for alcohol intoxication. *Nat. Nanotechnol.* **2013**, *8*, 187–192. [CrossRef] [PubMed]
112. Wang, W.; Duan, W.; Ahmed, S.; Mallouk, T.E.; Sen, A. Small power: Autonomous nano- and micromotors propelled by self-generated gradients. *Nano Today* **2013**, *8*, 531–554. [CrossRef]
113. Simmchen, J.; Baeza, A.; Ruiz-Molina, D.; Vallet-Regí, M. Improving catalase-based propelled motor endurance by enzyme encapsulation. *Nanoscale* **2014**, *6*, 8907–8913. [CrossRef] [PubMed]

114. Liang, S.; Liu, Y.; Jin, X.; Liu, G.; Wen, J.; Zhang, L.; Li, J.; Yuan, X.; Chen, I.S.Y.; Chen, W.; et al. Phosphorylcholine polymer nanocapsules prolong the circulation time and reduce the immunogenicity of therapeutic proteins. *Nano Res.* **2016**, *9*, 1022–1031. [CrossRef]
115. Zhang, L.; Liu, Y.; Liu, G.; Xu, D.; Liang, S.; Zhu, X.; Lu, Y.; Wang, H. Prolonging the plasma circulation of proteins by nano-encapsulation with phosphorylcholine-based polymer. *Nano Res.* **2016**, *9*, 2424–2432. [CrossRef]
116. Zhang, X.; Chen, W.; Zhu, X.; Lu, Y. Encapsulating Therapeutic Proteins with Polyzwitterions for Lower Macrophage Nonspecific Uptake and Longer Circulation Time. *ACS Appl. Mater. Interfaces* **2017**, *9*, 7972–7978. [CrossRef] [PubMed]
117. Zhang, X.; Xu, D.; Jin, X.; Liu, G.; Liang, S.; Wang, H.; Chen, W.; Zhu, X.; Lu, Y. Nanocapsules of therapeutic proteins with enhanced stability and long blood circulation for hyperuricemia management. *J. Control. Release* **2017**, *255*, 54–61. [CrossRef] [PubMed]
118. Danhier, F.; Feron, O.; Préat, V. To exploit the tumor microenvironment: Passive and active tumor targeting of nanocarriers for anti-cancer drug delivery. *J. Control. Release* **2010**, *148*, 135–146. [CrossRef] [PubMed]
119. Netti, P.A.; Berk, D.A.; Swartz, M.A.; Grodzinsky, A.J.; Jain, R.K. Role of Extracellular Matrix Assembly in Interstitial Transport in Solid Tumors Role of Extracellular Matrix Assembly in Interstitial Transport in Solid Tumors 1. *Cancer Res.* **2000**, *60*, 2497–2503. [PubMed]
120. Parodi, A.; Haddix, S.G.; Taghipour, N.; Scaria, S.; Taraballi, F.; Cevenini, A.; Yazdi, I.K.; Corbo, C.; Palomba, R.; Khaled, S.Z.; et al. Bromelain Surface Modification Increases the Diffusion of Silica Nanoparticles in the Tumor Extracellular Matrix. *ACS Nano* **2014**, *8*, 9874–9883. [CrossRef] [PubMed]
121. Villegas, M.R.; Baeza, A.; Vallet Regí, M. Hybrid Collagenase Nanocapsules for Enhanced Nanocarrier Penetration in Tumoral Tissues. *ACS Appl. Mater. Interfaces* **2015**, *7*, 24075–24081. [CrossRef] [PubMed]
122. Yan, M.; Du, J.; Gu, Z.; Liang, M.; Hu, Y.; Zhang, W.; Priceman, S.; Wu, L.; Zhou, Z.H.; Liu, Z.; et al. A novel intracellular protein delivery platform based on single-protein nanocapsules. *Nat. Nanotechnol.* **2010**, *5*, 48–53. [CrossRef] [PubMed]
123. Liu, C.; Wen, J.; Meng, Y.; Zhang, K.; Zhu, J.; Ren, Y.; Qian, X.; Yuan, X.; Lu, Y.; Kang, C. Efficient delivery of therapeutic miRNA nanocapsules for tumor suppression. *Adv. Mater.* **2015**, *27*, 292–297. [CrossRef] [PubMed]
124. Gu, Z.; Yan, M.; Hu, B.; Joo, K.L.; Biswas, A.; Huang, Y.; Lu, Y.; Wang, P.; Tang, Y. Protein nanocapsule weaved with enzymatically degradable polymerie network. *Nano Lett.* **2009**, *9*, 4533–4538. [CrossRef] [PubMed]
125. Biswas, A.; Joo, K.-I.; Liu, J.; Zhao, M.; Fan, G.; Wang, P.; Gu, Z.; Tang, Y. Endoprotease-Mediated Intracellular Protein Delivery Using Nanocapsules. *ACS Nano* **2011**, *5*, 1385–1394. [CrossRef] [PubMed]
126. Wen, J.; Anderson, S.M.; Du, J.; Yan, M.; Wang, J.; Shen, M.; Lu, Y.; Segura, T. Controlled protein delivery based on enzyme-responsive nanocapsules. *Adv. Mater.* **2011**, *23*, 4549–4553. [CrossRef] [PubMed]
127. Zhu, S.; Nih, L.; Carmichael, S.T.; Lu, Y.; Segura, T. Enzyme-Responsive Delivery of Multiple Proteins with Spatiotemporal Control. *Adv. Mater.* **2015**, *27*, 3620–3625. [CrossRef] [PubMed]
128. Meister, A.; Tate, S.S. Glutathione and Related γ-Glutamyl Compounds: Biosynthesis and Utilization. *Annu. Rev. Biochem.* **1976**, *45*, 559–604. [CrossRef] [PubMed]
129. Zhao, M.; Biswas, A.; Hu, B.; Joo, K.I.; Wang, P.; Gu, Z.; Tang, Y. Redox-responsive nanocapsules for intracellular protein delivery. *Biomaterials* **2011**, *32*, 5223–5230. [CrossRef] [PubMed]
130. Zhao, M.; Hu, B.; Gu, Z.; Joo, K.; Wang, P.; Tang, Y. Degradable polymeric nanocapsul for efficient intracellular delivery of a high molecular weight tumor-selective protein complex. *Nano Today* **2013**, *8*, 11–20. [CrossRef]
131. Ozaki, T.; Nakagawara, A. Role of p53 in Cell Death and Human Cancers. *Cancers* **2011**, *3*, 994–1013. [CrossRef] [PubMed]
132. Bell, S.; Klein, C.; Mü Ller, L.; Hansen, S.; Buchner, J. p53 contains large unstructured regions in its native state. *J. Mol. Biol.* **2002**, *322*, 917–927. [CrossRef]
133. Dutta, K.; Hu, D.; Zhao, B.; Ribbe, A.E.; Zhuang, J.; Thayumanavan, S. Templated Self-Assembly of a Covalent Polymer Network for Intracellular Protein Delivery and Traceless Release. *J. Am. Chem. Soc.* **2017**, *139*, 5676–5679. [CrossRef] [PubMed]